TESI DOCTORAL UPF / 2021

Universitat Pompeu Fabra Barcelona

Chimeric synthetic peptides as diagnostic tools. A novel IgM-specific immunoassay for the diagnosis of toxoplasmosis

Driving innovation towards next-generation IgM immunoassays

Greta Ripoll Pastor

Chimeric synthetic peptides as diagnostic tools. A novel IgM-specific immunoassay for the diagnosis of toxoplasmosis

Driving innovation towards next-generation IgM immunoassays

Greta Ripoll Pastor

UPF DOCTORAL THESIS / YEAR 2021

THESIS SUPERVISORS

Prof. David Andreu Martínez
Department of Experimental and Health Sciences
Universitat Pompeu Fabra

Dr. Roser Llevadot Esquerda
Biotechnology Integration
Biokit R&D

Department of Experimental and Health Sciences

Universitat Pompeu Fabra Barcelona

Aquesta tesi, aquest trosset de vida el dedico a les "M".

A qui em va donar la vida. La meva mare Marga.

Al meu gran descobriment de Biokit. La M Àngels.

A qui m'ha donat la mà durant aquest camí. La meva companya Maria.

"The wound is the place where the light enters you"

Rumi

Acknowledgements

Encara recordo com va començar tot. Puc visualitzar a la Roser i la Marta traient el cap pel laboratori buscant-me. Tot i que volien mantenir l'intriga uns minuts més, se'ls hi veia a la cara que portaven bones noticies; tenien el "sí" que faltava per donar llum verda al doctorat industrial. Quatre anys després, aquí estic, revivint tots els moments que han marcat aquest període, per donar-vos les gràcies a totes les persones que m'heu acompanyat. Al mirar enrere, sento una barreja molt gran de sentiments. Aquesta tesi ha suposat, en molts aspectes, un gran repte, però també una oportunitat única de col·laborar amb moltes persones de dins i fora de Biokit. Una cosa tinc clara, he après tot el que he pogut de cada una de vosaltres. Desitjo de tot cor que els que heu caminat al meu costat també us hagueu quedat amb un trosset de mi.

Primerament, moltes gràcies Roser i David per donar-me l'oportunitat de fer aquesta tesi. No sols m'heu fet créixer com a científica, sinó també com a persona. No ha set un camí fàcil, sens dubte, però tot plegat m'ha ajudat a coneixe'm, veure on estan els meus límits, assolir reptes i arribar a un punt millor. Gràcies a vosaltres he après ciència i també una gran lliçó de vida que mai oblidaré.

Vull donar-vos les gràcies als companys del laboratori de Proteòmica per fer-me sentir com una més, per ajudar-me sempre que us he necessitat: Yolanda, Maria, Mar, Sira, Clara, Ferran, Ariadna, Sara, Zoreh i, sobretot a tu Javi, per tot el que m'has ensenyat, per la confiança en què podria purificar sola, per aguantar la meva "fòbia" al tanc de nitrogen líquid, i per la teva infinita paciència. Segurament ho sabeu, però mai està de més que ens diguin les coses bones, sou gent molt maca i heu fet del meu pas pel PRBB una experiència meravellosa.

"*Merci*" a Maan Zrein, Elodie Granjon, Julie Caillaudeau, Lola Marqué i Peter Liehl, per com em vau acollir a InfYnity Biomarkers. Amb vosaltres no només vaig aprendre ciència, sinó que em vau ajudar a tenir una experiència a Lió fantàstica. Tanmateix, vull agrair a l'equip de ArkAb, en especial a la Pauline Monsbrot, per fer que la distància no fos un problema i fer fàcil aquesta col·laboració.

Des de què vaig arribar a Biokit he passat per diversos departaments, i de tots n'he après, però he sigut MOLT afortunada de què un d'ells fos innovació. Aquí he crescut com a científica, i en part això és gràcies a vosaltres. Marta P, Roser, Pepis, David, Anna, Marta C, Cris, Nuria, Alejandro, Paulina, etc.... Durant tot aquest camí m'he nodrit dels vostres coneixements i de la vostra energia! Moltes gràcies per formar part d'aquest treball, que ara també és vostre.

Gràcies a tota la gent de Biokit, en espacial a les persones de Biotecnologia i Assay Development, que durant aquests anys m'heu ajudat, des de fer un ELISA, passant per entendre els entrellats del BIO-FLASH®, i pel camí unes quantes ONCOTRAILS! Anna, Laura, Patri i Cris, he tingut la sort

de compartir "ofi" amb vosaltres durant gairebé l'últim any de tesi, us vull agrair tots els riures, els ànims i la força que m'heu transmès, sou genials. Laura, qué bien sabías por lo que estaba pasado estos últimos meses, a ti te venia de vuelta. Gracias por las charlas y tus "¡vamos Greta que tú puedes!". ¡Resultó, que sí que podía!. També vull donar-vos les gràcies a les Biokites; tot i què hem tingut diverses altes i baixes a la plantilla, el "*core team*" sempre heu estat allà!!!

Ara sí, a vosaltres, les Guachis, a totes i en majúscules, GRÀCIES!!!. No només per els innumerables esmorzars, dinars, cafès, sopars... (ondi, sembla que només haguem fet que menjar...), sinó també per tots els ànims en els moments difícils, perquè de cada una de vosaltres m'emporto ciència i amistat, què més podria demanar? Aquest temps a Biokit no hauria set el mateix sense vosaltres.

MÀngels, el meu gran descobriment de Biokit. Quantes converses, herbetes, riures, llàgrimes, consells, algun sermó, i molta paciència! Al poc de coneixe'ns ja em vas recollir en una d'aquelles abraçades que sense dir paraula, et col·loquen tot al seu lloc, d'aquelles que et fan saber que tot està bé. Quina sort tant immensa la meva de tenir una persona com tu al meu costat. Gràcies per ser el meu gran recolzament aquí dins, i la meva amiga (i també germana gran) fora de Biokit.

També et vull donar les gràcies a tu Lu; la teva implicació cap a mi, i en extensiu cap aquesta tesi ha fet que la visquessis, sobretot aquest últim any, gairebé com si fos teva. Gràcies per les teves revisions, la feinada immensa d'edició, el teu temps, afecte i comprensió. Gràcies per donar-me sempre la mà, per ajudar-me, per creure en mi, per confiar en mi... per la nostra família, en fi, gràcies per TOT.

Gràcies també a la meva família, a tots. Sé que, tot i que no sabeu ben bé que faig a la feina, em teniu present. Aquest últim any ha set difícil, i tant! Així que us vull donar les gràcies pel vostre suport, l'espai, la paciència i els ànims. Us estimo molt!

No vull deixar de donar-vos les gràcies a totes les persones que ja veníeu fent camí amb mi; Eva, Sandra, Cris, Linda, Reich, Shei, Fran, Yasbe, Merlin, Super (i Paula)... Sóc molt afortunada de tenir-vos. Gràcies per seguir amb mi, ara toca continuar endavant. Dintre de poc, si el virus ens deixa, ho celebrarem!

Per últim, vull agrair-vos a totes les persones que m'heu ajudat amb la redacció d'aquesta memòria; Sira, Leti, Anna, Nuria, Pepis, Maria, Susan, David, Roser, i també a les que us heu ofert a fer-ho. Aquesta no ha set una tasca senzilla per mi, i el vostre recolzament i temps ha significat molt per mi.

Gràcies de tot cor!

Greta

Barcelona, 2021

Abstract

Serologic tests detecting anti-*T. gondii* IgMs are the gold standard for the diagnosis of acute toxoplasmosis. Nevertheless, most commercial kits are based on lysate antigens obtained from tachyzoites grown in mice or tissue culture which present inherent limitations in terms of performance, providing erroneous results to the physicians, thus hindering patient management and requiring stringent regulation.

In this context, peptide-based antigens have emerged as an attractive alternative to overcome several of such issues. In this thesis, we focused on designing and synthetizing a novel *T. gondii* IgM-specific chimeric peptide that was used to develop a chemiluminescent immunoassay for the detection of anti-*T. gondii* IgMs. Additionally, we aimed to assess mouse monoclonal humanized chimeric antibodies as an alternative source to the human positive plasma-derived samples that are currently used to produce reference materials, such as calibrators and controls.

Along with its specific results, this thesis provides a set of innovative technologies to discover IgM-specific sequences translating them into robust antigens, to optimize immunoassay formulations, and to replace the current supply-chain of reference materials.

***Keywords**:* anti-*T. gondii* IgM, synthetic peptides, biomaterials, immunoassay performance, toxoplasmosis diagnosis.

Resum

Les proves serològiques que detecten IgMs contra *T. gondii* són referents en el diagnòstic de la toxoplasmosi aguda. No obstant, la majoria de kits comercials es basen en lisats antigènics obtinguts de taquizoïts cultivats en ratolins o cultius tissulars, els quals presenten limitacions inherents en termes de rendiment, proporcionant resultats erronis als metges, dificultant per tant el maneig dels pacients i exigint una rigorosa regulació.

En aquest context, els antígens basats en pèptids resulten una alternativa atractiva per a superar alguns d'aquests problemes. En aquesta tesi, ens hem centrat en el disseny i síntesi d'un nou pèptid quimèric específic per la detecció de IgM contra *T. gondii,* que hem utilitzat per a desenvolupar un immunoassaig quimioluminescent per a la detecció d'IgMs contra *T. gondii*. A més, la tesi ha tingut com a objectiu avaluar una font alternativa a les mostres positives derivades del plasma humà que actualment s'utilitzen per produir materials de referència com són els calibradors i controls.

Més enllà dels resultats, aquesta tesi proporciona un compendi de tecnologies innovadores per descobrir seqüències IgM específiques, traduint-les en antígens fiables, optimitzar la formulació dels immunoassaigs, i substituir l'actual cadena de subministrament de materials de referència.

Paraules clau: IgM contra *T. gondii*, pèptids sintètics, biomaterials, rendiment immunològic, diagnòstic de la toxoplasmosi.

Preface

During decades the healthcare system has been centered on the treatment of sick patients, with the greatest efforts aimed at a cure. Today, there is an increasing trend towards a new paradigm focused on prevention, where early diagnosis and health promotion programs are the protagonists. Within this new paradigm, the *in vitro diagnostic* industry has made significant efforts to improve two key aspects; time to market and accuracy, considering that there is no effective treatment if an accurate diagnosis is not provided on-time. Additionally, the development of novel assays devoted to detecting the acute phase of diseases, such as COVID-19, is fundamental. This trend is expected to continue rising to respond to the increasing demands of the health care sector.

Biokit is a biotechnology company that is part of Werfen with more than 45 years dedicated to the research, development and manufacture of assays and biomaterials for *in vitro diagnostics* use. To address the continuous challenges of this fast-paced industry, Biokit Innovation Department, in which I had the privilege to carry out this PhD thesis, was created with the aim to identify ideas and opportunities and implement them into high added value products.

Among the diagnostic challenges of the 21st century are the discovery of novel biomarkers that can be translated into innovative biomaterials improving the performance of diagnostic methods, especially those intended for IgM detection. With these demands in mind, the objective of this thesis was to overcome the diagnostic limitations offered by current commercial immunoassays for the early detection of IgM anti-*T. gondii*.

For decades, commercial kits for the diagnosis of toxoplasmosis were based on native antigens obtained from infected mice. This predominant approach has inherent limitations in terms of performance and regulatory requirements. In addition, the current source of standard materials (calibrators and controls) derived from seropositive plasma or serum, is difficult to obtain in large volumes and entails increasing drawbacks (see Introduction).

The main goals of the present thesis are therefore the identification of novel IgM-specific sequences that could be translated into synthetic antigens, the development of a prototype immunoassay that would demonstrate the usefulness of "artificial" antigens as diagnostic tools, and the evaluation of an alternative source to produce calibrators and controls.

Taken into account the above-mentioned ideas, the subsequent chapters progress as follows:

Introductory **chapter 1** is divided into four sections: i) a brief explanation of the role of the immune system in infectious diseases, and the importance of IgMs in microbial immunity; ii) a general background on *T. gondii* and toxoplasmosis, reviewing its main epidemiological indicators, and the

clinical distinction between acute and chronic disease; iii) current methodologies for toxoplasmosis diagnosis, focusing on serological tests, particularly those for IgM detection. Lastly iv) innovative technologies to discover and validate new IgM-specific biomarkers, methodologies to produce novel biomaterials that can replace the native antigens, and finally strategies to overcome the main drawbacks associated to the use of human derived state-plasma to produce reference materials for immunoassays. With these ideas in mind, **chapter 2** states the objectives of this thesis.

Subsequent chapters elaborate each objective, including a specific introductory section, which describes key concepts necessary for better understanding the contents of every result section.

Chapter 3 starts describing the study that set this project in motion, the discovery of new IgM-specific biomarkers from the main immunodominant proteins of *T. gondii*. The need to identify novel epitopes capable to detect specifically the IgM anti-*T. gondii,* motivated the collaboration with PEPperPRINT, a company specialized in the development of peptide microarrays.

With the sequences already identified, the obvious next step was to translate them into antigens that could be used to develop an IgM-specific immunoassay. Having joined Biokit R&D department to develop my master thesis about that time, I was put in charge of the project. To this end, a collaboration with the Proteomics and Protein Chemistry Research Group at UPF started with the objective to produce replicas of the identified sequences. Under the guidance of Prof. David Andreu and his group I learned to design and synthesize highly pure lots of synthetic peptides reproducing the sequences identified in the PEPperPRINT study. The chapter also describes the evaluation of these constructs by ELISA.

To optimize the evaluation of the 18 peptides produced at the UPF, we collaborated with InfYnity Biomarkers to develop a multiplex ELISA that allowed us to identify in a fast and efficient way which candidates reacted with the maximum number of IgM-positive samples. The results were reproduced at Biokit using singleplex ELISA. Additionally, we aimed to evaluate whether the combination of two peptides in solution could increase antigenic specificity.

Among the various peptides, the most promising results were encountered when the 3a and 6c constructs were combined in solution. With a view to further explore whether the incorporation of different epitopes into a single molecular entity could achieve higher IgM-specificity, we designed a second set of peptides. Accordingly, **chapter 4** depicts the synthesis of several chimeras designed to enhance IgM-specificity. Furthermore, other strategies to enhance assay performance were assessed: biotin labeling to control peptide orientation and the use of common IgM sequences.

After selecting the definitive candidate based on its promising antigenic characteristics, we set out to develop the proof of concept of a chemiluminescent immunoassay based on 3a6c synthetic peptide

in the BIO-FLASH® instrument. Thus, **chapter 5** describes the procedures and approaches followed to obtain a functional prototype assay based on paramagnetic microparticles coated with the 3a6c peptide (indirect assay), and an anti-IgM antibody labeled with a chemiluminescent tag, as a conjugate. To improve the attributes of the newly developed prototype, we tried to design an immunocapture assay, in which the 3a6c peptide was intended to act as conjugate. To this end, streptavidin had to be first conjugated with a chemiluminescent tag, and later combined with the biotin labeled 3a6c peptide. By this time, I became aware of the complexities of conjugate development, including purification and manipulation of chemiluminescent tags. Despite the months of troubleshooting and the hopes placed on the immunocapture approach, our assay unfortunately did not meet expectations. Therefore, we centered our efforts in the indirect assay. This period was one of the most demanding during my thesis, and I was fortunate to be instructed and guided by Dr. David Casagolda and M Àngels Cuerdo, of Biokit Biochemistry department.

To further increase the performance characteristics of the final indirect prototype, we applied the design of experiments (DOE) method to optimize the assay formulation. We deeply examined the role of each one of the main components of the assay, along with the instrument parameters. During this part of my thesis, I had the opportunity to learn from both Josep Serra and Dr. David Casagolda, who mentored me through the fascinating world of assay development and helped me to conceive the DOE study.

Once the previous achievements were completed, we wanted to go one step further. Particularly, we were interested in deciphering the performance of the 3a6c-PT1I versus a big sample panel, and also challenging the immunoassay in the presence of IgG anti-*T. gondii*. This work is described in **chapter 6.** To accomplish our aim, we designed both a method comparison and an interference study which allowed us to better understand the strengths and the shortcoming of our peptide-based immunoassay. During the most decisive, but also "struggling" periods, especially the analysis of the method comparison, and the IgG interference study, I had the chance to work along Dr. Nuria Tort, whose expertise in assay development and personal encouragement were decisive to surmount the multiple obstacles that I found on the way.

In parallel with the above-mentioned studies, we were interested in the development of an alternative source of reference materials, this is human derived-state plasma from patients suffering the disease. Aware of the challenges related to the current supply chain, **chapter 7** focuses on the evaluation of chimeric humanized monoclonal antibodies used to produce calibrators and controls for the newly developed immunoassay. The aim to obtain hybrid IgM, led us to collaborate with ArkAb, a division of B Cell Design company. This resulted in the obtention of two hybridoma cell lines that produce mice/human monoclonal IgM against the 3a6c chimeric peptide. Although the process to obtain the

cell lines was done outside Biokit, a close communication was established since the peptides used as immunogens were sent to ArkAb. Throughout the different steps to obtain the stable cell line, we were analyzing serum and supernatant samples from the different mice and cell lines to select which were the appropriate antibodies capable to be used as standard materials. This period gave me the opportunity to learn from Dr. Leticia Liste and Sonia Sanchez, who instructed me in the world of the cell culture. Their guidance boosted me to characterize the thermal stability of the new monoclonal antibodies, a key aspect to deal with, especially when considering the novelty of this biomaterial.

Along this project, I generated several sample panels which were crucial to the succeed of each step. Although it may seem a minor job, the limitations of the current commercial kits made this task highly complex, not only from the procedural point of view, but also considering the analysis of the results. In this point, the collaboration with Dr. Anna Rubio, and her high throughput Janus instrument was essential. She altruistically developed a protocol to perform ELISA which significantly simplified the manipulation work, also reducing the error rate usually encountered when manipulating hundreds of samples.

The last section, **chapter 8**, encompasses the conclusions of this PhD project. While I personally have no doubts that synthetic antigens will soon supersede both native and recombinant antigens, particularly in viral, parasitic, and autoimmune human diseases, meanwhile, the scientific community and the IVD industry have to continue developing breakthroughs to respond to the colossal challenges our society is living, not only the current pandemic, but also those that will come in the 21st century. Hopefully, the results presented here may constitute a forward step in this direction.

This doctoral thesis has been carried out in the frame of the program *Doctorats Industrials* of AGAUR (Agència de Gestió d'Ajuts Universitaris i de Recerca) of the *Generalitat de Catalunya*.

Glossary

aa	Amino acid
ABEI	Aminobutyl-ethyl isoluminol
ACN	Acetonitrile
AE	Acridinium esters
AGAUR	Agència de Gestió d'Ajuts Universitaris i de Recerca
AIDS	Acquired immunodeficiency syndrome
AMA	Apical membrane antigen
APC	Antigen-presenting cell
AU	Absorbance units
AUC	Area under the curve
BCA	Bicinchoninic acid
BSA	Bovine serum albumin
C	Constant
CB	Carbonate buffer
CE	*Conformité Européenne*
CI	Confidence interval
CLIA	Chemiluminescent immunoassay
CLSI	Clinical and laboratory standards institute
CMV	Cytomegalovirus
CTL	Cytotoxic T lymphocytes
Da	Daltons
DC	Dendritic cell
DCM	Dichloromethane
DIEA	N,N- diisopropiletilamine
DMF	N,N- dimethylformamide
DMSO	Dimethyl sulfoxide
DNA	Deoxyribonucleic acid
DOE	Design of experiments
ECLIA	Electrochemiluminescent immunoassay
ELFA	Enzyme-linked fluorescence assay
ELISA	Enzyme-linked immunosorbent assay
ESI-MS	Electrospray ionization mass spectrometry
Fc	Fragment crystallizable
FCS	Fetal calf serum
FDA	Food and drug administration
FIA	Fluoroimmunassay
Fmoc	Fluorenylmethyloxycarbonyl
FN	False negative

FNP	False negative proportion
FP	False positive
FPP	False positive proportion
GLP	Good laboratory practices
GMP	Good manufacturing practices
GPI	Glycosylphosphatidylinositol
GRA	Granular antigen
H	Heavy
HA	Human influenza hemagglutinin
HAMA	Human anti-mouse antibodies
HBTU	2-(1H-benzotriazol-1-yl)-1,1,3,3-tetramethyluronium hexafluorophosphate
HPLC	High-performance liquid chromatography
HRP	Horseradish peroxidase
HSV	Herpes simplex virus
ID	Identification
IEDB	Immune epitope database
IFNγ	Interferon gamma
Ig	Immunoglobulins
IgA	Immunoglobulin type A
IgE	Immunoglobulin type E
IgG	Immunoglobulin type G
IgM	Immunoglobulin type M
IMDV	Iscove's modified dulbecco's medium
IND	Indeterminate
IP	Isoelectric point
IVD	In vitro diagnosis
L	Light
LC-MS	Liquid chromatography mass spectrometry
Lys	Lysine
mAbs	Monoclonal antibodies
MEIA	Microparticle enzyme immunoassay
MHC	Major histocompatibility complex
MIC	Microneme protein
MJ	Moving junction
MP	Microparticles
MS	Mass spectrometry
MW	Molecular weight
NaCl	Sodium chloride
NC	Negative control

NEG	Negative
NHS	N-hydroxysuccinimide
NMPA	National medical products administration
NK	Natural killer
OD	Optical density
OFAT	One factor at a time
OT	Ocular toxoplasmosis
PAMP	Pathogen-associated molecular pattern
Parvo	Parvovirus
PB	Phosphate buffer
PCR	Polymerase chain reaction
PDB	Protein DataBank
PBS	Phosphate-buffered saline
PBST	Phosphate-buffered saline tween 20
PC	Positive control
PEG	Polyethylene glycol
POC	Point of care
POS	Positive
PRR	Pattern recognition receptor
P/S	Penicillin streptomycin
PV	Parasitophorous vacuole
PVM	Parasitophorous vacuole membrane
RAU	Relative absorbance units
RF	Rheumatoid factor
RIA	Radioimmunoassay
RLU	Relative light units
RMCB	Research master cell bank
ROC	Receiver operating characteristic
RON	Rhoptry neck protein
ROP	Rhoptry protein
RP-HPLC	Reversed phase high-performance liquid chromatography
RT	Retention time
RUB	Rubella
S/CO	Signal cut-off
SAG	Surface antigen
SD	Standard deviation
Se	Sensitivity
SEC	Size-exclusion chromatography
SLE	Systemic lupus erythematosus
SNR	Signal-to-noise ratio
Sp	Specificity

SPPS	Solid-phase peptide synthesis
SPR	Solid-phase receptacle
SRS	SAG-related sequences
SUMO	Statistical Utility for Microarray and Omics
T. gondii	*Toxoplasma gondii*
TAN	Triethanolamine
TB	Trypan blue
TCR	T cell receptor
TFA	Trifluoroacetic acid
T_H	T helper
TLA	Toxoplasma lysate antigens
TLR	Toll-like receptor
Toxo Ag	*T. gondii* native antigen
TMB	Tetramethylbenzidine
TN	True negative
TNP	True negative proportion
TP	True positive
TPP	True positive proportion
TV	Test value
US	United States
UV	Ultraviolet
V	Variable
VZ	Varicella zoster
WR	Working reagent
%bias	Percentage of bias
%CV	Coefficient of variation

List of Contents

Acknowledgements ..... **VII**

Abstract ..... **IX**

Resum ..... **XI**

Preface ..... **XIII**

Glossary ..... **XVII**

List of Contents ..... **XXI**

List of Figures ..... **XXVII**

List of Tables ..... **XXIX**

CHAPTER 1 – Introduction **1**

1.1. Infectious diseases, the importance of IgM 1

1.1.1. The role of the immune system in infectious diseases 1

1.1.2. The role of IgM in infectious diseases 3

1.2. *T. gondii*, the causative agent of toxoplasmosis 4

1.2.1. Population structure and geographic distribution 4

1.2.2. Proteins involved in cell invasion 5

1.2.3. Toxoplasmosis disease 7

1.2.4. Clinical features of toxoplasmosis 8

1.3. Toxoplasmosis diagnosis 10

1.3.1. Diagnosis based on microscopic observation and imaging techniques 11

1.3.2. The problems with serological detection 19

1.3.3. *T. gondii* antigens for serodiagnosis 21

1.4. Focus on innovation. New technologies to develop IgM-specific immunoassays 22

1.4.1. New technologies to identify IgM-specific epitopes 22

1.4.2. Synthetic peptides as diagnostic tools 25

1.4.3. Alternative sources to obtain immunoglobulins to be used as calibrators and controls in immunoassays 28

1.5. Final remarks 30

CHAPTER 2 – Objectives **31**

CHAPTER 3 – Synthetic peptides as antigens: from *T. gondii* peptide microarray to functional individual peptides **33**

3.1. *T. gondii* peptide microarray 34

3.1.1. Microarray characterization 34

3.1.2. *T. gondii* peptide microarray evaluation 36

3.2. From microarray to synthetic peptides 39

3.2.1. Identification and production of peptide sequences 40

3.3. Evaluation of synthetic peptides via ELISA 41

3.3.1. Screening panel characterization 41

3.4. Multiplex ELISA 44

3.4.1. Phase I: Optimizing printing conditions and setting up the screening conditions 44

3.4.2. Phase II: Evaluation of the synthetic peptides with the screening sample panel 50

3.5. Singleplex ELISA 53

3.5.1. Reproducing the multiplex parameters in singleplex ELISA 54

3.5.2. Optimizing the singleplex ELISA 55

3.6. Discussion 60

CHAPTER 4 – Peptide chimeras to enhance sensitivity **67**

4.1. Design and synthesis of chimeric peptides based on top-performing peptides 6c & 3a 67

4.1.1. Chimeric homotandems 68

4.1.2. Chimeric heterotandems 69

4.1.3. Biotin-labeled peptides 69

4.2. Evaluation of chimeric peptides via enzyme-linked immunosorbent assay 71

4.3. Evaluation of biotin-labeled peptides via ELISA 74

4.4. Discussion 76

CHAPTER 5 – Development of a chemiluminescent immunoassay based on synthetic peptides for the diagnosis of human toxoplasmosis **81**

5.1. Characterization of samples 82

5.2. Chemiluminescent immunoassay formats 83

5.2.1. Indirect assay using tosyl and streptavidin-activated magnetic beads 83
5.2.2. Immunocapture assay format 86
5.3. Reagent optimization using design of experiments method 87
5.3.1. Solid-phase formulation 88
5.3.2. Assay buffer formulation 92
5.3.3. Tracer formulation 94
5.4. Conjugate concentration study 96
5.5. Optimization of assay parameters 97
5.6. Discussion 100
CHAPTER 6 – Performance characteristics of the new immunoassay 105
6.1. Method-comparison study 106
6.1.1. Sensitivity, specificity and agreement evaluation 106
6.2. Analytical specificity 112
6.2.1. *T. gondii* IgG interference study 113
6.2.2. Cross-reactivity study 114
6.3. Discussion 116
CHAPTER 7 – Chimeric monoclonal IgM as an alternative source for calibrators and controls: Cell line generation and thermal stability characterization 121
7.1. Hybridoma cell line generation 122
7.2. Evaluation of the hybridoma supernatants' reactivity 122
7.2.1. Evaluation of hybridoma supernatants by ELISA 122
7.2.2. Evaluation of hybridoma supernatants by CLIA 123
7.3. Thermal stability of chimeric IgM 125
7.3.1. Hybridoma batch cell culture 125
7.3.2. Thermal stability characterization 126
7.3.3. Thermal stability at 2-8ºC 127
7.3.4. Freeze-thaw stability 128
7.3.5. Thermal stability of the final calibrators and controls 129
7.4. Discussion 132

CHAPTER 8 – Materials and methods 135

8.1. Instrumentation 135

8.2. Clinical samples 135

8.2.1. Samples for microarray study (Microarray panel) 135

8.2.2. Samples for initial testing (Screening panel) 135

8.2.3. Samples for CLIA reagent formulation 136

8.2.4. Samples for the feasibility study 136

8.2.5. Samples for interference and cross-reactivity studies 136

8.2.6. Laboratory investigation 136

8.3. *T. gondii* peptide microarray 138

8.3.1. Protein selection 138

8.3.2. Microarray content 138

8.3.3. Procedure 139

8.3.4. Statistical analysis 140

8.4. Solid-Phase Peptide Synthesis 140

8.4.1. Synthetic versions of the identified antigenic regions 140

8.4.2. Peptide cleavage and work-up 141

8.4.3. Peptide purification 141

8.4.4. $(6c)_2K_3$ branched peptide 142

8.4.5. Biotin peptide conjugation 142

8.5. Enzyme-linked immunosorbent assay 142

8.5.1. Multiplex ELISA 142

8.5.2. Singleplex ELISA 143

8.6. Chemiluminescent immunoassay 144

8.6.1. Solid-Phase 145

8.6.2. Assay buffer 145

8.6.3. Tracer 145

8.6.4. Protein quantification 146

8.6.5. BIO-FLASH® assay parameters 146
8.6.6. IgG interference study 146
8.6.7. Cross-reactivity study 146
8.6.8. Method comparison study 147
8.7. Chimeric monoclonal IgM. Cell line generation and characterization 147
8.7.1. Hybridoma cell line generation 147
8.7.2. Initial set-up and generation of research master cell bank of A12A and B12A hybridoma cell lines 147
8.7.3. Antibody titration 149
CHAPTER 9 – Conclusions 151
References 155

List of Figures

Figure 1-1: Schematic view of immune responses upon parasite infection. 2
Figure 1-2: Schematic structure of IgM. 4
Figure 1-3: Schematic representations of early and mid-invasion. 7
Figure 1-4: Anti-*T. gondii* immunoglobulin kinetics after primary infection. 11
Figure 1-5: Schematic view of ELISA types. 14
Figure 1-6: Reaction between Dynabeads® tosyl-activated magnetic beads and the amino group...16
Figure 1-7: Chemical reaction of ABEI to generate light emission....17
Figure 1-8: BIO-FLASH® Toxo IgM reaction scheme....19
Figure 1-9: Combinatorial synthesis of a peptide array with a laser printer....24
Figure 1-10: Schematic view of multiplex immunoassay in ELISA format....25
Figure 1-11: Schematic representation of peptide production by SPPS....26
Figure 1-12: Generation of mAb by immunizing laboratory animals with any target antigen. 29
Figure 3-1: Raw heatmaps of *T. gondii* peptide microarray. 37
Figure 3-2: *T. gondii* peptide microarray heatmap showing unpaired two-class t-test of differential IgM response. 38
Figure 3-3: Schematic view of the multiplex ELISA (phase I). 45
Figure 3-4: Scanned images for sample 4 with the 18 peptides. 49
Figure 3-5: Schematic view of the multiplex ELISA of phase II....51
Figure 3-6: Original image for positive sample 4, before and after processing....52
Figure 3-7: Schematic view of ELISA plates. 54
Figure 3-8: Correlation between multiplex and singleplex ELISA....55
Figure 3-9: Example of a checkerboard template. 56
Figure 3-10: Receiver operating characteristic curve of peptides 3a, 3b, 6c 7b and 3a+6c....58
Figure 4-1: Schematic representation of original and truncated version of peptide 6c....69
Figure 4-2: Schematic representation of the chimeric and biotin-labeled peptides. 71
Figure 4-3: Receiver operating characteristic curve of chimeric peptides. 73
Figure 5-1: Schematic representation of the microparticles used for the indirect approach....83
Figure 5-2: Pareto plot for solid-phase span variable. 90
Figure 5-3: Main effects plot for the span response in the solid-phase DOE....90
Figure 5-4: Pareto plot for solid-phase bound peptide variable. 91
Figure 5-5: Pareto plot for assay buffer span variable. 93
Figure 5-6: Main effects plot for span in the assay buffer DOE. 93
Figure 5-7: Pareto plot for tracer span variable. 95
Figure 5-8: Main effects plot for the span response in the tracer DOE. 96

Figure 5-9: Schematic view of the 3a6c-PT1I immunoassay.....98
Figure 6-1: ROC curve of 3a6c-PT1I and BIO-FLASH® vs. PLATELIA™. 112
Figure 7-1: Comparison of hybridoma supernatants' reactivity. 123
Figure 7-2: Hybridoma supernatant reactivity. 124
Figure 7-3: Reactivity of stabilized hybridoma supernatant. 124
Figure 7-4: A12A hybridoma cellular viability and reactivity against 3a6c-PT1I. 126
Figure 7-5: B12A hybridoma cellular viability and reactivity against 3a6c-PT1I. 126
Figure 7-6: Procedure followed to assess IgM thermal stability. 127
Figure 7-7: A12A and B12A Bias % plot. 128
Figure 7-8: Thermal stability of the final calibrators and controls. 130
Figure 8-1: General procedure for the generation of research, master, and working cell bank. 149

List of Tables

Table 3-1: List of the nine proteins used to build up the peptide microarray. 34
Table 3-2: Characterization of microarray serum panel. 35
Table 3-3: Top hits of differential IgM responses. 39
Table 3-4: Peptides used in the initial phase of this study. 40
Table 3-5: Screening panel composition. 41
Table 3-6: Commercial assays used to characterize screening panel. 42
Table 3-7: Detailed view of the screening panel characterization. 43
Table 3-8: Screening panel classification. 43
Table 3-9: Cut-off values for each peptide. 46
Table 3-10: Peptide screening via multiplex ELISA (phase I). 47
Table 3-11: Results overview for positive sample 4 (phase I). 50
Table 3-12: Peptide screening by multiplex ELISA (phase II). 52
Table 3-13: Results overview for positive sample 4 (phase II). 53
Table 3-14: Results overview of checkerboard optimization at original peptides. 57
Table 3-15: Area under the curve (AUC) of the ROC curve. 58
Table 3-16: Accuracy estimators for each peptide. 59
Table 4-1: Chimeric, biotin-labeled, and common IgG peptides used in this study. 70
Table 4-2: Checkerboard results overview of chimeric peptides. 72
Table 4-3: Accuracy estimators for each chimeric peptide. 73
Table 4-4: Area under the curve (AUC) of the ROC curve. 74
Table 5-1: Description of formulation panel (n=12) 82
Table 5-2: Evaluation of the formulation panel with 3a6c-ITPT1 and 3a6c-ISPT1. 84
Table 5-3: Accuracy estimators of 3a6c-ITPT1 at different cut-off levels. 85
Table 5-4: Variables and levels used for solid-phase formulation. 89
Table 5-5: Solid-phase DOE study. 91
Table 5-6: Variables and levels used for assay buffer DOE formulation. 92
Table 5-7: Assay buffer DOE study. 94
Table 5-8: Variables and levels used for tracer DOE formulation. 95
Table 5-9: Assay buffer DOE study. 96
Table 5-10: Conjugate concentration study. 97
Table 5-11: Results of the assay parameters optimization. 99
Table 6-1: Confusion matrix of diagnostic performance parameters. 105
Table 6-2: Method comparison of 3a6c-PT1I vs. BIO-FLASH® by Weighted Kappa. 107
Table 6-3: BIO-FLASH® Toxo IgM indeterminate samples. 108

Table 6-4: Final consensus for discrepant and indeterminate samples. 108
Table 6-5: Method comparison of 3a6c-PT1I vs. PLATELIA™ by Weighted Kappa. 109
Table 6-6: Diagnostic performance of 3a6c-PT1I without indeterminate sample. 109
Table 6-7: Samples around the 3a6c-PT1I gray zone. 110
Table 6-8: PLATELIA™ Toxo IgM indeterminate samples. 111
Table 6-9: Method comparison of 3a6c-PT1I vs. PLATELIA™ by Weighted Kappa for the *worst-case scenario*. 111
Table 6-10: 3a6c-PT1I *worst-case scenario* diagnostic performance. 111
Table 6-11: AUC of the ROC curve for 3a6c-PT1I, BIO-FLASH®, and PLATELIA™. 112
Table 6-12: Characterization of interference samples. 113
Table 6-13: Reported values of the interference study. 114
Table 6-14: Cross-reactivity evaluation with BIO-FLASH® Toxo IgM and 3a6c-PT1I. 115
Table 7-1: Supernatant stability at 2-8°C of A12A and B12A. 128
Table 7-2: A12A and B12A freeze-thaw stability. 129
Table 7-3: Thermal stability of the final calibrators and controls. 131

CHAPTER 1 – Introduction

1.1. Infectious diseases, the importance of IgM

1.1.1. The role of the immune system in infectious diseases

The human body is not a fortress. We are constantly interacting with a range of organisms, such as bacteria, viruses, fungi, and parasites, which can cause various infectious diseases. For years, our immune system has evolved to defend our body by producing immune cells and specific antibodies capable of recognizing and inactivating foreign agents.

Tackling infections is the job of different types of white blood cells which interact with the environment to detect infection or abnormal cell death. To identify pathogens, the immune system exposes antigens, which are unique molecular signatures for each pathogen. In the face of danger the immune system reacts in two ways:

Innate immunity is carried out by external physical barriers, and by cells that can be tissue-resident (macrophages and dendritic cells) or non-resident (monocytes, neutrophils, granulocytes and natural killers). Innate immune cells use specialized sensors encoded in the germline called pattern recognition receptors (PRRs), such as Toll-like receptors (TLRs), to recognize specific pathogen-associated molecular patterns (PAMPs) which are carbohydrate, polypeptide, and/or nucleic acid "signatures" not found among the molecules of host cells (1,2). In addition, they release signaling molecules that trigger an inflammatory response and begin to marshal the forces of the adaptive immune system (3–5). Innate response is defined by lack of immunogenic memory, fast kinetics and antigen-independent mechanism (6–9).

Adaptive immunity is slower than the innate one, as it depends on the latter, in particular on antigen-presenting cells (APCs) interacting with lymphocytes to trigger antigen-specific responses (10,11). Antigen specificity is mediated by receptors expressed on the surfaces of T and B lymphocytes. Unlike the germ line-encoded recognition molecules of the innate response, antigen-specific receptors of the adaptive response are encoded by genes assembled by somatic rearrangement to form intact T cell receptor (TCR) and immunoglobulin (B cell antigen receptor; Ig) genes (12,13).

There are two broad classes of adaptive responses, regulated by B and T cells, respectively: humoral through antibody production, and cell-mediated. In antibody responses, B cells are activated to secrete immunoglobulins (Ig) which bind specifically to the foreign antigens that stimulated their production. Antibodies play different roles in inactivating viruses and microbial toxins by blocking their ability to bind receptors on host cells, as well as marking the invading pathogens for destruction by phagocytic cells of the innate system (3). In cell-mediated responses, T cells engage in diverse set

of tasks, for example reacting against antigens presented by APCs to the major histocompatibility complex class I (MHC class I) when they are intracellular, or to MHC class II when they are extracellular. T cells also induce lysis of infected cells by cytotoxic T lymphocytes (CTLs or CD8+ T cells), which secrete signal molecules such as cytokines that activate macrophages to destroy invading microbes. They also stimulate B cells to produce Igs, and carry out helper (regulatory) functions (T_H cells or CD4+ T cells) (1,6,14). As part of the adaptive response, some B and T cells change into memory cells that stay in the lymph nodes and the spleen to quickly and vigorously fight infection if the immune system recognizes the same antigen again. A proper interaction between the immune cells and signaling molecular effectors is a prerequisite for an efficient immune response.

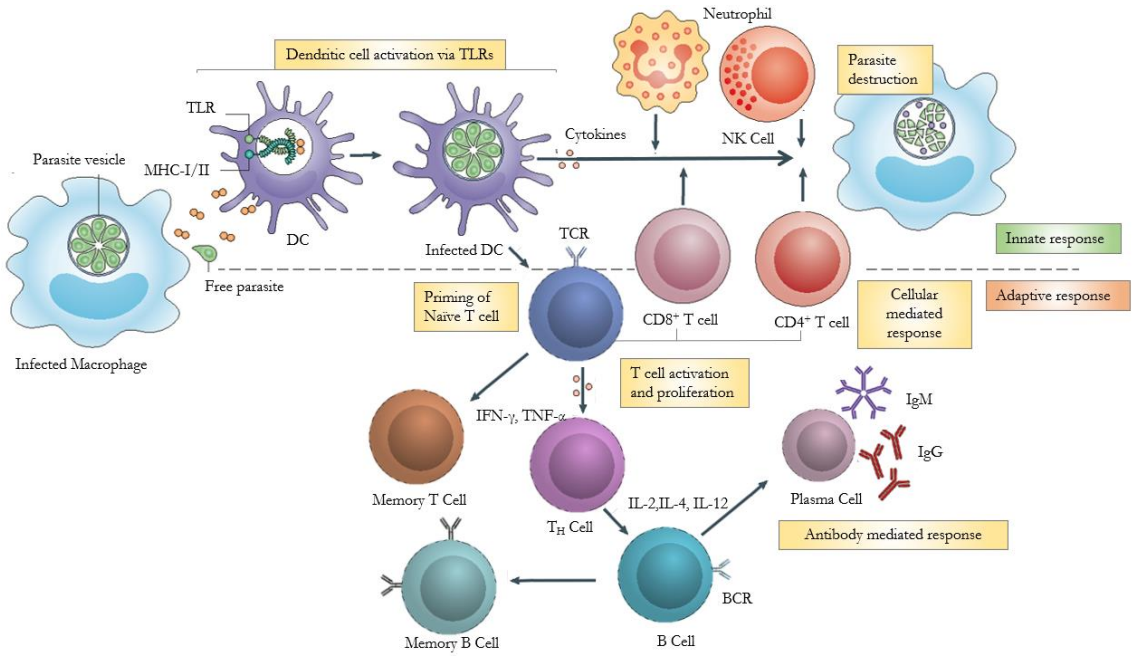

Figure 1-1: Schematic view of immune responses upon parasite infection. Cells involved in the innate and adaptive response are shown. Dendritic cells (DC) and macrophages are the first cells to respond against infection. Parasite secretions interact with Toll-like receptors (TLR) on antigen-presenting cells (APCs), inducing the production of pro-inflammatory cytokines. Innate immune cells, like neutrophils and natural killer (NK) cells, produce IFN-γ in response to infection, activating several host defense mechanisms for intracellular parasite elimination. Antigen presentation by major histocompatibility complex class I (MHC-I) on APCs triggers cell-mediated immune response. CD8+, CD4+ T cells, and B cells are activated in secondary lymphoid organs. Intricate communication and interaction between immune cells activate T helper and B cells, making the latter differentiate into plasma cells and start producing antibodies (IgM, and later IgG) that induce destruction of infected cells. Adapted from (15–17).

Microorganisms constitute an extraordinarily diverse group, found in all environments and infecting all living creatures. However, not all infections trigger disease. Many microorganisms coexist with their host, causing disease only when immune defenses are compromised (18,19). The immune system is constantly "deciding" if the presence of a certain antigen should lead to the beginning of a complex signaling cascade that gives rise to an immune response or if, on the contrary, the molecule does not present a threat (20–22).

1.1.2. The role of IgM in infectious diseases

The IgM, the primary humoral component elicited in immune response following infection, is produced by T-independent antigens (23).

Immune cells use different receptors to interrogate the environment. These have a common structure consisting of a combination of two identical heavy (H) and two light (L) chains formed by different domains designated as variable (V) and constant (C) regions. The variability is concentrated into three segments of each chain, entitled as hypervariable regions, which contain the amino acids that make contact with the antigenic determinant of an antigen (Figure 1-2).

Monomeric IgM (180,000 kDa) is expressed as a membrane-bound antibody on all naive B cells. It is formed by a dimer of a heavy and a light chain pair. The H chain contains five domains, each of approximately 110 amino acids, whereas the L chain consists of two domains. Each amino-terminal domain forms the antigen-binding site, which is different for each antibody. Multiple IgM monomers assemble through an interchain disulfide bridge between cysteines in the constant domains to form polymeric IgM, which is the most abundant IgM secreted version. It contains an additional small protein, the joining (J) chain, which bridges the cysteine residues within the tailpiece of two neighboring IgM monomers (24). Antibody secreting cells can also produce hexameric IgM, which lacks the J chain.

The pentameric structure generates ten linked antigen-binding sites, affording IgM a higher valency than other immunoglobulins to bind antigens with a wide range of avidities. However, as it is the first immunoglobulin secreted, it is typically of low affinity. Altogether, IgM is polyreactive, which means it can bind to a range of unrelated phylogenetically conserved structures, especially repeating epitopes, including nucleic acids, proteins, carbohydrates, and phospholipids (23,25).

The duration of IgM-mediated response is controversial; IgM immunity is usually considered to be transient, and therefore of little value for protection against re-infection. However, recent evidence indicates that it can be maintained for long periods after infection, especially in the case of intracellular bacterial infections (23).

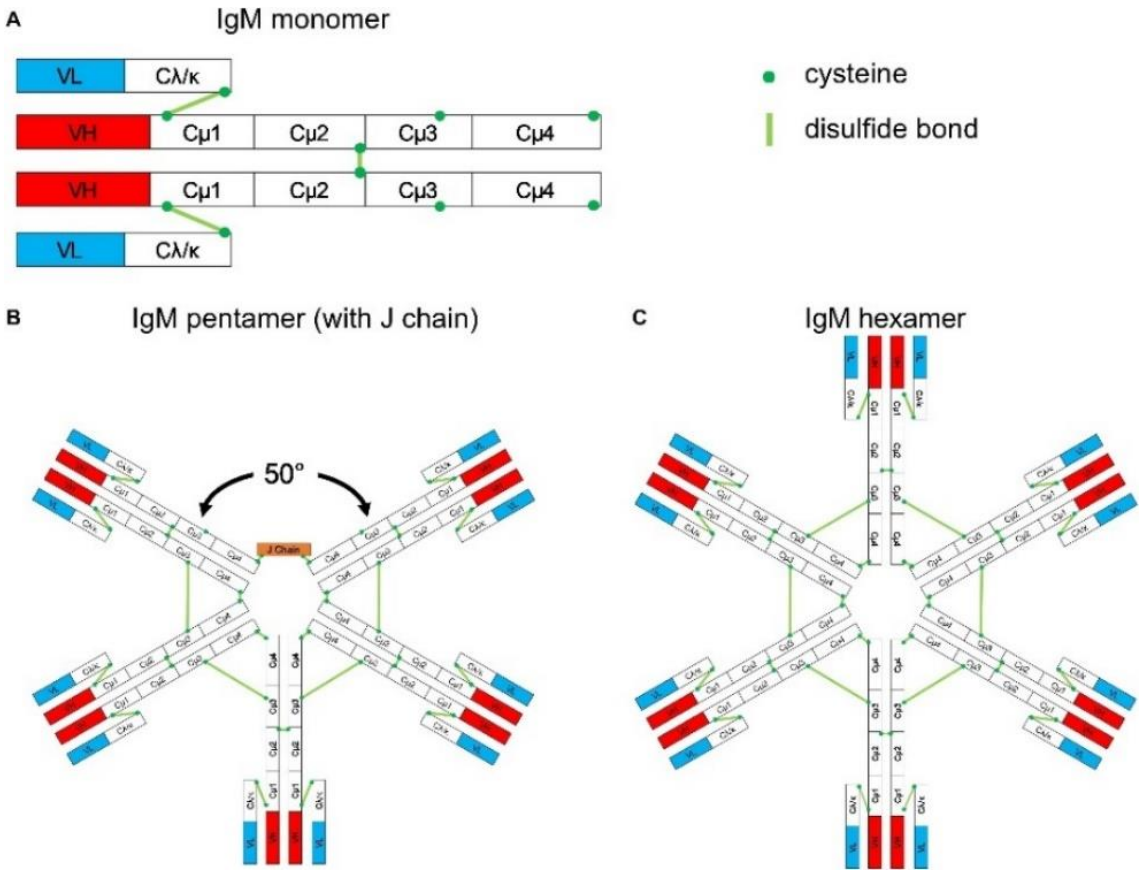

Figure 1-2: Schematic structure of IgM. (A) Monomeric IgM is composed of two heavy (μ) and two light (λ/κ) chains. Each heavy or light chain contains one variable region (V_H or V_L) and one constant region (Cμ1-4 and Cλ/κ). (B) Pentameric IgM contains five monomers and one J chain; disulfide bonds between each monomer form the pentamer; the structure shown in (B) is based upon the recent electron microscopy image presented by Hiramoto et al. (12). There is a 50° gap where the J chain resides. (C) The IgM hexamer contains six monomers and resembles a hexagon. The J chain is generally absent in hexamers.

1.2. *T. gondii*, the causative agent of toxoplasmosis

Infections caused by the protozoan *Toxoplasma gondii* (hereafter, *T. gondii*), the causative agent of toxoplasmosis, are widely prevalent in both humans and animals. With approximately two billion people infected, it is one of the most successful parasites worldwide (26,27).

1.2.1. Population structure and geographic distribution

Unlike other parasites, *T. gondii* possesses an extremely broad host range, infecting terrestrial and marine birds and mammals. Moreover, it seems to be nearly ubiquitous geographically, having been isolated from a variety of climatic regions on every continent surveyed.

With some exceptions, *T. gondii* has a clonal population structure in Europe and North America, in which the vast majority of strains can be grouped into three predominant lineages (types I, II, and III), type II being the most predominant (28–31). In South America however, strains appear to be more genetically diverse (32).

1.2.1.1.Parasite life cycle

The life cycle of *T. gondii* was completely understood with the discovery of the central role of the cat as a definitive host sheltering the sexual parasitic cycle and spreading oocysts through feces (33,34). There are three infectious stages: (i) tachyzoites, the fast replicate stage, found predominantly during the acute phase; (ii) bradyzoites, which multiply slowly within a tissue cyst in the chronic stage of the asexual cycle, and (iii) sporozoites, contained in sporulated oocysts (35,36). These three stages are connected in a complex life cycle that requires multiple hosts to complete a full cycle (35,37). Definitive hosts are members of the *Felidae* family, domestic cats. Intermediate hosts are probably all warm-blooded animals. Accordingly, the life cycle can be divided into feline and non-feline phases, which are in turn correlated with sexual and asexual replication, respectively (38,39).

Both animals and humans can become infected by several routes: eating raw or undercooked meat of animals harboring tissue cysts, and consuming food or water contaminated with cat feces. Additionally, humans are exposed in blood transfusion or organ transplantation (40).

The three parasitic stages are similar ultrastructurally but differ in certain organelles and inclusion bodies. From secretory organelles, we can distinguish dense granules, micronemes, and rhoptries. These organelles secrete proteolytic enzymes that allow the parasite to invade cells and create an intracellular environment suitable for their growth and development (41).

1.2.2. Proteins involved in cell invasion

T. gondii intracellular and extracellular forms represent two distinct biological states. Extracellular parasites do not divide, are highly motile, and secrete the contents of their secretory organelles. Intracellular parasites divide, are non-motile, and do not secrete (42). In the next sections, the role of the most relevant proteins—in terms of their potential use as antigens—will be addressed.

1.2.2.1. SAG 1 (P30) and host cell attachment

Most of the parasite's surface consists of a family of glycosylphosphatidylinositol (GPI)-linked proteins structurally related to the highly immunogenic surface antigen SAG1 (Surface Antigen 1), also known as Major Surface Antigen P30. Collectively, these surface antigens are known as the SRS (SAG1-related sequences), a family of proteins that includes at least 20 homologous proteins (43,44). They have an N-terminal signal peptide and share 24-99% of their sequence.

P30 has been identified as a homodimer with two dumbbell-shaped monomers that come together to form a deep, positively charged groove that bestows its attachment properties (45). Because of its structure, it has been implicated in the initial attachment to the host membrane, working as a receptor capable of initiating a cascade of interactions that facilitates parasite entry, and also activating host immunity to regulate the virulence of infection (46,47).

1.2.2.2. The role of MIC in cell invasion

Cell invasion is a rapid process (15 to 30") in which *T. gondii* forms a tight association between its apical end and the host cell membrane, forming a ring-like structure called the moving junction (48–50). This structure moves from the parasite's apical end to its posterior end, which leads *T. gondii* into a parasitophorous vacuole (51).

The moving junction is a cooperative structure between different proteins. One is AMA1, which is translocated from micronemes inside to the surface (52). The presence of this protein requires the secretion of different adhesins, such as MIC2, which recognize host cell receptors and promote parasite reorientation and attachment (51). At the same time, proteins residing in the rhoptry neck (RON proteins) and the rhoptry bulb (ROP proteins) are required to form a breach in the host's plasma membrane. The formation of the nascent parasitophorous vacuole membrane requires the secretion of both ROP and dense granule proteins, and the invagination of the host cell plasma membrane (48).

After the parasitophorous vacuole is formed, dense granules release their contents. Dense granule proteins like GRA1, GRA2, GRA4, and GRA6 are secreted into the lumen, and GRA3, GRA5, GRA8 are localized within the vacuolar membrane. The mechanism by which these proteins go from being soluble to having a transmembrane location is poorly understood but presumably involves a profound change in their topology (49). The parasitophorous vacuole membrane is a porous-like structure where GRA3, a soluble protein that oligomerizes and inserts into the membrane, may function as the pore-forming complex (38). Another function associated with GRA proteins, particularly GRA3 and GRA7, is their influence on antigen presentation (53).

1.2.2.3. Rhoptry bulb and neck proteins

The only circumstance in which rhoptries are known to secrete their contents is during invasion (54). Although some have putative transmembrane domains, unlike in dense granule proteins, no rhoptry membrane proteins are known (49).

ROP seems to have completely different functions from RON. However, both are released during invasion. ROP are dominated by a large family (ROP2 family) of protein kinase homologues of which only some possess all critical residues needed for kinase activity. In particular, ROP1 is released during invasion and accumulates within the lumen of the nascent parasitophorous vacuole (49,54) (Figure 1-3).

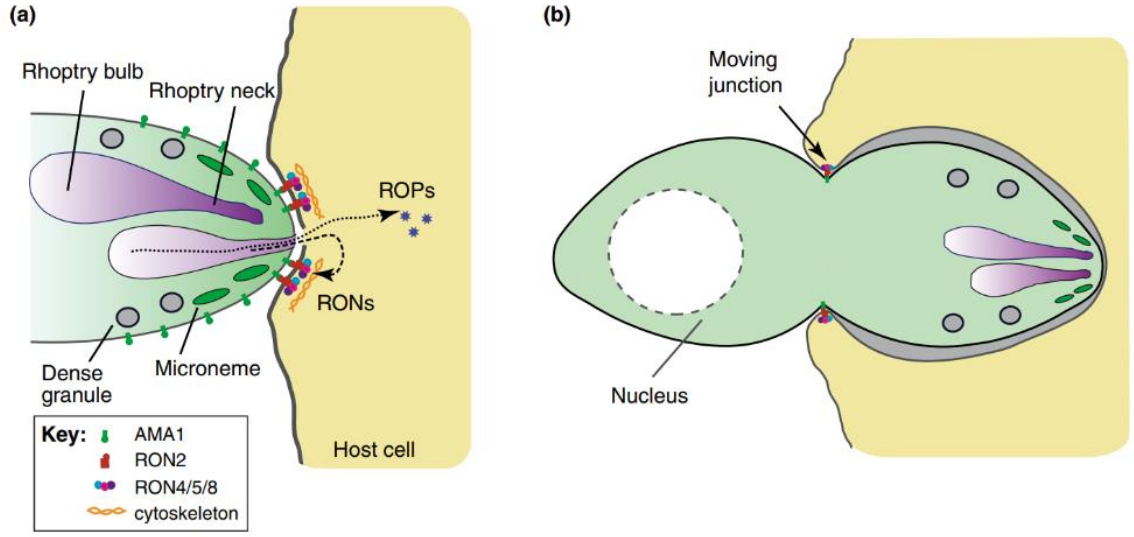

Figure 1-3: Schematic representations of early and mid-invasion. (a) Apical tip of *T. gondii* tachyzoite. The location of the secretory organelles is indicated: micronemes, rhoptries and dense granules (Box 1 for further details). (b) Partially invaded parasite. Adapted from (52).

The ROP2 family generally migrates to the parasitophorous vacuole membrane. Although no crystal structure of a ROP2 family member has been reported, it seems unlikely that a helix would be used to span a membrane, especially given the clear conservation of sequence on either side of the hydrophobic portion (55).

1.2.3. Toxoplasmosis disease

1.2.3.1. Distribution and prevalence

Toxoplasmosis is the most common parasitic infection in the world, surpassing even malaria (56). It is estimated to affect about a third of the world's human population, being more frequent in countries with a tropical climate (57–59). The prevalence of human toxoplasmosis increases with age and does not differ greatly between males and females (58). Three situations can be established depending on the host's immune system. In immunocompetent individuals, infection goes unnoticed or generates flu-like symptoms. In immunocompromised individuals, it has health-threatening and fatal implications. Finally, in congenitally infected fetuses, it can cause retinochoroiditis, hydrocephaly, mental retardation, seizures, or even death (60).

Seroprevalence studies done in Spain, estimate that around 25-50% of the population has been exposed to *T. gondii* (61,62). However, as it is not a disease of mandatory declaration, its prevalence is presumably underestimated. Additionally, the lack of clinical manifestations in the immunocompetent adult causes non-existing diagnosis in the healthy population, and therefore tests are limited to those cases with obvious clinical interest, such as pregnant or immunocompromised patients (63).

Toxoplasmosis prevalence depends on many factors: eating habits, environmental conditions, climate, the presence of definitive hosts, and socioeconomic level. Over the last decades, increased socioeconomic levels of most industrialized countries, together with an improvement in hygienic conditions, changes in farming systems, the consumption of frozen meat, and the feeding of cats with sterilized food, have led to a prevalence decrease (64). In countries where the number of cases in pregnant women is high (i.e., France, Germany, and the US), the prevalence has declined considerably, being France the most remarkable, with a decrease of 40% in the last 50 years (65,66).

1.2.3.2. Innate and adaptative immune responses against *T. gondii*

As an orally acquired pathogen, the innate immune response against *T. gondii* starts in the small intestinal mucosa (48), and adaptive immune responses in neural and muscular tissues. Its rapid dissemination throughout the body is mainly due to the ability of *T. gondii* to actively migrate across the gut epithelial barrier as well as invade migratory cells (dendritic cells and macrophages). The acute phase is associated with peripheral parasitemia with tachyzoites circulating freely, or within phagocytic cells, until the development of an effective immune response. Then, conversion of rapidly dividing tachyzoites to quiescent bradyzoites within tissue cysts occurs, which correlates with the beginning of the chronic phase (64,67,68).

It is well-established that the immunodominant antigens of *T. gondii* are recognized by $CD8^+$ T cells and associated with the parasitophorous vacuole; particularly GRA and ROP secreted proteins that reside within the lumen, or that localize to the limiting membrane (17,53,69–72).

1.2.4. Clinical features of toxoplasmosis

Regarding clinical aspects, although *T. gondii* infection in developed countries is asymptomatic in 80% of infected patients, there are several distinct clinical syndromes. Therefore, toxoplasmosis can be categorized as toxoplasmosis in immunocompetent patients, acquired or reactivated in immunodeficient patients, or acquired during pregnancy.

1.2.4.1. Toxoplasmosis in immunocompetent individuals

Primary infection is asymptomatic in more than 80% of immunocompetent subjects (58). In the remaining cases, patients may experience symptoms such as fever or cervical lymphadenopathy, sometimes associated with myalgia, asthenia, or other non-specific signs.

1.2.4.2. Toxoplasmosis in immunocompromised patients

In contrast to immunocompetent subjects, toxoplasmosis is always life-threatening in immunocompromised patients. However, the host immune background is of prime importance (51). As explained in previous sections, the containment of cysts by adapted immunity is a determining factor for the latency of toxoplasmosis reactivation (73).

Toxoplasmosis is a major opportunistic infection in immunodeficient patients, especially those suffering from acquired immunodeficiency syndrome (AIDS), and immunosuppressive therapies because of organ transplants. Because of its severity, this situation should be prevented by serological screening of donors and recipients and, afterward, by serological and PCR follow-up.

In the case of T-cell deficiency, as in AIDS-infected patients, bradyzoites can reactivate into tachyzoites. In these patients, reactivation of a latent infection might result in toxoplasmic encephalitis, which is the most predominant manifestation and potentially fatal if not treated properly (74,75). Various symptoms are associated, from headache, lethargy, lack of coordination, and ataxia to hemiparesis, loss of memory, dementia, or focal to major motor seizures, usually with fever.

1.2.4.3. Toxoplasmosis during pregnancy

T. gondii infection during gestation and fetal transmission continues to be the cause of tragic yet preventable disease in the offspring. Transmission to the fetus occurs almost solely in women who acquire their primary infection during or just before pregnancy. Rarely, congenital transmission occurs in chronically infected women whose infection was reactivated because of their immunocompromised state (76).

Toxoplasmosis seroprevalence in pregnant women in Spain is around 30%, 29% in Barcelona (62,77). The incidence of gestational toxoplasmosis is 1.9 ‰. However, this low incidence is because in most countries there is no regulated screening during pregnancy. Therefore, if a pregnant woman is tested for toxoplasmosis, this reflects her doctor's personal decision rather than clear regulations by health authorities.

As in immunocompetent, the symptoms manifested in pregnant women are non-specific and can be attributed to many different clinical situations. An interesting study carried out in 2005 revealed that 48% of mothers who gave birth to congenitally infected infants could recall clinical signs compatible with toxoplasmosis (malaise, low-grade fever, and lymphadenopathy) (76). This finding points to how often the infection goes undetected.

T. gondii infection during pregnancy and its potentially tragic outcome for the fetus and newborn continue to occur worldwide, even though it can be prevented by early diagnosis and treatment (78).

1.2.4.4. Congenital toxoplasmosis

T. gondii can cross the placenta causing congenital toxoplasmosis, which can result in miscarriage, fetal death, stillbirth, neurologic deficits, chorioretinitis, or child disability (51).

The risk of congenital infection and the severity of its symptoms depend on the gestational age at which the woman acquires the infection: the sooner the infection, the lower the risk but the greater

the severity of symptoms (74,79). The placental barrier is more efficient at the beginning of gestation (first trimester), leading to the passage of parasites in less than 10% of cases. However, it becomes more permeable throughout pregnancy, allowing parasite transmission in around 30% of cases in the second trimester and 60 to 70% of cases in the third trimester, and even more close to the time of delivery (79).

Globally 1.5 cases of congenital toxoplasmosis occur per 1000 live births. It has been estimated that between 500-5000 infants each year are born with congenital toxoplasmosis in the US (60).

France is one of the few countries in which guidelines recommend that non-immune pregnant women be tested every month throughout pregnancy to detect seroconversion to toxoplasma infection (79).

1.2.4.5. Ocular toxoplasmosis

Ocular toxoplasmosis is a disease that occurs when *T. gondii* infects the eyes and optic nerves. Retinochoroidal scars are its clinical hallmark and its worldwide prevalence has been estimated to be 2% (80–82).

The immune response of the host plays a similar role as in other tissues. It induces conversion from rapidly dividing tachyzoites to slowly dividing bradyzoites and their posterior encystment. The cyst may remain inactive in the scar or nearby for a long time. However, when the cyst ruptures into the surrounding retina, retinitis may be reactivated (80).

1.3. Toxoplasmosis diagnosis

T. gondii primary infection induces a humoral response with the appearance of different immunoglobulin isotypes with various kinetics. IgM and IgA appear during the first week and their levels reach a peak after approximately one month, before decreasing to undetectable levels after several weeks to years. IgE peaks after 2-3 months and then rapidly decreases. IgG appears two weeks after IgM and reaches a plateau after 2-3 months, and then steadily decreases to a residual lifelong titer (Figure 1-4).

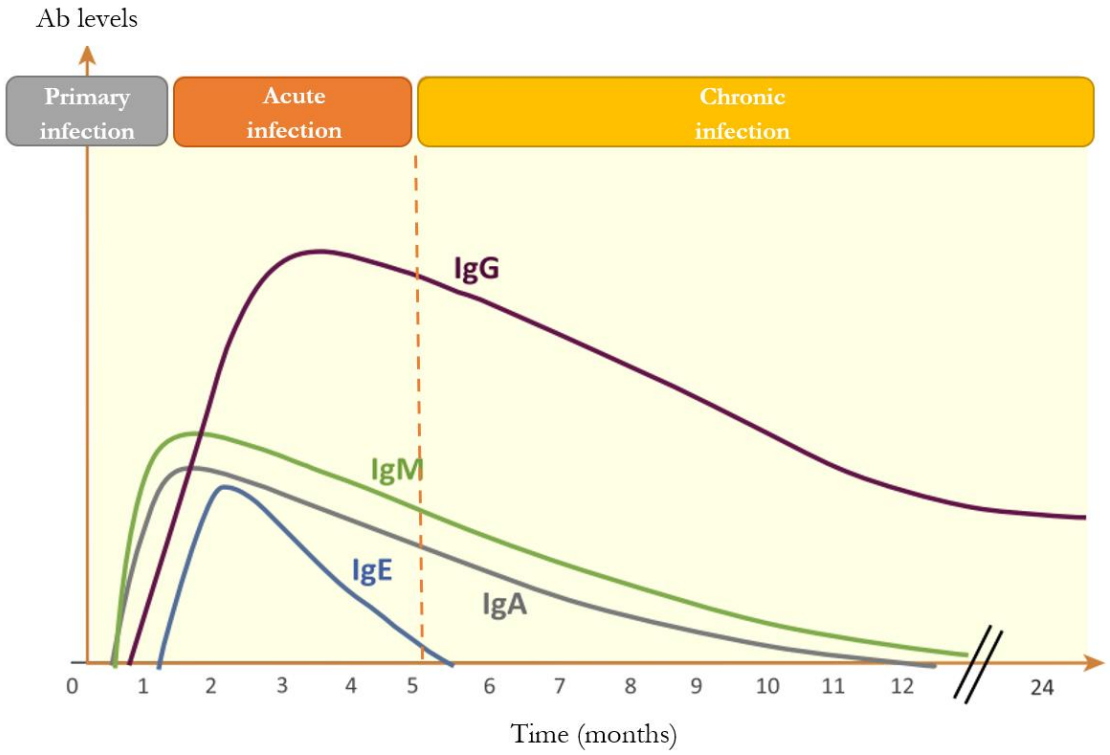

Figure 1-4: Anti-*T. gondii* immunoglobulin kinetics after primary infection. The average kinetics of the different isotypes are represented, but they may differ among patients and according to the serologic technique used. Adapted from (63).

The appearance of IgG after IgM allows the diagnosis of a primary infection with relative certainty. Nevertheless, it is important to remark that immunoglobulin kinetics vary depending on the patient, the antigens, and the technique used for serological detection (63). These antibodies are functionally important as they are known for blocking cell invasion, lysing parasites by activating complement pathways and the catalytic activity of natural killer and $CD8^+$ T cells, or by phagocytosis (83).

The recognition of the importance of toxoplasmosis in human and animal health since *T. gondii* discovery propitiated the development of different diagnostic tests to allow antemortem detection.

Depending on the patients' immune background and clinical signs, various techniques can be performed to achieve a diagnosis, either indirectly, by detecting antibodies, or directly, by identifying parasites or their DNA. The current section is an overview of the different diagnostic methods, their basis, and their routine use in clinical laboratories.

1.3.1. Diagnosis based on microscopic observation and imaging techniques

Detection of tachyzoites or cysts can be done by microscopic observation of tissue imprints, biologic fluids, or tissue biopsies. However, parasite identification based on light microscopy is less sensitive and accurate than other methods (64). Additionally, these approaches are time-consuming and require

considerable skills to obtain reliable results. In recent years, the electron microscope is also employed, but for obvious reasons, it is not easily applicable for routine laboratory use (84).

1.3.1.1.Serologic immunoassays

An immunoassay is a bioanalytical method that use an immunocomplex between antibodies and antigens (85,86). Because of its efficiency and relative simplicity, many serologic assays are available, all with strengths and shortcomings. They must be interpreted with a critical eye as the kinetics of the antibodies generated by the immune system do not always follow the same pattern.

Classically, an immunoassay uses one or more selected antibodies to detect the analytes of interest, either antigens or antibodies. These methods are based on a binding reaction between a specific antibody and an antigen. The basic components required for immunoassay development are the antibodies, the signal-generating labels, and the separation matrices.

Usually, the detection system requires the use of labeled material coupled with one of the immune-analytical components to measure the analyte of interest present in a sample. In most cases, the nature of this label serves as the basis for classifying different types of immunoassays.

The most common immunoassays are enzyme-linked immunosorbent assays (ELISA) based on an enzyme-coupled system, radioimmunoassay (RIA), which uses radioisotopes as a label, fluoroimmunassay (FIA), which employ a fluorophore as a label, and chemiluminescence immunoassay (CLIA) which utilize a chemiluminescent substance as a label.

1.3.1.1.1.Dye test

The first serologic method was developed by Sabin, Feldman (IgG), and Remington (IgM) in 1948 (87,88). Sabin and Feldman recognized that tachyzoites lose their affinity for methylene blue dye in the presence of anti-*T. gondii* antibodies so they used it to design a diagnostic method (89). Dye test is both specific and sensitive. However, it requires live parasites that must be maintained in infected mice, which implies a high cost, is potentially hazardous, and requires a high degree of technical expertise. Due to these requirements, it is implemented only in reference laboratories, such as the Toxoplasma Serology Laboratory at the Palo Alto Medical Foundation (Palo Alto, California, US).

1.3.1.1.2.Latex agglutination

In this test, soluble antigens are coated on latex particles, and agglutination is observed when the positive serum is added. Latex agglutination is rapid and easy to perform and can be used to detect anti-*T. gondii* antibodies. Although it varies between suppliers, it has a sensitivity of 86–94% and specificity around 100%. Therefore, it is often used as a screening tool in epidemiologic surveys due

to its simplicity. The main problem is that a positive result requires further confirmatory tests using other serologic tests (90,91).

1.3.1.1.3.Immunochromatographic test

It is a rapid technique in which a colloidal labeled antigen or antibody is used as a tracer, and a cellulose membrane is used as the solid support (92). The detection antibodies or antigens are dropped on the nitrocellulose membrane, which slowly infiltrates the conjugated pad through capillary action, and antibody-antigen complexes show a colloidal reaction. An immunochromatographic strip using anti-excretory/secretory antigens IgG antibodies was developed to detect *T. gondii* acute infection as early as 2-4 days post-infection, showing high agreement with ELISA (84,93,94).

1.3.1.1.4.Western blotting

In this test, sera are reacted with *T. gondii* antigen on a membrane transferred from a polyacrylamide gel, and the resulting banding patterns are matched with known molecular weight, which makes it possible to quantify specific proteins and compare antigenic profiles. In the toxoplasmosis field, it has been used as a complementary tool to demonstrate the presence of antigenic markers that help distinguish between acute and chronic phases (95–97). It has also been applied for the early diagnosis of congenital toxoplasmosis because the combination of IgA and IgM ELISA, IgG, and IgM western blot shows a sensitivity of 94-97% and specificity of 100% during the first three months of life (64,84,98).

1.3.1.1.5.Enzyme-linked immunosorbent assay (ELISA)

Immunoenzymatic assays are systems that involve the use of antigens, haptens, or antibodies labeled with an enzyme. These methods are now essential in toxoplasmosis serological testing. They were initially commercialized as high throughput, although they were manual methodologies. Automatization in toxoplasmosis serodiagnosis first appeared with such assays, providing good reproducibility and reduced testing delays, allowing systematic testing in immunosuppressed patients or pregnant women (84).

Different types of ELISA can be defined depending on the position of the antigens/antibodies with respect to the solid phase and depending on whether detection is done using a single step or more than one. The system includes the solid phase, a polystyrene 96-well plate, the enzyme-labeled antigen or antibody, and the substrate of the enzyme reaction, which can be modified to test both antibodies and antigens. There are different types of ELISA to detect *T. gondii* antigens and antibodies, such as direct, indirect, competitive, and sandwich (Figure 1-5).

Direct ELISA is the simplest and fastest format. Antigens are attached to the solid phase followed by an enzyme-labeled antibody. In indirect ELISA, the antigen is coated onto the solid phase, then the sample is added. The antigen-antibody reaction is enhanced by the addition of a secondary enzyme-linked antibody, and the reaction can be evaluated by quantification of the resulting color. These tests are almost all used to detect anti-*T. gondii* IgG, IgM, and IgA antibodies (99).

In sandwich ELISA, the capture antibody is immobilized on the solid phase and the enzyme-labeled antibody is used for coloration, which is directly proportional to the amount of antigen present (100). Competitive ELISA can be done to detect both antigens and antibodies. Specific antibodies to the analyte of interest are immobilized on the solid phase. Then, the enzyme-conjugated antigen is incubated with the capture antibody and the same antigen in its unconjugated form. In competitive ELISA, the higher the sample antigen concentration, the weaker the output signal obtained.

ELISA technique is simple, economical, easily adaptable, and automatable so that a large number of samples can be simultaneously tested. It is used to detect IgM, IgG, IgA anti-*T. gondii* antibodies, and circulating antigens. However, it is labor-intensive and time-consuming (84,89).

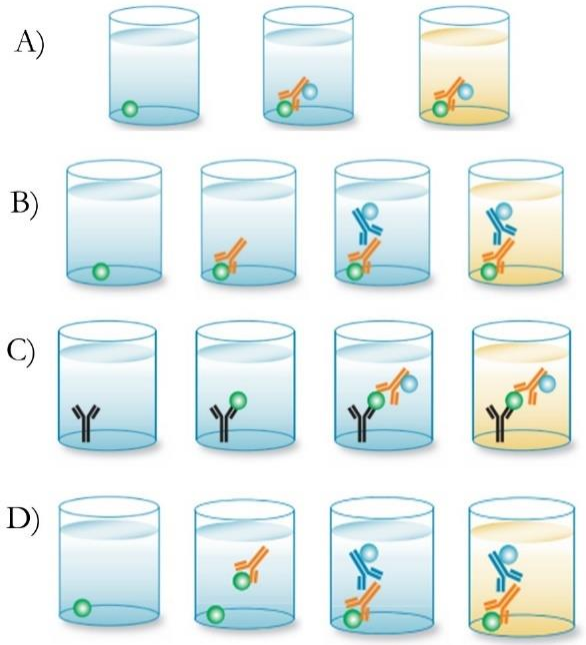

Figure 1-5: Schematic view of ELISA types. First, the capture molecule is immobilized onto the microtiter plate. The number of steps, or the disposition of capture molecule regarding the plate is used to classify the different ELISA. A) Direct: antigen is immobilized in the well and is detected by an antibody conjugated to an enzyme. B) Indirect: antigen is immobilized in the well and the detection can occur in a single or in a two-step process how it is represented. First, an unlabeled antibody binds to the antigen. Second, an enzyme conjugated antibody is added. C) Sandwich: it requires the use of matched antibody pairs (capture and detection antibodies) both specific for a different and non-overlapping antigenic regions. The capture antibody binds to the antigen that can be detected direct or indirectly. D) Competition: the sample antigen or antibody competes with a reference for binding to a limited amount of labeled antibody or antigen, respectively. The higher the sample concentration, the weaker the signal. Adapted from BIO-RAD website.

1.3.1.1.6.Chemiluminescent immunoassays

Traditional colorimetric immunoassays have been used successfully in research and clinical laboratories for more than 50 years. Despite their numerous advantages, some limitations have warranted the development of a new type of immunoassay, the chemiluminescent immunoassay (CLIA). This immunoassay offers an ultrasensitive and versatile tool with a wide range of applications in biotechnology. It has also become one of the most used diagnostic methods in clinical chemistry due to its high sensitivity and easy automation (101,102).

Luminescence is the emission of visible or near-visible (λ = 300-800 nm) radiation (103). It has long been known that organisms such as bacteria, fish, fungi, and insects are luminescent. However, the possible applications of luminescence were not clear until 1877, when green light was observed when lophine (2,4,5-triphenylimidazole) reacted with oxygen. It was not until nearly a century later, in 1976, that the first CLIA was produced (104).

CLIA reagents consist of two basic components; a solid-phase that supports the antigen or the antibody used to identify the molecule of interest, and a tracer, which is the mixture of the conjugate (capture molecule labeled with luminol-derived molecule) and the tracer diluent, in which the conjugate is diluted. Some CLIA also include an assay buffer, which is an aqueous solution in which the antigen-antibody reaction takes place (105).

a. Solid-phase

CLIA can be performed on different solid surfaces. Magnetic beads are widely used for capturing specific molecules thanks to their super-paramagnetic properties (106,107). There are several commercially available magnetic beads. Some are pre-activated or functionalized with different chemical groups, such as tosyl (which is the most frequently used), epoxy, and chloromethyl. These groups allow the ligand—either an antigen or an antibody—to be covalently bound.

Tosyl groups bind both amino and sulfhydryl groups depending on the pH used during the coating. Neutral pH is used for sulfhydryl, whereas basic is used for amino groups (Figure 1-6). These beads have great advantages (i.e., no pre-activation step—which helps to achieve a reproducible product, low non-specific binding, and stable covalent coupling). They have also some drawbacks, such as the lack of ligand orientation and conformation control, which is still a big challenge (106,108).

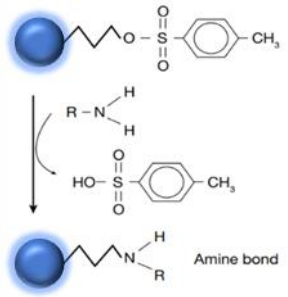

Figure 1-6: Reaction between Dynabeads® tosyl-activated magnetic beads and the amino group. Adapted from Byun et al.,(108).

Bio-activated magnetic beads aid to overcome some of the drawbacks of tosyl beads. They contain a surface biolink, such as streptavidin, biotin or protein A/G. These beads are expensive but highly effective if the ligand has to be non-covalently bound or in cases where the coupling requires extreme conditions. Streptavidin-activated beads use streptavidin, a small bacteria-derived protein that has an extraordinarily high affinity for biotin. The binding strength between them can withstand high temperatures, a wide range of pH values, variations in buffer salts and the presence of detergents (109). Nevertheless, their use might result in non-specific binding due to the presence of endogenous biotin, a phenomenon that is increasingly frequent (110).

b. Assay buffer

Assay buffer although is not essential, if present is designed to generate the perfect conditions for the reaction to achieve optimum assay performance, boost the antigen-antibody reaction and reduce non-specific interactions that could increase background (111).

c. Tracer: the mix of conjugate and tracer diluent

Several molecules are capable of being chemically excited and generating light when they return to a baseline state. Popular substrates employed in CLIA are luminol derivatives and, in recent years, acridinium esters (AE) or sulphonamides.

Tracer is composed of two components; i) the conjugate, which is a chemiluminescent-labeled active molecule that reports directly or indirectly the analyte presence, and ii) the tracer diluent, which is the solution in which the tracer is diluted. The tracer diluent has to promote adequate sensitivity, conjugate stability and low background. In assays where the assay diluent is not present, the conjugate diluent is normally the major component where the antigen-antibody reaction takes place, and therefore it must be formulated to guarantee optimal assay performance.

CLIAs have different label systems according to the mechanism of light emission (chemical, enzymatic or based on redox reactions). Luminol and its derivatives and acridinium ester and its derivatives are the most common. Exposure of such labels to an alkaline hydrogen peroxide solution triggers a flash of light that is measured in RLU (Relative Luminescent Unit) by the luminometer.

The mechanism of N-(4-aminobutyl)-N-ethylisoluminol (ABEI) light emission is shown in Figure 1-7.

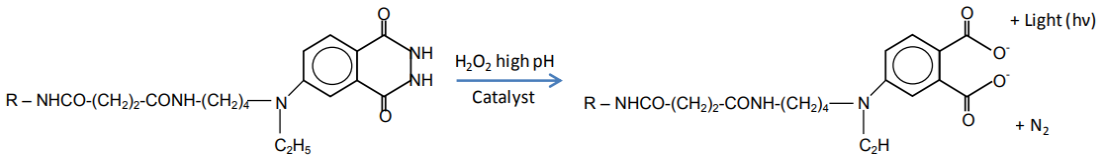

Figure 1-7: Chemical reaction of ABEI to generate light emission. Using an amide linkage, the analyte (either an antigen or an antibody molecule, R in the figure) is attached to the ABEI molecule separated by a spacer, therefore reducing the quenching effect of the protein. In the presence of H_2O_2, and high pH, light is emitted. From (105).

In overall, the combination of the unique mechanical characteristics of surface-functionalized paramagnetic microparticles coated with specific antigen or antibody and the specificity and sensitivity detection properties of a luminescent-labeled molecule that emits light when it is activated by specific triggers makes CLIA the technique of choice for immunodiagnosis.

d. Standard materials

Standard materials (calibrators and controls) are used to guarantee assay functionality. Although they are not essential for the reaction to take place, they are as important as any other component. In qualitative assays calibrators set up the threshold discriminating negative from positive samples. This threshold is known as the cut-off. In quantitative assays calibrators allow to generate calibration curves with which the analyte concentration can be extrapolated. They are constituted by a mix of the analyte of interest, diluted in a solution that maintains its integrity.

Controls are used to verify within each run that the reagent is functional. Although they can vary in number the most common controls are the negative control (NC) which mimics a negative sample, and the positive control (PC) which mimics a positive sample.

Same as ELISA, different types of CLIA can be defined considering the position of the antigens or the antibodies used as capture molecules with respect to the solid surface, and depending on whether detection is done using a single step or more than one. Direct CLIA detects antigens attached to the solid phase using labeled antibodies. In indirect CLIA, the sample is incubated with the solid phase which is coated with the antigen. This reaction is enhanced by the addition of a secondary labeled antibody, and the light emitted by the reaction can be detected and quantified. In immunocapture, the antibody is immobilized on the solid phase and the labeled antibody is used for detection, which is proportional to the amount of antigen present in the sample. Same competitive CLIA can be done to detect both antigens and antibodies. Specific antibodies to the analyte of interest are immobilized on the solid phase. Then, the conjugated antigen is incubated with the capture antibody and the same non-labeled antigen. In such assays the higher the sample antigen concentration, the weaker the output signal obtained.

The advantages of CLIA are numerous: it has an extremely elevated analytical sensitivity, absence of interfering emissions (i.e. high specificity), and a greater range of linearity than other methods. Additionally, its use is associated with automated analytical platforms that confer several advantages in routine clinical diagnosis, such as reduced incubation times, rapid acquisition of the analytical signal (30-40 min), high reagent stability, low consumption of materials, full compatibility with different assay protocols, standardization of the most critical analytical stages, and automatic processing of the result (which reduces human error). Some disadvantages are the limited availability of test panels and the high cost of the analytical platforms.

In summary, CLIA has contributed to the development of relatively uncomplicated automatic instrumentation that has progressively become routine in clinical laboratories. Today, it is used to detect and quantify hormones, drugs, vitamins, tumor markers, myocardial damage markers, and of course, infectious disease (103).

Several companies are developing antigens and antibodies that are the base of immunoassays, and top-class platforms. Biokit has developed an analytical platform based on CLIA technology, named BIO-FLASH®, which is a fully automated, simple-to-use benchtop autoanalyzer. The reagents developed use ABEI as the chemiluminescent label to detect analyte presence and concentration (105). The BIO-FLASH® has been used in this project to develop a proof-of-concept CLIA for the detection of IgM anti-*T. gondii*.

For the detection of specific anti-*T. gondii* IgG and IgM, Biokit has developed two reagents: the BIO-FLASH® Toxo IgG and the Toxo IgM. Both use paramagnetic microparticles coated with *T. gondii* lysate antigen, which are mixed and incubated with the sample. If the antibody (either IgG or IgM) is present, it binds to the antigens coated on the microparticles. Magnetic separation followed by a wash step removes non-specific interactions. Then, a tracer consisting of anti-human IgG or IgM isoluminol-labeled monoclonal antibody is added. The conjugate binds to the antibody captured on the surface of the microparticles. After a second incubation, magnetic separation, and a wash step, reagents that trigger a chemiluminescent reaction are added. The emitted light, which is measured by the BIO-FLASH® luminometer, is proportional to the concentration of anti-*T. gondii* antibodies (Figure 1-8).

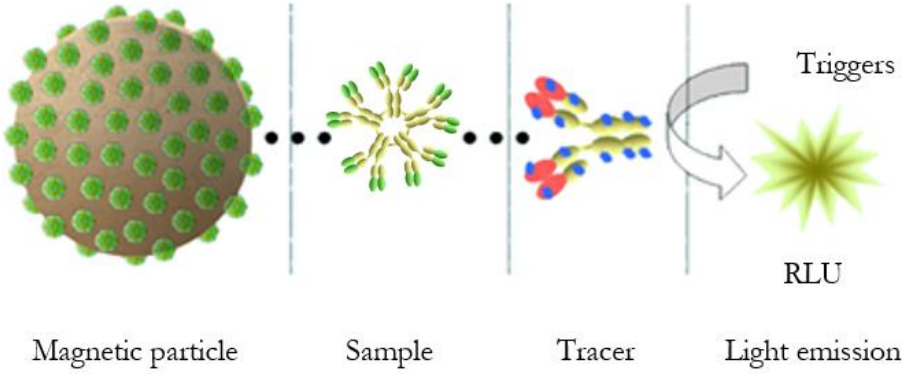

Figure 1-8: BIO-FLASH® Toxo IgM reaction scheme. Magnetic particles coated with toxoplasma antigen are incubated with the sample. Then, the tracer is added and may bind to the anti-toxoplasma IgM captured by the microparticles. Finally, the triggers are added. The emitted light is measured as relative light units (RLU).

1.3.2. The problems with serological detection

T. gondii infection consists of two phases: acute and chronic. Monitoring the humoral response nearly allows differential diagnosis. However, the production of specific anti-*T. gondii* antibodies does not always correlate exactly with the course of infection, especially in the high-risk population. In those cases, determining the serological status of the patient is only the tip of the iceberg. IgM and IgG interpretation may encounter different pitfalls.

1.3.2.1. Detection of low-IgG levels

Detection of IgG without IgM defines the serological pattern of past infection. However, for immunocompromised patients, who normally present low IgG levels, it is important to have a very sensitive serological test to avoid false negatives (112). The same happens during pregnancy, in which a chronic infection is not considered a risk for giving birth to a neonate with congenital infection. In these cases, the evaluation of results near or within the "gray zone" established by the manufacturers should be clearly stated using other techniques as dye test or western blot (51,113).

1.3.2.2. The limitation of IgM detection for dating the infection

The detection of IgM is commonly associated with acute or reactivated infection. While there are many scenarios in which this practice is clinically useful, there are multiple infections for which IgM testing should be avoided or interpreted with care. The identification of IgM is prone to false-positives as a result of the high cross-reactivity of IgM to other, closely related microorganisms or other interfering substances. Additionally, when considering IgM, the diagnostic window acquires special relevance. If the test is done before antibody development, results will be negative, when in fact the disease is present. However, if it is done later, it can lead to misdiagnoses because IgM may remain detectable for long periods (114).

Toxoplasmosis is a clear example of the difficulty associated with the interpretation of IgM levels, as they are not always a definitive marker of acute infection. In recent years, immunoassays have gained in specificity, but also sensitivity, which causes that IgM can be detected for months or years after infection. Several studies have evaluated the usefulness of IgM for dating the infection, demonstrating that some methods can detect it years after infection (115). Therefore, IgM is not a definitive marker of recent infection in some situations, unless it is found at high titers (51).

Primary infection during pregnancy entails the risk of a transplacental passage of *T. gondii* to the fetus. When the primary infection is diagnosed during pregnancy, monthly serological IgG and IgM screening until delivery is the initial approach (66,83,116). The results derived from this testing cannot always be evaluated in the same way. Immunological markers can vary depending on the trimester of infection, and maternal treatment during pregnancy can block or retard the immune response.

The lack of information that IgM titers give in some situations can be compensated by the IgG avidity test. This technique is based on the binding affinity of IgG for its antigen. IgG avidity is initially low after primary antigenic contact and, through antigen-driven B cell selection, it increases during the subsequent weeks. Thus, it can help to distinguish *T. gondii* acute and chronic infection (93).

The avidity test was initially carried out through in-house methods, but soon they began to be commercialized. In the US, the first FDA-approved test (VIDAS® Toxo IgG avidity assay; BioMérieux) was approved in 2011 (117,118). Despite its benefits, there are some limitations. For example, *T. gondii*-specific low-avidity IgG antibodies may persist for months, avidity maturation may be slow, and a high antibody concentration may affect the results. These drawbacks mean that antibody avidity detection methods need to be improved (96,99,119). Regarding its limitations, it is laborious, and its performance is similar to that of the reference method while being twice as cost-effective (120–122).

Overall, the reliance on a single serum test (i.e. an IgM-specific assay) to determine acute infection complicates the diagnosis of toxoplasmosis, because positive results are not always conclusive but can have dramatic consequences in the management of patients, especially pregnant women.

1.3.2.3. Variability among IVD immunoassays

Variability among different IgM-specific immunoassays prompted the FDA to reexamine their performance in 1997 (123). The clinical specificity of these kits varied between 77% and 99% compared to the reference IgM ELISA test performed by Palo Alto Medical Foundation (124). For this reason, the FDA currently requires additional evaluation of IgM-positive results by a reference laboratory (114,125–127). Although desirable, this practice is not mandatory in Europe. Therefore,

in many cases, toxoplasmosis diagnosis involves several repeated tests that have to be evaluated by numerous specialists.

1.3.3. *T. gondii* antigens for serodiagnosis

Immunological tests, especially ELISA and CLIA, are the preferred methods in clinical laboratories. Several are based on the recognition of *T. gondii* antigens by host anti-*T. gondii*-specific immunoglobulins. Researchers have worked toward simplifying methods and reducing production costs of these antigens. Today, both the widely used natural antigens and high-quality antigens based on recombinant proteins or peptides are available.

1.3.3.1. Toxoplasma lysate antigens

Currently, tests based on the whole intact tachyzoite are limited to a few assays performed in only a few laboratories. However, serologic methods based on toxoplasma lysate antigen (TLA) from tachyzoites grown in mice and/or tissue culture are still used routinely in the clinical setting (128). The high cost of maintaining the parasite and the scarcity of high-quality products obtained by other methods have forced manufacturers to invest in developing tests in which the live parasite is not necessary at all, which means large cost savings for the suppliers.

TLA-based products have prominent limitations: inability to estimate accurately the time of infection due to their use of a mixture of antigens, low sensitivity, and specificity—especially when detecting IgM—and difficult standardization (with huge lot-to-lot variability) (84,129,130).

1.3.3.2. Recombinant proteins

A recently developed approach to improve *T. gondii* diagnosis and also to discriminate between different phases of infection is to use recombinant antigens instead of TLA. Recombinant antigens, either proteins or peptides, avoid the associated cost of maintaining infected animals to obtain antigens directly from the parasite (131).

The use of recombinant products offers great advantages, as it allows the selection of a single antigen (84). In the past 20 years, numerous recombinant proteins, including granule antigens GRA1, GRA2, GRA4, GRA5, GRA6, GRA7 and GRA8, rhoptry proteins ROP1, ROP2, matrix protein MAG1, microneme proteins MIC2, MIC3, MIC4, and MIC5, and surface antigens SAG1, SAG2, SAG3, have been expressed in *E. coli* or *P. pastoris*, and their potential diagnostic value has been evaluated by ELISA to detect IgG and IgM (131–135).

Additionally, combinations of recombinant antigens are more sensitive and specific than the use of a single antigen (136). For example, combinations of SAG2, GRA2, GRA4, ROP2, GRA8, and GRA7 are potentially useful to detect IgG in humans with recently acquired infection (137,138), whereas

ROP1, SAG1, GRA7, GRA8, and GRA6 are promising for detecting specific IgM antibodies (128,139), and GRA7 and GRA8 are used to detect specific IgA antibodies (131,140).

The recomLine Toxoplasma (Mikrogen Diagnostik, GmbH, Germany) allows IgG and IgM detection by using ROP1, MIC3, GRA7, and GRA8 antigens and simultaneously differentiates antibody avidity using P30, MAG1, GRA1, and SAG1 (140). Although its performance for IgG is 100%, for IgM it is only 90%. Additionally, it is an assay whose results are subject to individual interpretations.

In the automated CLIA, two stand-out products based on recombinant antigens are the Elecsys Toxoplasma IgG (Roche Diagnostics, Mannheim, Germany), based on P30, and the ARCHITECT Toxo IgG (Abbott, GmbH, German) based on a mixture of P30 and GRA8.

Although several studies have been done on recombinant antigens, and various assays for the detection of both IgG and IgM can be found in the market, they have not successfully replaced TLA for several reasons. Despite its innumerable advantages, the use of recombinant proteins has limitations, including variations in sensitivity and specificity and contamination with foreign proteins. The use of synthetic peptides as antigens is an alternative approach that addresses these limitations.

1.4. Focus on innovation. New technologies to develop IgM-specific immunoassays

Technological improvements over the last years have revolutionized the health sector. Even though the field of immunoassays is mature, IVD companies are continuously developing new assays and platforms to offer higher quality products. The general trend is toward making multiplexing possible, miniaturizing point-of-care devices, and identifying and developing assays based on novel biomarkers, thus further expanding the potential of immunoassays in the future (141).

1.4.1. New technologies to identify IgM-specific epitopes

Testing for IgM is being performed routinely to achieve the diagnosis of acute infection, not only in the case of toxoplasmosis. However, the good performance of current immunoassays for IgM detection is not enough. False positive and false negative results are still a reality that clinicians have to contend with.

In the context of toxoplasmosis, the first improvement needed is related to the antigens used: new biomarkers that are characteristic of the acute and the chronic phase are an overriding need. To respond to this demand, innovative technologies that allow epitope identification become essential for obtaining good biomaterials and getting high-quality reagents (142).

1.4.1.1.Epitope mapping

The term "epitope mapping" can be defined as the experimental process of locating the epitope of a specific antibody on the antigen surface or in the antigen sequence (143). Next, some of the most cutting-edge technologies that allow identifying new epitopes will be summarized:

1.4.1.1.1.In-silico epitope prediction

The ability to computationally predict antibody epitopes to replace a whole protein, using only a small fragment that possesses the same antigenic properties is today a reality. In-silico prediction tools are built on relatively simple amino acid propensity scales based on characterized protein-protein interfaces to identify antigen regions that are likely to contain epitopes. Today, most efforts take advantage of existing antibody-antigen complexes in the PDB database (144,145). In the case of *T. gondii*, several proteins are considered to have a decisive antigenic role (53,146–150). Nevertheless, at the time of writing, only one of them has a PDB entry (151): the Major Surface Antigen, also known as P30 or SAG1. The fact that other proteins relevant to *T. gondii* are not included in the PDB database makes it more difficult to identify new epitopes using in-silico studies.

1.4.1.1.2.Mutagenesis

Site-directed mutagenesis is a simple and powerful approach toward epitope mapping. Loss of binding indicates that the modified residue could be associated with the epitope. However, it can be laborious since many mutants need to be produced and evaluated. Alanine scanning introduces an alanine, which has a simple methyl group as a side chain, for every residue in a given sequence. The resulting mutants can be analyzed for antigen binding (145). Such analyses have shown that between three and five residues of a structural binding interface can constitute a minimal binding epitope (20).

1.4.1.1.3.Peptide library screening by phage display

During the last two decades, phage display has contributed to the identification of a large number of small peptides or structured nucleic acids with diagnostic and/or therapeutic applications (152). These techniques are based on the use of filamentous bacteriophages (viruses that infect bacteria) to express and display foreign protein fragments or peptides on their surface (100).

T. gondii parasites have served as excellent models in studies involving phage display technology. To identify new epitopes, a phage-display library of *T. gondii* cDNA fragments was screened with sera of infected individuals. As a result, recombinant phage clones were identified carrying various epitopes present in SAG1, GRA1, GRA7, GRA8, and MIC5 (153). Using a similar approach, a panel of sera of pregnant women infected with *T. gondii* was screened and an antigenic peptide was identified within the sequence of GRA1 (154). In another study, phage display made it possible to identify an antigenic segment of GRA3 (155). Overall, these studies demonstrate the potential of this technology for antigen discovery (156).

1.4.1.1.4.Peptide microarray

Peptides can be arranged in microarrays, thus allowing simultaneous analysis of up to several thousand with a single serum sample. Peptide arrays were developed by Ronald Frank in 1984 (157) based on the Nobel-prize-winning solid-phase peptide synthesis invented by Bruce Merrifield. In the current version of the microarray technique, amino acid derivatives are incorporated into solid electrically chargeable "amino acid particles." These amino acid particles are placed on very small areas of a solid support, by a laser printer and helped by the electrical fields of computer pixel electrodes. Next, a coupling (peptide bond-forming) reaction is induced by melting the whole particle layer, which allows amino acid derivatives to react with amino groups on the surface of the support (Figure 1-9).

With this technique, global patterns of antibody responses to various infectious agents, such as *T. gondii*, have been studied (158,159). In some circumstances, a bioinformatic approach can be used for in-silico prediction of different B cell linear epitopes of interest. Then, the peptides need to be printed into a peptide microarray and validated by analyzing a large number of well-characterized human sera samples (142).

In this project, we used a peptide microarray to screen the nine most antigenic proteins of *T. gondii*, using sera samples of patients infected with *T. gondii* in different phases of the disease. For that purpose, we established a collaboration with the company PEPperPRINT GmbH (Heidelberg, Germany). PEPperPRINT develops custom peptide microarrays for several biomedical applications. These microarrays combine the synthesis of solid-phase Fmoc chemistry with a customized 24-color laser printer.

The results obtained were the starting point for identifying different peptides that were later synthesized and evaluated as antigens using several approaches. We designed those peptides to replace TLA in diagnostic assays, particularly for the detection of IgM anti-*T. gondii*.

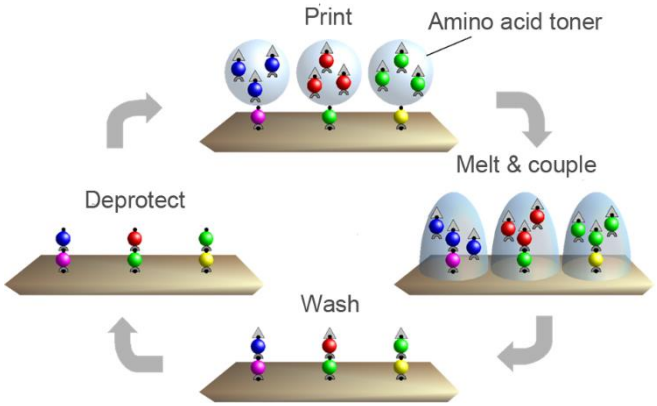

Figure 1-9: Combinatorial synthesis of a peptide array with a laser printer. The classic steps of SPPS are preserved.

1.4.1.1.5. Multiplex immunoassay

Classically, immunoassays measure the level of a single protein or antigen in a homogenous liquid sample and are, by definition, "singleplex." Although these methods are robust, they are not the best format when several target proteins need to be evaluated.

Over the past 20 years, the development of high-throughput technologies for genomic and proteomic analysis has brought in a novel era of biomarker discovery. Applied to immunoassay, this technology confers the attractive prospect of simultaneous measurement of multiple analytes in a single patient sample, thereby minimizing assay costs, time, and sample volume (Figure 1-10) (160).

In the early phases of this thesis, the need to quickly evaluate new peptides that we had identified using peptide microarrays led us to consider applying multiplexing technology to enhance the output that classic ELISA could offer. Therefore, we conducted the preliminary evaluation of the selected peptides in collaboration with InfYnity Biomarkers (Lyon, France), a company specialized in the identification of new biomarkers of clinical interest and developing innovative assays. Together, we developed a multiplex ELISA to evaluate the peptides that we had previously selected using a panel of anti-*T. gondii* IgM-positive and negative samples.

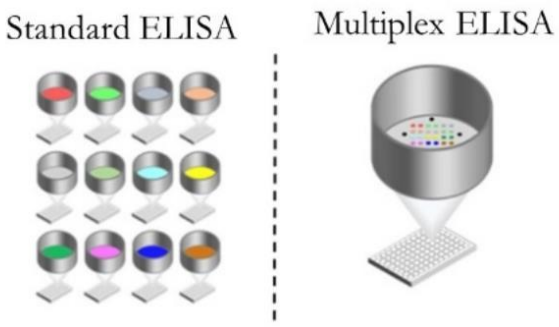

Figure 1-10: Schematic view of multiplex immunoassay in ELISA format. In standard ELISA each antigen is tested individually one by one. In multiplex ELISA, all antigens can be simultaneously scanned under the same experimental conditions. From http://www.infynity-biomarkers.com/.

1.4.2. Synthetic peptides as diagnostic tools

In the previous section, we summarized some of the current technologies that could be used to identify specific immunoglobulin epitopes. In this section, we focus on the need to develop new procedures to obtain reliable biomaterials.

Since the invention of solid-phase peptide synthesis (SPPS) by Merrifield in 1963 (161), the number of research groups focusing on peptide synthesis has grown exponentially. In 1968, the first automated solid-phase synthesizer was described. Today, new techniques for the synthesis of synthetic peptides have been developed in which both chemical ligation and microwave-assisted SPPS are successful for synthesizing long peptide sequences.

For SPPS, the first amino acid is coupled by its C-terminal residue to a resin (solid support) based on polymer material. The subsequent amino acids are coupled to the α-amino group of the nascent peptide through an amide (peptide) bond. To this end, the carboxyl group of the incoming amino acid must be activated to increase its electrophilicity vs. the resin-bound amino group (162,163). Once a new amino acid is attached to the resin, wash and filtration steps are performed to eliminate excess reagents, then the α-amino protecting group is removed, and the cycle is repeated until the desired peptide chain is obtained. During the chain assembly steps, any reactive functional groups (i.e., carboxyl, amino, hydroxy, etc.) on the side chains of trifunctional residues need to be maintained blocked (protected) with semi-permanent groups. Finally, the peptide-resin is treated (usually by acidolysis) to remove the side chain protections and cleave the peptide off the resin (Figure 1-11), after which it is purified by reverse-phase HPLC and lyophilized (164,165).

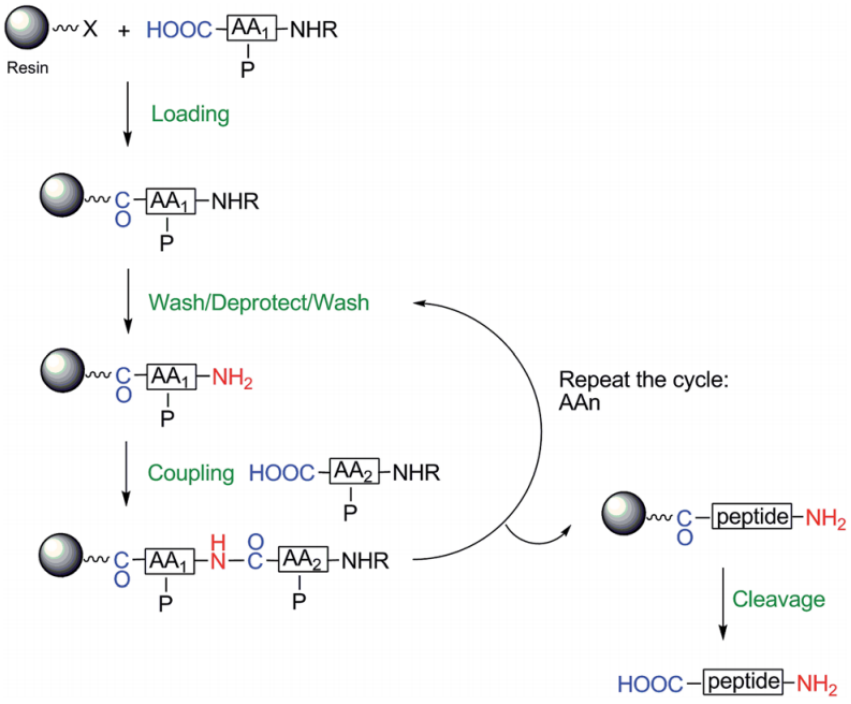

Figure 1-11: Schematic representation of peptide production by SPPS. From (162).

Synthetic peptides with antigenic properties are useful for developing new diagnostic methods. They minimize the non-specific reactions that sometimes arise in traditional immunoassays and help address the reproducibility problems that natural and recombinant antigen-based assays have. Another advantage of synthetic peptides is the possibility of modifying their chemical structure by the covalent attachment of a variety of chemical moieties such as biotin, cysteine residue, fatty acids, and carrier proteins, and also multimerizing the epitope sequence to enhance antigenic properties (166,167).

Nevertheless, the use of relatively short linear peptides is not without certain problems. Immobilization of peptides on the solid support (such as polystyrene plates) by passive adsorption poses difficulties, and peptide-surface interactions often alter the correct exposure of the epitopes in a manner that is difficult to predict. To overcome the low coating efficiency of highly hydrophilic peptides to solid surfaces and to avoid unpredictable orientations, the covalent attachment of the synthetic peptides is commonly used (168). The most frequent methods involve either the pre-activation of the biomolecules or the solid phase. Biotinylation—the process of attaching biotin to a protein or a peptide—is also a good strategy for peptide orientation, as the peptide can be immobilized onto the solid support which has been coated or coupled to avidin or streptavidin, enabling the binding of the peptide to be measured. Such immunoassays use a conjugate-labeled molecule or enzyme-labeled avidin or streptavidin.

1.4.2.1. Multimeric and chimeric peptides

In recent years, several studies reported an improvement in sensitivity and specificity when multimeric peptides that contain more than one epitope were used (169,170). Moreover, it has been demonstrated that chimeric peptides that combine different epitopes from various proteins within the same sequence amplify significantly the antigenicity of these biomolecules (166).

An interesting approach to increasing peptide antigenicity is the covalent attachment of epitopes to synthetic linear or branched polymeric scaffolds. Generations of branched poly-α-amino acid chains with a poly(L-lysine) backbone have been introduced for the rational design of polymeric homogeneous or heterogeneous polypeptides for the construction of synthetic antigens (171). The synthesis of such constructions can be performed using either SPPS or ligation (56,166).

1.4.2.2. Synthetic peptides for toxoplasmosis diagnosis

A growing number of studies have demonstrated the potential advantages of using synthetic peptides that mimic specific epitopes for the diagnosis of toxoplasmosis (172–174). Synthetic peptides have not only changed drastically the production procedures but also present higher sensitivity. As mentioned, they can include various immunoreactive specific-stage epitopes from different antigens, which increases the probability of discriminating different toxoplasmosis stages (138,175–179).

Several authors have studied the diagnostic utility of synthetic peptides in comparison with toxoplasma lysate or recombinant antigens, with promising results (128,149,180–183). Ferra et al. evaluated the diagnostic utility of five chimeric antigens vs. simple mixtures in solution. Synthetic peptides derived from SAG2, GRA3, GRA6, GRA7 have also been used to distinguish different *T. gondii* infecting strains using ELISA (172).

In this thesis, different synthetic peptides were designed and used as diagnostic tools to develop an immunoassay capable of detecting specifically the IgMs present in *T. gondii* positive samples. Based on the new approaches that have arisen to increase peptide antigenicity, we tested different peptide constructions (multiepitope and chimeric peptides) and evaluated their performance as antigens.

1.4.3. Alternative sources to obtain immunoglobulins to be used as calibrators and controls in immunoassays

In previous sections, we have reviewed some of the novel approaches used to identify IgM-specific sequences, and the technologies available to translate those sequences into antigens that can be used as capture molecules in diagnostic kits. However, little has been said about the importance of standards materials, which are essential to produce high quality assays.

In laboratory testing, when referring to standards, it concerns calibrators and controls. In quantitative assays, calibrators allow to quantify the analyte concentration by the generation of calibration curves. In qualitative assays, they set up the cut-off values used to discriminate positive from negative samples. Controls are routinely used to confirm assay integrity and adequate performance characteristics (184,185). Both materials are as essential as any other assay component to deliver reliable results which can help clinicians with disease management.

A *'good'* diagnostic test need to be accurate, which means to provide consistent and meaningful results (186,187). An intrinsic part of test accuracy relies on the use of well-characterized standards materials. Therefore, aware of this reality, IVD industry is constantly improving the manufacturing procedures of the biomaterials used as standards in commercial kits.

Most of manufacturers use sera pooled from individuals with confirmed cases of specific diseases to produce reference materials. However, such materials have significant disadvantages, including difficulty in sourcing large volumes with high titer and specificity, especially in rare or exotic diseases. This is even harder if IgMs are required, as high titers occur early in disease progression, often before diagnosis. Also, they present high lot-to-lot variability, which means that each finite lot requires standardization due to different antibody titers. Furthermore, ethical problems arise from human blood collection, and safety concerns exist when dealing with potentially infectious sera. Finally, other limitations regarding characterization and cost are inherent to the use of human sera (185).

The development of an alternative method for manufacturing non-serum-derived calibrators and controls that avoids the use of human samples represents a significant advance. Such a product must fulfill two essential criteria: it must specifically bind to a particular antigen, and it must contain epitopes recognized by the conjugated anti-human antibody used to generate the assay endpoint.

1.4.3.1. Humanized monoclonal antibodies

Georges Kohler and Cesar Milstein invented in 1975 the hybridoma technology, for which they received the Nobel Prize in 1984 in physiology and medicine (188). Hybridomas are formed via fusion between a short-lived antibody-producing B cell and an immortal myeloma cell. Each hybridoma constitutively expresses a large amount of one specific monoclonal antibody (mAb) (189–191).

Hybridoma obtention takes advantage of a host animal's natural ability to generate functional, highly specific and high-affinity mAb. In brief, it is a five-step process, first an immunogenic antigen must be developed and optimized (192). Next, a host animal is immunized with the antigen to elicit an immune response and initiate the process of B cell maturation (193,194). Third, to generate hybridomas from the spleen of the host animal and fuse with myeloma cells (185). Next, the generated hybridomas are subject to multiple rounds of screening and selection in order to identify the ones producing the best mAbs for the intended downstream application. The final step is the amplification of these specific hybridomas and the subsequent mAb purification (193).

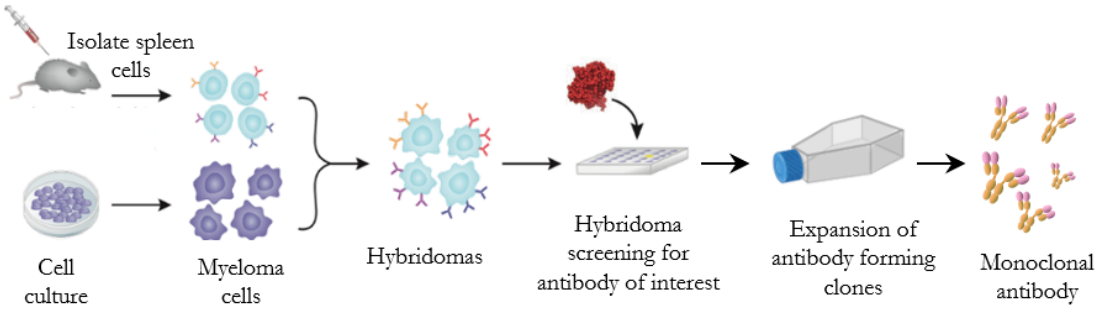

Figure 1-12: Generation of mAb by immunizing laboratory animals with any target antigen. After immunization, hybridoma cells are generated by the fusion between B cells and the myeloma cells. Hybrid cells are selected and finally, cells secreting desired antibodies are expanded. Adapted from (190).

To date, several mAbs have been developed on a large scale using this technology, and are used with several in vivo applications for diagnosis, prevention, and treatment of different diseases (195).

When considering immunodiagnostic applications, animal antibodies do not react '*per se*' in the assay format required for the measurement of specific human immunoglobulins, and therefore are not useful as standard materials (196). With the discovery of recombinant DNA technology and the most recently developed tools for antibody engineering, it has become possible to generate chimeric antibodies by the combination of the heavy and light chain variable regions of a desired mouse monoclonal antibody with the human constant regions (197). Furthermore, to avoid the multistep process of humanization, the concept of transgenic mice harbouring the human antibody repertoire has gain attention. Those, chimeric antibodies can be reproducibly generated in virtually unlimited quantities and are homogeneous in specificity and affinity in front of a certain antigen (196).

1.4.3.2. Standard materials for *T. gondii* serodiagnosis

The prevalence of toxoplasmosis infections in healthy people is quite low, so the obtention of blood bank samples with a sufficiently negative IgM titer to fulfill the demand for assay development is feasible. However, to find sufficient positive sera to develop biomaterials, calibrators and controls and meet current industry demands is a complex task. At the time of writing, no suitable artificial material was commercially available, and thus, this material is still being sought from specialized suppliers. In view of this, the intrinsic properties of chimeric monoclonal antibodies made more attractive their use to produce standard materials (198).

Therefore, a clear purpose of this project was to develop such biomaterials to address the drawbacks of current production methods. Monoclonal chimeric IgM has been produced, in collaboration with ArkAb, to be used as calibrators and controls for the development of an IgM-specific immunoassay for toxoplasmosis diagnosis.

ArkAb develops and manufactures human chimeric antibodies to replace human plasma currently used as calibrators and positive controls. It holds a patent for a transgenic mouse, InEps™, which produces human chimeric IgM and IgE by an in vitro induced class switching (198). Due to the fact that the murine model used in this project for the development of the specific hybridomas is protected by intellectual property rights, we can only provide general information. To generate the transgenic mouse, a cassette carrying the human gene of the immunoglobulin heavy chain constant region was inserted into the endogenous locus of the mouse. This insertion leads to the expression of human chimeric antibodies directly by the mouse lymphocytes (100,199).

1.5. Final remarks

In overall, although the innovation model and the technologies applied in this thesis can be used in different fields and with a huge variety of purposes, we focused on toxoplasmosis, due to its uniqueness. The need to improve current diagnostic kits, particularly the ones aimed to detect IgM, is conspicuous. First, there is a need for innovative antigens capable to differentiate the two disease phases more reliably, besides being produced without using animals. Second, the current methods for producing standard materials are not optimal. The difficulty of finding sera with high IgM concentration is evident. Therefore, there is a need to replace human-derived materials for toxoplasmosis diagnosis.

CHAPTER 2 – Objectives

The main goal of this thesis consists of **exploring the potential of synthetic peptides as diagnostic tools**. Due to its singularity, we focused on **the serologic detection of IgM anti-*T. gondii*** as a model to develop a proof of concept of a novel peptide-based immunoassay.

Aware of the challenges to successfully leading new immunoassays into the market, we concentrated our efforts on the following sub-objectives:

1. **Identifying new IgM-specific sequences** within several highly immunogenic proteins of *T. gondii*.
2. **Designing and synthesizing novel peptides** reproducing the sequences previously identified.
3. **Exploring the usefulness of the synthetic peptides as antigens** for the detection of IgM-positive samples. Assessing if peptide chimeras enhance IgM-specificity.
4. **Developing and optimizing the proof of concept of a chemiluminescent immunoassay** intended for IgM anti-*T. gondii* detection.
5. **Evaluating the performance of the new immunoassay**, establishing sensitivity and analytical specificity.
6. **Obtaining chimeric monoclonal IgMs** using our synthetic peptide as immunogen and utilize it as an alternative source to produce calibrators and controls.

CHAPTER 3 – Synthetic peptides as antigens: from *T. gondii* peptide microarray to functional individual peptides

The diagnosis of acute toxoplasmosis is based mainly on serological tests that detect anti-*T. gondii* IgM antibodies. The commercial kits available in the market are usually based on *T. gondii* lysate antigens (TLA) from different sources (i.e., infected mice and / or tissue cultures). The use of *T. gondii* lysate antigens presents inherent limitations in terms of performance (the inability to estimate the time of infection due to the use a mixture of antigens), difficult standardization and strong regulation (39,84). In recent years, purified recombinant antigens have become a promising alternative with proved diagnostic utility (137,200–204). However, several problems are associated with their use for the serological diagnosis of *T. gondii* infection such as low inter-assay reproducibility, laborious and expensive production and low immunoreactivity (166,170,205,206). As a result, none of the assays based on recombinant antigens have all the characteristics required to replace the *T. gondii* lysate antigens to detect either IgG or IgM. Additionally, only one commercial kit has been developed so far, thus limiting its use in patient diagnosis (131). In short, further work is needed, because we are still far from meeting the needs for toxoplasmosis diagnosis, and this shortcoming has a direct impact on the clinical management of infected patients.

Discovering new epitopes that could help in the clinical management of toxoplasmosis is one of the foci of this thesis. Identifying which proteins of the *T. gondii* parasite could be used as new potential biomarkers for the diagnosis of the acute phase of the disease is an obvious starting point, thus a first objective of the present work is to study the main antigenic proteins of *T. gondii*.

Given the drawbacks of *T. gondii* lysate antigens and recombinant product-based assays, we opted for a peptide-based approach aimed at identifying epitope sequences with potential application in an immunoassay for anti-*T. gondii* IgM detection. To this end, we first used an epitope mapping technology involving a peptide microarray developed by PEPperPRINT GmbH (Heidelberg, Germany) to find new antigens specific for IgM and with no or little reactivity to other Ig types (i.e. IgG).

In a subsequent step, we used solid phase peptide synthesis (SPPS) to produce scaled-up, high-quality synthetic versions of relevant sequences identified in the PEPperPRINT scan as free (i.e., not microarray-bound) soluble peptides to be incorporated into diagnostic kits, a frequent strategy in various immunoassays (166,170,172–174,205–207).

Finally, we evaluated the antigenic capacity of the peptides using an ELISA. To this end, we collaborated with InfYnity Biomarkers, which is specialized in the identification of new biomarkers of clinical interest by developing high-throughput immunoassays. Initially, we developed a multiplex

ELISA to evaluate the feasibility of synthetic peptides for detecting anti-*T. gondii* IgM. Once we identified the best peptides, we used a singleplex ELISA to validate the results obtained by the multiplex ELISA. Finally, the singleplex ELISA was optimized to improve the performance of the assay to detect anti-*T. gondii* IgM-positive samples.

3.1. *T. gondii* peptide microarray

To identify new *T. gondii* epitopes that could be incorporated as diagnostic tools in an immunoassay for detecting anti-*T. gondii* IgM, we initiated a collaboration with PEPperPRINT GmbH to design a peptide microarray that displayed all peptides covering different antigenic proteins from *T. gondii*. A complete list of the nine proteins selected, identified by means of UniProt (https://www.uniprot.org/) and the Immune Epitope Database (IEDB) (https://www.iedb.org/), is shown in Table 3-1.

#	Source Molecule Name	Protein acronym	Alternative name	UniProt ID	Length (aa)
1	Major Surface Antigen P30 Precursor	SAG1	P30	P13664	336
2	Surface Antigen P22, Putative	SAG2	P22	Q9NBH1	186
3	Dense Granule Protein 2 Precursor	GRA2	-	P13404	185
4	Dense Granule Protein GRA3	GRA3	-	B6KEU8	222
5	Dense Granule Protein 4 Precursor	GRA4	Antigen H11	Q27002	345
6	Granule Antigen Protein GRA6	GRA6	P32	Q27003	230
7	Granule Antigen Protein GRA7	GRA7	P29	O00933	236
8	Microneme Protein 3	MIC3	-	Q9GRG4	359
9	Rhoptry Protein 1, putative	ROP1	P66	B6KA38	446

Table 3-1: List of the nine proteins used to build up the peptide microarray. ID: identification. aa: amino acid. From **https://www.uniprot.org/**.

3.1.1. Microarray characterization

For a preliminary assessment of the selected proteins in the epitope mapping microarray experiment, a panel of 13 human serum samples (henceforth microarray serum panel) obtained from Cerba Laboratory and Biokit biobank was fully characterized for *T. gondii* IgM and IgG immunoreactivity.

Different immunoglobulins, in particular IgG and IgM, exhibit distinct profiles and kinetics during toxoplasmosis, so it was essential to ascertain which antibody types were present in the microarray serum panel. Due to the high prevalence of the disease (57,58), *T. gondii* IgG-positive samples lacking IgM are the more frequent type observed in clinical routine. In contrast, *T. gondii* IgM-positive samples devoid of IgG, characteristic of initial phases of the disease, are difficult to obtain. This is

mainly because early diagnosis of toxoplasmosis is unusual, since immunocompetent patients remain asymptomatic in most cases, or the clinical picture is complex and can be confused with a variety of other diseases. Therefore, the most usual scenarios are that either both anti-*T. gondii* IgG and IgM are normally found together, or IgG alone is detected (58,208).

For our microarray evaluation it was essential that samples containing only IgM were adequately represented. To this end, three samples (MA10, MA11 and MA12) were IgG-depleted to remove anti-*T. gondii* IgG; thus, depleted and non-depleted samples were included in the microarray panel.

Characterization of the microarray panel was done by means of the commercial BIO-FLASH® Toxo IgG and the BIO-FLASH® Toxo IgM immunoassays. Results are shown in Table 3-2.

Sample ID	BIO-FLASH® Toxo IgG (IU/mL)	Interpretation	BIO-FLASH® Toxo IgM (S/CO)	Interpretation
MA1	613	positive	0.5	negative
MA2	787	positive	0.7	negative
MA3	762	positive	0.6	negative
MA4	841	positive	0.7	negative
MA5	736	positive	0.6	negative
MA6	< 0.9	negative	4.3	positive
MA7	< 0.9	negative	6.6	positive
MA8	< 0.9	negative	4.7	positive
MA9	500	positive	0.8	negative
MA10	240	positive	4.4	positive
MA11	410	positive	1.7	positive
MA12	448	positive	11.2	positive
MA13	< 0.9	negative	6.3	positive
MA10d	< 0.9	negative	3.5	positive
MA11d	< 0.9	negative	1.7	positive
MA12d	< 0.9	negative	9.3	positive

Table 3-2: Characterization of microarray serum panel. For both assays, the mean of two replicates was interpreted according to manufacturer's instructions. For BIO-FLASH® Toxo IgG immunoassay, samples with concentrations ≥10.00 and ≤8.00 IU/mL, respectively, were considered positive and negative. In the BIO-FLASH® Toxo IgM assay, signal cut-off (S/CO) ≥1.00 and ≤0.80 were considered positive and negative, respectively. Depleted samples are labelled with a "d" after the Sample ID. ID: identification.

Analysis of the microarray serum panel revealed that six samples were positive according to the BIO-FLASH® Toxo IgG immunoassay and negative according to the BIO-FLASH® Toxo IgM (MA1 to MA5 and MA9), four samples were positive for IgM and negative for IgG (MA6 to MA8 and MA13), and three samples were IgG- and IgM-positive (MA10 to MA12). Depleted samples (MA10d to MA12d) showed 99% IgG titer reduction relative to the non-depleted samples. Therefore, they were classified as IgG-negative. The depletion process caused a 17-20% reduction in IgM reactivity compared to non-depleted ones.

3.1.2. *T. gondii* peptide microarray evaluation

The sequences of the nine selected *T. gondii* proteins were evaluated by PEPperPRINT GmbH, in a peptide microarray vs. the microarray serum panel. Goat anti-human IgG (Fc) fluorescent conjugated DyLight680 and goat anti-human IgM (μ chain) fluorescent conjugated DyLight800 were used as secondary antibodies to differentiate either type of antibody response in each group of samples. IgG and IgM heatmaps of the unprocessed fluorescent images are presented Figure 3-1.

The IgG response heatmap shows that IgG-positive samples (MA1 to MA5) had a similar fluorescent signal profile and intensity. For their part, IgG-negative samples (MA6 to MA8) exhibited no unspecific binding to any epitopes evaluated, altogether highlighting a clear difference between both groups of samples. As expected, depleted samples (*MA10d, to MA12d)* showed no response for IgG compared with non-depleted ones (MA10, to MA12), which were positive for some epitopes. Sample MA13, despite being initially classified as IgM-positive, showed no differences between both IgG and IgM peptide microarrays and was thus considered an outlier, not included in the statistical analysis (Figure 3-1A).

As we expected, the IgM response heatmap revealed a more complex profile than that of the IgG. IgM-positive samples, regardless if IgG-positive or negative (MA6 to MA8, MA10 to MA12 and *MA10d* to *MA12d*), demonstrated a distinctly stronger response than IgM-negative ones (MA1 to MA5 and MA9). Sample MA7 had the highest reactivity within the IgM-positive group, consistent with the results from the previous BIO-FLASH® Toxo IgM (6.6 S/CO). In contrast, samples MA12 and *MA12d,* with high IgM titers in the BIO-FLASH® Toxo IgM characterization (11.2 and 9.3 S/CO respectively), showed weaker reactivity (Figure 3-1B).

For data analysis, the microarray serum panel was classified into four different groups as follows: Group 1 (G1): IgM-positive (MA6, MA7, MA8, MA10, MA11, *MA11d*, MA12, *MA12d* and MA13); G2: IgG-positive (MA1, MA2, MA3, MA4, MA5, MA9, MA10, MA11 and MA12); G3: IgG-negative (MA6, MA7, MA8, *MA10d*, *MA11d* and *MA12d*) and G4: IgM-negative (MA1, MA2, MA3, MA4 and MA5).

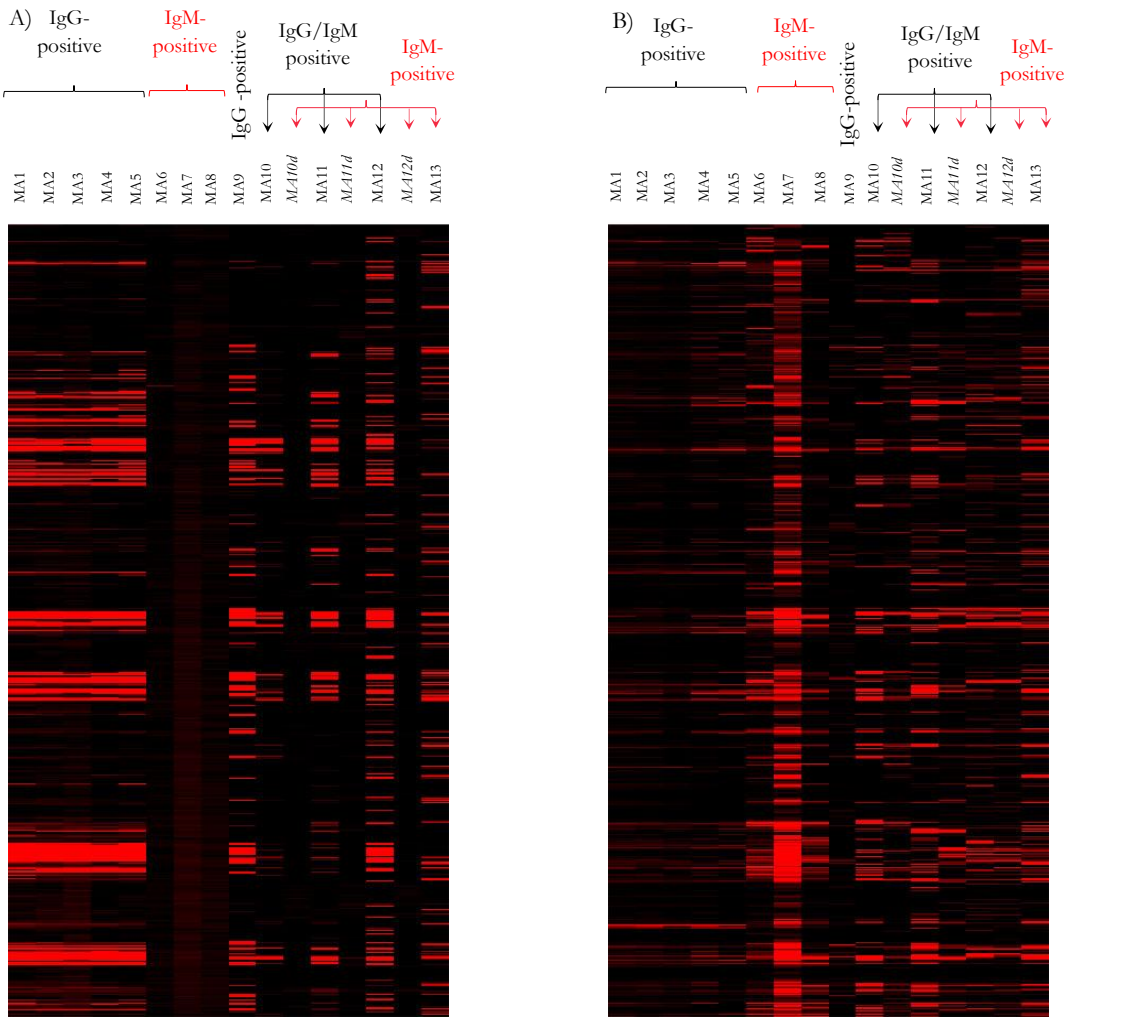

Figure 3-1: Raw heatmaps of *T. gondii* peptide microarray. The heatmaps are represented on a two-color code: red for strong and black for weak or no antibody responses. (A) IgG response heatmap using goat anti-human IgG (Fc) fluorescent secondary antibody and (B) IgM response heatmap using goat anti-human IgM (μ chain) fluorescent secondary antibody. (PEPperPRINT GmbH source).

The results obtained were statistically analyzed using the Statistical Utility for Microarray and Omics data (SUMO) software (Heidelberg, Germany), based on the unprocessed averaged spot intensities without data normalization. As a noise filter, a minimum spot intensity of 50 fluorescence units was defined, (i.e., all interactions below the threshold were set to 50 and had no influence on the statistical analysis). Unpaired two-class t-test were performed to identify: (i) common IgG responses (IgG-positive against IgG-negative samples), (ii) common IgM responses (IgM-positive against IgM-negative samples) (data not shown), and (iii) differential IgM (henceforth G1-G2) (IgM-positive against IgG-positive samples).

To elucidate which epitopes were specific for IgM, differential IgM responses were evaluated. Averaged spot intensities of IgM-positive sera (MA6, MA7, MA8, MA10, MA11, *MA11d*, MA12, *MA12d* and MA13) vs. IgG-positive sera (MA1, MA2, MA3, MA4, MA5, MA9, MA10, MA11 and

MA12) were distributed in a response matrix that included 82 peptides with a p-value of p < 1.00E-02. From 82 peptides, up to 39 were statistically significant and thus upregulated in the IgM-positive vs. IgG-positive samples. Based on the information in the differential IgM response heatmap, top peptide hits exhibited G1-G2 differences of >400 units, which were predominantly assigned to dense granule protein GRA3, rhoptry protein, granule antigen protein GRA7 and major surface antigen P30 (Figure 3-2).

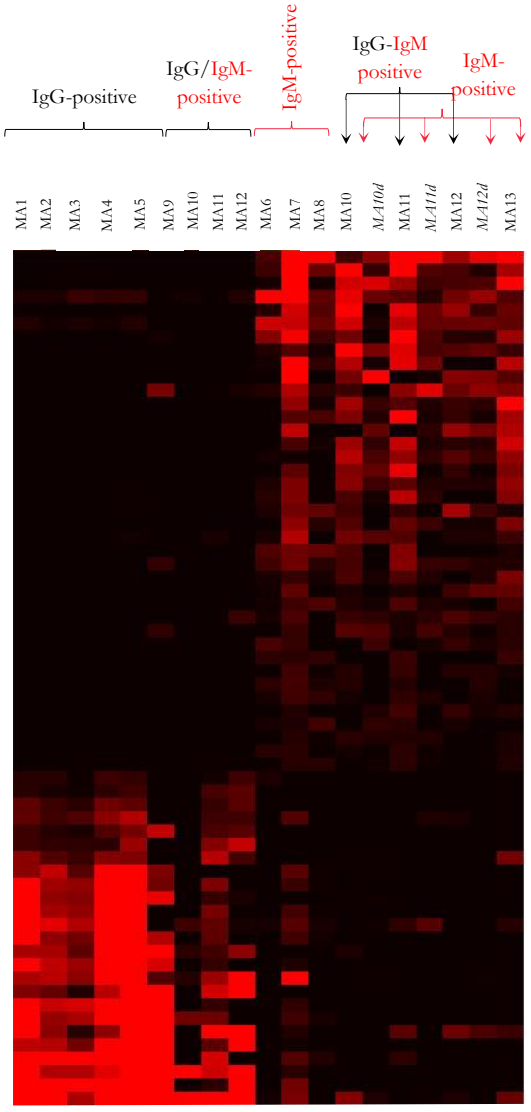

Source Molecule	G1-Mean	G1-G2 difference	p-Dist.
Dense Granule Protein Gra3	1408.410	1358.410	5.77E-003
Rhoptry Protein, Putative	734.640	684.007	5.58E-003
Rhoptry Protein, Putative	712.840	662.729	6.90E-003
Rhoptry Protein, Putative	647.040	520.718	4.08E-003
Rhoptry Protein, Putative	497.020	446.020	1.05E-003
Rhoptry Protein, Putative	522.700	442.444	9.27E-005
Granule Antigen Protein Gra7	477.640	424.162	4.15E-003
Major Surface Antigen P30 Precursor	455.560	405.560	6.33E-003
Surface Antigen P22	447.330	397.330	7.78E-003
Dense Granule Protein 4 Precursor	414.900	364.900	7.33E-003
Dense Granule Protein Gra3	418.230	316.374	2.86E-003
Granule Antigen Protein Gra6	354.500	304.500	8.62E-003
Granule Antigen Protein Gra6	344.690	294.690	8.40E-003
Surface Antigen P22, Putative	322.470	272.470	6.44E-003
Surface Antigen P22, Putative	320.600	270.600	8.60E-003
Major Surface Antigen P30 Precursor	311.160	261.160	3.02E-003
Surface Antigen P22, Putative	306.280	256.280	8.72E-003
Surface Antigen P22, Putative	274.270	224.270	2.30E-003
Rhoptry Protein, Putative	260.330	209.808	9.74E-003
Rhoptry Protein, Putative	247.300	197.300	4.86E-003
Rhoptry Protein, Putative	242.970	192.970	4.37E-003
Major Surface Antigen P30 Precursor	247.300	189.711	8.57E-003
Rhoptry Protein, Putative	223.460	173.460	5.98E-003
Granule Antigen Protein Gra7	235.460	169.716	2.13E-003
Rhoptry Protein, Putative	186.860	136.860	4.70E-003
Mic3 Microneme Protein	182.300	132.300	7.78E-003
Mic3 Microneme Protein	167.000	117.000	2.00E-003
Dense Granule Protein 4 Precursor	178.000	108.778	1.79E-003
Mic3 Microneme Protein	170.080	104.669	7.54E-003
Dense Granule Protein 4 Precursor	146.300	95.333	2.98E-003
Mic3 Microneme Protein	122.300	72.300	8.58E-003
Mic3 Microneme Protein	121.160	71.160	6.33E-003
Dense Granule Protein, Putative	117.340	67.340	6.07E-003
Dense Granule Protein, Putative	117.040	67.040	5.21E-003
Dense Granule Protein 4 Precursor	114.130	64.130	9.16E-003
Dense Granule Protein, Putative	109.670	59.670	9.43E-003
Mic3 Microneme Protein	102.500	52.500	2.75E-003
GSGSGSG Neoepitope	94.100	44.100	9.72E-003
Mic3 Microneme Protein	93.060	43.060	9.97E-003
Dense Granule Protein 2 Precursor	56.100	-80.233	8.57E-003
Dense Granule Protein 2 Precursor	50.000	-114.622	6.44E-003
Dense Granule Protein 2 Precursor	50.000	-195.556	1.63E-003
Dense Granule Protein 4 Precursor	88.840	-216.193	7.80E-003
Dense Granule Protein 2 Precursor	50.000	-250.233	4.15E-003
Dense Granule Protein 2 Precursor	50.000	-258.511	8.60E-003
Dense Granule Protein 2 Precursor	91.200	-262.833	5.05E-003
Dense Granule Protein 4 Precursor	80.200	-433.100	9.99E-003
Dense Granule Protein 4 Precursor	68.700	-573.278	2.30E-003
Dense Granule Protein 4 Precursor	51.470	-587.786	2.03E-003
Dense Granule Protein 4 Precursor	72.270	-632.063	8.51E-003
Dense Granule Protein 2 Precursor	140.960	-641.284	9.33E-003
Dense Granule Protein 4 Precursor	72.400	-655.078	6.36E-003
Dense Granule Protein 2 Precursor	56.870	-715.352	1.53E-003
Dense Granule Protein 4 Precursor	56.870	-777.430	4.25E-003
Dense Granule Protein 2 Precursor	151.360	-790.184	6.46E-003
Dense Granule Protein 2 Precursor	50.000	-852.078	9.54E-003
Dense Granule Protein 4 Precursor	63.930	-930.448	6.37E-003
Dense Granule Protein 2 Precursor	74.040	-945.260	2.17E-003
Granule Antigen Protein Gra6	167.340	-947.871	4.31E-003
Dense Granule Protein 2 Precursor	51.900	-1104.956	1.95E-003
Granule Antigen Protein Gra6	98.900	-1561.756	4.72E-003
Dense Granule Protein 2 Precursor	61.030	-1636.203	5.33E-003
Granule Antigen Protein Gra6	88.570	-1653.708	2.20E-003
Dense Granule Protein 2 Precursor	191.730	-1801.503	1.89E-003

Figure 3-2: *T. gondii* peptide microarray heatmap showing unpaired two-class t-test of differential IgM response. Source molecule name: protein to which each peptide belongs (sequence not shown). G1-Mean: mean value of all IgM-positive samples. G1-G2 difference: the result of the two-class t-test. Peptides are sorted by decreasing G1-G2 differences.

A detailed view of the two-class t-test analysis performed on the 21 statistically significant peptides previously seen in Figure 3-2, which exhibited the highest G1/G2 ratios, is shown in Table 3-3. The top upregulated peptides (peptides I to VIII) showed G1-G2 differences of >400 units and almost

all showed G1/G2 ratios of >5, which indicated that they were 5-fold more reactive for the IgM-positive samples (G1) in comparison with the IgG-positive samples (G2). The same peptides presented low reactivity for IgG-positive samples, G2 $\bar{x}$ between 50 and 126, which highlighted their specificity for IgM-positive samples.

Microarray Peptide ID	Prot. acronym	G1 $\bar{x}$	G1 σ	G2 $\bar{x}$	G2 σ	G1-G2 diff.	G1/G2 ratio	t-value	p-value (*E-03)
I	GRA3	1408.4	1358.9	50	0.0	1358.4	28.2	3.2	5.7
II	ROP1	734.6	696.7	50.6	1.9	684	14.5	3.1	5.6
III	ROP1	712.8	703.2	50.1	0.3	662.7	14.2	3	6.9
IV	ROP1	647	496.1	126.3	64.2	520.7	5.1	3.3	4.1
V	ROP1	497	343	51	2.1	446	9.7	4.1	1
VI	ROP1	522.7	240.4	80.3	35.9	442.4	6.5	5.7	9.3
VII	GRA7	477.6	408.8	53.5	10.4	424.2	8.9	3.3	4.1
VIII	SAG1	455.6	413.3	50	0.0	405.6	9.1	3.1	6.3
IX	SAG2	447.3	422.3	50	0.0	397.3	8.9	3	7.8
X	GRA4	414.9	383.1	50	0.0	364.9	8.3	3	7.3
XI	GRA3	418.2	270.3	101.9	138.1	316.4	4.1	3.3	2.9
XII	GRA6	354.5	337.9	50	0.0	304.5	7.1	2.8	8.6
XIII	GRA6	344.7	325.2	50	0.0	294.7	6.9	2.9	8.4
XIV	SAG2	322.5	285.2	50	0.0	272.5	6.4	3	6.4
XV	SAG2	320.6	293.6	50	0.0	270.6	6.4	2.9	8.6
XVI	SAG1	311.2	238.2	50	0.0	261.2	6.2	3.5	3.0
XVII	SAG2	306.3	278.9	50	0.0	256.3	6.1	2.9	8.7
XVIII	SAG2	274.3	195.3	50	0.0	224.3	5.5	3.6	2.3
XIX	ROP1	260.3	238.7	50.5	1.6	209.8	5.2	2.8	9.7
XX	ROP1	247.3	191.0	50	0.0	197.3	4.9	3.3	4.9
XXI	ROP1	243.0	187.8	50	0.0	193	4.9	3.2	4.4

Table 3-3: Top hits of differential IgM responses. Protein acronym (Prot. acronym) refers to the protein to which each peptide belongs. G1 and G2 Mean ($\bar{x}$) refer to the central tendency of both groups of samples, and their corresponding standard deviation (σ). G1 $\bar{x}$-G2 $\bar{x}$ (G1-G2 diff.) refers to the result of subtracting G2$\bar{x}$ from G1$\bar{x}$. The G1/G2 ratio resulted from dividing G1 Mean by G2 Mean. T and p-value resulted from the unpaired two-class t-test of IgM responses obtained using SUMO software.

3.2. From microarray to synthetic peptides

As mentioned earlier, the drawbacks of TLA or recombinant antigens contrast with the proven advantages of synthetic constructs, such as minimizing non-specific interactions, higher reproducibility and the possibility of adapting their chemical structure to enhance their antigenic properties (166,174). Therefore, we chose an approach based on synthetic peptides to reproduce the sequences identified in the above screening.

3.2.1. Identification and production of peptide sequences

Based on the results of the microarray analysis, we identified the sequences that had the potential to perform best. We based our selection on the following: i) IgM specificity based on G1-G2 differences and G1/G2 ratio for differential IgM responses, ii) homology to *T. gondii* B cell epitopes found in IEDB, and iii) peptide length. Thus, we designed the peptides to include the areas within the studied proteins that were most specific for IgM but limiting peptide length to around 50-60 residues, which is the approximate threshold after which the quality of synthetically produced peptides could be compromised. The 18 selected peptides, were synthesized in C-terminal carboxamide form using Fmoc solid phase synthesis, purified to >95 % homogeneity using HPLC (high performance liquid chromatography) and satisfactorily characterized using MS (mass spectrometry). Note that their sequences cannot be revealed due to confidentiality and industrial property concerns (see Table 3-4).

Peptide ID	Prot. acronym	Theo. mass[a] (Da)	Size (aa)	Net charge[b]	RT[c] (min)	ACN grad[d]	ACN[e] (%)	Purity[f] (%)
1a	SAG1	1587	15	0	5.1	10-35	23	97
1b		2345	22	+1	4.8	20-50	34	99
2a	GRA4	2730	27	-6	7.5	5-40	20	97
3a	GRA3	3827	40	-5	5.4	20-50	35	95
3b		4011	41	-6	5.7	10-50	27	95
3c		3083	31	-7	5.4	20-60	38	96
4a	GRA7	3344	31	-3	6.5	25-50	32	96
4b		3036	25	-1	6.3	5-40	20	95
4c		1585	15	-6	6.7	5-40	21	95
5a	SAG2	2757	27	-2	n/d	5-95	47	n/d
5b		2476	23	-2	10.1	15-40	30	96
5c		1468	15	-1	4.9	0-40	15	98
6a	ROP1	2641	24	-4	4.9	15-50	29	95
6b		2483	23	-7	6.0	10-40	25	96
6c		2915	27	-4	6.9	10-40	27	95
6d	GRA6	1586	15	-2	5.5	0-40	17	99
7a		2275	23	-3	6.3	10-35	23	96
7b		3134	31	-8	4.6	20-40	25	96
ctrl[g]	-	2521	23	+3	5.4	15-50	27	99

Table 3-4: Peptides used in the initial phase of this study. [a]Theoretical mass (Theo. Mass) was calculated using GPMAW software version 8.10. [b]Net charge was calculated using the ExPASy ProtParam website (https://web.expasy.org/protparam/). [c]Retention time (RT) is time elapsed from injection to peak detection. [d]Analytical RP-HPLC was performed using linear gradients of solvent B (0.036% TFA in ACN) into A (0.045% TFA in H_2O) over 15 min at 1 mL/min flow rate and with UV detection at 220 nm. [e]% acetonitrile (ACN) at peptide elution time. [f]% purity was calculated using the percentage of peak area at the chromatographic profile. [g]The control peptide (ctrl) does not belong to *T. gondii* proteome. ID: identification.

The only sequence posing synthesis problems was peptide 5a, which was obtained in poor yield and required two syntheses to finally obtain 5 mg of material. Its purity was not determined with the same accuracy as the other sequences due to difficulties in HPLC peak integration. Even so, the purified material showed via MS a molecular mass consistent with theory. Thus, the synthetic peptide panel was altogether satisfactorily produced and characterized, and hence ready to be evaluated against *T. gondii* IgM-positive samples.

3.3. Evaluation of synthetic peptides via ELISA

Once the new synthetic peptides were produced, we wanted to evaluate their functionality using both multiplex and singleplex indirect ELISA.

3.3.1. Screening panel characterization

To evaluate the selected peptides, a panel of 110 human sera (hereafter screening panel) was acquired from several suppliers. AbBaltis, ABO Pharma, and Biomex as external vendors provided *T. gondii* IgM-positive samples (n=46). Two IgM-positive samples from the microarray panel were included to verify the results obtained by the peptide microarray (MA10, and MA11). Sixty samples that came from Banc de Sang i de Teixits de Catalunya were acquired in two different batches as *T. gondii* IgM-negative. To preliminary study cross-reactivity, Biokit biobank provided two supplementary *T. gondii* negative samples that were positive for cytomegalovirus (CMV), as this virus was described by other commercial assays as a possible cross-reactant. The composition of the sample panel before the internal characterization can be seen in Table 3-5.

Supplier		External vendors	Biokit biobank	Blood bank	Microarray serum panel	n
Type of sample	Positive	46	-	-	2	48
	Negative	-	2	60	-	62
Total number of samples						**110**

Table 3-5: Screening panel composition. Samples came from different suppliers (external and internal). (n) sum of each type of sample.

Samples provided by external vendors were previously characterized for *T. gondii* IgM using different commercial assays (data not shown). The two negative samples provided by Biokit biobank were classified as negative according to previous serologic information (data not shown). Samples acquired from the blood bank were not previously tested for toxoplasmosis infection. The three IgM-positive samples belonging to the microarray panel were tested within this study (see 3.1.1).

To validate the results provided by the suppliers and the agreement between IgM anti-*T. gondii* detection methods (123), the screening panel was fully characterized for the presence of IgM by means of four commercial assays that were selected considering i) assay performance (high sensitivity

and specificity), ii) system requirements (i.e., methodology or specific instrumental requirements) and iii) the capacity to obtain reagents and technical support. BIO-FLASH® Toxo IgM immunoassay (Biokit), bioelisa TOXO IgM (Biokit) and PLATELIA™ Toxo IgM (BIO-RAD) were selected. Additionally, VIDAS® TOXO Competition (BioMérieux) for the detection of total anti-*T. gondii* Ig was included as a preliminary screening method (Table 3-6).

Commercial name	Supplier	Technology	Capture Antigen	Tracer
BIO-FLASH® Toxo IgM	Biokit	CLIA	*T. gondii* lysate antigen	anti-human IgM monoclonal antibody
bioelisa TOXO IgM	Biokit	ELISA	anti-human IgM rabbit antibodies	*T. gondii* antigen
PLATELIA™ Toxo IgM	BIO-RAD	ELISA	anti-human µ-chains antibodies	*T. gondii* antigen and anti-*T. gondii* monoclonal antibody
VIDAS® TOXO Competition	BioMérieux	ELFA	*T. gondii* lysate antigen	monoclonal anti-P30 antibody

Table 3-6: Commercial assays used to characterize screening panel. Commercial assays are classified according to the information present in the intended use data sheet.

To characterize the screening panel, we designed a strategy to prioritize analyzing positive samples from external vendors (n=46) using the four assays (BIO-FLASH® Toxo IgM, bioelisa TOXO IgM, PLATELIA™ Toxo IgM and VIDAS® TOXO Competition). Finally, from the two microarray serum panel samples, due to the available volume of each sample, we tested MA10 and MA11 samples with only two commercial assays.

The 60 samples provided by the blood bank, which we expected to be mostly negative, were tested using one or two assays considering both the sample volume and the assays available in-house when the samples were received. When a result was positive, we expanded the screening using a second or third assay. The first batch consisted of 20 samples that were tested using two assays (blood bank batch I). From those 20 samples, one gave a positive result; thus, it was evaluated by a third assay, which gave a negative result. In the second batch 40 samples were received and tested using two assays (blood bank batch II). From those, one gave a positive result; hence it was tested using a third assay, which gave a negative result. Table 3-7 details the results of the screening panel characterization.

The results we obtained with the 46 samples purchased as IgM anti-*T. gondii* positive varied among the four commercial assays used to characterize the samples, ranging from 45 to 30 positives. VIDAS® TOXO Competition was the assay that classified the greatest number of samples as positive (n=45), whereas BIO-FLASH® Toxo classified the lowest number of samples as positive (n=30). Regarding negative samples, the same estimations could not be performed, because not all samples were evaluated by the same assays.

	Commercial name	VIDAS®	PLATELIA™	bioelisa	BIO-FLASH®	Result
Sensitivity -Specificity (%)		99.4 - 99.3	100 - 99.9	88 - 95.2	96.9 - 93.8	
Supplier	External vendors (n=46)	45	41	36	30	Positive
		1	1	10	11	Negative
		-	4	-	5	Indeterminate
	Biokit biobank (n=2)	1	-	-	1	Positive
		1	2	2	1	Negative
	MA 10-11 microarray panel (n=2)	-	2	2	-	Positive
		-	-	-	-	Negative
	Blood bank (batch I) (n=20)	4	1	0	-	Positive
		16	19	1	-	Negative
	Sample 7	pos	pos	neg	-	-
	Blood bank (batch II) (n=40)	-	1	0	0	Positive
		-	19	1	20	Negative
	Sample 95	-	pos	neg	-	-
Total samples		68	90	52	69	-

Table 3-7: Detailed view of the screening panel characterization. The left column classifies samples according to the supplier (external vendors, Biokit biobank, microarray panel and blood bank). The number of samples included in each group is specified in brackets. Blood bank samples (batch I and II) include the information of those samples that were initially positive. Each group of samples is classified according to manufacturer instructions as represented in the right column (positive, negative or indeterminate).

These results show that the four commercial assays did not agree on the positivity of the samples. Since discerning positive from negative samples was key for our study, we classified the panel according to the agreement across the assays used to evaluate each sample. The classification is shown in Table 3-8.

Classification	Nº samples	Explanation	Final classification
Total positive	28	All the results obtained agree	
Total negative	60		
Total pos cond	4	One indeterminate result assumed as positive	Conditional (n=94)
Total pos cond 2	2	Two indeterminate results assumed as positive	
2 pos 1 neg	4	Two positive and one negative results	
2 neg 1 pos	10	Two negative and one positive result	Excluded (n=16)
Pos neg	1	One positive and one negative[a]	
Pos neg ind	1	Total disagreement[b]	
Total	110		

Table 3-8: Screening panel classification. [a]Sample tested by two methods. [b]Sample tested by three methods; all of them gave different results.

Samples that showed total agreement among all the methods used were classified as total positive (n=28) or total negative (n=60). Samples that were purchased from external vendors as positives, but during our characterization showed one indeterminate result, were classified as total positive conditional (total pos cond) (n=4) or as total positive conditional 2 (total pos cond 2) for samples that presented two indeterminate results (n=2). That group of samples (total positive, total negative and samples with one or two indeterminate results) was named as "*conditional*" (n=94). The group of samples with final classification as "*excluded*" (n=16) correspond to samples that showed different degrees of disagreement, either the same number of positive and negative results or even one result of each type (positive, negative and indeterminate). These samples were excluded from the study.

3.4. Multiplex ELISA

The microarray study elucidated 18 different peptides that potentially reacted with IgM anti-*T. gondii* positive samples and did not react with anti-*T. gondii* IgG-positive samples. The sequences of the selected peptides were synthesized by SPPS (see section 3.2). To identify which reacted with the maximum number of IgM-positive samples in a fast and efficient way, and considering that the sample volume was scarce, we designed a multiplex ELISA in collaboration with InfYnity Biomarkers.

3.4.1. Phase I: Optimizing printing conditions and setting up the screening conditions

To elucidate which were the best peptides, we initially needed to design the optimal assay with the appropriate assay conditions. To establish optimal peptide concentration, three peptide dilutions (5, 50 and 100 μg/mL) were spotted in duplicate and organized in a 6x6 array in each well of a 96-well plate (Figure 3-3). In addition, positive control (PC) was spotted in triplicate to check the reactivity in each well and for array space-orientation. Two different conjugate dilutions were tested (1/1500 and 1/3000). Eight total positive (4, 5, 24, 31, 36, 37, 40 and 46) and eight total negative (52, 54, 55, 56, 58, 60, 61 and 62) samples from the conditional panel were selected and diluted 1/50. The ELISA plate design is shown in Figure 3-3.

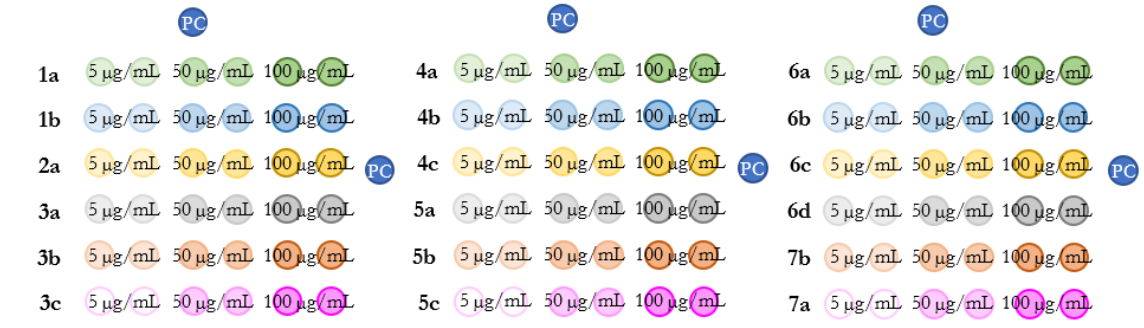

	1	2	3	4	5	6	7	8	9	10	11	12
A	4	52	4	52	4	52	4	52	4	52	4	52
B	5	54	5	54	5	54	5	54	5	54	5	54
C	24	55	24	55	24	55	24	55	24	55	24	55
D	31	56	31	56	31	56	31	56	31	56	31	56
E	36	58	36	58	36	58	36	58	36	58	36	58
F	37	60	37	60	37	60	37	60	37	60	37	60
G	40	61	40	61	40	61	40	61	40	61	40	61
H	46	62	46	62	46	62	46	62	46	62	46	62

Figure 3-3: Schematic view of the multiplex ELISA (phase I). The upper panel represents the spotting pattern within each section of the 96-well ELISA plate (1 to 3 upper row of the ELISA plate) represented in the lower panel. The first four columns of the ELISA plate were printed with peptides 1a to 3c, Columns 4 to 7 were printed with peptides 4a to 5c, and columns 8 to 12 were printed with peptides 6a to 7b. The eight positive and negative samples were evaluated following the pattern shown in the picture. PC=positive control.

Fluorescent net intensity (mean value of duplicated spots) was established for the 16 samples included in the study. The mean value of negative samples was used to establish individual cut-off for each peptide (Table 3-9). Almost all cut-off values were under 600 units. Peptides 6d, 7a and 7b showed higher reactivity (672, 723 and 625, respectively). Two peptides showed cut-off values 2- and 3-fold higher than the others (cut-off of peptide 1a was 1545 and 5b was 3953).

Peptide ID (100μg/mL)	Cut-off (fluorescent units)
1a	1545
1b	592
2a	156
3a	350
3b	394
3c	736
4a	289
4b	577
4c	220
5a	464
5b	3953
5c	287
6a	421
6b	495
6c	597
6d	672
7a	723
7b	625

Table 3-9: Cut-off values for each peptide. Cut-off values are expressed in relative fluorescence units. ID: identification.

Net intensity of each peptide for positive or negative samples was converted into positive or negative reactivity according to the cut-off value. Signal-to-cut-off value (S/CO) of each sample is presented in Table 3-10. Also, final S/CO was calculated by subtracting mean negative value from mean positive value. Samples with S/CO values ≥1 were considered positive and samples with S/CO <1 were considered negative. Peptides that showed final S/CO values >1 were considered specific in front anti-*T. gondii* IgM-positive samples.

Positive samples were reactive to almost all peptides (1a, 2a, 3a, 3b, 3c, 4a, 4b, 4c, 5a,5b, 5c, 6b, 6c, 6d and 7b). Peptides 3a, 3b, 3c, 6c, and 7b showed higher final S/CO (≥ 3,5). Peptides 5a and 5c showed final S/CO ≥1. The final S/CO for peptide 4a was equal to 1. Peptides 5b, 6a, and 7b reacted more for negative samples compared to positive samples. This outcome suggests that those peptides were non-specific for IgM-positive samples.

#	Interp.	1a	1b	2a	3a	3b	3c	4a	4b	4c	5a	5b	5c	6a	6b	6c	6d	7a	7b
4	Pos	3.2	0.4	1.4	23.0	14..4	8.1	5.9	4.6	1.8	2.1	2.3	2.8	0.4	0.3	25.8	0.2	0.3	2.7
5	Pos	0.5	0.4	1.4	0.9	1.4	1.4	2.7	1.2	1.8	1.1	0.3	4.1	0.8	1.0	8.4	0.6	1.0	1.3
24	Pos	1.6	0.7	0.0	6.3	2.3	1.5	0.2	0.2	0.7	0.4	0.5	3.1	0.7	1.3	1.6	0.7	0.5	1.0
31	Pos	2.3	0.4	1.0	48.0	40.3	13.4	2.6	1.5	1.4	12.0	3.4	7.4	1.8	3.9	8.4	2.7	2.3	5.5
36	Pos	0.3	0.1	0.4	0.8	1.0	3.0	2.9	2.3	2.1	1.0	0.8	0.7	1.2	1.3	5.2	1.7	1.4	2.7
37	Pos	0.8	0.0	0.0	1.0	0.6	0.4	0.4	0.4	1.3	0.6	0.7	2.8	0.2	0.4	22.6	0.2	0.4	0.9
40	Pos	1.8	1.6	3.2	4.7	3.0	2.3	0.3	1.4	0.3	16.1	0.4	1.2	0.0	0.2	10.5	0.2	0.2	37.4
46	Pos	0.5	0.2	0.5	5.7	7.7	8.3	0.6	0.2	0.1	0.8	1.8	1.6	0.3	0.6	5.7	6.2	0.4	2.6
52	Neg	0.8	0.0	0.0	0.3	0.0	0.7	0.7	1.0	2.3	0.2	1.2	0.3	1.5	0.4	0.5	0.4	0.1	0.1
54	Neg	0.3	0.5	2.2	1.2	1.8	0.8	0.5	1.0	0.2	0.3	0.1	0.6	2.5	1.5	1.8	1.6	1.6	2.1
55	Neg	0.1	0.3	0.6	0.1	0.8	1.0	0.5	1.8	0.5	0.5	0.6	1.0	1.0	0.9	0.6	0.8	0.8	0.6
56	Neg	3.9	0.2	0.8	2.7	2.4	0.3	2.6	0.5	0.6	1.9	1.7	1.0	0.5	1.0	0.8	0.6	0.6	1.2
58	Neg	0.6	0.1	0.0	0.0	0.0	1.1	0.5	0.2	0.4	0.4	2.0	0.8	0.3	0.5	1.0	0.6	0.5	0.7
60	Neg	1.0	5.1	3.0	0.8	1.6	0.9	1.8	2.3	1.5	1.3	0.1	1.9	1.4	2.0	1.3	1.8	1.7	1.7
61	Neg	0.7	1.4	1.2	2.7	1.2	0.0	1.0	0.4	2.6	1.6	1.9	1.4	0.3	1.3	1.3	1.3	1.7	1.2
62	Neg	0.6	0.5	0.2	0.2	0.2	3.1	0.4	0.9	0.0	1.7	0.4	1.0	0.5	0.6	0.7	0.9	1.1	0.5
mean pos		1.4	0.5	1.0	11.3	8.8	4.8	2.0	1.5	1.2	4.3	1.3	3.0	0.7	1.1	11.0	1.6	0.8	6.8
mean neg		1.0	1.0	1.0	1.0	1.0	1.0	1.0	1.0	1.0	1.0	1.0	1.0	1.0	1.0	1.0	1.0	1.0	1.0
Final S/CO		0.4	-0.5	0.0	10.3	7.8	3.8	1.0	0.5	0.2	3.3	0.3	2.0	-0.3	0.1	10.0	0.6	-0.2	5.8

Table 3-10: Peptide screening via multiplex ELISA (phase I). S/CO value of each peptide for each sample (#). Final S/CO is shown using color labeling (red for reactive (S/CO >1) and black for non-reactive (S/CO ≤1)).

An example is shown below. Reactivity of 18 peptides for sample 4 can be visually explored in Figure 3-4 and correlated with numerical cut-off values presented in Table 3-11. For each peptide, as non-specific results could be reported when precipitates appeared, all scanned images were visually reviewed and contrasted with their net intensity values. Peptide 6c, one of the best performing (together with 3a), is marked with a yellow hyphened-line rectangle in Figure 3-4. 6c presented the most intense spots visually, correlating with its S/CO of 25.8, the highest of all peptides (see Table 3-11). One example of non-specific results is observed when peptides 5b and 5c are compared. Visually, spot intensities of 5b were higher than 5c. In contrast, cut-off values were higher for peptide 5c (2.8 S/CO vs. 2.3 S/CO, respectively). This example illustrates the importance of comparing the numerical result obtained by the software and prioritizing the visual exploration of the images, to avoid erroneous interpretations of the results.

Multiplex ELISA phase I allowed us to establish the optimal assay conditions (peptide concentration at 100 μg/mL, samples at 1/50 and conjugate at 1/1500). The results obtained indicate that peptides 3a and 6c were reactive for IgM anti-*T. gondii* for the eight positive samples analyzed and non-reactive for the eight negative samples. In contrast, peptides 1a, 5b and 7a presented cross-reactivities with the negative samples which may indicate that they were non-specific for IgM anti-*T. gondii*. Even so, the study of the 18 peptides was extended to phase II, with a higher number of samples (the complete sample panel consisting of 110 samples) using the assay conditions established in phase I.

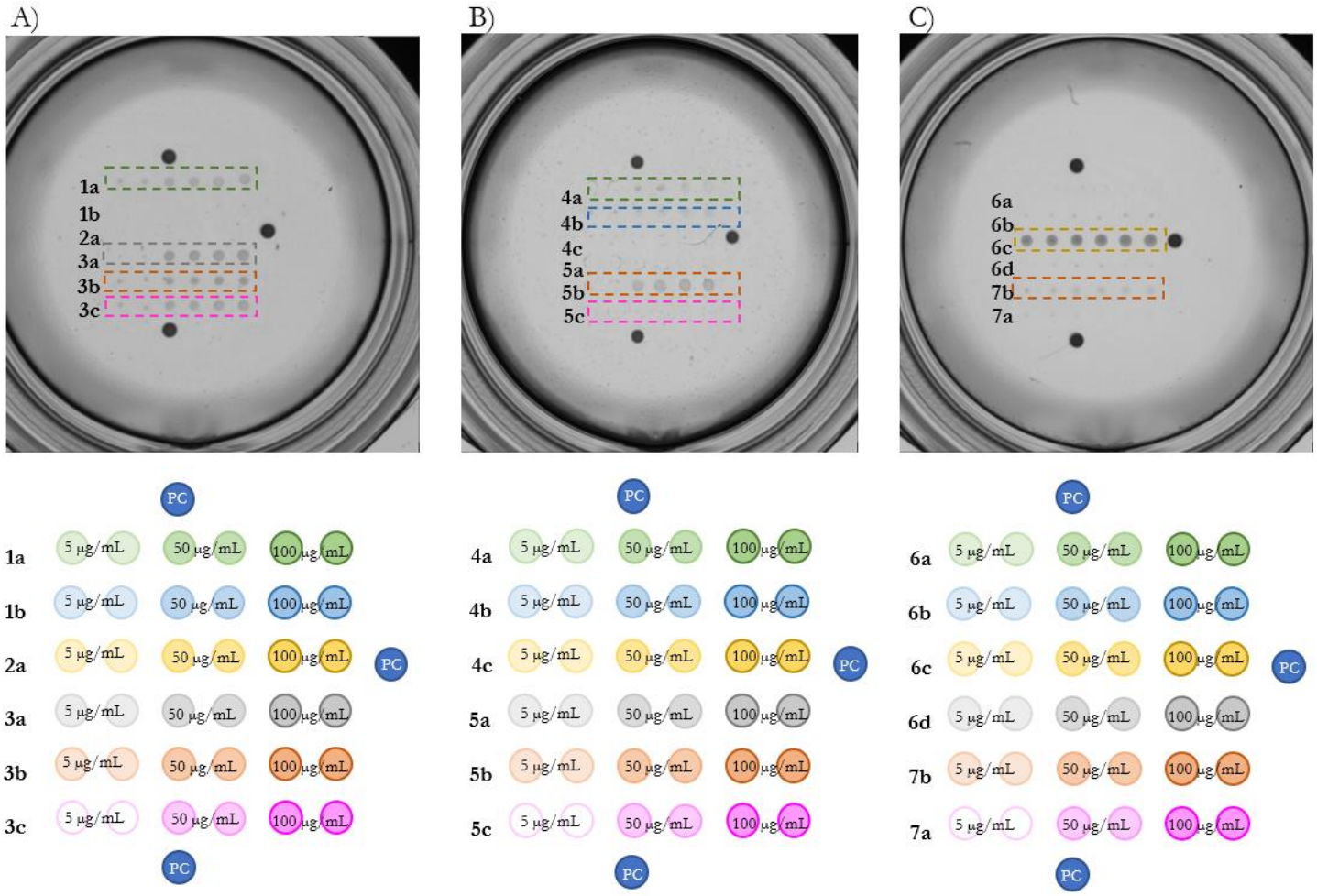

Figure 3-4: Scanned images for sample 4 with the 18 peptides. Panel a) corresponds to scanned images of peptides 1a to 3c. Panel b) corresponds to scanned images of peptides 4a to 5c. Panel c) corresponds to scanned images of peptides 6a to 7a. A schematic view of the spotting pattern of each well is showed in the right side of each panel. The reactivity of peptides which showed S/CO ≥ 2.2 is highlighted with a hyphen-line figure. (PC: positive control).

Peptide ID	Net intensity	Cut-off	S/CO	Interpretation
1a	4969	1545	3.2	reactive
1b	249	592	0.4	non-reactive
2a	225	156	1.4	non-reactive
3a	8050	350	23.0	reactive
3b	5663	394	14.4	reactive
3c	5940	736	8.1	reactive
4a	1704	289	5.9	reactive
4b	2640	577	4.6	reactive
4c	392	220	1.8	non-reactive
5a	973	464	2.1	non-reactive
5b	9161	3953	2.3	reactive
5c	809	287	2.8	reactive
6a	188	421	0.4	non-reactive
6b	171	495	0.3	non-reactive
6c	15413	597	25.8	reactive
6d	160	672	0.2	non-reactive
7a	215	625	0.3	non-reactive
7b	1657	723	23	reactive

Table 3-11: Results overview for positive sample 4 (phase I). Net intensity, cut-off and S/CO for each peptide are presented. The interpretation column shows the classification of each peptide for sample 4. Peptides with S/CO ≥2.3 were interpreted as reactive. Peptides with S/CO < 2.3 were interpreted as non-reactive. ID: identification.

3.4.2. Phase II: Evaluation of the synthetic peptides with the screening sample panel

As explained in the previous section, Phase I allowed us to establish the appropriate assay conditions for the 18 peptides. In phase II, our objective was to identify which peptides had the best antigenic properties. To do so, we analyzed the performance of each peptide – the number of samples that were correctly classified as positive or as negative – by using the assay conditions established in phase I with the complete screening panel (see section 3.3.1).

Peptides at 100 μg/mL were spotted in duplicate and organized in a 7x6 array in each well of a 96-well plate (Figure 3-5). Additionally, native antigen of *T. gondii* produced by Biokit was included as an extra control. Biokit Toxo antigen was spotted in duplicate at three different concentrations (5, 50 and 100 μg/mL).

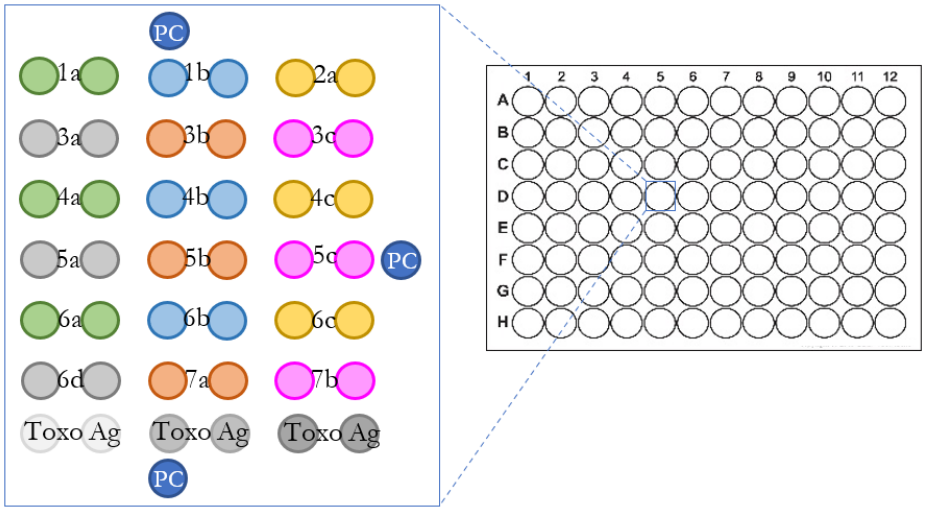

Figure 3-5: Schematic view of the multiplex ELISA of phase II. Each well of two 96-well plates was printed with the 7x6 spotting matrix represented in the figure. (PC: positive control, Toxo Ag: native antigen of *T. gondii*).

In phase II, InfYnity Biomarkers changed the plate reader and the software used to capture and analyze images from the 96-well plate. The new software establishes the cut-off level according to the data overall. Then, net intensity of each antigen for positive and negative samples was converted into positive or negative reactivity according to the cut-off value established by the software.

Although the complete screening panel (n=110) was used, data analysis was performed only on the conditional panel (see Table 3-8) (samples that were characterized as total positive, total pos cond, total pos cond 2 and total negative) (n=94). Only samples that reported high homogeneity among the assays used to characterize the samples were considered for the analysis, in order to minimize the possibility of including false positives or false negatives, which could have led to data misinterpretation and choice of non-specific peptides. Results are shown in Table 3-12.

Peptide ID	Mean pos samples [AU]	Mean neg samples [AU]	Result (S/CO)	Interpretation
1a	13.1	9.5	3.6	non-reactive
1b	2.5	2.8	-0.4	non-reactive
2a	1.0	1.0	0.0	non-reactive
3a	16.9	5.3	11.6	reactive
3b	19.6	7.0	12.6	reactive
3c	13.9	9.8	4.1	non-reactive
4a	5.7	3.1	2.6	non-reactive
4b	8.0	6.0	2.0	non-reactive
4c	0.2	0.2	0.0	non-reactive
5a	6.4	3.1	3.3	non-reactive
5b	16.3	22.0	-5.7	non-reactive
5c	2.3	1.9	0.4	non-reactive

Peptide ID	Mean pos samples [AU]	Mean neg samples [AU]	Result (S/CO)	Interpretation
6a	2.1	4.5	-2.4	non-reactive
6b	0.8	0.7	0.2	non-reactive
6c	24.1	8.9	15.2	reactive
6d	2.7	0.6	2.1	non-reactive
7a	0.8	0.3	0.5	non-reactive
7b	10.0	1.9	8.2	non-reactive
Toxo Ag 5 μg/mL	1.1	0.9	0.2	non-reactive
Toxo Ag 50 μg/mL	31.5	19.6	11.9	reactive
Toxo Ag 100 μg/mL	39.4	25.8	13.6	reactive

Table 3-12: Peptide screening by multiplex ELISA (phase II). The mean of all positive and negative samples included in the conditional panel is presented. The result column is calculated by subtracting mean neg samples from mean pos samples. The interpretation column was done according to the following criteria; non-reactive for S/CO ≤3 and reactive for S/CO >10. (Toxo Ag: native antigen of *T. gondii*, AU: Absorbance units).

The reactive peptides showing the highest S/CO were 3a, 3b, 6c. Native antigen of *T. gondii* was positive only when tested at 50 and 100 μg/mL. Even so, the mean values of the negative samples were the highest shown in the study, followed by peptide 5b, which may suggest that the use of native antigen of *T. gondii* is not a good approach for detecting IgM anti-*T. gondii*-positive samples.

A specific example is shown in Figure 3-6 and Table 3-13. The original image obtained with sample 4 was processed using the software according to the parameters established. Numerical results were then obtained. Interpretation was provided according to the established cut-off and an indeterminate zone was proposed by the software.

Figure 3-6: Original image for positive sample 4, before and after processing. Left image before analysis. Right image after software processing.

Peptide	Result (S/CO)	Interpretation
1a	24.6	reactive
1b	4.3	indeterminate
2a	0.3	non-reactive
3a	46.7	reactive
3b	38.3	reactive
3c	31.3	reactive
4a	16.0	reactive
4b	7.6	indeterminate
4c	0.0	non-reactive
5a	0.9	non-reactive
5b	35.1	reactive
5c	0.0	non-reactive
6a	1.8	non-reactive
6b	1.6	non-reactive
6c	70.5	reactive
6d	0.0	non-reactive
7a	0.6	non-reactive
7b	15.1	reactive
Tx Ag 5 μg/mL	0.0	non-reactive
Tx Ag 50 μg/mL	37.6	reactive
Tx Ag 100 μg/mL	47.5	reactive

Table 3-13: Results overview for positive sample 4 (phase II). Signal to Cut-Off (S/CO) and interpretation are shown. Interpretation was done according to the following criteria; non-reactive for S/CO ≤3 and reactive for S/CO >10. Indeterminate was established between >3 and ≤10 (Tx Ag: *T. gondii* native antigen).

The results we obtained with the multiplex ELISA phase II suggested to us that the best candidates were peptides 3a, 3b and 6c. Although we initially classified peptide 3c as non-reactive, we considered it for study in the next step due to its sequence overlapping with peptides 3a and 3b. Also, we retained peptide 7b to be studied in the next step, despite having initially considered it non-reactive when we analyzed the conditional panel (see Table 3-12), due to its high reactivity to *T. gondii* IgM-positive samples.

3.5. Singleplex ELISA

The multiplex ELISA elucidated which of the peptides initially selected were reactive to anti-*T. gondii* IgM-positive samples and non-reactive or little reactive to anti-*T. gondii* IgM-positive samples and which of them were cross-reactive with *T. gondii* negative samples. Additionally, multiplex ELISA allowed us to define the best assay conditions (peptide concentration, sample and conjugate dilutions). Once the assay parameters were established and the number of final candidates reduced from 18 to 5, the next step was to set up an indirect ELISA in its singleplex classic version.

The objectives were, first, to ascertain if we could reproduce the results obtained with the multiplex ELISA during the collaboration with InfYnity Biomarkers. Then, if the first objective was accomplished, the second was to establish an in-house protocol to perform an indirect ELISA. The new indirect ELISA would use the synthetic peptides as antigens, thus validating the functionality of the selected peptides as new diagnostic tools for detecting *T. gondii* IgM-positive samples.

3.5.1. Reproducing the multiplex parameters in singleplex ELISA

During the collaboration with InfYnity Biomarkers, we showed that the selected peptides could be directly attached to the solid surface of the 96-well plates, instead of being used as a conjugate (which is the common approach used by other commercial available immunoassays, as seen in Table 3-8). Thus, we decided to design an indirect ELISA to validate the results obtained with the multiplex ELISA, both in phase I and II. The indirect approach allowed us to simplify the method, since we did not have to label all the peptides with peroxidase.

Several ELISA plates were coated with the five selected peptides at 100 μg/mL, following standard in-house coating procedures (see section 8.5.2) using single strip-detachable 96-well plates. The strip-detachable 96-well plates allowed us to easily reassemble ELISA plates and customize the final ELISA plate to perform the functional assay (see Figure 3-7).

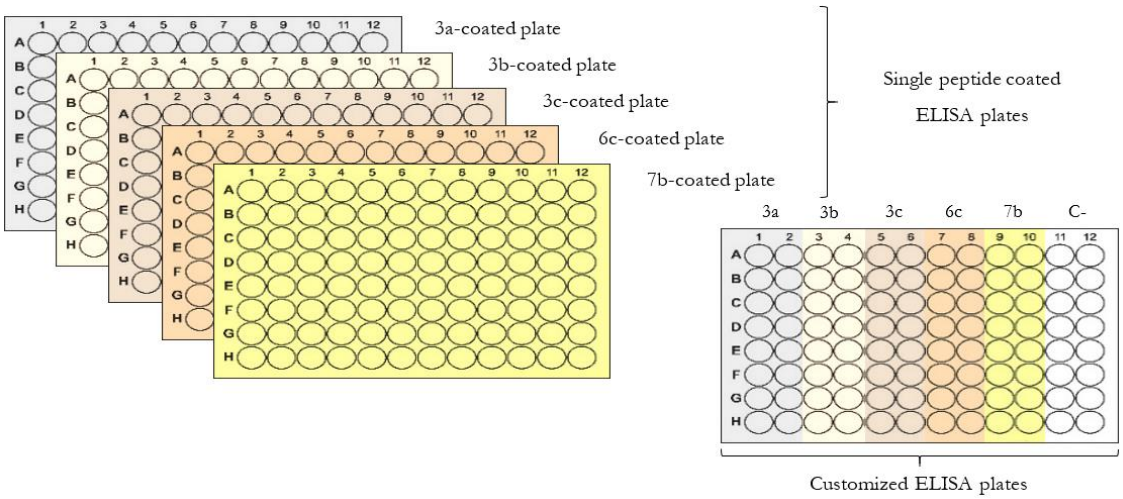

Figure 3-7: Schematic view of ELISA plates. ELISA plates coated with a single peptide were initially produced in single strip-detachable 96-well plates. Ready-to-use, customized ELISA plates were easily obtained using strips from the original plates on demand. C- strips refers to control strips, for which we followed the same coating procedure but without peptide.

To validate the results obtained by multiplex ELISA, two positive and two negative samples that were tested in phase I were selected. Using the ELISA format shown in Figure 3-7, 1/50 samples and 1/1000 conjugate dilutions were evaluated. Once the ELISA protocol was completed (see section 8.5.2), the optical density (OD) of each plate well was read using a 630 nm filter. Relative absorbance units were calculated by subtracting blank results (read at 450 nm with the blank well). The cut-off

value was calculated as the average result of the absorbance of all negative samples (0.187 OD). Signal-to-noise ratio (SNR) was then calculated according to the absorbance value of each positive sample divided by the cut-off value. Results are shown in Figure 3-8.

The results of the singleplex ELISA showed a good correlation with those of the multiplex ELISA developed in collaboration with InfYnity Biomarkers. Peptides 3a, 3b, and 6c showed higher fluorescent units and SNR, followed by 3c and 7b. Because the units of the two techniques were not comparable, we calculated the standard deviation and extrapolated the result to a percentage value with respect to the highest value (data not shown). In doing so, we observed an interesting fact. In multiplex ELISA, the standard deviation of sample #31 for 3a, 3b and 6c peptides was 979, which represented 14% with respect to the highest reactivity value (6912). The same determination in singleplex ELISA gave a standard deviation of 3.7, i.e. 28% with respect to the highest reactivity value (13.3). This difference (twice as high in the singleplex than in the multiplex) was not observed in sample 46; the difference could be attributed to sample degradation or to a manipulation error.

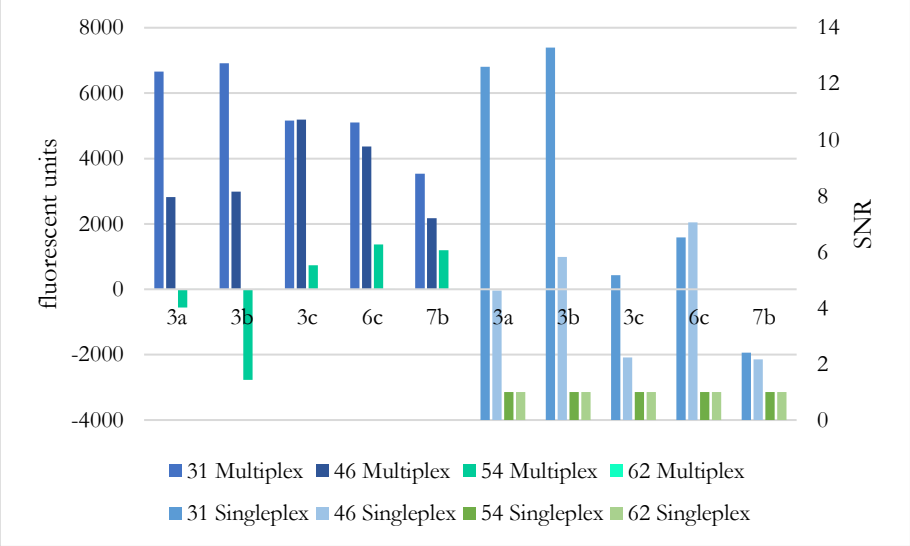

Figure 3-8: Correlation between multiplex and singleplex ELISA. Positive samples (31 and 46) and negative samples (54 and 62) are represented for each technique with their corresponding units (fluorescent units and signal-to-noise ratio (SNR)respectively. Al peptides were tested at 100µg/mL.

3.5.2. Optimizing the singleplex ELISA

The multiplex ELISA had allowed us to establish the optimal working ranges for each assay condition studied (peptide, sample and conjugate concentrations) and to identify which were the best performing peptides. We next translated the assay conditions established with the multiplex ELISA to a singleplex format. However, due to the methodological differences between multiplex and singleplex, such as coating of the plates (peptide printing versus precipitation from carbonate buffer, among others), we decided to examine in more depth the assay conditions established by the

multiplex ELISA and optimize them to a singleplex context with the objective of improving performance of the latter. To this end, we performed a checkerboard titration.

In all immunoassays it is important to optimize the concentration of the sample and the antigens or the antibodies used to capture or detect the samples. If the sample or antigen/antibodies are too concentrated, there is a risk of saturation. On the contrary, if samples or antibodies are not concentrated enough, the signal will be weak and difficult to detect. Checkerboard titration can be used to assess two variables at once: in this case, we decided to study the concentration of the peptide that would be used to coat the ELISA plates to capture the IgM anti-*T. gondii*, and the conjugate concentration. By running each well with a different ratio of peptide and conjugate, not only the optimal concentration of each one can be found, but also the optimal ratio of both concentrations. An example of a checkerboard titration is shown in Figure 3-9. Each one of the columns 1-12 corresponds to different peptide dilution factors in decreasing order and rows A-H to conjugate dilution factors also in decreasing order.

1/500 → 1/4000 Conjugate dilution; Peptide concentration (µg/mL) 50 → 0

		1	2	3	4	5	6	7	8	9	10	11	12
1/500	A	50	50	12.5	12.5	3.1	3.1	0.8	0.8	0.2	0.2	0	0
	B	50	50	12.5	12.5	3.1	3.1	0.8	0.8	0.2	0.2	0	0
1/1000	C	50	50	12.5	12.5	3.1	3.1	0.8	0.8	0.2	0.2	0	0
	D	50	50	12.5	12.5	3.1	3.1	0.8	0.8	0.2	0.2	0	0
1/2000	E	50	50	12.5	12.5	3.1	3.1	0.8	0.8	0.2	0.2	0	0
	F	50	50	12.5	12.5	3.1	3.1	0.8	0.8	0.2	0.2	0	0
1/4000	G	50	50	12.5	12.5	3.1	3.1	0.8	0.8	0.2	0.2	0	0
	H	50	50	12.5	12.5	3.1	3.1	0.8	0.8	0.2	0.2	0	0
Sample 1/50		PS	NS	PS	NS	PS	NS	PS	NS	PS	NS	PS	NS

Figure 3-9: Example of a checkerboard template. Every two columns the peptide concentration was reduced 1:4. The two last columns are used as a negative control. Every two rows the conjugate was diluted 1:2. One column of each condition is used to test a positive sample (PS) and the other to test a negative sample (NS). The sample dilution is fixed at 1/50 with sample diluent.

Table 3-14 summarizes the concentration range assessed for each peptide, the peptide concentration finally selected, the absorbance of the positive and negative samples that were used and the SNR. For all peptides, the best dilution of conjugate was 1/2000. Peptide 6c required the lowest peptide concentration, however it showed the highest SNR. In contrast, peptide 7b required the highest peptide concentration to reach a SNR of 1.9.

Peptide ID	**3a**	**3b**	**3c**	**6c**	**7b**	**3a+6c**
Range of concentrations tested (µg/mL)	50-0.2	250-0.2		50-0.2		10 to 0.6 0.2 to 0.05[a]
Samples used (pos/neg)				46/88		
Final concentration (µg/mL)	10	0.2	-	0.2	50	1.25-0.2[b]
Conjugate dilution				1/2000		

Peptide ID	3a	3b	3c	6c	7b	3a+6c
$A_{450/630}$ sample 46	0.66	0.65	0.42	0.65	0.40	0.98
$A_{450/630}$ sample 88	0.20	0.15	0.34	0.15	0.20	0.23
SNR	**3.3**	**4.3**	**1.2**	**4.4**	**1.9**	**4.3**

Table 3-14: Results overview of checkerboard optimization at original peptides. [a]Peptide 3a was tested from 10 to 0.6 μg/mL and peptide 6c from 0.2 to 0.05 μg/mL. [b]Selected concentration for 3a and 6c peptides, respectively.

Once the optimal assay conditions of the indirect ELISA were established, the conditional panel (see Table 3-8) was evaluated with peptides 3a, 3b, 6c and 7b. Due to low volume, sample 49 was excluded from the study (n=93). Peptide 3c was excluded due to the low reactivity showed during the checkerboard (SNR of 1.2).

For the evaluation, three 96-well plates were coated with each peptide (3a, 3b, 6c, 7b) at the selected peptide concentrations. Each sample was evaluated in duplicate, including the blank. Optical density of each well was read using a 630 nm filter. Relative absorbance units were calculated by subtracting blank result (read at 450 nm). The net absorbance of each sample was reported and its status (negative or positive) was used to generate a receiver operating characteristic curve (ROC curve) using Analyse-it® software. The ROC curve is a graphical plot that illustrates the diagnostic ability of a binary classifier system as its discrimination threshold is varied. Thus, the ROC curve was created by plotting the true positive proportion (TPP, also known as sensitivity) against the false positive proportion (FPP, also known as probability of false alarm or false positive, calculated as 1 – specificity, at various threshold settings).

Additionally, we wanted to evaluate whether the combination of two peptides could have synergy, thus increasing the SNR obtained individually. Peptide 7b was discarded as its reactivity to IgM-positive samples was low. Peptide 6c was selected because it was the best candidate so far. To decide between peptides 3a and 3b, we set up a tentative cut-off (0.21) and analyzed the number of true positives, true negatives, false positives and false negatives obtained after screening with the conditional panel (data not shown). The number of false positives and false negatives results coincided, although peptide 3a showed two additional true positive results, and one additional true negative result. Therefore, we decided to test the combination of peptides 3a and 6c. A checkerboard was performed with a mixture of the two peptides at different concentrations. The checkerboard revealed that when both peptides were used together as antigens, a high SNR could be obtained with a concentration of 3a nearly 10 times lower than when 3a was used on its own (see Table 3-14). Once the assay conditions were established, the conditional panel (see Table 3-8) minus the sample 49 (n=93) was evaluated with the combination of peptides 3a and 6c. (see Figure 3-10).

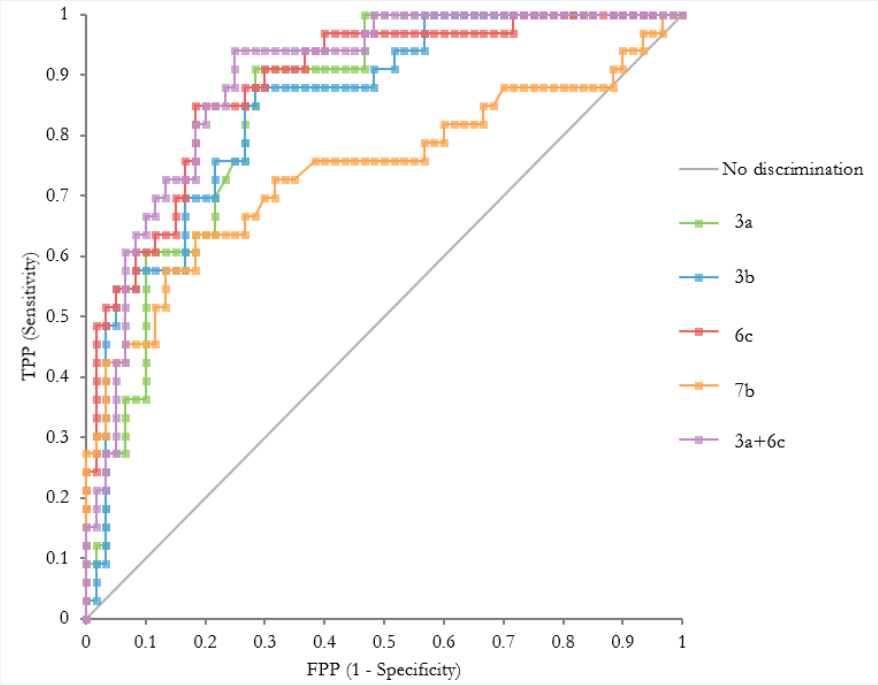

Figure 3-10: Receiver operating characteristic curve of peptides 3a, 3b, 6c 7b and 3a+6c. The diagnostic performance of each peptide is represented by a different-colored line. The solid gray line indicates the non-discrimination area of the ROC curve. The conditional sample panel, minus sample 49 was used to generate the curve (n=93).

As can be seen in Figure 3-10, peptide 7b was not a good candidate, because at some point the line approaches the non-discrimination area (random classification), which indicates that 7b does not reliably classify samples as positive or negative. Additionally, its area under the curve (AUC) is the lowest, 0.741 with a 95% confidence interval (CI) of 0.624 to 0.859 (see Table 3-15).

Peptides 3a, 3b, and 6c showed better diagnostic performance, as their ROC curves are closer to the upper left corner (see Figure 3-10). That corner, also known as the 0.1 point or perfect classification, represents 100% sensitivity (no false negatives) and 100% specificity (no false positives). Additionally, their AUC values are around 0.85 or even higher in the case of peptide 6c and the combination of 3a and 6c which were both 0.89 with a 95% CI of 0.82 to 0.95. (see Table 3-15).

Peptide ID	AUC	95% CI
3a	0.85	0.77 to 0.92
3b	0.85	0.77 to 0.93
6c	0.89	0.82 to 0.95
7b	0.74	0.62 to 0.86
3a+6c	0.89	0.82 to 0.95

Table 3-15: Area under the curve (AUC) of the ROC curve. For each peptide, the AUC and its 95% confidence interval (CI) is calculated according Wilcoxon-Mann-Whitney test.

The ROC curve allowed us to establish the best threshold or cut-off level in which each peptide reaches its best diagnostic performance. Accuracy estimators, sensitivity (Se) and specificity (Sp) for

each peptide was calculated using Analyse-it® software. We determined that the combination of peptides 3a and 6c acted synergistically in terms of sensitivity; however, we also observed that the specificity when peptides were used together was the lowest (see Table 3-16).

		cut-off (RAU)	TP	FP	TN	FN	TPP (Se)	TNP (Sp)	FPP	FNP
Peptide ID	3a	0.21	22	11	49	12	0.65	0.82	0.18	0.35
	3b	0.20	24	12	48	10	0.71	0.80	0.20	0.29
	6c	0.22	26	10	50	8	0.76	0.83	0.17	0.23
	3a+6c	0.20	32	15	45	2	**0.94**	**0.75**	0.25	0.06

Table 3-16: Accuracy estimators for each peptide. Cut-off is expressed in relative absorbance units (RAU). TP: true positive, FP: false positive, TN: true negative, FN: false negative. TPP: true positive proportion, also known as sensitivity (Se), TNP: true negative proportion, also known as specificity (Sp). FPP: false positive proportion and FNP: false-negative proportion.

3.6. Discussion

Discovering new IgM-specific antigens that might be used in an immunoassay for *T. gondii* detection remains a pressing need in the clinical management of toxoplasmosis. In this chapter, the epitope mapping study of nine *T. gondii* proteins using customized peptide microarray is presented. The study allowed us to identify different specific IgM sequences in *T. gondii* positive samples.

As an alternative to the commercially available *T. gondii* lysate antigens, we produced "artificial" antigens obtained by peptide synthesis. Then, we evaluated the potential application of the synthetic peptides as antigens for detecting IgM anti-*T. gondii* positive samples, in both multiplex and singleplex ELISA formats.

The microarray study revealed a homogeneous response profile among the IgG-positive samples evaluated. These data are consistent with the high specificity of IgG molecules selected by the immune system during a complex maturation process to recognize specifically certain proteins of *T. gondii*. In contrast, the response pattern of IgM-positive samples was heterogeneous and weaker, a fact that can be attributed to the intrinsically lower specificity of IgM antibodies (209), thus hindering the identification of IgM-specific sequences.

To select the sequences that could detect the greatest number of IgM-positive samples and not react to IgG-positives, we performed a statistical analysis that subtracted the response of IgG-positive from that of IgM-positive ones. Thus, we identified nearly 40 sequences that were upregulated in the IgM-positive vs. IgG-positive samples. Those sequences belonged mainly to dense granule protein GRA3, rhoptry protein 1 (ROP1), granule antigen protein GRA7 and major surface antigen P30. Our results are in accordance with previous findings that demonstrate the serological applications of those proteins as recombinant antigens for detecting different anti-*T. gondii* immunoglobulins (139,181,202,210,211). When using a recombinant protein as antigen, a priori, the native conformation of the protein is preserved, thus maintaining the conformational epitopes. In our approach, the peptide microarray used was based on linear epitopes, that is, non-conformational epitopes. Despite these differences, our results are consistent with those based on native proteins, and therefore we suggest that epitope mapping via peptide microarray is an appropriate technology for identifying specific antigens that are useful for detecting either anti-IgM or IgG.

In our study, we used a sera panel consisting of 16 samples (from 13 different patients, plus three depleted samples). We depleted three IgG/IgM-positive samples to increase the number of samples representing the acute phase of the disease, in which just IgM anti-*T. gondii* are present (137). However, the number of samples used is smaller than other published studies based on peptide microarray (142,159), which used around 20 samples classified as acute toxoplasmosis. In the study

carried out by Maksimov et al., none of those samples were IgG-negative, whereas in ours we were especially interested in evaluating both IgM-positive / IgG-negative and IgM-positive / IgG-positive samples. This goal was complicated by the difficulties in obtaining IgM-positive samples without IgG and justifies our decision to use IgG depletion. To our knowledge, no studies have used IgG depletion process to obtain IgM-positive samples. In taking this approach, we were able to increase the number of IgM-positive samples and to detect possible cross-reactivities among IgM and IgG, thus identifying which epitopes are specific for each type of immunoglobulin. This outcome has special relevance, as we discarded epitopes that were reactive to non-depleted samples (which had both types of immunoglobulins) but non-reactive to depleted samples (which contained only IgM anti-*T. gondii).*

The sample panel we used was characterized by means of commercial BIO-FLASH® Toxo IgG and Toxo IgM immunoassays. For all samples, we were able to correlate results obtained with the peptide microarray with those from the BIO-FLASH®, except for sample MA12, which reported the highest IgM titer among *T. gondii* IgM-positive samples. Nonetheless, when we evaluated sample MA12 with the peptide microarray, we found a weaker IgM profile than other samples reporting lower IgM titers with BIO-FLASH® Toxo IgM assay (e.g., MA7). This may reflect methodological differences between both technologies, and/or the antigens used. The BIO-FLASH® Toxo IgM assay is based on TLA, whereas the microarray contains just nine parasite proteins. Hence, IgM of sample MA12 may not be specific for any of the proteins in the array or may bind a conformational epitope not represented in the microarray.

In our study, one GRA3 peptide showed the highest score for IgM-positive sera (mean value of spot intensities), and, additionally, gave the highest value in the T-test to evaluate which peptides were upregulated in IgM-positive vs. IgG-positive samples. Robben et al. first reported that monoclonal antibodies (mAbs) obtained by immunizing mice with sonicated tachyzoites bound to a specific region of the *T. gondii* GRA3 protein. They used a novel epitope screening approach based on the display of genomic DNA fragment-encoded peptides on filamentous phage (155). Later, Beghetto et al. reported the presence of an immunoreactive region within GRA3 broadly recognized by human antibodies, especially during the first months after infection (153). GRA proteins are highly expressed by *T. gondii*; thus, anti-GRA circulating antibodies are characteristic in both acute and chronic phases of *T. gondii* infection, and, consequently they have special relevance in host immunity. GRA3 is a 30 kDa protein located in dense granule organelles. Following invasion and exocytosis, the granule content empties into the parasitophorous vacuole. The association with the vacuolar membrane makes GRA3 a good specific antigen candidate for detecting anti-*T. gondii* IgM. Therefore, our findings confirm work by the above authors identifying relevant regions in GRA3 reactive to *T. gondii* positive samples.

In a study aimed at identifying epitopes allowing to distinguish different *T. gondii* strains, Kong et al. found that GRA3 discriminated type II from non–type II infections in mice (172). Different *T. gondii* strains have been correlated with the severity of infection in mice and humans. Typically, type I is highly virulent, type II relatively avirulent and type III is intermediate (212). While the issue of severity and its obvious impact on clinical management is beyond the scope of the present work, it is worth mentioning that type II is the strain most commonly linked to both human and animal infections in Europe and the United States. Our findings, together with the evidence that strain II has a different allele encoding GRA3 protein (155,213), could suggest that GRA3-derived antigens are good diagnostic candidates to detect patients infected with strain II. Even so, further studies are needed to determine whether specific GRA3 allele differences among *T. gondii* strains are enough to make GRA3 a useful diagnostic antigen.

Several studies support the notion that ROP1 protein is involved at an early stage of *T. gondii* invasion of host cells. They show that ROP1 is secreted into the parasitophorous vacuole during parasite entry into host cells and a few hours after the invasion, the expression of ROP1 is inhibited (214–216). This rapid disappearance suggests that ROP1 plays a role in early invasion. This interpretation is what leads diagnosticians to consider ROP1 to be a marker that differentiates acute and chronic toxoplasmosis.

The peptide microarray used in this project elucidated for the first time eight different peptides within ROP1 protein which are specific for IgM anti-*T. gondii* positive samples. Aubert et al. have demonstrated higher reactivity of ROP1 for samples that contained *T. gondii*-specific IgA, IgM, and IgG (87.6% [78 out of 89 samples]) compared to samples classified as chronic infection (21.9% [23 out of 105 samples]) (200). Holec-Gasior et al. reported the usefulness of ROP1-derived recombinant antigens in an IgG ELISA avidity test for serodiagnosis of *T. gondii* infection in humans (211,217). The ROP1 recombinant protein used by Holec-Gasior encoded from the amino acid residues 85 to 396. However, our study allowed us to find a peptide with just 27 residues within the same region studied by Holec-Gasior which concentrated the highest reactivity of ROP1. Contrary to what was found by Holec-Gasior, that region was non-reactive to the IgG-positive samples used in our study. This difference could be explained by the fact that the reactivity of those samples is related to conformational epitopes that are not present when using linear peptides, but are highly conserved in recombinant constructs.

Mezzasoma et al. demonstrated equivalence between the results from a peptide microarray containing antigens of *T. gondii*, rubella virus, cytomegalovirus and herpes simplex virus types 1 and 2 (ToRCH antigens) and different commercial ELISA tests (158). Within our study, the reproducibility between the microarray and the ELISA was a key issue. To address it, we included in the multiplex ELISA

(3.4) two IgM-positive samples that were previously tested in the microarray study. Additionally, when we contrasted the results obtained by both techniques, we found that peptides 3a, 3b and 6c, which belong to proteins GRA3 and ROP1 respectively, were highly specific for IgM-positive samples. This finding was consistent with the results obtained using the microarray study, in which GRA3 and ROP1 proteins also contained most of the regions that were specific for IgM-positive samples. Thus, despite the methodological differences between Mezzasoma et al. and our study, we were able to demonstrate that the results of the peptide microarray were equivalent to those obtained with multiplex ELISA.

In that same study (158), the authors could not ascertain a similar equivalence for IgM-positive samples due to an insufficient number of IgM-positive samples. In contrast, in our study the two samples used to evaluate the equivalence (MA10 and MA11) were IgM-positive. Altogether, our findings indicate that peptide microarray is a suitable technology to identify specific antigens for detecting infectious diseases such as toxoplasmosis.

In the market one can find the BioPlex® 2200 ToRC IgM, a multiplex flow immunoassay intended for the qualitative detection of IgM antibodies anti *T. gondii*, rubella and cytomegalovirus (218,219). Guigue et al., evaluated its performance in critical cases of toxoplasmosis compared to routine technologies (i.e., PLATELIA™ IgG/IgM (ELISA) (BIO-RAD Laboratories) and Toxo-Screen direct agglutination assay (BioMérieux, Lyon, France)) (220). They included samples from patients that were monitored during seroconversion and chronification. These authors found that patients showed a trend toward a more rapid decrease of IgM titers with BioPlex® 2200 than with PLATELIA™. These results could be explained by a weaker detection of residual IgM by the BioPlex®. We were not able to include any series of samples from same patient during the course of the disease. Nonetheless, like Guigue et al., we used the PLATELIA™ among other commercial kits to characterize our samples.

Beyond characterization of the sample panel, we also used the PLATELIA™ immunoassay in the later phases of development as a confirmatory assay (see 6.1.1.3) due to the high sensitivity and specificity reported in the manufacturing data sheet (100% and 99.9%, respectively). The PLATELIA™, unlike our ELISA, captures the anti-*T. gondii* IgM using an anti-human μ chain antibody as surface coating, and for detection a mixture of *T. gondii* antigen and peroxidase-labelled murine anti-*T. gondii* P30 monoclonal antibody. This format, known as immunocapture, differs from our indirect ELISA where the synthetic peptide is the coating antigen and an anti-human μ chain antibody (peroxidase-labeled) is used for detection. These methodological differences do not necessarily justify the differences we observed in some samples that were classified as positive by our ELISA but negative by the PLATELIA™ or vice versa.

Despite the excellent performance proclaimed in the PLATELIA™ manufacturing data sheet, a study by Liesenfeld et al. highlighted a high number of false positive results compared with reference IgM ELISA (221). Despite this caveat, we used the PLATELIA™ as an FDA- (and CE) approved kit. However, some limitations have to be considered as acute infection can only be diagnosed if an increase of anti-*T. gondii* IgG antibodies in two samples drawn at a 3-week interval is observed, with presence of anti-*T. gondii* IgM at a significant level. Thus, the fact that we could not characterize samples drawn at a different time-points is a limitation of our study.

Before our sample panel was characterized, it consisted of 48 positive and 62 negative samples. Afterwards, just 28 samples tested as positive for all the methods, and 60 samples as negative. Wilson et al., found that six commercial kits for the detection of IgM anti-T. *gondii* reported more equivocal results in the false positive than the false negative group (124). These results not only coincide with our observations, but also suggest the need to improve both sensitivity and specificity to have robust diagnostic methods offering comparable and reliable results.

Given these circumstances, instead of using a reference method—the approach chosen by most studies (140,222)—we selected only the samples with total agreement across the four methods used.

The concordance between multiplex and singleplex ELISA was also a key issue. To our knowledge, apart from Baschirotto et al., no studies compares the performance of multiplex vs. singleplex immunoassays in the context of toxoplasmosis (223). This study used *T. gondii* lysate antigens as well as recombinant antigens from P30, GRA7, GRA1, ROP4, MIC3 and two GRA7, P30 and GRA8 chimeric antigens coupled onto fluorescent beads for detecting IgG anti-*T. gondii.* In both multiplex and singleplex ELISA, authors outlined good performance correlation. Singleplex ELISA reported ~100 sensitivity and 99% specificity with TLA. In contrast, multiplex ELISA showed 96-100 % sensitivity and 100% specificity with chimeric antigens. Here, we report for the first time the comparison between multiplex and singleplex ELISA based on synthetic peptides for detecting IgM anti-*T. gondii*. In our study, peptide 6c showed one-half the reactivity of 3a and 3b, while in the multiplex ELISA it showed the highest reactivity. This issue could be attributed to either sample degradation or to a manipulation error. No additional tests were performed to clarify this question, since in any case 3a, 3b, 3c and 6c were the top performers.

As mentioned, peptide 6c reported the highest sensitivity and specificity, which was corroborated in the ROC analysis, with the highest area under the curve. However, if we compare our data with other ELISA based on ROP1 recombinant antigens, particularly the study performed by Holec-Gasior et al. (211,224), both the sensitivity and specificity obtained by synthetic peptides were lower. This issue could be attributed to the higher number of epitopes present (either linear or conformational) in a

recombinant protein vs. in small peptides, a fact that could evidently influence the ability to recognize a specific type of immunoglobulin.

Considering the limitations of single peptides and the excellent results obtained in other studies based on chimeric antigens (102,177), we considered testing peptides 3a and 6c in combination, to assess if synergy was achievable. Interestingly, we observed a higher signal-to-noise ratio, even with peptide 3a concentrations nearly 10-fold lower. Additionally, we found that the combination increased sensitivity to levels comparable with other assays based on recombinant antigens (211,224). These findings led us to investigate whether fusing the 3a and 6c sequences into a single peptide molecule would improve the results relative to simple peptide combination in solution. This issue will be addressed in Chapter 4.

Overall, in the present chapter we have demonstrated that innovative technologies such as peptide microarrays are useful to identify new antigens for the diagnosis of toxoplasmosis. Additionally, we have described for the first time the use of multiplex ELISA to study synthetic peptides from *T. gondii* GRA3 and ROP1 instead of lysates (TLA) as antigens for detecting IgM-positive samples.

CHAPTER 4 – Peptide chimeras to enhance sensitivity

In the previous chapter, we showed that combining two peptides in solution enhanced reactivity compared to their individual use. In view of this, a logical next step was to design and evaluate chimeric peptides that combined the sequences of the better candidates identified in Chapter 3. The rationale for designing the chimeric peptide was thus threefold: i) to increase IgM specificity, ii) to control peptide orientation on the solid surface (i.e., polystyrene plate or magnetic particles), and to assess if, using peptides reactive not only to IgM-positive but also to IgG-positive samples, one could increase the performance of the assay.

Multimeric peptides, displaying several B and/or T cell epitopes on a single molecular scaffold, have shown to possess a wide array of biomedical applications as tools in drug design, targeted delivery, serodiagnosis, oncology and vaccinology (182,225–229). These chimeric molecules present demonstrable advantages, in that they are versatile, highly stable (i.e., compared to native proteins), easy to produce at moderate cost, and have good immunogenicity (230,231).

For that purpose, we first selected two best-performing sequences from the microarray study in Chapter 3. Next, we produced synthetic versions of those peptides using SPPS. We also included peptide 7b, after having initially discarded it, because in the microarray study it showed specific reactivity to IgG-positive samples. Finally, we labeled with biotin some of the chimeric peptides to evaluate whether peptide orientation on the solid surface could affect the assay performance.

We used a singleplex ELISA to evaluate the performance of the new chimeric constructions with IgM anti-*T. gondii* positive samples. We selected the same approach as in section 3.5 to establish the optimal assay conditions for the new peptides.

4.1. Design and synthesis of chimeric peptides based on top-performing peptides 6c & 3a

Many immunoassays rely on the attachment of antigens onto solid surfaces such as polystyrene plates or magnetic particles to detect the molecule of interest. Short synthetic peptides that are easily produced through chemical synthesis are commonly used antigens because of the high specificity they confer (9). However, many of them show less than ideal ability to bind to solid surfaces. Multimeric peptide constructs, particularly those with dendrimeric (branched) arrangements, tend to be much better than linear ones in overcoming such limitations. This is probably because those peptides tend to adopt a more extended spatial organization than linear species, providing increased

surface-binding properties and enhanced sensitivity, thus becoming more effective in disease diagnosis (99,228,232).

Multiepitope linear peptides contain more than one repeat of a given epitope in juxtaposed fashion. Multiepitope dendrimer peptides, for their part, have branched architectures with high molecular organization and stability. In dendrimers, the molecular scaffold is built around a core matrix to which different branches are tethered. Different amino acids are used for core formation, but lysine (Lys) is used preferentially because its two amino groups (α, ε) can be utilized as branching points to generate multiplicity (171,225).

In this work we have designed and produced both types of multiepitope peptides, i.e. constructs with various repeats of the same epitope (chimeric homotandems), in both linear and branched versions as well as constructs with more than one repeat of different epitopes, those always in linear fashion. Additionally, we produced peptide constructs to optimize peptide immobilization by biotin labeling. All peptides were synthesized in C-terminal carboxamide form using Fmoc solid phase synthesis, purified to >95% homogeneity using HPLC, and satisfactorily characterized using MS.

4.1.1. Chimeric homotandems

Although the sequences used in this project cannot be revealed due to confidentiality and industrial property concerns, it is worth mentioning an interesting feature of peptide 6c, composed of a tandem repeat of eight residues, *BBBJOUXZ*, where residue *O* is altered in each repeat (i.e., *O, O'* and *O"*, Figure 4-1). Given the presence of those block-tandem sequences in ROP1 protein (234) we hypothesized that these eight residues might be involved in recognizing IgM.

On that basis, we designed and produced other chimeric peptides with more than one repetition of the 6c sequence minus the two N-terminal residues (hereinafter named truncated 6c) as a motif for three different constructions, namely i) homotandem with two consecutive stretches of truncated peptide 6c (ID 6c*2), ii) homotandem with two truncated 6c peptide sequences separated by a flexible spacer (8-amino-3,6-dioxaoctanoic acid (O_2Oc)) (ID 6cO36c†), and iii) branched bivalent peptide based on a lysine core from which two truncated 6c peptide sequences branched out (ID $(6c^*)_2K_3$) (Figure 4-2).

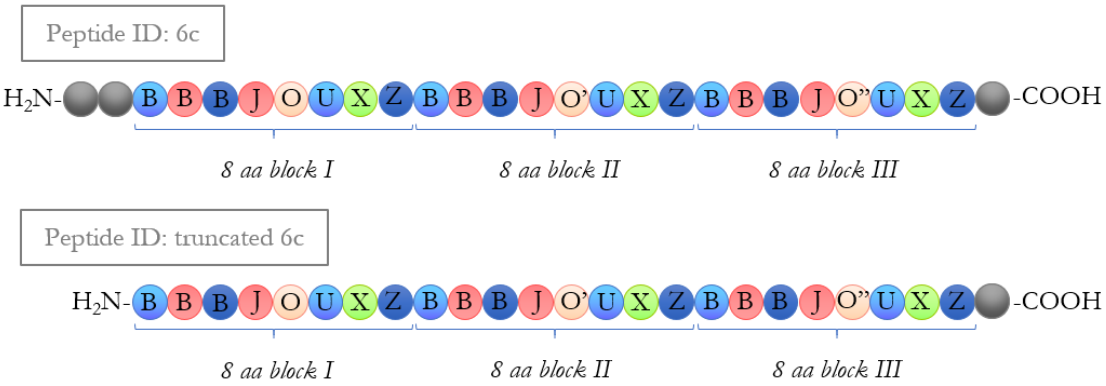

Figure 4-1: Schematic representation of original and truncated version of peptide 6c. 6c peptide consisted of the tandem repetition of three blocks of eight amino acids plus two amino acids in the N-terminus, and one amino acid in the C-terminus (27aa). Truncated 6c peptide consisted of the same block tandem repetition minus two amino acids in the N-terminus (25 aa). Each different amino acid within the block is named with a different letter. O, O' and O" represent the single amino acid that changes within the block.

4.1.2. Chimeric heterotandems

To assess whether the combination of peptides 3a and 6c in a single construction could enhance the reactivity achieved with the original sequences tested together in solution (see Chapter 3), we designed and produced two chimeric peptides as follows i) a heterotandem construct combining truncated 6c and 3a sequences using 8-amino-3,6-dioxaoctanoic acid (O_2Oc) as a flexible spacer between them (ID 6c3a), and ii) the reverse heterotandem version in which we merely changed the sequence order of truncated 6c and 3a peptides (ID 3a6c) (Figure 4-2).

4.1.3. Biotin-labeled peptides

In many instances, proteins or peptides are randomly immobilized by simple adhesion to immunoassay solid surfaces, which results in a loss of functional epitopes that are responsible for bestowing specificity for the molecule that we aim to capture. Biotin labeling has been used for several decades for protein and peptide orientation as well as for numerous laboratory research techniques (i.e., label, detect, and purify). The biotin moiety has a very strong affinity for streptavidin (K_d <10^{-10}M) and biotinylation is, therefore, an efficient method for specifically binding peptides to streptavidin-coated surfaces. Biotinylation can be performed either at the N- or C-terminus. At the N-terminus it can be conducted directly on the primary-terminal amino group, which was the strategy we selected.

We synthesized and purified different biotin-labeled peptides to study how distinct peptide orientations on the immunoassay surface could affect the reactivity of the resulting assay; i) biotin-labeled 3a sequence (ID 3ab), ii) biotin-labeled truncated 6c peptide (ID 6c*b), iii) 3a6c biotin-labeled heterotandem (ID 3a6c*b) and iv) biotin-labeled 7b peptide (ID 7bb).

A complete list of all new chimeric peptides can be seen in Table 4-1 and a schematic representation in Figure 4-2.

Peptide ID	Prot. Acronym	Theoretical mass[a] (Da)	Size (aa)	Net charge[b]	RT[c] (min)	ACN grad[d]	ACN[e(%)]	Purity[f] (%)
$6c^*_2$	ROP1	5260	50	-6	6.6	15-40	29	98
$6cO_36c^\dagger$		5695	52	-6	7	15-40	31	97
$(6c^*)_2K_3$		6092	55	-6	8	10-60	32	96
$6c^*b$		2912	25	-3	6.9	15-50	30	98
3ab	GRA3	4052	40	-5	10	25-70	42	98
$6c^*3a$	ROP1-GRA3	6828	67	-8	12	20-60	40	97
$3a6c^*$	ROP1-GRA3	6828	67	-8	8	15-60	34	97
$3a6c^*b$	ROP1-GRA3	7055	67	-8	8.5	15-60	39	97
7bb	GRA6	3361	31	-8	7	15-40	28	96

Table 4-1: Chimeric, biotin-labeled, and common IgG peptides used in this study. [a]Theoretical molecular mass was calculated using GPMAW software (version 8.10). [b]Net charge of the peptide was calculated using ExPASy ProtParam website (https://web.expasy.org/protparam/). [c]Retention time (RT), referred as the minutes from injection to detection. [d]Analytical RP-HPLC was performed using linear gradients of solvent B (0.036% TFA in ACN) into A (0.045% TFA in H2O) over 15 min at 1 mL/min flow rate and with UV detection at 220 nm. [e]% acetonitrile (ACN) at peptide elution time. [f]Peptide purity was calculated using the percentage of peak area at the chromatographic profile. 6c* indicates the 6c truncated peptide.

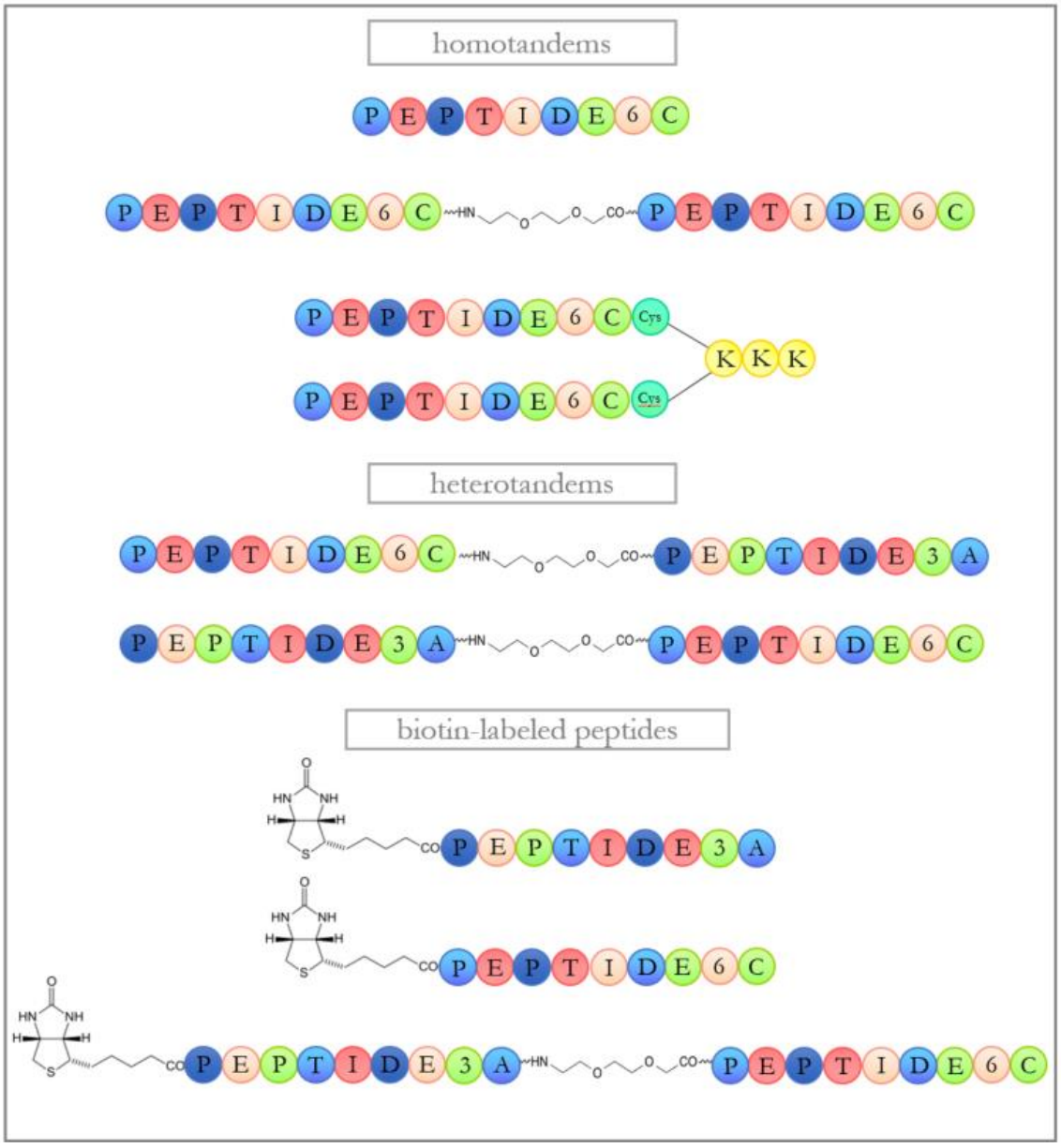

Figure 4-2: Schematic representation of the chimeric and biotin-labeled peptides. 6c homotandems consisted in tandem repetition of the 6c peptide in three different formats. 3a and 6c heterotandems consisted of tandem repetition of 3a and 6c sequences using O_2O_c as a spacer, in different orientations. 3a and 6c truncated peptide were biotin-labeled.

4.2. Evaluation of chimeric peptides via enzyme-linked immunosorbent assay

Once we had synthesized the chimeric peptides, we evaluated their ability to detect IgMs compared with the original peptides. Initially, we established the optimal assay conditions. To do so, we reproduced the procedure used with the original sequences (see 3.5.2). Since we knew the optimal assay conditions of the original sequences with which we designed the chimeric peptides, we established the different concentration ranges to be tested based on previous data. Thus, we used

from 0.2 to 8 x 10^{-4} μg/mL for all chimeric peptides. For common IgM-IgG peptides, since they were being tested for the first time, we evaluated wider concentration ranges (from 50 to 0.2 μg/mL) (Table 4-2).

The checkerboard evaluation revealed that the signal-to-noise ratio (SNR) of chimeric peptides increased almost two-fold compared with that obtained by the combination of 3a and 6c peptides in solution (Table 4-2). The chimeric peptide that showed the lowest SNR ratio was $(6c^*_2)K_3$. In contrast, 3a6c* showed the highest SNR. The common IgM-IgG sequences (peptides 8a and 9a) showed lower SNR compared with the original sequences tested in Chapter 3, indicating they were not good candidates to be used as antigens.

Peptide ID	**Chimeric peptides**					**Original peptides**
	$6cO_36c$	$6c^*_2$	$(6c^*_2)K_3$	$6c^*3a$	$3a6c^*$	3a+6c
tested concentration (μg/mL)	0.2 - 8 x 10^{-4}					10 to 0.6 0.2 to 0.05[a]
samples used (pos/neg)	46/87					46/88
selected concentration (μg/mL)	0.2					1.25-0.2[b]
conjugate dilution	1/2000					
$A_{450/630}$ pos sample	2.29	2.53	2.34	2.15	2.29	0.98
$A_{450/630}$ neg sample	0.22	0.27	0.31	0.25	0.21	0.23
Signal-to-noise-ratio	10.3	9.3	7.5	8.5	11	4.3

Table 4-2: Checkerboard results overview of chimeric peptides. [a]Peptide 3a was tested from 10 to 0.6 μg/mL and peptide 6c from 0.2 to 0.05 μg/mL. [b]Selected concentration for 3a and 6c peptide, respectively.

Once we evaluated the chimeric peptides with the checkerboard, we analyzed their performance with the conditional sample panel (n=94).

The use of chimeric peptides did not increase assay performance compared with the peptide combination in solution (3a+6c), except for 3a6c (see Table 4-3) which reached the same number of true positives (TP), one true negative (TN), one false positive (FP) and one false native (FN) fewer than 3a+6c.

		cut-off (RAU)	TP	FP	TN	FN	TPP (Se)	TNP (Sp)	FPP	FNP
Peptide ID	3a+6c	0.20	32	15	45	2	**0.94**	**0.75**	0.25	0.06
	$6c_2$*	0.31	30	22	38	3	0.91	0.63	0.37	0.09
	$6cO_36c$*	0.22	30	23	37	3	0.91	0.62	0.38	0.09
	$(6c_2)K_3$	0.31	31	22	38	3	0.91	0.63	0.37	0.09
	6c3a	0.31	31	16	44	3	0.91	0.73	0.27	0.09
	3a6c*	0.29	32	14	46	1	**0.97**	**0.77**	0.23	0.03

Table 4-3: Accuracy estimators for each chimeric peptide. Cut-off is expressed in relative absorbance units (RAU). TP: true positive, FP: false positive, TN: false negative, FN: false negative. TPP: true positive proportion, also known as sensitivity (Se), TNP: true negative proportion, also known as specificity (Sp). FPP: false positive proportion and FNP: false-negative proportion.*n=93 due to lack of sample volume.

Figure 4-3 presents the ROC curve of all chimeric peptides. $6cO_36c$ peptide runs at some point on the non-discrimination area, indicating that it is not able to classify samples according to their real status (sensitivity of 91% and specificity of 63%). Although the sensitivity is the same and the specificity is similar to that of $6c_2$, 6c3a, and $(6c_2)K_3$ peptides, none of the other ROC curves crossed the non-discriminatory line, which indicates that for this specific threshold, only $6cO_36c$ peptide classified the samples incorrectly.

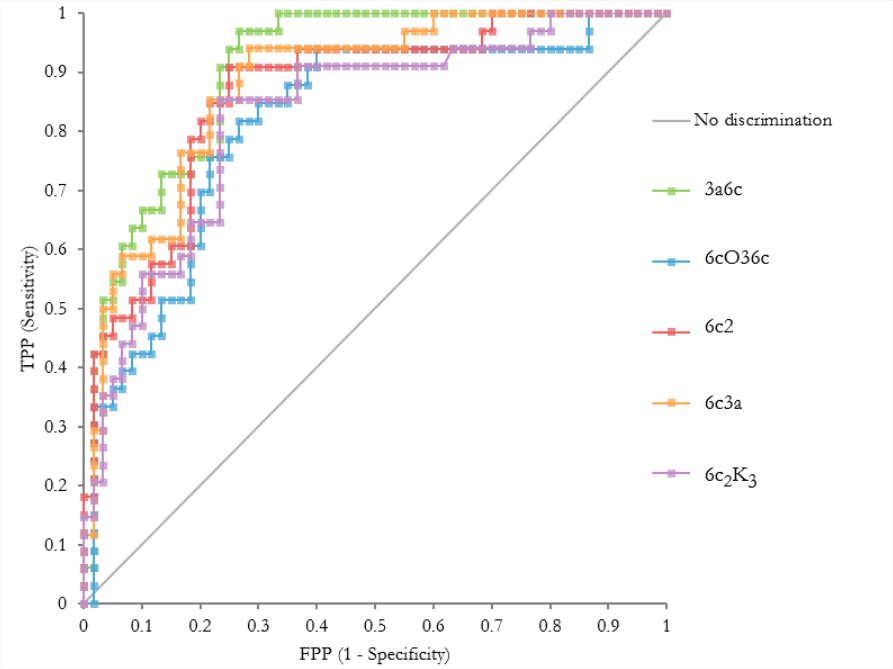

Figure 4-3: Receiver operating characteristic curve of chimeric peptides. The diagnostic performance of each peptide is represented by a different color line. The solid gray line indicates the non-discrimination area. The conditional sample panel, minus samples 49 and 31 (n=92) were used to generate the ROC curve for peptides $6c_2$, $6cO_36c$ and 3a6c. For peptides $(6c_2)K_3$ and 6c3a, the conditional sample panel, minus sample 31, (n=93) was used.

We also calculated the area under the curve (AUC) of each ROC with a 95% confidence interval (Table 4-4). Peptide 3a6c showed the highest AUC (0.90), followed by 6c3a peptide (0.88).

Peptide ID	AUC	95% CI
3a6c	0.90	0.85 to 0.96
6c$O_3$6c	0.82	0.72 to 0.91
6c$_2$	0.86	0.79 to 0.94
6c3a	0.88	0.81 to 0.94
(6c$_2$)K$_3$	0.82	0.74 to 0.91

Table 4-4: Area under the curve (AUC) of the ROC curve. For each chimeric peptide, the AUC and its 95% confidence interval (CI) were calculated using a Wilcoxon-Mann-Whitney test.

4.3. Evaluation of biotin-labeled peptides via ELISA

Until now, we have seen that 3a6c chimeric peptide, which combined the sequence of 3a and 6c peptides within the same molecule, increased assay performance compared with the performance obtained with the same peptides tested together in solution (3a+6c). As explained above, peptides that are randomly immobilized on the surface of ELISA plates are prone to lose by occlusion functional epitopes, with a direct impact on assay performance. Thus, we wanted to elucidate if we could obtain better assay performance by controlling orientation by using biotin-labeled peptides.

Although we knew that the best candidate hitherto was the 3a6c chimeric peptide, we went on to evaluate the biotin-labeled truncated 6c peptide (6c*b). We performed a checkerboard to establish the optimal assay conditions. Since we already knew the optimal conditions for its non-labeled analogue, we started with a peptide concentration of 2.5 μg/mL on a streptavidin-coated 96-well plate (see section 3.5.2).

Surprisingly, we were not able to obtain a control condition with acceptably low reactivities. The absorbance of the strips containing no peptide (blank) was similar to that obtained using 2.5 μg/mL of biotin-labeled peptide (data not shown). We wondered whether this was due to an inappropriate blocking step (performed with commercial blocking reagent) or to damaged streptavidin-coated plates. Thus, we repeated the same experiment twice with new lots of peptide, new streptavidin-coated 96-well plate, and new buffers, but we obtained similar results (data not shown).

Because we could not validate the functionality of the 6c*b peptide using streptavidin-coated plates, we performed the same experiment using standard ELISA plates. When we did so, the absorbance of the blank was what we expected, and the absorbance of the strips that contained 2.5 μg/mL of 6c*b peptide, despite being lower than that obtained with 6c peptide was three times higher than the blank (data not shown).

These results triggered a period of troubleshooting in which different biotin-labeled peptides, including the 3a6c* chimeric peptide, were evaluated together with different positive and negative samples, and we obtained similar results. Additionally, despite the fact that MS showed that the 6c*b peptide had a molecular mass consistent with theory and acceptable purity, we repeated the synthesis and the experiments, obtaining similar outcomes. At this point, since we had an optimal chimeric peptide to work with, we decided to move forward and re-evaluate the biotin-labeled peptides when we started the chemiluminescence-based assay, using streptavidin-coated magnetic beads.

After all the troubleshooting, we postulated that biotin-labeling was affecting the ability of the peptide to recognize IgM. If confirmed, this would imply that the recognition of IgM is closely related to the N-terminus, considering that we had used NHS-maleimide biotin to label the N-terminus of the peptide.

4.4. Discussion

The number of studies that have demonstrated the potential advantages of chimeric or synthetic peptides as antigens for the serological diagnosis of *T. gondii* infection is growing. In comparison to recombinant proteins, they stand out for their simple standardization, high sensitivity, low contamination with foreign proteins, low production cost, and higher probability of discriminating between the different stages of toxoplasmosis (138,142,178,179,235,236).

Chimeric synthetic peptides are designed to include various epitopes from different *T. gondii* antigens properly selected according to their immunoreactivity. In recent years, a variety of innovative tools have been developed to predict specific *T. gondii* epitopes, including immunoassays based on chimeric synthetic antigens.

As described in this chapter, we evaluated the diagnostic utility of different chimeric peptides based on two antigenic regions of GRA3 and ROP1 *T. gondii* proteins to replace the lysate antigen in serologic tests. We also assessed the utility of including in the immunoassay peptides that were common for both IgM and IgG anti-*T. gondii*. Additionally, to elucidate how peptide orientation affects assay performance, we evaluated biotin-labeled peptides.

In the literature several studies have demonstrated the usefulness of recombinant antigens produced either in *E. coli* or in *P. pastoris,* which combined different epitopes in a single molecule for the serological diagnosis of toxoplasmosis. These antigens included dense granule proteins, rhoptry antigens, microneme proteins, and surface antigens (37,138,175,176,178,179,181,210,237,238). However, the exact composition of a recombinant cocktail that mimics the antigenic repertoire present in *T. gondii* lysate antigen and is adequate for the detection of IgM antibodies is still an open question (175,200). Our study presents for the first time the use of synthetic chimeric peptides (non-recombinant) as antigens for the detection of IgM-anti-*T. gondii*.

Holec-Gasior highlighted the importance of selecting the proper protein fragments to construct recombinant chimeric antigens to have the highest reactivity in ELISA (181). Our rationale to select the epitopes was based on previous studies that analyzed the usefulness of GRA3 and ROP1 in diagnostic tests and described them as potential markers of recent *T. gondii* infection. These studies are described in Chapter 3, where we additionally demonstrated that the combination in solution of 3a and 6c peptides enhanced assay performance compared with the peptides alone. Based on these results, we designed and produced different synthetic chimeric peptides combining such peptides and evaluated their performance in a singleplex ELISA.

From our list of *T. gondii* antigens, only SAG1 (also known as P30) has been crystallographed (45). Despite the lack of conformational studies about ROP1, several articles elucidate its role and correlate

it with its sequence (215,216,234). The amino acid sequence of ROP1 contains an interesting charge asymmetry; an acidic N-terminal and central region due to the presence of a series of tandem octapeptide repetitions rich in proline and glutamic acid, and a basic C-terminal region, rich in arginine (181). Based on this observation, we proposed for the first time that the capacity of ROP1 to recognize IgMs is related to the octapeptide repetitions. Thus, we designed both a truncated version, which lacked two amino acids in the N-terminus, and different chimeric homotandems based on those sequences, and we evaluated their performance in front of a panel of *T. gondii* positive and negative samples.

The use of synthetic chimeric homotandems for the diagnosis of infectious diseases is not new. Kim et al. compared the reactivity of several immunoassays based on different peptide constructions made from the HIV-1 V3-loop peptide. These included two-to-five tandem repetitions and two-to-eight branched peptides (239). In their study, the V3-loop linear peptide showed low reactivity due to low solid-phase binding efficiency and loss of native conformation. However, when tandem repetition and branched peptides were used, they observed that the reactivity of the immunoassay increased. That increase could be explained by a gain of interaction (mainly hydrophobic) between the peptide and the solid phase. Regarding the loss of conformation, the use of tandem and branched peptides could be an advantage, as other parts of the molecule remain conformationally available and free for antibody binding. In our study, contrary to what Kim et al. described, we found that 6c peptide showed good reactivity to IgM anti-T. *gondii* positive samples (see Chapter 3). However, unlike what they observed, in our study not all chimeric homotandem peptides enhanced assay performance compared to monomeric peptides. Additionally, Kim et al. reported an improvement limit related to peptide repetitions, as above three peptide repetitions or four branches, the assay sensitivity remained stable. However, in our study we did not evaluate the performance of chimeric homotandems with more than two peptide repetitions, either in linear or branched format.

Kim et al. concluded that branched peptides are better than tandem repeats because of their higher sensitivity and lower production cost. A possible explanation is the greater antigen density of branched peptides (i.e., the number of binding sites per surface area). However, our study does not lead to the same conclusion because, on the one hand, all our chimeric homotandems showed similar performance, and on the other hand, we did not synthesize a branched heterotandem combining both 3a and 6c peptides. Thus, we could not evaluate if such a conformation increases the performance obtained by the 3a6c linear peptide. Given this, our results could be related to the combination of two different epitopes in a single molecule, more than with conformation. Even so, since every peptide has different chemical and physical properties, more studies would be needed to clarify if branched conformation combining both peptides could be applied to our assay and what their performance would be.

In addition to synthetic chimeric peptides, we synthesized and evaluated the performance of IgM-IgG common peptides. Both 8a peptide, which belongs to MIC3, and 9a peptide, which belongs to GRA4, have been previously described by different researchers as good markers for the detection of recently acquired infections and therefore as potential antigens for diagnosing the acute phase of toxoplasmosis (135,142,213). To see the value of using MIC and GRA proteins as biomarkers, it is important to understand their role during *T. gondii* invasion.

The mechanisms underlying the invasion of host cells by *T. gondii* have not been completely clarified. However, several studies indicate that unlike the endocytosis processes used by bacteria and viruses, *T. gondii* actively invades cells, and it seems that MIC proteins are essential in this process. When the parasite contacts the host cells, it first pushes the conoid outside the body, and then, micronemes discharge a large number of MIC proteins through the conoid. MIC proteins, including MIC3, interact with their receptors on the host cell membrane and are distributed on the parasite's surface. At the front end of the parasite, MICs move to the rear end through the force produced by actin proteins, which allows cell invasion through the moving junction (135). In this way, MICs play a bridging role between parasites and host cells. Beyond invasion, MIC3 is expressed at all stages of the life cycle of *T. gondii*, which makes this antigen a promising candidate for the diagnosis of toxoplasmosis. GRA proteins, which are equally indispensable for *T. gondii,* are contained in a structure called dense granules, which are secretory vesicular organelles that participate in the modification of the parasitophorous vacuole and their membrane, which is fundamental for the maintenance of intracellular parasitism in almost all nucleated host cells (240). GRA proteins constitute the main circulating antigens in both acute and chronic phases of *T. gondii* infection and therefore they are widely used as antigens for toxoplasmosis detection (149).

Several researchers have used MIC and GRA proteins to develop methods to detect IgG anti-*T. gondii*. Beghetto et al. established an IgG avidity assay based on MIC3 recombinant antigens to detect low-avidity IgG antibodies in sera collected within two months after primary infection (202). Maksimov et al. developed a peptide microarray-based on different *T. gondii* linear epitopes from GRA1, GRA2, GRA4, and MIC3 and evaluated their reactivity to sera from patients with acute, latent, and ocular signs of toxoplasmosis. GRA4- and MIC3-derived peptides recognized up to 60% of the acute patients, but only 40% of latent patients (142). Nigro et al. developed an immunoassay based on recombinant GRA4 antigen to detect IgG anti-*T. gondii* in patients with acute toxoplasmosis (241). Thus, both MIC3 and GRA4 have been demonstrated to be effective for detecting the acute stage of *T. gondii* infection. However, in our study, these peptides failed to detect IgM-positive samples, despite the microarray results reported in Chapter 3. These differences with our results could be related to the fact that for the first time we aimed to use those antigens to detect IgM anti-*T. gondii*, not IgG, which was the target of Beghetto et al., Maksimov et al., and Nigro et al.

When immobilizing target molecules such as synthetic peptides on a solid surface, it is essential to control the orientation. There are several approaches for immobilizing peptides, including passive adsorption, chemical fixation and specific protein-protein interactions (i.e., streptavidin-biotin) (242). Passive adsorption may be highly variable depending on protein composition and exposure of hydrophobic patches, which could directly affect assay sensitivity. This phenomenon could be pronounced during immobilization of a mixture of multiple proteins, as in the case of the immunoassays based on *T. gondii* lysate antigens (109,243). In the present study, we aimed to evaluate how peptide orientation on the solid surface could affect assay performance. For this purpose, we used biotin labeling. However, none of the tests we performed gave us significant results. The different troubleshooting experiments we performed did not clarify the reason why the biotin-labeled peptides were not able to detect the IgM-positive samples. In a further step, the same peptides will be used in streptavidin functionalized magnetic beads.

Altogether, with the results obtained using singleplex ELISA we were able to select which synthetic chimeric peptide was appropriate to be used as an antigen for detecting IgM-positive samples instead of *T. gondii* lysate antigen. In the next chapter, we will evaluate 3a6c chimeric peptide as antigen in a chemiluminescence based immunoassay, thus replacing the polystyrene solid surface of the ELISA plate with magnetic beads and the manual procedure for a fully automated chemiluminescent autoanalyzer.

CHAPTER 5 – Development of a chemiluminescent immunoassay based on synthetic peptides for the diagnosis of human toxoplasmosis

Detection methods as radioimmunoassay (RIA) and enzyme-linked immunoassay (ELISA) have been utilized for decades for a variety of biological, chemical, and clinical purposes. Despite so, some of their drawbacks (i.e., use of radioactive reagents, high costs, long reactions, lack of reproducibility, etc.) fostered the development of new technologies adapted to laboratories' needs (107,127,160,244).

Chemiluminescent immunoassays (CLIA) are based on the detection of conjugated proteins that emit light in a chemiluminescent reaction. This technology offers several advantages over manual techniques, such as extreme analytical sensitivity under low analyte concentrations (it can reach the range of zeptomoles of protein (10^{-21} mol)), shorter incubation steps, non-hazardous materials are required, and also, it can be automated with the use of a luminometer (103,107).

With the consolidation of chemiluminescence in serological testing, clinical laboratories opt for such technology not only to reduce costs in the medium and long term but also, with automation, to avoid human error and deliver clinicians reliable results that directly impact the management of patients and their quality of life (245,246).

In previous chapters, we have seen how chimeric synthetic peptides are suitable to be used as antigens to detect IgM anti-*T. gondii* in ELISA. However, in response to current laboratory demands, in the present chapter we describe the development of a CLIA based on the chimeric synthetic peptide that demonstrated the greatest capacity to distinguish IgM anti-*T. gondii* positive samples (see Chapter 3).

One of the most effective approaches of CLIA to detect a particular analyte is to attach the capture molecule onto paramagnetic beads. The paramagnetic properties of these particles allow detection and isolation steps to occur concurrently. Besides, the pair analyte and conjugate can be quickly separated from any contaminants or free substrate and concentrated at the same time, which makes it possible to reach higher sensitivity.

To achieve our goal, we first assessed if the selected peptide remained functional after being coupled onto magnetic beads and therefore, if our prototype could detect positive samples. Then, we evaluated preliminary assay performance, and finally, we used design of experiments (DOE) method to optimize assay formulation. Additionally, we studied if different assay definitions on the BIO-FLASH® autoanalyzer could improve assay performance.

5.1. Characterization of samples

Forty-nine human sera coming from Biokit biobank were selected and evaluated by means of the BIO-FLASH® Toxo IgG and Toxo IgM. We aimed to obtain a representative panel of what the assay might encounter in the laboratory: i) negative samples from patients not suffering the disease and/or blood-bank samples (apparently healthy individuals), ii) positives samples with concentrations covering all the expected assay range, including cut-off and high positive samples, iii) samples selected with other criteria (i.e., known potentially interfering conditions).

According to BIO-FLASH® results, and the volume available, some samples were pooled, and others were maintained as individual samples. We classified them into four groups considering the presence or absence of IgG and IgM anti-*T. gondii*; i) G neg/M neg, ii) G pos/M neg, iii) G pos/M pos and iv) G neg/M pos. Then, we pooled several samples within each group to obtain higher volumes of each subgroup. Hence, the formulation panel was composed of 12 samples (Table 5-1).

Group	G neg/ M neg	G pos/M neg	G pos/M pos	G neg/M pos
Subgroup	1) NEG POOL 1	6) POOL LOW G	8) SD7106	*
	2) NEG POOL 2		9) 2574Q	
	3) NEG POOL 3		10) POS POOL 1	
	4) NEG POOL 4	7) POOL HIGH G	11) SD7106/5713	
	5) NEG 5713		12) 2574Q/5713	

Table 5-1: Description of formulation panel (n=12). The presence or absence of IgG and IgM anti-*T. gondii* was used to classify the samples. Each group was subdivided into different subgroups considering the reported value or the volume to generate different pools of samples. * These samples were excluded.

We pooled the IgG/IgM-negative samples, named G neg/M neg (n=26), into four subgroups according to anti-*T. gondii* IgG titer. NEG POOL 1 corresponds to samples that reported values <0.9 IU/mL. NEG POOL 2 and 3 was formed by samples reporting 1 and 5 IU/mL respectively. NEG POOL 4 included samples <5 IU/mL. NEG 5713, of which we had a large volume, was maintained as an individual sample, constituting an independent subgroup.

IgG-positive/IgM-negative samples, named as G pos/M neg (n=13), were pooled into two subgroups. POOL LOW G was made of samples that reported <12 IU/mL, whereas POOL HIGH G comprised samples that reported >12 IU/mL.

Unlike previous groups, IgG/IgM-positive samples, G pos/M pos (n=7), were pooled according to their IgM anti-*T. gondii* titer. We pooled together the samples that reported results between 1 and 5 S/CO, (POS POOL 1). SD7106 and 2574Q, of which we had large volumes, were maintained as individual samples. Additionally, to increase the number of samples in the medium assay range, we

diluted SD7106 and 2574Q with sample 5713 (G neg/M neg), generating two additional samples; SD7106/5713 and 2574Q/5713.

IgG-negative/IgM-positive samples, G neg/M pos, were difficult to obtain. Of the 49 samples initially screened, only three had these characteristics. We decided to exclude them, anticipating that the volume (~3 mL) would not be enough to be used throughout the proof of concept phase.

5.2. Chemiluminescent immunoassay formats

CLIA assay can be classified, depending on the disposition of the molecule used to capture the analyte of interest, in regards to the solid-phase (102). In this project, we evaluated two different formats: indirect, in which the capture molecule is directly coated onto the magnetic beads, and immunocapture, in which anti-IgM antibodies are coupled to the magnetic beads. Additionally, for the indirect format, we tested two types of magnetic particles: tosyl and streptavidin-activated beads.

5.2.1. Indirect assay using tosyl and streptavidin-activated magnetic beads

Following in-house standard procedures, we produced two lots of tosyl and two lots of streptavidin magnetic beads. One lot of tosyl beads was coated with the 3a6c chimeric peptide, named 3a6c-Indirect Tosyl Prototype 1 (3a6c-ITPT1). A different lot was blocked with BSA and used as a control.

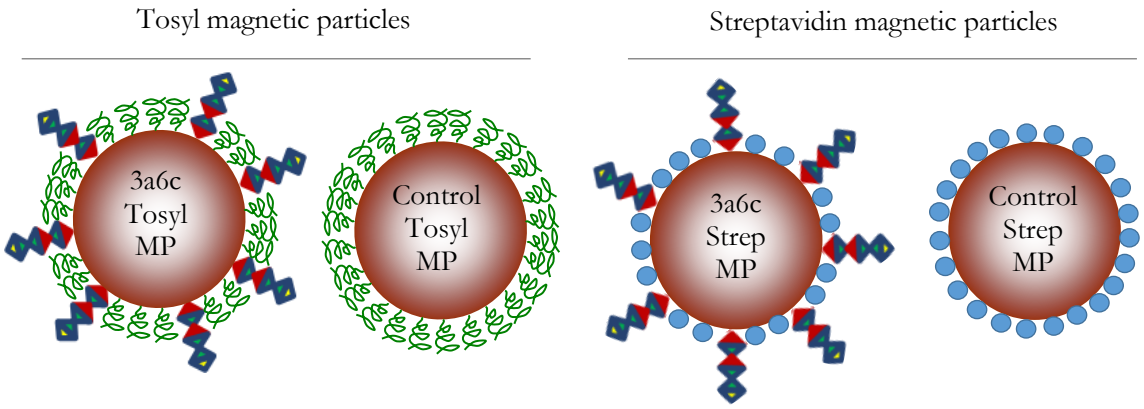

Figure 5-1: Schematic representation of the microparticles used for the indirect approach. Tosyl and streptavidin magnetic beads coated with the 3a6c peptide and their respective controls are represented.

Regarding streptavidin beads, one lot was coated with the 3a6c-biotin-labeled chimeric peptide, named 3a6c-Indirect Strep Prototype 1 (3a6c-ISPT1), a second lot was blocked with biotin and used as a control.

To evaluate each new microparticle lot we tested both, the formulation panel (n=12), and the commercial BIO-FLASH® Toxo IgM calibrators and controls (n=4) (Biokit, Spain). Calibrator 1 and negative control allowed to measure the assay background, while calibrator 2 and positive control

were used to estimate the reactivity of positive samples. For the evaluation, we used standard assay buffer and tracer formulations. At the same time, all samples were tested with the commercial BIO-FLASH® Toxo IgM (Biokit, Spain).

To determine if the new lots were able to distinguish positive from negative real samples (not standards), we calculated different assay estimators: the mean of both negative and positive samples, as well as the span (mean of positive divided mean of negative samples). Results can be seen in Table 5-2.

Sample class.	Sample ID	Interp.[a]	BIO-FLASH® Toxo M	3a6c-ITPT1	Control Tosyl	3a6c-ISPT1	Control Strep
Standards (n=4)	Cal 1	NEG	667	309	294	490	624
	Cal 2	POS	13371	1369	328	4205	813
	NC	NEG	3867	686	299	1383	339
	PC	POS	26859	3841	324	14280	694
Formulation panel (n=12)	NEG POOL 1	NEG	2919	413	360	3645	5958
	NEG POOL 2	NEG	2021	572	397	3355	3431
	NEG POOL 3	NEG	3514	913	439	7732	10164
	NEG POOL 4	NEG	3324	711	568	2070	5073
	NEG 5713	NEG	719	345	338	456	673
	POOL LOW G	NEG	2793	1378	472	6752	4089
	POOL HIGH G	NEG	2690	806	419	4477	8299
	SD7106	POS	57287	4204	692	72780	21919
	2574Q	POS	78394	25969	392	103042	2931
	POS POOL 1	POS	28324	7742	412	34134	6901
	SD7106/5713	POS	37954	2250	572	33422	10482
	2547Q/5713	POS	53543	11375	326	45264	1618
Assay estimators	Mean Neg		2569	734	428	4070	5384
	Mean Pos		51101	10308	479	57728	8770
	Span		20	14	1	14	2

Table 5-2: Evaluation of the formulation panel with 3a6c-ITPT1 and 3a6c-ISPT1. All results are shown in RLU. [a]Interpretation was done according to BIO-FLASH®. (NC: negative control and PC: positive control).

Calibrators and controls reported expected results when they were analyzed with the BIO-FLASH® Toxo IgM. Additionally, the RLU of the calibrator 1 tested with the 3a6c-ITPT1 were lower than with the BIO-FLASH® Toxo IgM, indicating the absence of non-specific binding.

The RLU of the positive control with the 3a6c-Indirect Tosyl Prototype 1 were 5-fold the negative, indicating that the assay was able to distinguish positive from negative standards. Regarding the formulation panel, the difference between positive and negative samples increased respect standards (span = 14).

Interestingly, contrary to what we observed in streptavidin-coated ELISA plates (see Chapter 3), 3a6c-Indirect Strep Prototype was able to distinguish negative from positive in both standards and real samples.

While the reactivity of the control tosyl particles remained below 1000 RLU in both standard and real samples, the control strep particles reactivity increased 10-fold in the real samples compared to the standards, suggesting the presence of some interferent component (i.e., endogenous biotin).

Overall, preliminary data indicated that both 3a6c-ITPT1 and 3a6c-ISPT1 were specific for anti-*T. gondii* IgM. However, although both assays reported the same span, the higher risk of interference (i.e., endogenous biotin) and foreseeing the higher costs of streptavidin magnetic beads, we did not pursue the 3a6c biotinylated peptide, therefore continuing the study only with the tosyl magnetic beads.

5.2.1.1. Evaluation of the screening panel with the indirect CLIA prototype

Once we demonstrated that the CLIA based on 3a6c chimeric peptide was functional and able to discriminate the sample status of the formulation panel (n=12 pooled samples), we evaluated its performance with part of the screening panel (3.3.1). This panel (n=94 non-pooled samples) was previously generated to scan the peptides with the multiplex ELISA.

We represented the reactivity versus the samples' status on a ROC curve using Analyse-it® software (data not shown). Based on the accuracy estimators, we established a tentative cut-off at 1229 RLU (Table 5-3).

cut-off	TP	FP	TN	FN	TPP (Se)	TNP (Sp)	FPP	FNP
998	29	9	51	5	0.85	0.85	0.15	0.15
1229	29	8	52	5	**0.85**	**0.87**	0.13	0.15
1093	28	8	52	6	0.82	0.87	0.13	0.18

Table 5-3: Accuracy estimators of 3a6c-ITPT1 at different cut-off levels. Cut-off is expressed in RLU. TP: true positive, FP: false positive, TN: true negative, FN: false negative. TPP: true positive proportion, also known as sensitivity (Se), TNP: true negative proportion, also known as specificity (Sp). FPP: false positive proportion and FNP: false-negative proportion.

At that cut-off, the number of false positive and false negative results was the minimum, therefore our prototype reported 85% sensitivity and 87% specificity. Although the preliminary results were acceptable, the next step was to optimize the formulation to increase assay performance (see section 5.3).

5.2.2. Immunocapture assay format

Contrary to indirect, IgM immunocapture assays use anti-IgM antibodies attached to the solid-phase to capture the IgMs present in the sample. However, with this approach all types of IgMs present in the sample are captured by the microparticles, hence is the conjugate responsible for making the assay-specific to detect only the ones of interest, in our case, the IgM anti-*T. gondii*.

Our immunocapture prototype was based on biotinylated 3a6c chimeric peptide coupled with isoluminol-labeled streptavidin as a conjugate, immunocapture paramagnetic beads, and standard assay buffer. All reagent components were prepared following internal standard procedures.

None of the initial tests performed gave us satisfactory results. Therefore, we initiated troubleshooting to assess which of the two main components (microparticles or conjugate) was responsible for the lack of reactivity. The microparticles demonstrated to be functional, however when we tested the conjugate, we obtained no reactivity.

We established two hypotheses:

i) Streptavidin could be poorly isoluminol-conjugated.

We confirmed the presence of isoluminol-conjugated streptavidin by performing a light-check assay. This assay is performed as part of routine instrument maintenance to assure the functionality of the BIO-FASH® luminometer. It consists of measuring the RLU of a reference material, which contains an isoluminol-labeled IgG antibody diluted in a standard buffer.

ii) The conjugate could be non-stable.

Free 3a6c-biotinylated peptides could bind IgM anti-*T. gondii*, but that reaction could not be monitored, since the peptides were not conjugated. Additionally, free 3a6c-biotinylated peptides could interfere with the binding of the stable conjugate. To remove possible non-bound peptides present in the conjugate, we performed a purification by size exclusion chromatography (SEC), however, we obtained similar results.

After troubleshooting (data not shown), we rejected both hypothesis. Overall, as the immunocapture approach was unable to discriminate positive from negative samples, we decided to use only the indirect assay format for the optimization phase.

5.3. Reagent optimization using design of experiments method

The diluents of an immunoassay are formulated to prevent any of the assay components from degradation or aggregation, while ensuring accurate, optimal, and repeatable results. Initially, we adapted our peptide-based assay to the formulation of the BIO-FLASH® Toxo IgM reagent for three reasons i) it is an in-house product, so we had deep knowledge on the formulation, ii) we could evaluate the functionality of our peptide in a chemiluminescent assay reducing significantly the period dedicated to assay development, and iii) we could assess the impact on assay performance associated with the replacement of a native antigen by a synthetic chimeric peptide.

Although the initial formulation was functional, the need to apply powerful optimization methods during the development of the proof of concept was obvious: our initial prototype reported only 85% sensitivity and 87% specificity. Therefore, our goal was to find an assay formulation giving the lowest background in the negative samples (high specificity) and the highest signal in the positive samples (high sensitivity).

The traditional optimization approach, varying one factor at a time (OFAT) have drawbacks (i.e., it is time and resource-intensive, rarely uncovers the optimal conditions as it is highly dependent on the starting point, and it is unable to separate the "noise" (the inherent run-to-run variation) of a reaction from significant improvement unless a high number of reactions are repeated (247,248).

As an alternative, Design of Experiments (DOE), is a statistical method based on organizing and designing a series of experiments so that, with the minimum number of tests, it is possible to investigate the impact of changes in system parameters (249,250). The systematic approach inherent in DOE has two main advantages; i) eliminates researcher bias and often leads to experimental conditions not considered previously, and ii) detects interactions between factors and estimates their effect. Generally, there are three key points in the life of a product when DOE may be used; early in development when the best conditions are not obvious, when exploring robustness, and when optimizing conditions for established products (247).

To conduce a DOE, the first step is to define an objective (i.e., optimize a process or a product), then the factors or variables and their ranges, as well as the response, followed by the selection of the appropriated experimental design. The next step is to generate a worksheet into DOE software, and finally, to perform the experiments, to collect and to analyze the data to find which factors influence the results in a statistically relevant manner and which of those are interdependent (248,251).

We performed the DOE sequentially, analyzing first the solid-phase, second the assay buffer, and subsequently the tracer, using the optimized formulation established within each step, to perform the DOE of the next assay component.

5.3.1. Solid-phase formulation

The process to bind the capture molecule on the solid-phase—the coating procedure—is crucial since it directly affects the orientation and the availability of the capture molecule.

Passive adsorption relies on hydrophobic interactions to bind the capture molecule onto the bead surface. It allows little control over the final orientation, resulting in multiple layers of the capture molecule. This method is typically linked to low specificity and stability problems. To avoid such limitations, we covalently bound the capture molecule onto the solid-phase using tosyl pre-activated magnetic beads.

We defined as relevant variables for the coating process:

- Peptide/magnetic bead ratio: To establish optimal peptide concentration, it is important to control the peptide surface density on the magnetic beads. On the one hand, using too little peptide may result in sub-optimal coating and therefore low reactivity. On the other hand, using too much may cause steric effect with diminished activity or background increase, or may simply waste expensive reagent (252–255).
- Salt: Ionic components as sodium chloride are present in many buffers to increase the solubility of the capture molecule. Their presence increases the net charge of both peptides and proteins by joining hydrophilic domains. This increases electrostatic repulsion promoting interaction with H_2O molecules and favoring its re-solubilization. However, if salt concentration is too high, the effect can be the opposite, preventing the binding of the capture molecule with the tosyl groups. Usually, salt has a low effect in this component; nonetheless, it is important to determine if its presence during coating is necessary for the reaction (256,257).
- Buffer pH: It affects both the solubility of the capture molecule and the reaction between the tosyl and the amino groups of the biomolecule which is meant to attach onto the solid surface. Tosyl-chemistry is favored at basic pH, however, the isoelectric point (IP) of the capture molecule has to be considered. As the 3a6c chimeric peptide has an IP of 3.71, we decided to use a pH between 7 and 9 to favor peptide solubility and the coupling reaction. Additionally, the hydrophobicity of the molecule is important, as tosyl groups can easily interact with the hydrophobic parts of a protein or a peptide. Seeing that our peptide has more than 50% hydrophobic residues, we considered the binding between the two molecules to be suitable (92,106,258,259).
- Blocking agent: Blockers are commonly used to fill the gaps not covered by the capture molecule, therefore inactivating remaining active groups. They are often attached via adsorption after coating the capture molecule to reduce non-specific interactions between

the beads and non-targeted molecules present in the sample or hydrophobic interaction between proteins and polymer surfaces. The blocking species have to minimize non-specific interactions, and therefore reduce assay background. Some common blockers are BSA (bovine serum albumin) and PEG (polyethylene glycol) (257,260,261).

For each variable we proposed two levels represented in Table 5-4. Additionally, for peptide/microparticles ratio and pH, we added a central level (peptide ratio 10 $\mu g_{peptide}/mg_{microparticles}$ and pH 8.45).

Variables	**Levels**		
	LEVEL -	CENTRAL LEVEL	LEVEL +
Peptide/microparticles ratio ($\mu g_{peptide}$ / mg_{MP})	5	10	15
Buffer pH	PB pH 7.4	PB pH 8.45	CB pH 9.5
Salt	NaCl 0 mM	-	NaCl 154 mM
Blocking agent	PEG 0.1%	-	BSA 0.5 g/L

Table 5-4: Variables and levels used for solid-phase formulation. Different coating ratios, expressed as the amount of peptide (μg) per milligram (mg) of microparticles (MP) were studied. The coating buffers were prepared at different pH, salt concentrations and with different blocking agents. PB: phosphate buffer, CB: carbonate buffer, NaCl: sodium chloride.

In addition to define the factors that could affect the coating process, we established the response variables we would use to decide which formulation gives better assay performance:

- Span: It is the ratio between the average result of positive samples and the average result of negative samples. The first is directly affected by the presence of 3a6c chimeric peptide, therefore this variable should have a similar performance as "bound antigen" response variable. The second measures how effective the blocking agent is.
- Bound antigen: To quantify the amount of bound peptide, each time we performed a coating, we kept a sample of the solution that contained the peptide before and after the coupling between the solid-phase and the capture molecule. Then, we performed a micro BCA assay to calculate the amount of bound antigen in absolute value.

Considering the number of variables, the experimental design selected was factorial fractional 1/2, 2^{4-1} with one central level, which equals 12 experiments. According to DOE specifications, we prepared different coating (n=6), blocking (n=12) and the resuspension (n=12) formulations to obtain 12 different mini lots of microparticles. For assay buffer and tracer, standard formulations as for ITPT1 were used. Each new prototype was named from dPTmp1 to dPTmp12 and tested with the formulation panel (n=12). Span and bound antigen response variables were individually studied with Minitab® 18 to determine how the factors analyzed affect each variable.

5.3.1.1. Span

The impact of the variables studied on span was analyzed, and the pareto chart obtained (Figure 5-2). The bars that exceed the red line in the plot are said to have statistically significant effect. The results obtained showed that the blocking agent (D) had the highest effect on span followed by buffer pH (B).

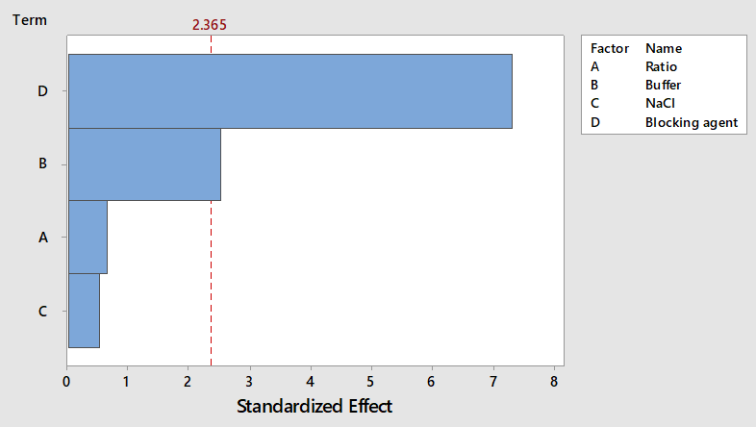

Figure 5-2: Pareto plot for solid-phase span variable. The standardized effect of each variable was represented. Statistically significant level α=0.05.

Additionally to pareto chart, the main effect plot was obtained. It represents the mean of the results per level connected by a line. When a horizontal line is present, there is no effect. The greater the line slope, the higher the effect of that variable.

As seen in Figure 5-3, the blocking influences the span, as its line presents the most pronounced slope. When BSA 5 g/L was used, a higher span was observed compared with PEG 1%. Buffer pH also affects span but to a less extent.

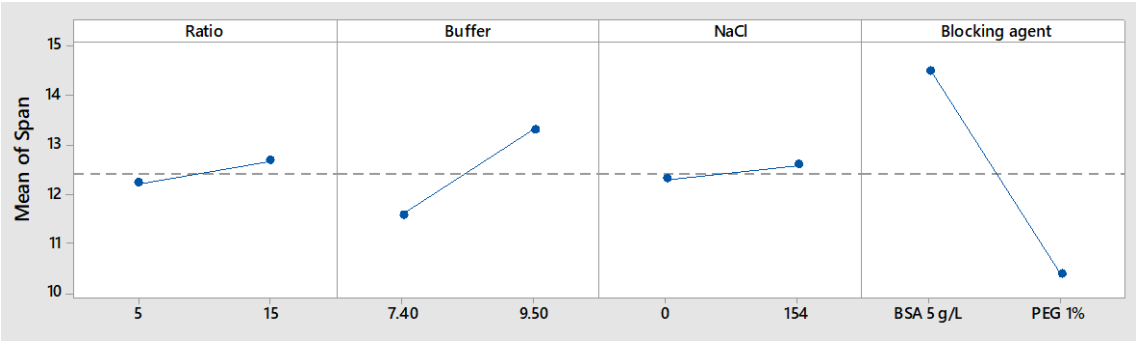

Figure 5-3: Main effects plot for the span response in the solid-phase DOE. The mean of the span was represented per each variable level. The slope of the line connecting both results is a measure of the impact of the variable on the span.

5.3.1.2. Bound peptide

The pareto chart showed that none of the variables studied were statistically significant for bound antigen (Figure 5-4). Therefore we did not perform additional analyses about the effect of each level.

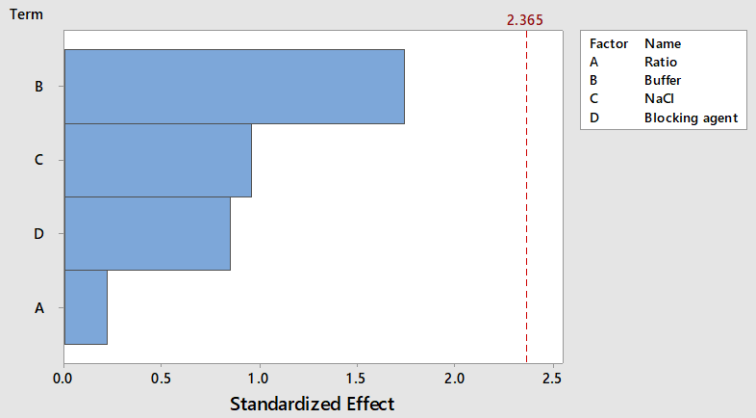

Figure 5-4: Pareto plot for solid-phase bound peptide variable. The standardized effect of each variable was represented. Statistically significant level α=0.05.

The overall results obtained with the evaluation of the 12 mini lots of microparticles with the formulation panel can be seen in Table 5-5. On the one hand, the highest span was obtained with the formulation containing peptide ratio 5, BSA 5 g/L, and buffer pH 9.5. On the other hand, the highest values of bound antigen were obtained with the same formulation but with buffer pH 7.4.

Considering the results, we selected the formulation with peptide ratio 10, NaCl 154 mM, BSA 5 g/L, and buffer pH of 8.45. Despite the slightly lower span (15.4 vs 15.8), the bound antigen was significantly higher than that of the formulation with the highest span (24.3 vs 13.3).

R	pH	NaCl (mM)	Blocking agent	Bound peptide (µg/mg)	$\bar{X}$ neg	$\bar{X}$ pos	Span
15	7.4	154	BSA 5 g/L	22.5	719	10366	14.4
5	9.5	154	BSA 5 g/L	13.3	870	13702	15.8
15	9.5	154	PEG 1%	17.7	746	7760	10.4
5	7.4	154	PEG 1%	15.6	699	6472	9.3
15	9.5	0	BSA 5 g/L	15.3	727	11001	15.1
10	8.45	0	BSA 5 g/L	8.9	773	10982	14.2
10	8.45	0	PEG 1%	11.7	786	7793	9.9
5	7.4	0	BSA 5 g/L	31.9	886	10582	11.9
10	8.45	154	PEG 1%	24.2	816	8309	10.2
5	9.5	0	PEG 1%	8.9	803	9526	11.9
15	7.4	0	PEG 1%	18.4	663	7041	10.6
10	8.45	154	BSA 5 g/L	**24.3**	806	12441	**15.4**

Table 5-5: Solid-phase DOE study. For each coating ratio (R) at different pH, salt (NaCl) concentration and blocking agent, the response variables are represented: bound peptide ($\mu g_{peptide}/mg_{MP}$), $\bar{X}$ neg/pos: average of positive / negative samples and span.

5.3.2. Assay buffer formulation

Once we established the optimal solid-phase formulation, we studied the assay buffer. The variables assessed were:

- Salt: Sodium chloride or other salts are used to provide suitable ionic strength to favor the recognition between the analyte and the capture molecule. We mimicked physiologic sodium plasma concentration (135-145 mmol/L), which is where antigen-antibody reactions take place (256,262).
- Buffer pH: Small pH changes can affect the binding between the antigen and the analyte, in our case IgM anti-*T. gondii*. Usually, physiologic pH contributes to antigen-antibody recognition (92,106,258,259).
- Detergent: It prevents non-desired interactions affecting the capture molecule or the analyte of interest. Normally, it reduces background and increases the signal, thus improving the signal-to-noise ratio (SNR). Nevertheless, excessive detergent causes foaming which can affect performance. Considering that the background of our assay was low, we studied the absence of detergent (257,263).
- Blocking agent: Like detergents, blocker species prevent non-specific interactions. Common blockers are fetal calf serum (FCS) and BSA (257,260,261,264).

For each variable, we proposed two different levels shown in Table 5-6.

Variables	**Levels**	
	LEVEL -	LEVEL +
Buffer pH	TRIS pH 7.6	TRIS pH 8.2
Salt	NaCl 0.15 mM	NaCl 150 mM
Detergent	-	Tween 20 0.05%
Blocking agent	BSA 0.5 g/L	FCS 50%

Table 5-6: Variables and levels used for assay buffer DOE formulation. Different formulations were prepared at different pH, salt concentrations, detergents and blocking agents.

Considering the number of variables, we selected the DOE experimental design full factorial 2^4 with 16 experiments with full resolution.

According to DOE specifications, we prepared different assay buffer formulations (n=16). The microparticles used were those selected in the DOE of the solid-phase (ratio 10, NaCl 154 mM, BSA 5 g/L and pH of 8.45). The standard formulation of the tracer used for ITPT1 was maintained. Each new prototype was tested with the formulation panel (n=12). We used the span to select the optimal assay buffer formulation.

5.3.2.1. Span

The significance of the variables studied on the span was analyzed with the pareto plot (Figure 5-5), which showed that the blocking agent (D) had the highest effect.

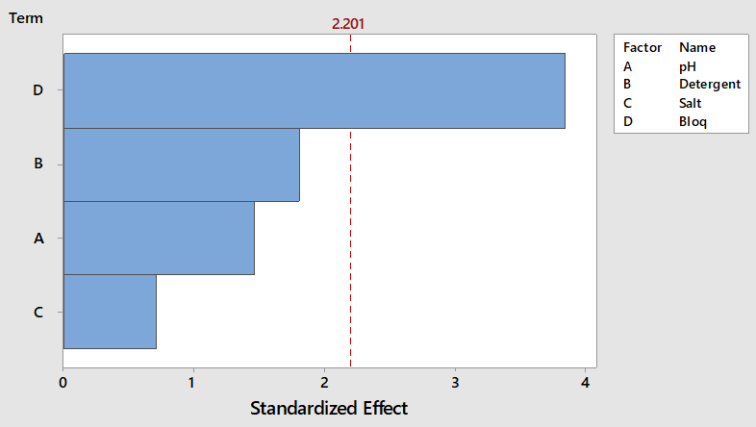

Figure 5-5: Pareto plot for assay buffer span variable. The standardized effect of each variable was represented. Statistically significant level α=0.05.

Besides to pareto chart, the main effect plot presented in Figure 5-6 shows how each variable level affected the span. FCS caused a span that was two units higher than the observed with BSA. After blocking agent, detergent showed the highest impact.

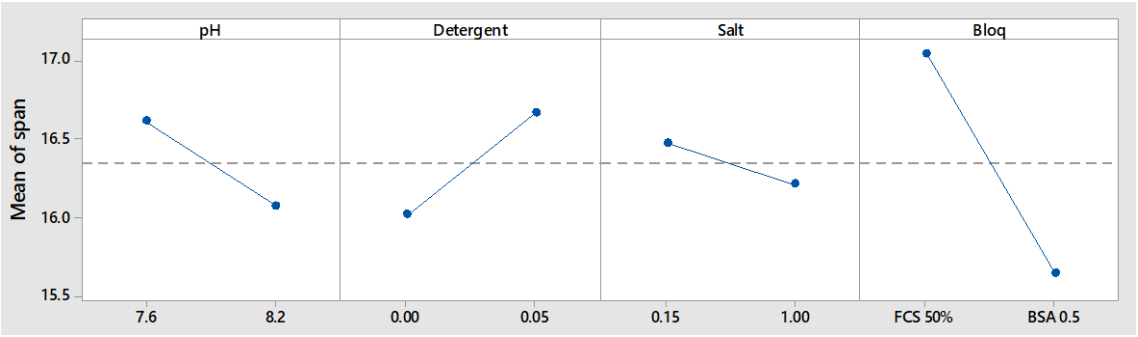

Figure 5-6: Main effects plot for span in the assay buffer DOE. Mean of span was represented per each variable level. The slope of the line connecting both results is a measure of the impact on the span.

The results obtained when the 16 assay buffer formulations were tested with the formulation panel can be seen in Table 5-7. The highest span was obtained with pH 7.6, Tween 20, 150 mM NaCl, 50% FCS, which was the assay buffer formulation selected.

pH	Detergent	NaCl (mM)	Blocking agent	$\bar{X}$ neg	$\bar{X}$ pos	Span
8.2	0	150	BSA 0.5 g/L	719	10732	14.9
7.6	0.05	150	FCS 50%	542	9994	**18.4**
7.6	0	150	FCS 50%	549	9028	17.2
7.6	0.05	150	BSA 0.5 g/L	620	10194	16.4
7.6	0	0.15	BSA 0.5 g/L	818	13354	16.3

pH	Detergent	NaCl (mM)	Blocking agent	$\bar{X}$ neg	$\bar{X}$ pos	Span
8.2	0	150	FCS 50%	543	8855	16.3
7.6	0.05	0.15	FCS 50%	655	11402	17.4
8.2	0.05	150	FCS 50%	513	8785	17.1
8.2	0.05	0.15	BSA 0.5 g/L	674	10775	16
8.2	0.05	150	BSA 0.5 g/L	608	9483	15.6
8.2	0.05	0.15	FCS 50%	676	10879	16.1
7.6	0	0.15	FCS 50%	668	11322	17
7.6	0.05	0.15	BSA 0.5 g/L	703	11526	16.4
8.2	0	0.15	FCS 50%	655	11100	16.9
8.2	0	0.15	BSA 0.5 g/L	834	13086	15.7
7.6	0	150	BSA 0.5 g/L	791	10931	13.8

Table 5-7: Assay buffer DOE study. For each pH, detergent, salt (NaCl) concentration, and blocking agent, the response variables are represented: $\bar{X}$ neg/pos: average of negative/positive samples and span.

5.3.3. Tracer formulation

The tracer is formed by the conjugate concentrate and the tracer diluent. Thus, we studied the effect of both components separately, starting with the tracer diluent, and then analyzing the concentration of the conjugate in the selected tracer diluent. To study the diluent, we used a pre-established conjugate concentration of 100 ng/mL.

We defined as relevant factors for tracer diluent:

- Buffer pH: It affects the binding between the conjugate (anti-human IgM monoclonal antibody) and the analyte of interest, in our case, IgM anti-*T. gondii*. As for the assay buffer, physiological pH values favor recognition between both antibodies (92,106,258,259).
- Detergent: The presence of detergent avoids the formation of non-specific interactions between the conjugate and random molecules that may have joined with the capture molecule. It decreases the background and increases the signal, thus intensifying the SNR. As with the assay buffer, considering that the background of the ITPT1 was low, we studied the absence of detergent (257,263).
- Non-ionic molecules: Usually metal ion chelators prevent non-desired interactions, decreasing assay background and increasing SNR (263).
- Blocking agent: Blockers avoid non-desired interactions. Common blockers are FCS and BSA (257,260,261,264). Additionally, we studied casein.

For each factor, we proposed two levels which are presented in Table 5-8.

Variables	Levels	
	LEVEL -	LEVEL +
Buffer pH	TRIS pH 7.6	TRIS pH 8
Detergent	-	Tween 20 0.05%
Non-ionic components	-	5 mM
Blocking agent	BSA 0.5 g/L	FCS 50%
Casein	-	5 g/L

Table 5-8: Variables and levels used for tracer DOE formulation. Different formulations were prepared at different pH, detergents, non-ionic components and blocking agents.

Considering the number of variables, the experimental design selected was full factorial 2^{5-1} with full resolution, which requires 16 experiments.

Different tracer diluents (n=16) were prepared according to DOE specifications. We used the formulations selected previously for the solid-phase (ratio 10, NaCl 154 mM, BSA 5 g/L at pH 8.45) and for the assay buffer (150 mM NaCl, Tween 20, 50% FCS, at pH 7.6). Each new prototype was tested with the formulation panel (n=12). We used the span response variable to select the appropriate tracer diluent formulation.

5.3.3.1. Span

The effect of the factors studied on span was analyzed and a pareto chart was generated. The pareto plot showed that detergent (A), blocking agent (D) and non-ionic components (C) had a significant effect on span.

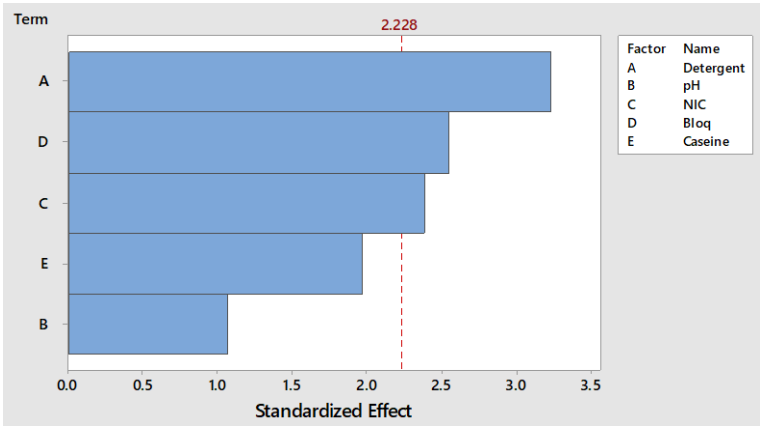

Figure 5-7: Pareto plot for tracer span variable. The standardized effect of each variable was represented. Statistically significant level α=0.05.

The presence of detergent in tracer diluent increased the span by two units. After detergent, non-ionic components showed the highest impact. We observed similar results with blocking agent and casein, in favor of the presence of BSA 5 g/L and casein.

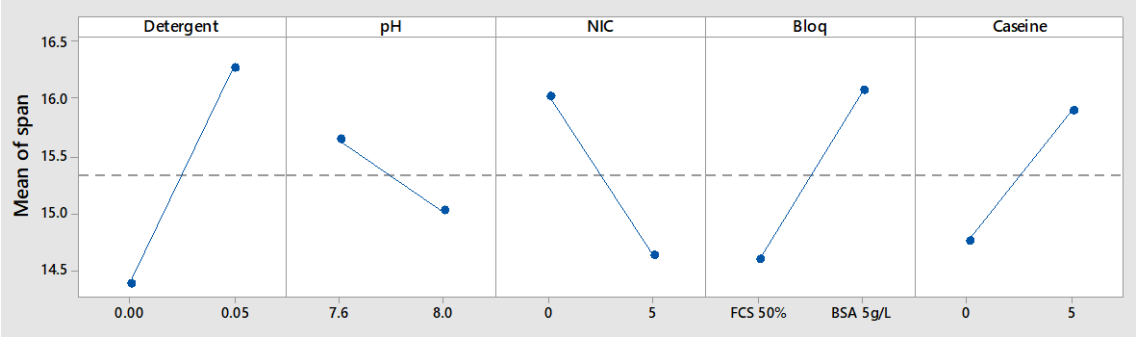

Figure 5-8: Main effects plot for the span response in the tracer DOE. Mean of span was represented per each variable level. The slope of the line connecting both results is a measure of the impact on span variable.

The results obtained after the evaluation of the different tracer diluents (n=16) with the formulation panel are shown in Table 5-9. The highest span was obtained with Tween 20, absence of non-ionic components, BSA 5g/L at pH 7.6 which was the tracer diluent formulation we selected.

pH	Detergent	NaCl (mM)	Blocking agent	$\bar{X}$ neg	$\bar{X}$ pos	Span
8.2	0	150	BSA 0.5 g/L	719	10732	14.9
7.6	0.05	150	FCS 50%	542	9994	**18.4**
7.6	0	150	FCS 50%	549	9028	17.2
7.6	0.05	150	BSA 0.5 g/L	620	10194	16.4
7.6	0	0.15	BSA 0.5 g/L	818	13354	16.3
8.2	0	150	FCS 50%	543	8855	16.3
7.6	0.05	0.15	FCS 50%	655	11402	17.4
8.2	0.05	150	FCS 50%	513	8785	17.1
8.2	0.05	0.15	BSA 0.5 g/L	674	10775	16
8.2	0.05	150	BSA 0.5 g/L	608	9483	15.6
8.2	0.05	0.15	FCS 50%	676	10879	16.1
7.6	0	0.15	FCS 50%	668	11322	17
7.6	0.05	0.15	BSA 0.5 g/L	703	11526	16.4
8.2	0	0.15	FCS 50%	655	11100	16.9
8.2	0	0.15	BSA 0.5 g/L	834	13086	15.7
7.6	0	150	BSA 0.5 g/L	791	10931	13.8

Table 5-9: Assay buffer DOE study. For each pH, detergent, salt (NaCl) concentration, and blocking agent, the response variables are represented: $\bar{X}$ neg/pos: average of negative/positive samples and span.

5.4. Conjugate concentration study

Once we selected the optimal tracer diluent using DOE, we studied different conjugate concentrations (50 to 500 ng/mL). To do so, we manufactured four tracers using the diluent previously selected versus the formulation panel, and we evaluated how the span was affected.

Sample ID	Toxo IgM[a]	3a6c (RLU)	Tz1 (RLU)	Tz2 (RLU)	Tz3 (RLU)	Tz4 (RLU)
NEG POOL 1	NEG	413	1033	602	2312	3607
NEG POOL 2	NEG	572	909	817	1934	2825
NEG POOL 3	NEG	913	1785	1326	4809	6215
NEG POOL 4	NEG	711	1869	911	4292	5956
NEG 5713	NEG	345	329	296	567	799
POOL LOW G	NEG	1378	1624	1479	4069	5953
POOL HIGH G	NEG	806	1516	1111	3699	5509
SD7106	POS	4204	10461	15925	29254	50230
2574Q	POS	25969	17576	31444	49819	80921
POS POOL 1	POS	7742	7384	10992	20511	32044
SD7106/5713	POS	2250	4946	6022	13458	22620
2574Q/5713	POS	11375	7939	31590	21823	36435
$\bar{x}$ neg		734	1295	935	3097	4409
$\bar{x}$ pos		10308	9661	19195	26973	44450
span		14.0	7.5	20.5	8.7	10.1

Table 5-10: Conjugate concentration study. The formulation panel was evaluated with four different conjugate concentrations Tz1, Tz2, Tz3, Tz4 at 50, 100, 200, and 500 ng/mL, respectively. Toxo IgM[a] refers to the presence or absence of anti-*T. gondii* IgM antibodies. The 3a6c (RLU) column is used as a reference; 100 ng/mL of the conjugate was used in standard tracer diluent. $\bar{x}$ neg/pos: average of negative/positive samples.

As the highest span was obtained with the conjugate at 100 ng/mL, we selected it as the optimal concentration. When we tested both lower and higher concentrations, the span decreased due to the higher reactivity of negative or positive samples, indicating that assay background and non-specific interactions increased (see Table 5-10). Overall, we selected the tracer formulation with detergent, absence of non-ionic components and BSA, at pH 7.6 with a concentrate conjugate at 100 ng/mL.

5.5. Optimization of assay parameters

Besides of each reagent component, the instrument used to run the assay plays a key role, conditioning assay performance. The BIO-FLASH® platform allowed to modify several assay parameters (i.e., volumes, incubation times, etc.). As a starting point, we used the BIO-FLASH® Toxo IgM assay definition which includes: i) sample pre-dilution, ii) mix and incubation of the magnetic beads with pre-diluted sample, iii) wash steps, iv) tracer incorporation and incubation, v) triggers addition, and vi) chemiluminescent read-out (5,8). A scheme of the assay is shown in Figure 5-9.

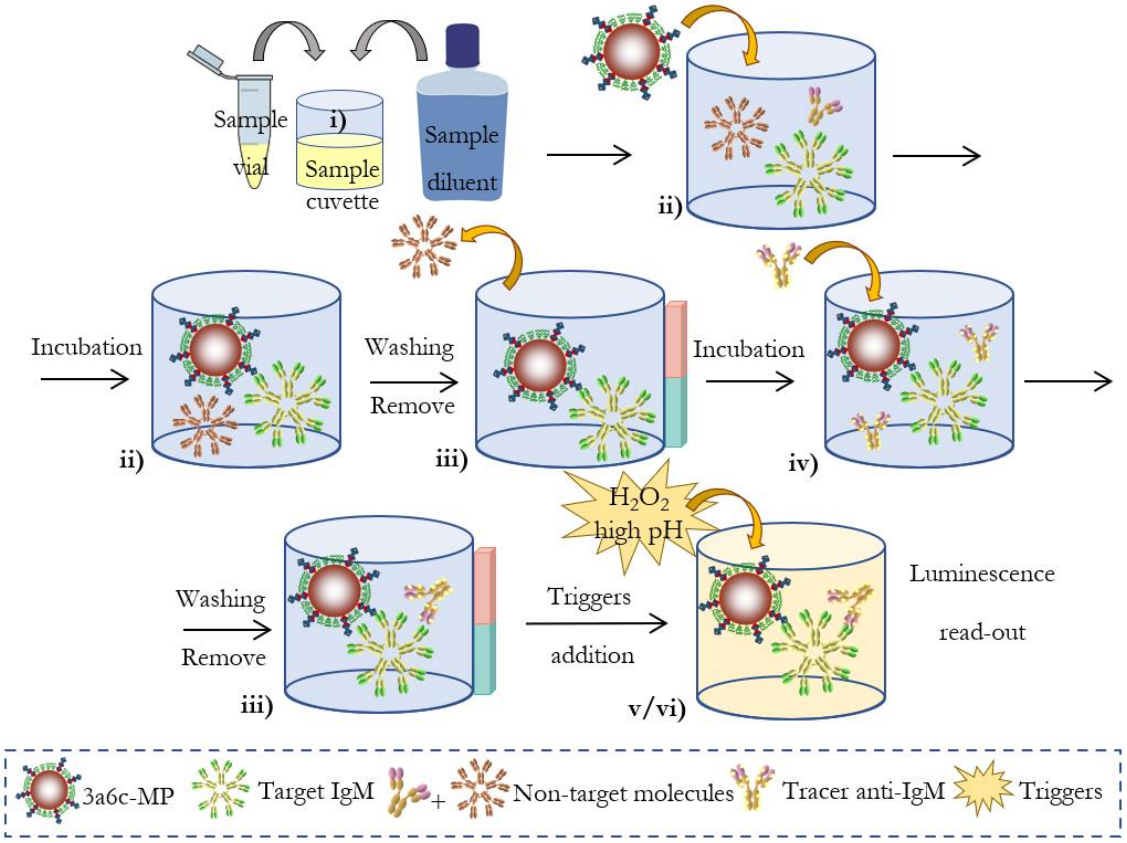

Figure 5-9: Schematic view of the 3a6c-PT1I immunoassay. The 3a6c peptide-coated magnetic beads capture the IgM antibodies from the pre-diluted sample; signal recognition is done by the addition of ABEI-labelled antibody followed by chemiluminescent measuring. Main steps are separated by two washing steps, all performed automatically by BIO-FLASH® instrument. Adapted from Mahler et al.,(105).

Once selected the optimal reagent formulation, we studied different assay definitions in the BIO-FLASH® platform. We focused on the magnetic beads and the sample mix (Figure 5-9). As in previous sections, we used span as a response.

Based on BIO-FLASH® immunoassay (Toxo_ref) assay, we developed Toxo_d100 and Toxo_nd, increasing 5 and 10-fold respectively, the sample volume incubated with the magnetic particles, compared with the reference assay. We tested the three assay definitions with the formulation panel (n=12). Results are shown in Table 5-11.

The span increased as the sample volume incubated with the magnetic particles increased (Table 5-11). Additionally, we calculated the ratio between the highest value of the negative samples (Pool low) and the lowest value of the positive samples (Pool SD7106/5713)—named R-value—to determine how the two groups of samples (negative vs. positive) were separated with the different assay definitions. The R-value of the reference assay was 1.8, whereas with Toxo_nd the R-value was 2.9. Our results indicated that the more sample volume, the better the separation between negative and positive samples.

Estimators	Toxo_ref (RLU)	Toxo_d100 (RLU)	Toxo_nd (RLU)
Mean negative samples	745	2265	4871
Mean positive samples	10847	51222	127819
Span	15	23	26
R-value	1.8	2.2	2.9

Table 5-11: Results of the assay parameters optimization. Different estimators are represented per assay definition. RLU: Relative luminescent units. R-value: ratio between the highest value of the negative samples (Pool low) and the lowest value of the positive samples (Pool SD7106/5713).

Considering that the results obtained with the reference assay were good enough and foreseeing the risk of increasing false-positive and false-negative results if more sample volume was incubated with the beads, we decided to conserve the reference assay parameters to continue with the proof of concept.

Overall, the final reagent formulation consisted of i) magnetic beads with a peptide ratio of 10 µg/mg bead, 154 mM NaCl and BSA 5 g/L at pH of 8.45, ii) an assay buffer containing detergent, NaCl 150 mM, FCS 50%, at pH 7.6, and iii) a tracer with detergent, BSA at pH 7.6 and a conjugate concentration of 100 ng/mL.

5.6. Discussion

Although the serological tests play a key role in the diagnosis of both human and animal toxoplasmosis, the insufficient accuracy which characterizes some of them is highly correlated with significant variations in the antigen manufacturing procedures (236). Therefore, the biggest challenges for researchers are to identify novel antigens that possess high immunoreactivity and to develop accurate diagnostic assays that can replace current immunoassays which are mainly based on the *T. gondii* lysate antigens.

According to the above remarks, the emergence of chemiluminescent immunoassays in the field of toxoplasmosis diagnosis meant a significant improvement. A proof of it is an increasing number of studies demonstrating that CLIA are more useful than the conventional methods, such as ELISA, for the serological diagnosis of toxoplasmosis (101,102,235,265).

First, their wide dynamic range implies ultra-sensitive detection limits and therefore high capacity to detect accurately the presence of antibodies at extremely low concentrations. This is especially advantageous when detecting IgMs that could be present at low concentrations at the beginning of the acute phase. Second, the use of chemiluminescent immunoassays ushers in a new era, thanks to the use of automated analytical platforms, where the most critical analytical stages are controlled by highly advanced software. Third, their short execution time (30-40 min) with considerably reduced immunochemical reactions, allows clinical laboratories to carry out a greater number of tests and reduces the time to result (103). This panorama gave us a clear idea of where to direct this project once we had a promising synthetic peptide candidate.

Apart from the importance of the analytical method, it is well known that the effectiveness and especially the sensitivity of immunoassays depend mainly on the antigen used and its capacity to bind specific immunoglobulins (102,266,267). Here we describe the development of a chemiluminescent-based immunoassay prototype using as antigen the chimeric synthetic peptide depicted in previous chapters, containing fragments of two highly immunogenic *T. gondii* antigens, on the BIO-FLASH® platform. Using this internally developed autoanalyzer allowed us to develop the proof of concept as well as study and modify each assay parameter to get a promising reagent prototype for the detection of IgM anti-*T. gondii*.

Although indirect approaches are the most common in commercial ELISA kits to detect IgM anti-*T. gondii*, most CLIA use immunocapture, in which, instead of an antigen, an anti-IgM antibody is attached to the solid-phase, and therefore the antigen is used as a conjugate.

The immunocapture approach is performed by the ARCHITEC Toxo IgM. First, the pre-diluted sample is incubated with anti-human IgM mouse monoclonal antibody-coated magnetic beads. Then,

after washing, the conjugate consisting of native *T. gondii* lysate antigen complexed to an acridinium-labeled anti-*T. gondii* P30 mouse monoclonal F(ab')2 fragment, is added and bound to anti-*T. gondii* IgM previously captured by the microparticles, forming an antibody-antibody-conjugate complex, which is detected in the presence of the triggers (118).

To our knowledge, the BIO-FLASH® Toxo IgM is the only commercial CLIA that uses the indirect approach with native *T. gondii* lysate antigen to capture the IgMs present in the sample. A commercial assay that uses the same approach, although is not chemiluminescent based, is the AxSYM system (Abbott Laboratories, Chicago, US). This microparticle enzyme immunoassay (MEIA) uses polystyrene microparticles coated with cell-cultured *T. gondii* antigen and alkaline phosphatase-labeled anti-human IgM as a conjugate with final fluorescence detection. This assay has good performance; however, some studies have found low agreement percentages compared with other immunoassays (122,268).

Other commercial kits use the streptavidin-biotin system with satisfactory results. The Roche Elecsys Toxo IgM (Roche Diagnostics, Mannheim, Germany) is an electrochemiluminescent immunoassay (ECLIA), in which the luminescent reaction is produced during an electrochemical reaction due to the generation of molecules that emit light when they are relaxed to an electronically lower-level state from an excited state. This assay uses a ruthenium-labeled recombinant surface antigen SAG 1 (P30) designed to contain multiple IgM binding sites. First, the diluted sample is incubated with the labeled antigen. Then, a biotinylated monoclonal anti-human IgM antibody is added, together with the streptavidin-coated microparticles. Finally, the complex formed by the biotin-labeled antibody, the IgM anti-*T. gondii* and the labeled antigen become bound to the solid phase through the biotin-streptavidin interaction, and in presence of the triggers, the electrochemical reaction is detected by the optical system (222,269).

If we compare our CLIA assay with Elecsys Toxo IgM, two important aspects stand out: i) in the Roche Elecsys Toxo IgM, the biotin-labeled molecule is a recombinant antibody, whereas we used a chimeric peptide, and ii) in Elecsys Toxo IgM, the complex between the biotin-labeled molecule and the streptavidin is not pre-formed; rather, the solid phase (which is streptavidin pre-activated) is added at the same time as the biotin-labeled molecule. This allows the capture molecule to interact freely with the IgM present in the sample, and then, with the solid-phase. This approach favors the antigen-antibody complex to form partially in liquid phase—non-bound to the solid phase—which has been linked to smaller steric effect, higher sensitivity, smaller amount of sample required, shorter incubation time and lower manufacturing costs (270).

This scenario led us to evaluate both approaches (immunocapture and indirect). From a manufacturing point of view, immunocapture has a clear advantage, since magnetic particles are

universal to all IgM assays, thus simplifying production procedures and reducing costs. To develop the immunocapture, we used magnetic beads coated with anti-human IgM antibodies, and a conjugate complex made with biotin 3a6c chimeric peptide and isoluminol-labeled streptavidin molecule. Our first prototype was not able to distinguish negative from positive samples, and the troubleshooting to find the root cause was non-satisfactory. With our research we rejected the possibility that the streptavidin could be poorly isoluminol-conjugated, and we demonstrated that our conjugate was stable and there were no free peptides interfering with the assay. However, our assay was still not functional.

All things considered, we hypothesize that the cause of our non-functional immunocapture assay could be related to the 3a6c peptide. In chapter 3, we demonstrated that biotin labeling did not affect peptide functionality, since when we used it to develop indirect ELISA with standard plates, the assay was functional. However, although not described in the literature, it remain possible that binding between streptavidin and the biotin-labeled peptide affects the ability of the peptide to recognize IgM, therefore we attribute our negative results to an impaired ability to recognize the IgM by the 3a6c peptide once bound to streptavidin.

Regarding the indirect assay, it allowed us to demonstrate the reactivity of our chimeric peptide either using tosyl or streptavidin magnetic beads, as we obtained satisfactory results using both approaches. Interestingly, while the CLIA based on streptavidin beads was able to distinguish positive from negative samples, its analog ELISA was not functional. Initially, we suggested that the ability of the peptide to recognize the IgMs, if dependent on the peptide N-terminus, could be affected by the biotin labeling, since we used NHS-maleimide biotin to label the N-terminus (see chapter 3). However, according to the results presented here, we rejected this possibility. Therefore, we attribute the lack of functionality of the ELISA to a manipulation error or to a failure caused by the streptavidin plates.

Our preliminary CLIA prototype reported balanced performance (85% sensitivity and 87% specificity). Similar results were observed by Holec-Gasior and her colleagues when they developed a CLIA based on a new SAG2-GRA1-ROP1L recombinant chimeric protein (102). However, they used an acridinium ester to tag the conjugate, while we used an isoluminol derivate. This difference conferred the CLIA developed by Holec-Gasoir an advantage, as acridinium esters do not necessarily require catalyst in the luminescent reaction to trigger the emission of light. Thus, low background signals and ultra-high sensitivities can be reached (235). Even though our assay used luminol, we had extremely low background and therefore we opted not to explore other tags.

DOE methodology has effectively been used in assay development to provide critical insight for optimizing experimental conditions and to study the outcome of analytical methods by different authors (247,248,271,272). However, its potential is not fully exploited to optimize immunoassays.

Joelsson et al., conducted a DOE approach to quickly optimize conventional ELISA when adapting into an automated platform (251). Same as Joelsson, we studied four variables for the solid-phase, which would require 32 runs in a full factorial design; however, doing fractional design, the number of runs was reduced to eight. Although Joelssons' aim was focused on assay robustness and precision, aligned conclusions can be extracted: the use of DOE allowed assessing multiple factors with significant time and cost savings, otherwise, it would be extremely complex and difficult by routine methods.

In this project, the systematic approach on which DOE is based makes it possible to explore different formulations for each reagent component (microparticles, assay diluent, and conjugate) with a relatively low number of experiments in a short period.

Regarding the microparticles, we opted for buffers at pH 8.45, since the proportion between bound antigen and span was more balanced compared with the buffers at a lower pH. Those findings were aligned with the coating conditions which are normally required for tosyl magnetic particles (106).

Interestingly, our results regarding both assay buffer and tracer were contrary to those of Petzold, and Chapman et al. They found that high pH buffers are advantageous to increase the binding of lower-affinity antibodies, which is the case of IgM (256,262). Nevertheless, our results showed a clear trend to neutral pH in both cases. This tendency was aligned with the fact that antigen/antibody reactions are favored in buffers mimicking physiological conditions, as the epitopes relevant for antibody recognition are prone to be exposed.

Overall, the results presented here demonstrate that our synthetic chimeric peptide can be used in chemiluminescent immunoassay, replacing *T. gondii* parasite native proteins and it is useful to detect IgMs anti-*T. gondii* in human sera. Additionally, we proved that DOE is an excellent tool to study and optimize the formulation of IVD reagents. Thus, we encourage researchers to use this approach to obtain improved assays, reduce the execution time of development phases, and achieve a high level of understanding of the behavior of their products. Nevertheless, although results presented in this study are promising, further work is needed to assess the performance of the assay with a high number of samples, besides evaluating potential interferents, especially those from IgG anti-*T. gondii*.

CHAPTER 6 – Performance characteristics of the new immunoassay

In clinical chemistry, the perception of what is a '*good*' test and therefore the term '*quality*' can be considered from different points of view. Performance is just the tip of the iceberg of what expert commissions consider when they evaluate in vitro medical tests (273–276). It includes i) analytical performance (i.e., precision, stability, interference, etc.), and ii) method-comparison studies. According to Clinical & Laboratory Standards Institute (CLSI) guidelines, whose purpose is to establish high-quality standards to improve clinical laboratory practices, method-comparison studies are used to determine if a new diagnostic method is equivalent to an established one already in clinical use (184).

The method-comparison study is included in the validation and verification processes that IVD companies must perform to obtain the regulatory agencies' certification (CE, FDA, and NMPA), which is mandatory to commercialize new assays. The process to design, analyze and interpret such a study is complex, time-consuming, and requires the understanding of several statistic methods (184,277). In this study, the current method is called the reference and the new method is called the test. Of course, both are known to measure with a certain degree of imprecision. However, the true state (presence or not of the disease) is by consensus defined by the reference method (277).

Two important parameters can be used to evaluate the performance of a diagnostic test: sensitivity and specificity. Sensitivity (also known as true positive proportion (TPP)) is the percentage of patients with the disease, called true positives (TP), in a group of subjects with the disease. Specificity, also called true negative proportion (TNP), is the percentage of patients who do not have the disease and whose assay result is negative, called true negatives (TN), in a group of healthy subjects. If the test is not able to classify a sample appropriately, we find false positive (FP) that is an error in data reporting in which the result is positive, when in fact the disease is not truly present; and false negative (FN) which is an error where the result is negative when the disease is present (see Table 6-1) (186,278).

		True State*		
		Positive	Negative	
Test Results	Positive	a	b	a+b
	Negative	c	d	c+d
		a+c	b+d	n

Table 6-1: Confusion matrix of diagnostic performance parameters. a: true positive: the patient has the disease and the test is positive, b: false positive: the patient does not have the disease, but the test is positive, c: false negative: the patient has the disease, but the test is negative, d: true negative: the patient does not have the disease and the test is negative, a+b: total of positive results, a+c: total diseased, c+d: total of negative results: b+d: total non-diseased, n: total number of patients/samples tested. *Defined by a reference method.

The equations to calculate terms of Table 6-1 are:

$$Sensitivity\ \% = \ a/(a+c) \cdot 100$$

$$Specificity\ \% = \ d/(b+d) \cdot 100$$

$$False\ Negative\ rate = \ c/(a+c) \cdot 100$$

$$False\ Positive\ rate = \ b/(b+d) \cdot 100$$

In the present project, once we had developed the prototype of the new 3a6c peptide-based immunoassay, and optimized its formulation, we performed a method-comparison study to establish its diagnostic performance.

In previous chapters, we emphasized the importance of the new assay being IgM-specific, which means that it is not affected by the presence of other immunoglobulins, especially by IgG. Hence, in the present chapter, we evaluated the potential interference that anti-*T. gondii* IgG immunoglobulins could have in the assay. Apart from IgG anti-*T. gondii* interference, we also evaluated the cross-reactivity by other disease conditions described in the literature (i.e., IgMs of other infectious diseases, rheumatoid factor (RF), and Human Anti-Animal Antibodies (HAMA)) (110,279,280).

6.1. Method-comparison study

We acquired a panel consisting of 316 samples (hereafter feasibility panel). All samples were selected following *T. gondii* IgM-positive and negative criteria (see 8.2.4). The panel contained 216 positive samples provided by Biokit biobank, and 100 non-selected samples provided by Banc de Sang i de Teixits de Catalunya.

In Spain, toxoplasmosis is not a notifiable disease, hence the blood bank samples are not tested for toxoplasmosis. However, considering toxoplasmosis prevalence, we used it as a probable source of IgM anti-*T. gondii* negative samples. To perform the method-comparison, despite it is not the gold standard method for toxoplasmosis diagnosis, we chose the BIO-FLASH® Toxo IgM as the reference assay as it is an in-house developed indirect CLIA, using *T. gondii* lysate antigen.

6.1.1. Sensitivity, specificity and agreement evaluation

Qualitative immunoassays classify samples as negative if their reactivity is under the cut-off and as positive if it is above the cut-off. Additionally, immunoassays can establish a gray zone around the cut-off where samples are classified as indeterminate or equivocal. If so, the assay supplier must specify how to proceed to solve the result (i.e., repeat the test with a new sample obtained after one or two weeks, use an alternative method, etc.).

Before performing the method-comparison, we defined the study design and the strategy to anticipate how to proceed in case of obtaining indeterminate results and/or discrepancies between the methods:

i. We first analyzed the feasibility panel with both, the new 3a6c prototype (test) and the BIO-FLASH® Toxo IgM (reference).
ii. We used a second method to solve discrepancies between the test and the reference assay and to define the status of BIO-FLASH® indeterminate samples. For its excellent performance, we selected the BIO-RAD PLATELIA™ Toxo IgM.
iii. We calculated the sensitivity, specificity, and agreement. If the PLATELIA™ Toxo IgM assay classified any sample as equivocal, we excluded it for the calculations.
iv. We studied how a gray zone affected the performance of the 3a6c prototype. To do so, we re-calculated sensitivity, specificity, and agreement including gray zone. Samples within it were excluded to perform the calculations.
v. To include indeterminate samples, we applied the *worst-case scenario*. That was to classify the samples against the result reported by the test assay. Therefore, if the sample was classified as positive, its true state was considered negative, and if the sample was classified as negative, its true state was considered positive. This strategy allowed us to predict the performance of our assay in the worst conditions, which means that the 3a6c-IPT1I would have classified incorrectly all indeterminate samples.

After analyzing the feasibility panel (n=316) with the test and the reference assay in parallel, we classified the samples according to the BIO-FLASH® package insert (positive ≥1 S/CO, negative <0.8 S/CO and indeterminate ≥0.8 and <1.0 S/CO). We initially did not consider a gray zone for the 3a6c-PT1I immunoassay; thus, we classified samples as positive when their S/CO were ≥1 and negative when it was <1. The results are shown in Table 6-2.

		3a6c-PT1I	
BIO-FLASH®	POS	NEG	TOTAL
POS	171	13	184
NEG	23	103	126
IND	3	3	6
TOTAL	197	119	316

Table 6-2: Method comparison of 3a6c-PT1I vs. BIO-FLASH® by Weighted Kappa. Weighted Kappa ($\varkappa$): 0.72 Wald 95% CI 0.64 to 0.80. POS: positive, NEG: negative and IND: indeterminate.

The comparison revealed 36 discrepant samples, 23 were positive for 3a6c-PT1I, but negative for BIO-FLASH®, and 13 were negative for 3a6c-PT1I but positive for the BIO-FLASH®. Additionally, six samples were classified as indeterminate by the BIO-FLASH®. Of these, three of

them were positive for the 3a6c-PT1I (samples 8, 136, and 299) and the other three were negative for the 3a6c-PT1I (samples 11, 189, and 290) (Table 6-3).

Sample ID	BIO-FLASH® (S/CO)	BIO-FLASH® Interp.	3a6c-PT1I (S/CO)	3a6c-PT1I Interp.
8	0.95	IND	2.57	POS
11	0.85	IND	0.60	NEG
136	0.88	IND	3.15	POS
189	0.85	IND	0.25	NEG
290	0.81	IND	0.40	NEG
299	0.80	IND	1.40	POS

Table 6-3: BIO-FLASH® Toxo IgM indeterminate samples. Results are shown in S/CO. Interp.: Interpretation according to each method. POS: positive, NEG: negative and IND: indeterminate.

6.1.1.1. Sensitivity, specificity and agreement evaluation after discrepancy resolution

To solve the six BIO-FLASH® indeterminate samples and to define the status of the 36 discrepant samples we used PLATELIA™ assay. Results along with the strategy used to classify the samples are presented in Table 6-4.

If 3a6c-PT1I was…	If BIO-FLASH® was…	If PLATELIA™ was…	Consensus was…	N° samples
NEG	POS	NEG	TN	11
NEG	POS	POS	FN	1
POS	NEG	NEG	FP	4
POS	NEG	POS	TP	19
POS	IND	POS	TP	3
NEG	IND	NEG	TN	3
NEG	POS	IND	FN	1

Table 6-4: Final consensus for discrepant and indeterminate samples. The number of samples within each condition is shown in the rightmost column. POS: positive, NEG: negative, and IND: indeterminate, TN: true negative, TP: true positive, FP: false positive, FN: false negative.

From the 42 samples, 36 coincided between the 3a6c prototype and the PLATELIA™. Fourteen agreed as negative, and therefore they were classified as true negatives (TN), and, 22 agreed as positive; hence they were considered true positives (TP).

Only six samples were discrepant between the 3a6c prototype and PLATELIA™. According to Table 6-4, we classified by consensus the four samples that were positive for 3a6c-PT1I but negative for PLATELIA™ as false positives (FP), and the only sample that was positive for PLATELIA™ but negative according to 3a6c-PT1I as false negative (FN). The sample classified as indeterminate by

PLATELIA™ (#78) was temporarily excluded to perform the calculations. The final status of the feasibility panel after discrepancy resolution is shown in Table 6-5.

	3a6c-PT1I		
Sample status*	POS	NEG	TOTAL
POS	194	1	195
NEG	4	116	120
TOTAL	199	117	315

Table 6-5: Method comparison of 3a6c-PT1I vs. PLATELIA™ by Weighted Kappa. Weighted Kappa (ϰ): 0.96 Wald 95% CI 0.93 to 0.99. Indeterminate sample (#78) was excluded. *Sample status combined the results of PLATELIA™ and BIO-FLASH®.

Based on Table 6-5, we calculated the diagnostic performance (see Table 6-6). Sensitivity or TPP was 99.5% and specificity or TNP was 96.7%. False positive result was 3.3% and false negative result was 0.5%.

Test assay	**3a6c-PT1I**	
Reference assay	PLATELIA™	
	Value	95% CI
Sensitivity (TPP)	99.5	97.2.4 - 99.9
Specificity (TNP)	96.7%	91.7 - 98.7
False positive	3.3%	1.3 - 8.3
False negative	0.5%	0.1 - 2.8
Agreement (ϰ)	97%	94.0 - 100.0

Table 6-6: Diagnostic performance of 3a6c-PT1I without indeterminate sample. Agreement was calculated by Weighted Kappa with Wald 95% CI.

6.1.1.2. Sensitivity, specificity and agreement evaluation considering 3a6c-PT1I gray zone

Once we evaluated the diagnostic performance after discrepant and indeterminate sample resolution using PLATELIA™, we aimed to study how the performance of the 3a6c-PT1I prototype was affected after considering a gray zone. We analyzed the results reported by the two methods after sorting the samples from lowest to highest RLU. Results are shown in Table 6-7.

	3a6c-PT1I Interp.			**BIO-FLASH®**		**PLATELIA™**		
#	S/CO[a]	w/o gray-zone	with gray-zone	S/CO	Interp.	RAU	Interp.	Consensus
228	0.79	NEG	NEG	0.1	NEG	-	-	NEG
186	0.80	NEG	IND	0.0	NEG	-	-	NEG
52	0.86	NEG	IND	0.26	NEG	-	-	NEG
5	0.86	NEG	IND	0.78	NEG	-	-	NEG

#	3a6c-PT1I Interp.			BIO-FLASH®		PLATELIA™		Consensus
	S/CO[a]	w/o gray-zone	with gray-zone	S/CO	Interp.	RAU	Interp.	
78	0.87	NEG	IND	1.67	POS	0,91	IND	IND
68	0.89	NEG	IND	0.62	NEG	-	-	NEG
47	1.01	POS	POS	1.92	POS	-	-	POS

Table 6-7: Samples around the 3a6c-PT1I gray zone. # Sample ID. #186, 52, 5, and 68, as their result agreed between the 3a6c-PT1I and the BIO-FLASH®, were not evaluated using PLATELIA™. Consensus column refers to the sample status for each sample. One sample above and below the gray zone is shown (samples 228 and 47).[a]Samples are sorted by 3a6c-PT1I S/CO.

The only sample incorrectly classified by the test versus the reference assay was the #78. According to its S/CO (0.87), we proposed to establish a gray zone between ≥0.80 and <1.00 S/CO. Once it was considered, the result of sample #78 coincided between PLATELIA™ and 3a6c-PT1I, being indeterminate in both cases. This scenario led us to remove it from the calculations; therefore, the performance of the assay remained the same as the previous (99.5% sensitivity and 96.7% specificity).

6.1.1.3. Additional evaluation using PLATELIA™ Toxo IgM

After the initial evaluation, we selected 80 additional samples to be tested with PLATELIA™. The criterion used was defined considering the result reported by both the BIO-FLASH® and the 3a6c-PT1I as follows:

From the non-selected samples coming from the blood bank:

- Eleven coincided as positive. Therefore, we decided to re-test them to rule out the possibility that they were false positives.
- Eight coincided as negative with a result close to the cut-off.

From the *T. gondii* IgM-positive samples provided by Biokit biobank:

- Thirty-two coincided as negative, contradicting their initial clinical status.
- Twenty-nine coincided as positive with a result close to the cut-off.

After PLATELIA™ evaluation, five samples were classified as indeterminate. Of these, two were also classified as indeterminate by the 3a6c-PT1I (see Table 6-8).

#	3a6c-PT1I		PLATELIA™		BIO-FLASH®	
	S/CO	Interp.	RAU	Interp.	S/CO	Interp.
5	0.86	IND	0.87	IND	0.78	NEG
68	0.89	IND	0.92	IND	0.62	NEG

#	3a6c-PT1I		PLATELIA™		BIO-FLASH®	
80	0.77	NEG	0.80	IND	0.66	NEG
112	0.73	NEG	0.84	IND	0.21	NEG
312	0.72	NEG	0.84	IND	0.13	NEG

Table 6-8: PLATELIA™ Toxo IgM indeterminate samples. The result and interpretation of each sample per assay are shown using the units described in the user instructions. #: Sample ID.

We re-calculated diagnostic performance excluding the two new samples classified as indeterminate by the 3a6c-PT1I (#5, and #68). Regarding samples 80, 112, and 312, we applied the worst-case scenario strategy. We used the confusion matrix shown in Table 6-9 to calculate the final sensitivity and specificity.

	3a6c-PT1I		
Sample status*	POS	NEG	TOTAL
POS	194	4	198
NEG	4	111	115
TOTAL	198	115	313

Table 6-9: Method comparison of 3a6c-PT1I vs. PLATELIA™ by Weighted Kappa for the *worst-case scenario*. Weighted Kappa (κ): 0.95 Wald 95% CI 0.91 to 0.98. *Sample status merges the results of PLATELIA™ and BIO-FLASH®.

The 3a6c-PT1I showed a sensitivity or TPP of 98.0% and specificity or TNP of 96.5% with an agreement of 0.95%.

Test assay	**3a6c-PT1I**	
Reference assay	PLATELIA™	
	Value	95% CI
Sensitivity (TPP)	98.0%	94.9 - 99.2
Specificity (TNP)	96.5%	91.4 - 98.6
False positive	3.5%	1.4 - 8.6
False negative	2.0%	0.8 - 5.1
Agreement (κ)	95%	91.0 - 98.0

Table 6-10: 3a6c-PT1I *worst-case scenario* diagnostic performance. Agreement was calculated by Weighted Kappa with Wald 95% CI.

We represented the performance of both assays (3a6c-PT1I and BIO-FLASH®) in a receiver operating characteristic (ROC) curve, considering PLATELIA™ the reference. Results are shown in Table 6-11 and Figure 6-1.

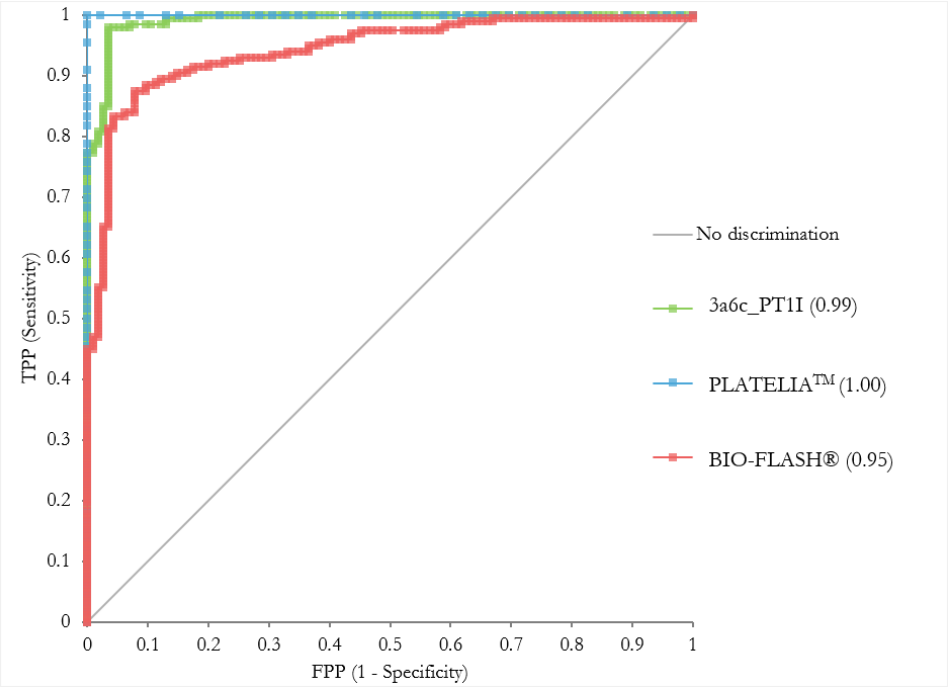

Figure 6-1: ROC curve of 3a6c-PT1I and BIO-FLASH® vs. PLATELIA™. The diagnostic performance of each assay is represented by a different colored line. The solid gray line indicates the non-discrimination area of the ROC curve. The feasibility panel, minus samples 5, 68, and 78 was considered for each assay (n=313).

The area under the curve (AUC) of each ROC was calculated along with its 95% confidence interval (CI). The 3a6c-PT1I showed an AUC of 0.99, whereas BIO-FLASH® showed an AUC of 0.94. As in this case we used PLATELIA™ as a reference, it presented the maximum performance (AUC equal to 1.00 without confidence interval).

Assay ID	AUC	95% CI
3a6c-PT1I	0.99	0.98 to 1.00
BIO-FLASH®	0.94	0.92 to 0.97
PLATELIA™	1.00	-

Table 6-11: AUC of the ROC curve for 3a6c-PT1I, BIO-FLASH®, and PLATELIA™. For each assay, the AUC and its 95% CI were calculated according to the Wilcoxon-Mann-Whitney test.

6.2. Analytical specificity

Analytical specificity is the assay's ability to detect the intended target. It includes two aspects, cross-reactivity and interference (281).

In immunoassays, interference phenomena occur when a substance alters the measurable concentration of the analyte of interest or modifies the antibody-binding capacity causing an erroneous result (110). Interference can be endogenous, caused by substances naturally found in the sample (i.e., lipids, proteins, antibodies, etc.), or exogenous, originated by foreign substances (drugs, poison, preservatives from the collection tube, etc.) (280).

Cross-reactivity is a type of interference created by a substance present in the sample, which has a structural similarity with the analyte aimed to detect. Due to this, the cross-reactant competes with the analyte for the capture molecule. Cross-reactivity is probably the most common type of interference in immunoassays. It usually causes positive interferences, which means that the sample is overrated. However, negative interferences are also possible with certain assay designs (282).

In the present project, we focused on two types of endogenous interference: i) caused by IgG anti-*T. gondii* and ii) originated by specific antibodies against other disease conditions. This type of interference study is known as a cross-reactivity study. The cross-reactants were selected based on data provided by the user instructions of the commercial kits.

6.2.1. *T. gondii* IgG interference study

To study the interference of endogenous IgG anti-T. *gondii* in the 3a6c-PT1I immunoassay, we adapted internal procedures which follows CLSI guidelines (EP07-A2) (110,283). Briefly, interference was calculated based on the measurement of the analyte of interest (IgM anti-*T. gondii*) in a sample containing the potential interferent (the IgG anti-*T. gondii*) versus a control sample that did not contain the interferent. We established at ±5% the acceptance criterion to determine whether IgG was interfering in the assay.

We selected two samples containing IgM anti-*T. gondii*—positive according to 3a6c-PT1I—but negative for IgG anti-*T. gondii* (samples #35 and #74 of the conditional panel (Table 3-8)), and two samples containing the potential cross-reactant (the IgG anti-*T. gondii*) but not the analyte of interest; that is, samples that were negative for IgM anti-*T. gondii* (named IgG1 and IgG2). The immune status of each sample and the assay used to perform the analysis are shown in Table 6-12.

The samples containing the IgM anti-*T. gondii* were divided into three aliquots, one aliquot was diluted with an IgG and IgM-negative sample (#5713) and was used as control (C). The other two aliquots were spiked each one with the IgG1 and IgG2 samples. Those were the test (T). To study interference, we performed 30 replicates of each aliquot with the 3a6c-PT1I.

	BIO-FLASH® Toxo IgG			**BIO-FLASH® Toxo IgM**			**3a6c-PT1I**	
#	Interp.	RLU	IU/mL	Interp.	RLU	S/CO	Interp.	RLU
35	NEG	1724	1.5	POS	48126	4.8	POS	51283
74	NEG	527	< 0.9	POS	96865	9.7	POS	254359
5713	NEG	365	< 0.9	NEG	871	0.02	NEG	345
IgG1	POS	9369	21.3	NEG	2793	0.2	NEG	1278
IgG2	POS	18757	38.7	NEG	2690	0.2	NEG	806

Table 6-12: Characterization of interference samples. IgG and IgM anti-*T. gondii* evaluation shown in RLU, IU/mL, or S/CO according to the package insert. Interp.: interpretation.

For the analysis, we calculated the mean RLU value of the 30 replicates, the standard deviation (SD), the coefficient of variation (%CV), and the percentage of bias (%bias) between (C) and (T). Results are shown in Table 6-13. If the bias was <5%, we considered that the IgG anti-*T. gondii* did not interfere in the assay.

The dilution with IgG1 and IgG2 entailed a reduction or an increase in the reported RLU. Nevertheless, none of the samples evaluated showed a bias higher than 2.5%, which was the case of sample 35. Therefore, the presence of IgG anti-*T. gondii* did not interfere in the performance of the 3a6c-IPT1I.

#	Sample type	Mean (RLU)	SD	%CV	%bias
35-IgG1	(C)	21039.1	618.5	2.9	-2.5
	(T)	20521.0	513.1	2.5	
35-IgG2	(C)	21039.1	618.5	2.9	-1.7
	(T)	20681.0	756.1	3.7	
74-IgG1	(C)	114154.1	827.3	0.7	-1.1
	(T)	112874.2	1109.3	1.0	
74-IgG2	(C)	114157.2	827.3	0.7	-0.9
	(T)	113123.3	1237.7	1.1	

Table 6-13: Reported values of the interference study. Mean (RLU), standard deviation (SD), and coefficient of variation (%CV) for each pool are shown for control (C) and test (T) samples.

6.2.2. Cross-reactivity study

In the current section, we present the study of potential cross-reactive antibodies in samples from donors infected with other diseases or with anti-animal antibodies for the 3a6c-PT1I immunoassay. Among the commonly studied cross-reactive antibodies, anti-animal antibodies stand out. These usually appear in sera of animal workers, patients treated with monoclonal antibodies for therapy or imaging, and others exposed to mice antigens (111,284,285).

To perform the study, we followed internal procedures. According to BIO-FLASH® Toxo IgM user instructions, the cross-reactants prone to alter assay results were human anti-mouse antibodies (HAMA), varicella zoster (VZ), systemic lupus erythematosus (SLE), rubella (RUB), rheumatoid factor (RF), parvovirus (Parvo), herpes simplex virus (HSV) and cytomegalovirus (CMV).

For the present study, we used as a reference method the BIO-FLASH® Toxo IgM. We considered potential cross-reactivity when the status of IgM anti-*T. gondii* was different between the 3a6c-PT1I and the BIO-FLASH® Toxo IgM.

Sample	BIO-FLASH® Toxo IgM		3a6c-PT1I		Agree
	S/CO	Interp.	S/CO	Interp.	
VZ 1	0,1	NEG	0,4	NEG	YES
VZ 2	2,1	POS	2,0	POS	YES
VZ 3	0,0	NEG	0,5	NEG	YES
SLE 1	0,1	NEG	0,0	NEG	YES
SLE 2	0,3	NEG	0,2	NEG	YES
RUB 1	0,4	NEG	0,1	NEG	YES
RUB 2	0,4	NEG	0,6	NEG	YES
RUB 3	1,4	POS	0,3	NEG	NO
RF 1	0,7	NEG	0,5	NEG	YES
RF 2	0,0	NEG	0,1	NEG	YES
PARVO 1	0,0	NEG	0,2	NEG	YES
PARVO 2	0,2	NEG	0,6	NEG	YES
PARVO 3	0,3	NEG	0,5	NEG	YES
HSV 1	0,1	NEG	0,8	NEG	YES
HSV 2	0,6	NEG	0,6	NEG	YES
HAMA 1	0,2	NEG	11,2	POS	NO
HAMA 2	0,1	NEG	4,7	POS	NO
CMV 1	0,3	NEG	0,6	NEG	YES
CMV 2	0,1	NEG	0,3	NEG	YES
CMV 3	1,1	POS	0,6	NEG	NO

Table 6-14: Cross-reactivity evaluation with BIO-FLASH® Toxo IgM and 3a6c-PT1I. The agreement between the reference assay (BIO-FLASH®) and the test (3a6c-PT1I) is represented in the rightmost column. VZ: varicella zoster, SLE: systemic lupus erythematosus, RUB rubella, RF: rheumatoid factor, Parvo: parvovirus, HSV: herpes simplex virus, HAMA: human anti-mouse antibodies, and CMV: cytomegalovirus.

The analysis of the potential cross-reactants showed total agreement and therefore no interference in the cases of varicella zoster, systemic lupus erythematosus, parvovirus and herpes simplex virus. In contrast, the results for both rubella and cytomegalovirus were discrepant; one out of three samples was classified as negative by the 3a6c-PT1I and positive by the BIO-FLASH® Toxo IgM. For the two samples with HAMA, the 3a6c-PT1 reported positive results, whereas BIO-FLASH® classified them as negatives. These results indicated that HAMA, rubella and cytomegalovirus antibodies are potential cross-reactants for 3a6c-PT1I immunoassay.

6.3. Discussion

The process to validate an immunoassay comprises several well-defined stages, from early feasibility studies to the determination of assay performance characteristics (184).

Even though the conception of this project was to perform the proof of concept of a new peptide-based IgM-specific immunoassay, and that objective has been already completed in previous chapters, we considered it relevant to have a greater understanding of its performance. Therefore, in the present study, the potential clinical utility of a novel assay for the qualitative detection of IgM anti-*T. gondii* has been comprehensively assessed by using clinical sera samples, resulting in a sensitivity and specificity of 98% and 96.5% respectively.

The regulatory agencies often recommend the use of at least 40 and preferably 100 patient samples to compare two methods. However, the number of samples used in such studies varies considerably. Gay-Andrieu et al., performed a comparative evaluation of the ARCHITECT Toxo IgG and IgM immunoassays with 730 samples from pregnant women (118). The study conducted by Kaul et al., which aimed to develop a new toxoplasma bead-based IgM immunoassay, included 402 non-selected healthy donors and pregnant women (125). The study performed by Beghetto et al., which evaluated the diagnostic utility of six antigenic regions of *T. gondii*, used 127 samples from adults and 30 samples from infants born to mothers with primary toxoplasmosis (175). Baschirotto et al., developed a multiplex microarray for the diagnosis of toxoplasmosis and rubella infection, including 92 positive and 30 negative samples (223).

Although we have cited only a few of the many studies in this area, we can see the lack of consensus when choosing the number and type of samples. Usually, the studies that assess commercial immunoassays use larger panels compared to those that evaluate methods that have not been commercialized. However, more important than the number is the alignment between the scope of the study, or the intended use of the product and the type of samples tested.

For the method-comparison, we tested 316 samples. Although this may seem like a large number, especially considering that this is a proof of concept, it is important to point out that we did not use pregnancy-selected samples. The 3a6c-PT1I was designed for the detection of IgM anti-*T. gondii*, which is especially relevant in pregnant women, and therefore it may appear logical to study those kinds of samples. However, two main reasons made us decide not to use them: the difficulty to obtain these samples, and that we did not want to condition our results to a single casuistry. Rather, we used non-selected samples to have a more generic picture of the assay performance when used in the general population. Nevertheless, this must be considered when comparing our results with other studies.

Seroconversion panels that include sequential samples from subjects who were initially *T. gondii*-negative are one of the most valuable tools to evaluate sensitivity since the positives are known to result from an acute infection (125,286). Besides, IgM-positive and IgG-negative samples at the first test are also valuable, since this pattern suggests recent infection. Despite the usefulness of these samples, they are not used in many studies given the difficulty of finding them. As far as we know, the study done by Kaul et al., which included 10 toxoplasma seroconversion panels analyzing 44 samples overall, is the study aimed to evaluate an IgM-specific immunoassay that included the highest number of seroconverted samples (125).

The ideal assay has a sensitivity and specificity of 100%. When this is not possible, the cut-off impacts directly on both parameters. Concerning IgM in the context of toxoplasmosis, specificity is important because a positive result during pregnancy is highly distressing for the patient and therefore false positive results should be avoided. Similarly, high sensitivity is also desirable as the consequences of not treating pregnant women with acute toxoplasmosis (false negative) can be fatal. For this reason, to decide whether an assay with greater sensitivity and few false negatives is preferable, or on the contrary, the assay should have greater specificity and few false positives is not trivial.

In the clinical context, the predictive value of a *T. gondii* IgM-positive result varies from one assay to another, thus complicating toxoplasmosis diagnosis (287). Different studies support such data. The FDA toxoplasmosis Ad Hoc working group evaluated the diagnostic performance of six IgM anti-*T. gondii* FDA-cleared commercial kits after the same FDA detected an increased number of false positive results (123). For the method-comparison, they selected as reference assay a double-sandwich IgM ELISA performed by the Toxoplasma Serology Laboratory, Palo Alto Medical Foundation. They found that except for two, all kits showed 100% sensitivity and specificities between 99 and 84% respectively. One of the commercial assays evaluated was the Abbott Toxo IMx, which reported 95.6% sensitivity and 99.8% specificity in a study performed by Luyasu et al., (288) two years before, whereas, a similar study performed by Liesenfeld et al., showed 97.8% sensitivity and 99.0 specificity using as a reference the Sabin-Feldman dye test (289).

In Europe, Roberts et al., performed the biggest study done to date, comparing the diagnostic performance of 20 *T. gondii* immunoassays (seven of them intended for IgM detection) using samples coming from 11 European centers. This study also included the Abbott Toxo IMx, which reported 93% sensitivity and 92% specificity (287).

Garry et al., although did not focus on any particular assay, found the more dramatic results (100% sensitivity and 11.4% specificity) when they reviewed the clinical utility of commercial laboratory tests aimed to detect specific IgM versus the results found in the reference Toxoplasmosis Serology Lab, Research Institute, Palo Alto Medical Foundation (290).

Several studies can be found exemplifying such performance differences in regards to different commercial and in-house assays (51,221,269,291,292). This data points out two important aspects concerning IgM immunoassays: i) laboratory testing for toxoplasmosis varies greatly by method and kit, and ii) exist a need to design immunoassays capable not only to increase both sensitivity and specificity but also to provide reliable and robust results.

In regard to the performance differences encountered by the several studies mentioned, one aspect must be highlighted. We found a trend that indicates that most of the false positive results were concentrated in IgG-positive and IgM-negative samples, this observation was found in particular in the immunoassays that used antigens as a capture molecule (123,269,293). In the study performed by Marianna et al., they deduced that immunocapture formats could reduce the number of false positive results in IgG-positive patients as, by its very nature, this approach theoretically provides complete elimination of all isotypes other than IgM in the initial step of the assay (123).

Aware of the reality that exists around the IgM serodiagnosis, our immunoassay directly impacts several of the limitations that current kits manifest. We used a synthetic peptide as an antigen, which has demonstrated to be an excellent diagnostic tool in several human diseases (56,166,170,174). Avoiding the use of native antigens, which has been largely related to performance drawbacks (131,224), we obtained good diagnostic performance. Additionally, we proved that our prototype is IgM-specific, and the presence of IgG does not interfere with our assay.

Here we have confirmed that the antigen used, rather than the assay itself, directly affects the ability to recognize IgM. In contrast to what Kaul et al., observed in their bead-based immunoassay, which yields a differential response to IgM anti-*T. gondii*, with reduced sensitivity to IgM from samples with high-avidity IgG (125). That observation was associated with the assay (ELISA vs. bead-based) rather than a characteristic of the antigen. In the present project, although we encountered differences between the 3a6c-ELISA and the 3a6c-PT1I, those were minor and can be easily attributed to the greater CLIA dynamic range compared to ELISA. However, in comparison with Kaul et al., it is important to mention a limitation of our study, as we did not test IgG anti-*T. gondii* seroprevalence in the feasibility panel. Therefore, we do not know whether the false positive samples we found were IgG-positive or not.

To perform the method comparison, we initially selected as reference the BIO-FLASH® Toxo IgM, as we wanted to compare our synthetic-peptide assay with one that uses native *T. gondii* antigen as a capture molecule. Additionally, to solve discrepant and indeterminate results, we selected the PLATELIA™ Toxo IgM because of its excellent performance (221). The study performed by Kaul and colleagues also compared the performance of their bead-based assay with the PLATELIA™ Toxo IgM. They observed that in the group of pregnant women both assays reported the same

number of positive results; however, six samples reported contradictory results. To solve the status of those samples they analyzed them at the Toxoplasma Serology Laboratory, Palo Alto Medical Foundation, concluding that they were IgM-negative (125). This study suggests that the false positive ratio we obtained (3.5%) could be inaccurate if our assay were more IgM-specific than the reference method. It is important to mention that the PLATELIA™ Toxo IgM, although is an immunocapture assay, it uses native *T. gondii* antigen as a conjugate, which could pose a disadvantage with respect to its specificity.

As mentioned, IgG interference was a crucial factor in developing our assay. For their very nature, IgGs have a higher affinity than IgMs, which could displace in favor of IgG the kinetics of the immunological reaction in the context of an immunoassay. For that reason, we studied in detail the immunoreactivity of our peptides in the early development phases; starting with the use of a peptide microarray to identify the IgM-specific regions, and later using a multiplex ELISA to evaluate their reactivity with a large number of IgM-positive samples. Finally, we designed a synthetic peptide based on GRA3 and ROP1 epitopes which have been demonstrated to be IgM-specific, despite other studies use ROP1 for IgG detection (181). Additionally, in the present chapter, we aimed to assess IgG interference. Our design allowed us to evaluate how IgG concentration affected the result. Thanks to the set of tests performed, we could affirm that our assay is IgM-specific and is not affected by the presence neither the concentration of IgG.

The evaluation of the potential cross-reactants showed that both rubella and cytomegalovirus, although positive by the BIO-FLASH® Toxo IgM, were not detected by the 3a6c-PT1I. One of the rubella samples was also positive for IgG (data not shown), which made us to deduce that it could be also IgM-positive, and therefore a false negative for our assay. Regarding the cytomegalovirus positive sample, our results could be explained if it was a false positive of the BIO-FLASH® Toxo IgG, especially considering its result near the cut-off (1.16 S/CO). A particular case is the HAMA samples, which reported all discrepant results versus the reference. HAMA interference is more prone to occur in immunocapture immunoassay (294); however, that was not the case in our peptide-based assay. Therefore, we attribute it to a chance finding, probably related to excessive concentrations of plasma constituents (i.e., free fatty acids, hemolysis, hyperbilirubinemia, etc.) or due to the presence of compounds of similar molecular structure or which carry similar immunoreactive epitopes. Regarding our cross-reactivity study, we found a limitation the lack of a confirmatory test capable of decanting doubtful samples.

Despite the huge effort made in IgM immunoassays, there is still an urgent need for a test that can determine the true nature of *T. gondii* infection given the long half-life of some IgM antibodies (125). Our results demonstrate that the new immunoassay here presented has performance characteristics

comparable to those of assays using the native *T. gondii* antigen (175,200) with an additional advantage, since it does not require the use of animals for the production of the antigen. These not only represent big savings in production costs but also facilitate the obtention of more reproducible biomaterials.

Altogether, we hope the work presented here opens the door to the use of these "artificial" antigens for the development of a new generation of IgM-specific immunoassays, more ethical, and capable of diagnosing the acute phase of toxoplasmosis with maximum reliability.

CHAPTER 7 – Chimeric monoclonal IgM as an alternative source for calibrators and controls: Cell line generation and thermal stability characterization

Immunoassay quantitation requires one or more components used as standards —calibrators and/or controls— containing the molecule to be measured. Therefore, their production depends on the availability of reference sera that has been characterized in terms of antibody content (196).

In quantitative assays, calibrators are used to generate calibration curves, which allows interpolating sample reactivity between two points in the calibration curve to determine the sample concentration. Conversely, in qualitative assays they work as the assay cut-off that permit discriminating positive from negative samples. Controls are utilized to establish assay performance characteristics, and when they are used within a run are useful indicators of assay integrity (196,295).

Conventional manufacturing procedures to generate both calibrators and controls require collecting and processing large volumes of sera from infected individuals. This modus operandi has several drawbacks, especially when detecting IgM, which includes difficulty to obtain large volumes with high IgM titer (as in most cases it is present in blood for less time than IgG), adequate specificity, and low variability between lots. Altogether, these factors make obtaining good reference materials an expensive and time-consuming process (86,185).

Consequently, finding alternative methods to produce calibrators and controls that avoid the use of human sera would represent a significant advance, as it would contribute to develop a new generation of calibrators and controls that did not depend on highly prized raw materials.

This section presents the collaboration with ArkAb, a division of B Cell Design (Limognes, France), which has developed several hybridoma cell lines producing specific chimeric humanized monoclonal antibodies. This source is a promising alternative supply for antibodies found in sera of infected individuals.

As an alternative to sera from patients with acute toxoplasmosis, we developed two hybridoma cell lines that produce chimeric monoclonal IgM specific to our synthetic peptide to be used as standard materials for our 3a6c-PT1I immunoassay.

Initially, we evaluated if the chimeric monoclonal IgM could serve as calibrators and controls, using two different buffers as diluent, to reach the required reactivity. Additionally, we aimed to investigate whether the storage time and temperature conditions influenced the reactivity of the chimeric monoclonal IgM and therefore if those novel biomaterial have comparable thermal stability to the current calibrators and controls (296).

7.1. Hybridoma cell line generation

Hybridoma technology offers an indefinite supply of murine monoclonal antibodies, which have several applications in biochemistry, molecular biology, and biomedicine (190,297). However, these antibodies do not react in the assay format required to measure specific human IgG or IgM and therefore cannot be used to standardize anti-human antibodies assays (196).

Recombinant DNA technology allows the obtention of chimeric humanized antibodies, as it has become possible to combine the heavy and light chain variable regions of a desired murine monoclonal antibody with human constant regions, creating hybrid antibody molecules (189,197,298). Additionally, in the last years, the use of transgenic non-human models that incorporate such genetic modification and are capable to produce chimeric human immunoglobulins had become a reality with attractive advantages over recombinant products (193).

To achieve our aim of generating chimeric humanized monoclonal IgM to be used as reference materials, we collaborated with ArkAb which developed and patented InEps® transgenic mouse model (198). These mice possess a cassette carrying the human gene of the immunoglobulin heavy chain constant region in the endogenous immunoglobulin locus. Therefore, the mouse lymphocytes secrete chimeric antibodies with a human heavy chain constant region and mouse variable regions.

To obtain the hybridomas, five InEps® mice were immunized with the 3a6c synthetic peptide selected in previous chapters. After immunization, ArkAb followed mice polyclonal response using ELISA, therefore identifying which animals were secreting specific antibodies against the 3a6c peptide. Four mice were selected for B cells immortalization. The cellular fusion process yielded different number of hybridomas per mice. The reactivity assessment revealed that 12 hybridomas from two different mice were specific for the 3a6c peptide and showed non-polyreactive response (data not shown). We selected eight hybridomas (seven from one mice, and one from a second) as final candidates to initiate cellular stabilization and master cell bank generation.

7.2. Evaluation of the hybridoma supernatants' reactivity

As mentioned in previous chapters, we have developed both ELISA and CLIA prototype assays using as antigen the 3a6c synthetic chimeric peptide. We used ELISA to monitor the response of the hybridomas. Additionally, we evaluated the reactivity of the final hybridomas with our 3a6c-PT1I CLIA.

7.2.1. Evaluation of hybridoma supernatants by ELISA

Based on ArkAb results, we selected eight hybridomas showing specific and maintained antibody titer production (A12, B12, H3, A11, F3, B6, G7, B3). The supernatants of the final hybridomas were

sent to Biokit to determine the reproducibility of the results obtained by ArkAb and to evaluate its reactivity with CLIA. Results of ELISA evaluation are shown in Figure 7-1.

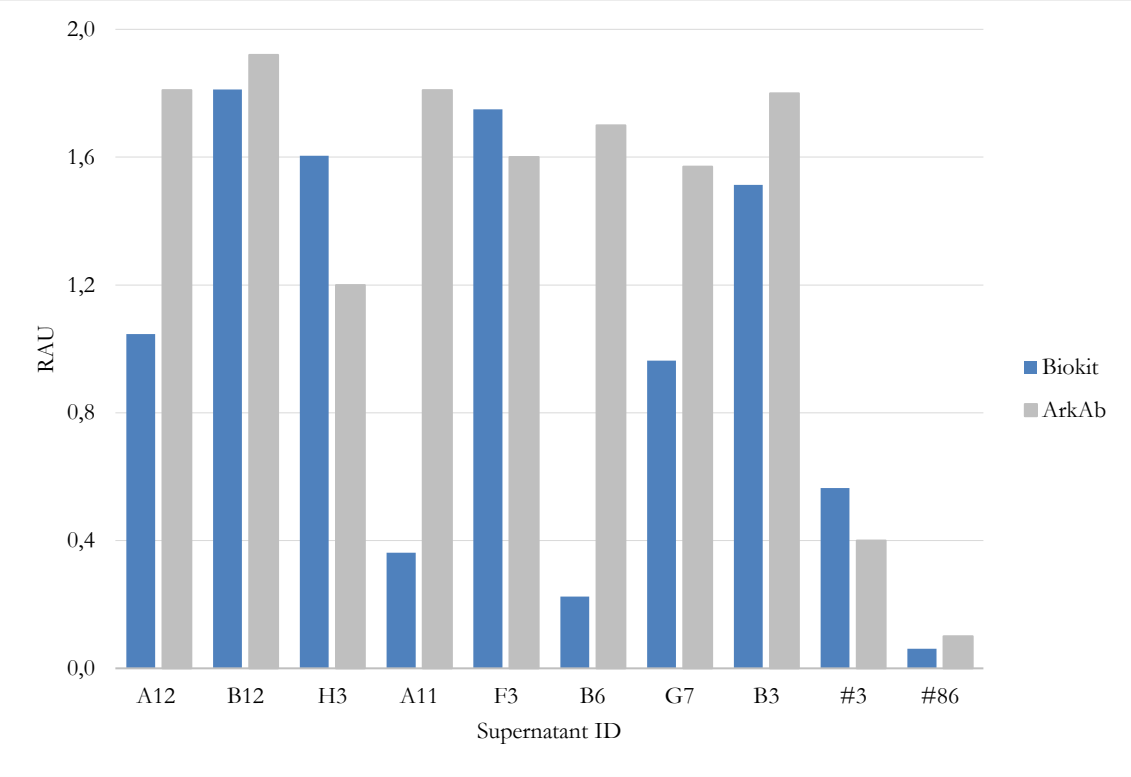

Figure 7-1: Comparison of hybridoma supernatants' reactivity. Reactivity is expressed in Relative Absorbance Units (RAU). As controls, high positive (#3) and negative sample (#86) were used.

Similar reactivities were found in all supernatants except for A11 and B6 supernatants. As controls, we used one positive and one negative sample from the conditional panel (see Chapter 3). We considered "reactive" those supernatants with RAU higher than 0.4. Our results demonstrated that A12, B12, H3, F3, G7 and B3 hybridomas were specific for the 3a6c chimeric peptide.

7.2.2. Evaluation of hybridoma supernatants by CLIA

We evaluated the supernatants received from ArkAb with the 3a6c-PT1I CLIA. In parallel, we used the BIO-FLASH® Toxo IgM, which is based on *T. gondii* lysate antigen to assess the specificity of the antibodies. As a control, we used control tosyl magnetic particles (see 5.2.1.1).

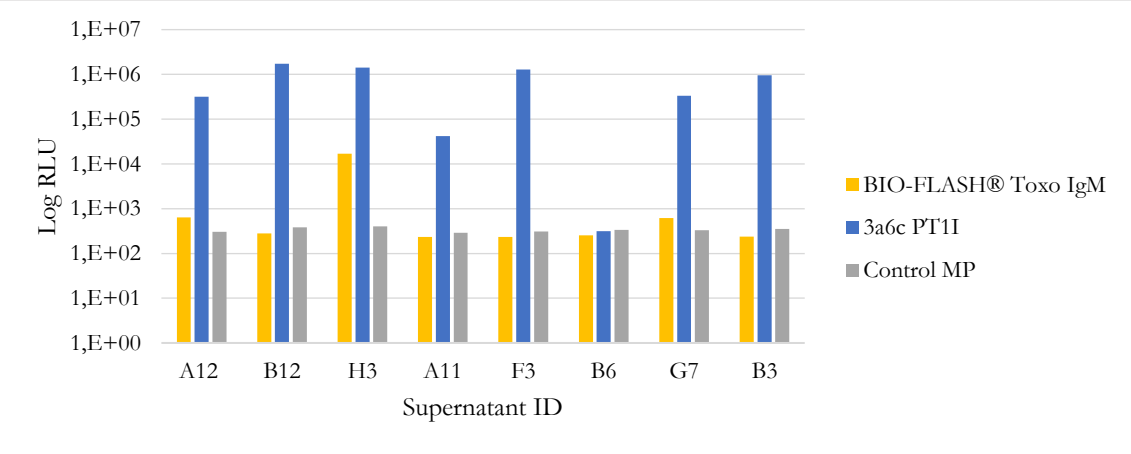

Figure 7-2: Hybridoma supernatant reactivity. Supernatants were evaluated with BIO-FLASH® Toxo IgM, and 3a6c-PT1I. As a control, non-functionalized magnetic particles were used.

The results obtained were consistent with those reported by ELISA. Based on their reactivity, we selected A12, B12, H3, F3, G7 and B3 hybridomas to continue the stabilization process. Each selected clone was stabilized by ArkAb before proceeding to obtain the master cell bank. After the stabilization, the two best derived clones (A12A, A12B, B12A, B12B, etc.) were sent to Biokit to assess their reactivity with the 3a6c-PT1I (see Figure 7-3).

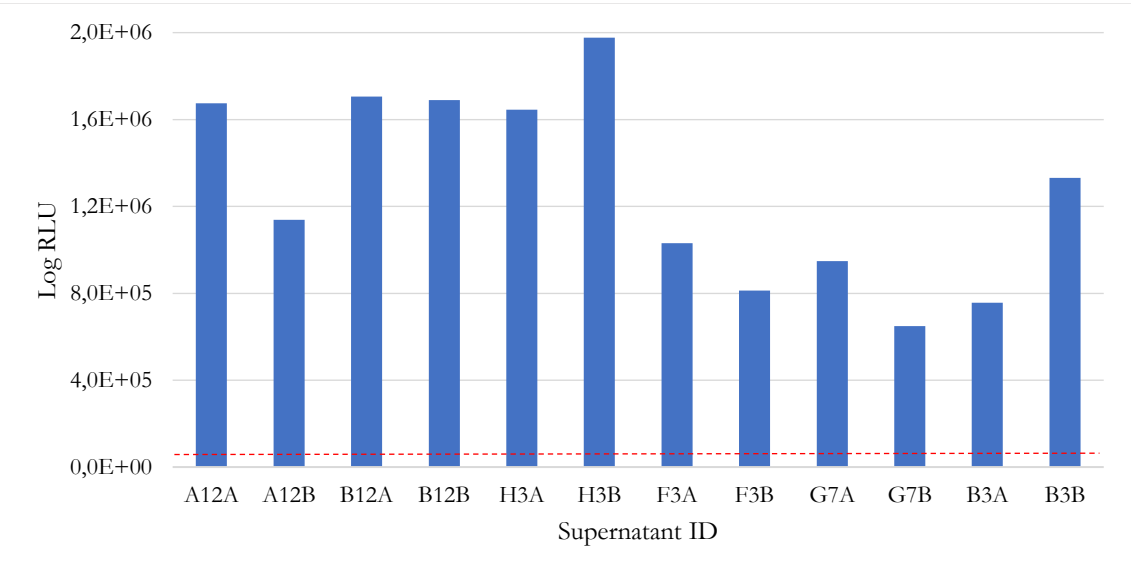

Figure 7-3: Reactivity of stabilized hybridoma supernatant. Each supernatant was analyzed with the 3a6c-PT1I. The red-dash line indicates the positive threshold defined by the BIO-FLASH® Toxo IgM calibrator 2.

To determine if the clones were reactive and suitable as new calibrators and controls, we used as a threshold the RLU reported by the BIO-FLASH® Toxo IgM calibrator 2 (between 10,000 and 20,000 RLU). This value is represented in Figure 7-3 as a red-dash line. Although all supernatants were highly reactive to the 3a6c-PT1I, we selected as final candidates A12A, B12A and H3B hybridomas to constitute the master cell banks.

At the time of writing, only A12A and B12A cell lines had been validated and delivered to Biokit. Thus, no further information can be provided regarding the H3B hybridoma.

7.3. Thermal stability of chimeric IgM

7.3.1. Hybridoma batch cell culture

In addition to assess the reactivity and specificity against the 3a6c chimeric peptide, we studied the IgMs thermal stability. To do so, we evaluated the reactivity of the supernatants after exposing them to different temperature and freeze/thaw cycles. To mimic current calibrators and controls, we diluted the supernatants to reach working concentrations of 1 and 3 S/CO, which correlates with BIO-FLASH® Toxo IgM calibrator 2 and positive control S/CO, respectively. As diluents, we used both generic buffer and specific diluent formulated to stabilize IgMs.

To produce enough quantity of supernatant to assess IgM stability, we performed a batch cell culture for each hybridoma cell line, A12A and B12A. It consists in maintain cells and media in a culture platform for a certain period of time with no nutrient addition, sub-metabolite or product removal. During cell growth, parameters such as cell density, viability, and production of the antibody of interest were assessed. We maintained the cell culture until cell viability was ≤20%, moment at which we harvested the supernatants to perform the thermal stability study.

7.3.1.1. A12A cell line

From the second day of culture, supernatant samples were collected every 24 hours until the cellular viability was ≤20%. Each sample was diluted 1/100 with generic buffer and analyzed with the 3a6c-PT1I. Reactivity against 3a6c-PT1I and cell viability percentages are shown in Figure 7-4. In the first two checkpoints, RLU remained stable; however, at 96h the reactivity decreased. Later, at 120h, reactivity was recovered and even increased, and was maintained stable until the end of the culture. In terms of cellular viability, we observed a peak at 72h of culture. Thereafter, the cell viability gradually decreased until it reached 18% at 192h.

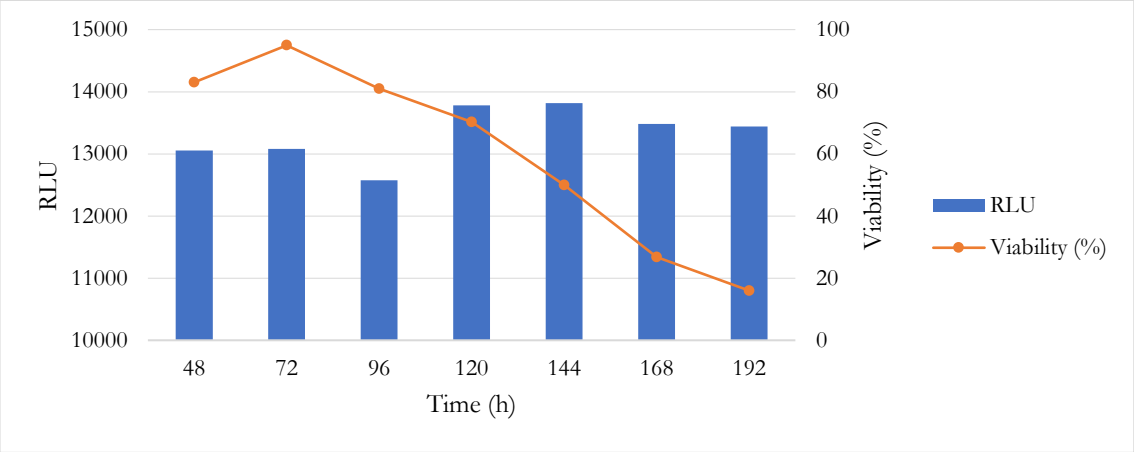

Figure 7-4: A12A hybridoma cellular viability and reactivity against 3a6c-PT1I. During batch culture, each supernatant sample collected was evaluated with the 3a6c-PT1I to assess reactivity and checked for cellular viability until it was ≤20%.

7.3.1.2. B12A cell line

The procedure followed to assess cellular viability and hybridoma reactivity was the same as for A12A cell line. Results showed that both hybridomas behave differently either in reactivity and cellular viability. B12A reactivity against 3a6c-PT1I, although it grew continuously until the last check point at 144h, it was 10-fold lower than that of A12A (7392 vs. 13817 RLU). Cell viability dropped from 72 to 144h, reaching 17% at 144h, moment in which we stopped the cell culture (see Figure 7-5).

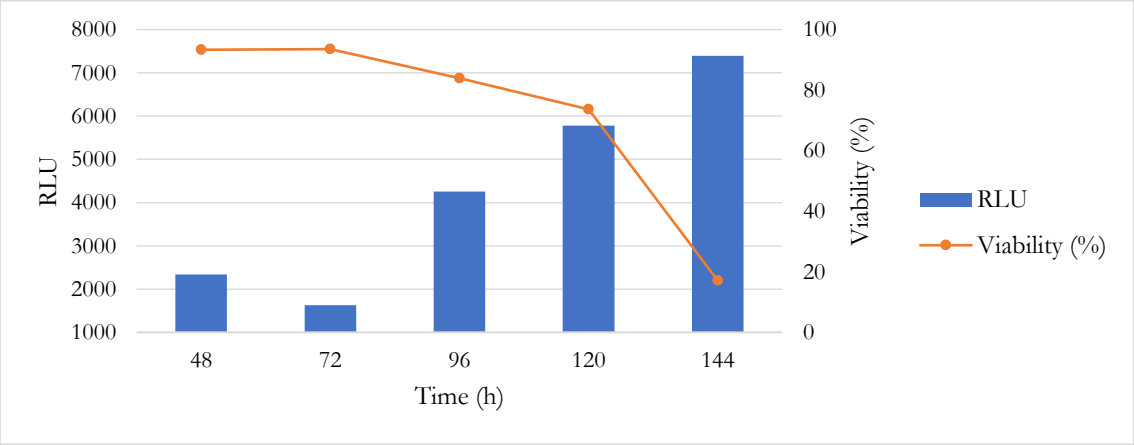

Figure 7-5: B12A hybridoma cellular viability and reactivity against 3a6c-PT1I. During batch culture, cellular viability was assessed and supernatant samples were evaluated with the 3a6c-PT1I.

7.3.2. Thermal stability characterization

To study antibody stability at different storage and handling conditions, we kept the supernatants at different temperatures (2-8°C, and successive freeze-thaw cycles at -70°C). Both studies were conducted following the procedure shown in Figure 7-6.

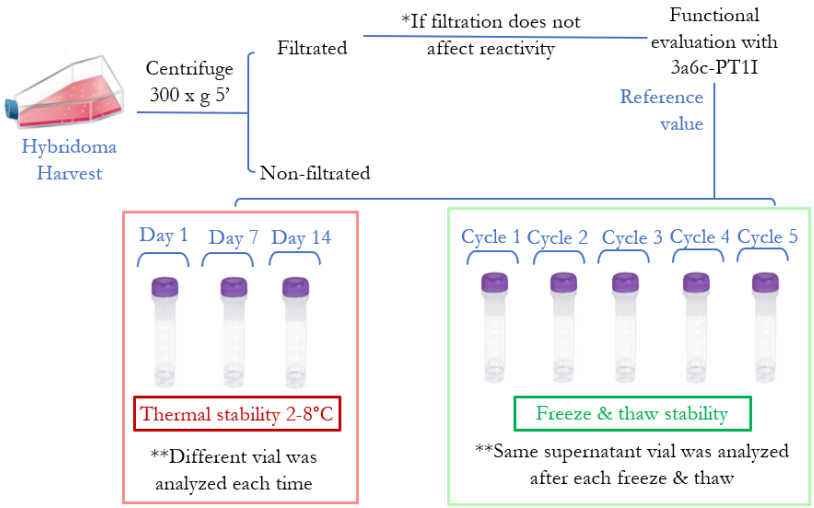

Figure 7-6: Procedure followed to assess IgM thermal stability. Batch culture was harvested and centrifugated. An aliquot of both filtered and non-filtered supernatants was analyzed (reference value). Supernatants stored at 2-8°C were evaluated at days 1, 7 and 14. One aliquot was stored at -70°C and subjected to five freeze-thaw cycles.

7.3.3. Thermal stability at 2-8°C

Harvested hybridoma supernatants were filtered in sterile conditions to avoid possible contamination. Both, filtered and non-filtered supernatants were evaluated at day 0, showing that the filtration did not result in antibody loss (data not shown). We wanted to prepare two sets of materials; one reaching approximately 1 S/CO and a second at 3 S/CO. As we demonstrated previously that the reactivity of each hybridoma was different, we performed serial dilutions with each supernatant to assess the optimal dilution with which the reactivity was 1 and 3 S/CO (data not shown).

The A12A hybridoma supernatant was diluted 1/500 to reach 1 S/CO (1254 RLU) and 1/150 to reach 3 S/CO (3940 RLU) and then, stored at 2-8°C (see Table 7-1). At each checkpoint, we tested the vials with the 3a6c-PT1I. Results showed that the reactivity of both materials decreased except for the day 1. The same procedure that for A12A supernatant was followed to assess the stability of the B12A supernatant at 2-8°C. B12A supernatant was diluted 1/450 to reach 1.6 S/CO (2631 RLU) and 1/150 to reach 3.5 S/CO (5406 RLU). Results showed that B12A reactivity decreased gradually, until day 14 when it recovered and even overcame the reference values. Overall, the results indicated that both supernatant were unstable at 2-8°C, hence different storage conditions must be studied.

Sample ID		Reactivity	Day 0	Day 1	Day 7	Day 14	Major Bias (%)
A12A	1 S/CO	RLU	1254	1411	809	466	-62.8
		S/CO	1.0	1.1	0.5	0.1	-
	3 S/CO	RLU	3940	4318	3635	950	-75.9
		S/CO	3.0	3.8	3.1	0.6	-

Sample ID		Reactivity	Day 0	Day 1	Day 7	Day 14	Major Bias (%)
B12A	1 S/CO	RLU	2631	2117	1229	3240	-53.3
		S/CO	1.6	1.3	0.6	2.0	-
	3 S/CO	RLU	5406	4517	3599	6492	-33.5
		S/CO	3.5	2.9	2.3	4.3	-

Table 7-1: Supernatant stability at 2-8°C of A12A and B12A. Bias (%) vs. Day 0 was calculated for each time point. Only major bias (%) is represented. Results are given in Relative Luminescence Units (RLU) and Signal to Cut-Off (S/CO).

7.3.4. Freeze-thaw stability

Apart from 2-8°C, we aimed to assess stability of the IgM after several freeze-thaw cycles. Once filtrated, supernatants were frozen at -70°C. Then, after a minimum of 24h frozen, they were thawed, diluted to reach approximately 1 and 3 S/CO using generic buffer and tested with the 3a6c-PT1I. Results obtained after successive freeze-thaw cycles are shown in Table 7-2 and Figure 7-7.

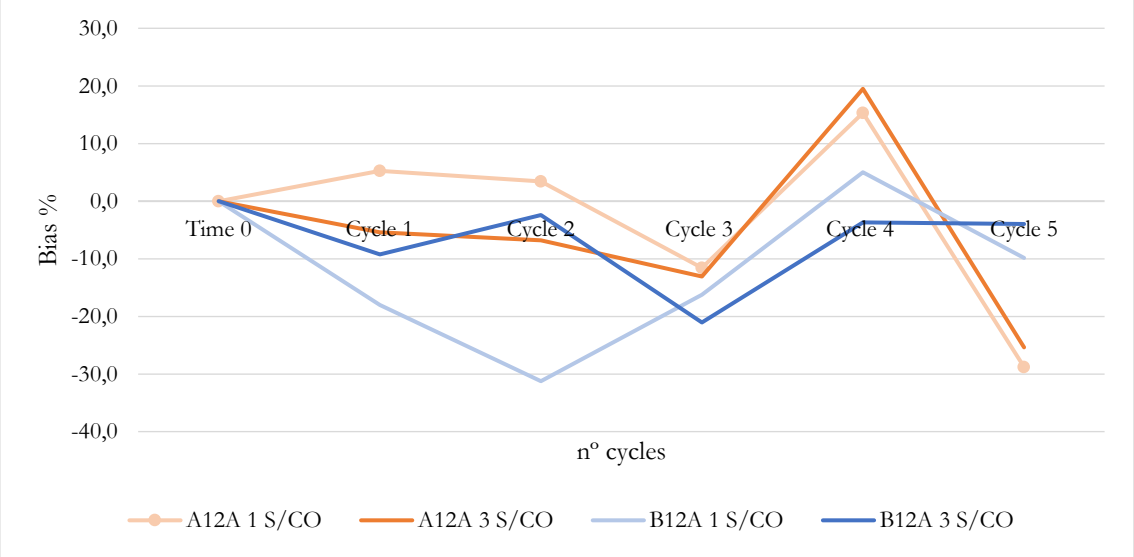

Figure 7-7: A12A and B12A Bias % plot. The reactivity of each sample after several freeze-thaw cycles was measured and the bias vs. Time 0 was calculated.

Bias % vs. nº cylces plot represented in Figure 7-7 shows that the reactivity drop was lower when the supernatants were more concentrated (3 S/CO), especially in the first and second freeze-thaw cycles. In contrast, higher dilutions presented larger variation percentages bias (31% in the second cycle of B12A supernatant). In general, B12A supernatant diluted to reach 3 S/CO showed higher stability.

In terms of S/CO, the reactivity of A12A diluted to reach 1 S/CO remained stable for the first three cycles, then it showed a clear downward trend. However, at 3 S/CO a reactivity drop was observed in the first checkpoint, and afterwards it was maintained stable. In contrast, the reactivity of B12A showed no clear trend, with alternating increments and drops.

Sample ID		Reactivity	Day 0	Cycle 1	Cycle 2	Cycle 3	Cycle 4
A12A	1 S/CO	RLU	1254	1320	1297	1109	893
		S/CO	1.0	1.0	1.0	0.9	0.6
	3 S/CO	RLU	3940	3729	3672	3425	2940
		S/CO	3.4	3.2	3.2	2.9	2.5
B12A	1 S/CO	RLU	2631	2157	1809	2204	2372
		S/CO	1.6	1.3	1.0	1.3	1.4
	3 S/CO	RLU	5406	4905	5276	4268	5192
		S/CO	3.5	3.2	3.5	2.8	3.4

Table 7-2: A12A and B12A freeze-thaw stability. Reactivity results of both cell lines and materials (1 and 3 S/CO) at successive freeze-thaw cycles are given in Relative Luminescence Units (RLU) and Signal to Cut-Off (S/CO).

7.3.5. Thermal stability of the final calibrators and controls

Since the antibodies were not stable at 2-8°C using generic buffer as diluent, we wanted to assess their stability in a specific buffer formulated for IgM stabilization (appropriated pH and salt concentration). We performed the same procedure shown per the generic buffer.

In addition to 2-8°C, we aimed to assess 25°C as the samples (patient besides calibrators and controls) on-board the instrument are not refrigerated. After dilution with the specific buffer to reach desired reactivities, we kept the supernatants at 2-8ºC and 25°C for 1, 7, 14 and 28 days. For each checkpoint, we measured the reactivity with the 3a6c-PT1I, and we calculated the bias respect the day 0. Following current CLSI guidelines (299), we established as acceptance criteria the bias ±20%.

As shown in Figure 7-8 and Table 7-3 the reactivity of supernatant A12A diluted at 1 and 3 S/CO meets the acceptance criteria for both storage conditions until day 14. B12A supernatant at 1 S/CO and stored at 2-8°C fulfill the acceptance criteria until day 28. However, the rest of samples (1 S/CO stored at 25°C and 3 S/CO at 2-8 and 25°C), were stable for 14 days. Our results indicated that both supernatants used as calibrators and controls were stable for 14 days when IgM stabilization buffer was used as diluent.

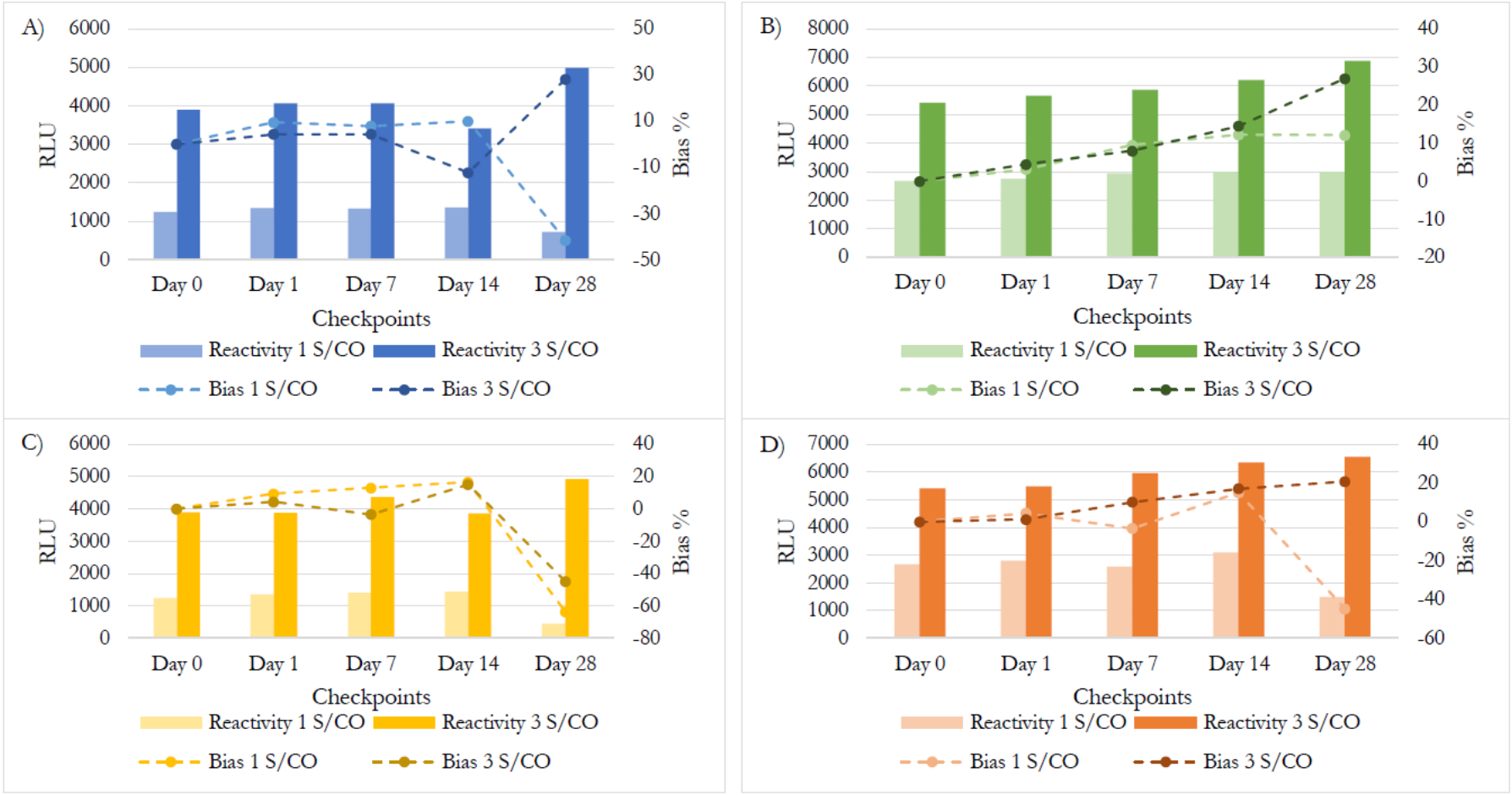

Figure 7-8: Thermal stability of the final calibrators and controls. A and B) A12A and B12A stored at 2-8°C respectively, C and D) A12A and B12Astored at 25°C. RLU and bias % are presented for each time point.

Storage condition			2-8°C					25°C			
Sample ID		Reactivity	Day 0	Day 1	Day 7	Day 14	Day 28	Day 1	Day 7	Day 14	Day 28
A12A	1 S/CO	RLU	1233	1350	1330	1356	721	1348	1394	1438	449
		Bias (%)	-	9.5	7.9	10.0	-41.5	9.3	13.1	16.6	-63.6
		S/CO	1.0	1.0	1.0	1.0	0.4	1.0	1.0	1.1	0.1
	3 S/CO	RLU	3889	4059	4058	3412	4985	3872	4367	3857	4923
		Bias (%)	-	4.4	4.3	-12.3	28.2	-0.4	12.3	-0.8	26.6
		S/CO	3.0	3.4	3.4	3.2	4.4	3.0	3.8	3.3	4.4
B12A	1 S/CO	RLU	2678	2762	2932	3005	3001	2794	2586	3082	1477
		Bias (%)	-	3.1	9.5	12.2	12.1	4.3	-3.4	15.1	-44.8
		S/CO	1.6	1.7	1.8	2.0	2.0	1.6	1.5	2.0	1.1
	3 S/CO	RLU	5416	5655	5847	6198	6877	5479	5965	6341	6541
		Bias (%)	-	4.4	8.0	14.4	27.0	1.2	10.1	17.1	20.8
		S/CO	3.5	3.6	3.7	4.0	4.5	3.5	3.7	4.1	4.4

Table 7-3: Thermal stability of the final calibrators and controls. RLU, Bias % and S/CO are presented for each time point.

7.4. Discussion

Two circumstances exist in which obtaining large amounts of sera to produce reference materials is especially difficult: one is rare or emerging diseases and the second is diseases against which people are widely immunized, as is the case when detecting IgM against *T. gondii* (185,196). Under these circumstances, IVD suppliers often encounter difficulties to find enough disease state plasma to respond to market demands.

Different studies have demonstrated the usefulness of chimeric immunoglobulins as alternative to plasma-derived antibodies, since they eliminate most of their associated disadvantages (196,295,300). Plasma-derived material is finite, and so new batches must be routinely procured. Conversely, chimeric antibodies are obtained from a stable cell line, which allows consistent and continuous production while reducing standardization requirements. This also avoids the ethical problems associated with sera collection from sick individuals and safety issues involving handling of infectious materials (195).

Hackett et al. described the use of recombinant chimeric antibodies as calibrators for the detection of IgG and IgM antibodies anti-*T. gondii*. The technology used to obtain the mouse-human antibodies, unlike the one we used, consisted of generating immunoglobulin expression vectors that were transfected by electroporation into the receiving cells. Although the obtention of chimeric IgG was successful, the levels of IgM achieved were insufficient even after using protoplast fusion to enhance expression (196).

Because of their size, complexity and high level of glycosylation, the recombinant expression of IgM is still not routinely achieved. Like Hackett et al., other authors have encountered difficulties in producing IgM using recombinant methods (301–304). However, in recent years, the use of transgenic mouse models has demonstrated several advantages over recombinant methods, such as: long-term production of reproducible lots, high affinity and specificity, high-titer production in vitro, and maintained mouse repertoire architecture to target all kinds of antigens (305,306).

In the present chapter, we describe the development of chimeric antibodies to replace human disease state plasma in automated chemiluminescent immunoassays measuring IgM anti-*T. gondii*.

In collaboration with ArkAb, we obtained two hybridoma cell lines producing human-murine monoclonal antibodies against 3a6c chimeric peptide to be used as calibrators and controls. Chimeric IgM antibodies were produced using a transgenic mouse model (InEps®), whose sequence for the IgM heavy chain constant region was replaced by the corresponding human sequence.

The analysis of the anti-3a6c IgM chimeric antibodies produced by both hybridoma cell lines (A12A and B12A) revealed that they were fully functional in the new immunoassay (either ELISA or CLIA). Additionally, the signal obtained in the functional evaluation (over one million RLU) far exceeded the reactivity of current commercial calibrators (around 25,000 RLU) produced using pooled human sera, making it suitable to use both A12A and B12A supernatants as a source of standard materials.

The high reactivity obtained with chimeric antibodies led us to work with extremely diluted samples to obtain reference materials similar to the commercial ones. Therefore, reproducing the culture conditions used in this project to supply that biomaterial, we could produce around 50,000 1 mL vials at 3 S/CO with significant reduction of time, production costs, and without impacting the functionality of the delivered products.

During hybridoma batch cell culture, we monitored both supernatant reactivity and cellular viability. Although minor, we found a reactivity loss in the A12A cell line at 96 h, which could be caused by degradation of the monoclonal antibody due to the presence of proteases released into the cell media when cellular lysis started. However, as we did not observe a parallelism between the reactivity loss and cell death, we also contemplated the formation of protein aggregates which could also explain the reactivity drop.

Reference materials, not only have to mimic the sample aimed to detect in order to guarantee precise and accurate results, besides adequate performance, but they also must be stable for a period comparable with the reagent (295). Therefore, during the development and verification phases of new immunoassays, the stability of the calibrators and controls is established (299). Several studies describe the relevance of handling conditions for collected serum and how different sample preparation and storage procedures can impact on antibody preservation (307,308). Additionally, numerous articles focus on the stability of recombinant antibodies (309,310). Nevertheless, little is found regarding the stability of chimeric antibodies when used as standard materials. In the present project, we analyzed the behavior of chimeric monoclonal antibodies as calibrators and controls when stored at different temperatures and handling conditions.

Han et al., studied the consequences on the measurements of anti-PLA2R, anti-GBM, anti-MPO and anti-PR3 antibodies (kidney disease biomarkers) when sera samples where incubated at 2-8°C for extended periods of time (six weeks) (307). Similar as our results, they found significant differences in the measured antibodies. Although we limited the duration of our study at two weeks, no satisfactory results were found at the different checkpoints when generic buffer was used as diluent.

These findings were not unexpected as the formulation of the diluent was not appropriate to stabilize antibodies. However, the use of specific IgM diluent conferred 14 days stability to both antibodies at

both storage conditions studied (2-8°C and 25°C). Additionally, considering that the bias at day 14 was significantly lower compared to the established acceptance criteria (±20%), if more check controls were done between day 14 and 28, presumably longer stability could be established.

Regarding freeze-thaw stability, no significant effect on kidney biomarkers measurements after repetitive freeze-thaw cycles was found by Han et al., which was consistent with our findings when supernatants were freeze-thaw up to five cycles. Our study was performed on the undiluted supernatant because, although we demonstrated that both antibodies diluted with specific buffer were stable at 2-8°C (which could be appropriate for final customers), this approach is preferable for several reasons: to avoid intermediate manipulation steps, to prevent contamination and also to reduce storage space. Surprisingly, we found that the two antibodies presented different behaviors, being B12A supernatant more sensitive at different freeze-thaw cycles. We also observed that lower dilutions (used to reach 3 S/CO) tended to be more stable. However, considering our experimental design in which the frozen materials were not diluted, such differences may be related to the dilution performed after the thaw step.

Our freeze and thaw study was performed without establishing any acceptance criteria, as we aimed to assess the preliminary stability of the new biomaterials, and also, because one of the main advantages of freezing the undiluted supernatant is that after each thaw, the performance could be re-evaluated and the final reactivity adjusted according to the requirements of the material that needs to be produced.

For decades, the IVD industry has faced the drawbacks of using plasma-derived antibodies. The present study provides robust data for using mouse-human chimeric antibodies as calibrators and controls for the measurement of human IgM anti-*T. gondii* antibodies. Additionally, we evaluated the thermal stability of those novel biomaterials in an attempt to provide background knowledge to encourage the use of such materials for the development of reliable diagnostic kits.

CHAPTER 8 – Materials and methods

8.1. Instrumentation

- Microplate reader equipped with 450 nm and 620 nm filters.
- Microplate incubator thermostatically set at 37±1°C.
- Automatic microplate washer.
- Vortex and roller.
- Automatic or semi-automatic, adjustable or preset, pipettes or multipipettes, to measure and dispense 0.2 µL to 1000 µL, and 1 mL, 2 mL, and 10 mL.
- Automated analyzers: BIO-FLASH® (Biokit, Spain), and VIDAS® (BioMérieux, France).

8.2. Clinical samples

Samples were provided by Biokit biobank, which is responsible for supplying samples on-demand. The internal quality system of Biokit guarantees that all procedures regarding handling and storage conditions of clinical samples are done according to GLP and GMP regulations.

No clinical analysis certificates are available for any sample used in this study. Additionally, no information regarding gender, age, or race was considered.

Samples were stored frozen at -70°C until tested. Before testing, samples were completely thawed and homogenized at room temperature in a roller. If the samples were cloudy or with the presence of clots, they were centrifuged at 300 x g for 5 min. Results for each sample served to classify and generate panels that were used during the different project phases with several objectives.

8.2.1. Samples for microarray study (Microarray panel)

A panel consisting of 13 human samples was screened for anti-*T. gondii* IgG and IgM with BIO-FLASH® Toxo IgG and IgM (Biokit, Spain). This panel was used for the microarray study.

Three samples (MA10, MA11, and MA12) were IgG-depleted by the Biochemistry Department of Biokit following standard internal procedures.

8.2.2. Samples for initial testing (Screening panel)

Forty-six human samples fulfiling *T. gondii* IgM-positive criteria were purchased from external vendors (AbBaltis, ABO Pharma, and Biomex). Sixty samples were provided by Banc de Sang i de Teixits de Catalunya as non-selected samples. Biokit biobank provided two cytomegalovirus (CMV)-positive and *T. gondii*-negative samples.

All samples were tested for anti-*T. gondii* IgM with the following commercial immunoassays; PLATELIA™ TOXO IgM (BIO-RAD, France), VIDAS® TOXO Competition (BioMérieux, France), Bioelisa TOXO IgM (Biokit, Spain), and BIO-FLASH® Toxo IgM (Biokit, Spain). This panel was used for the peptide screening with the multiplex ELISA.

8.2.3. Samples for CLIA reagent formulation

Forty-nine human samples were screened for anti-*T. gondii* IgG and IgM with BIO-FLASH® Toxo IgG and IgM (Biokit, Spain). These samples were used to generate a panel to be used throughout the formulation phase.

8.2.4. Samples for the feasibility study

Two hundred sixteen samples fulfiling *T. gondii* IgM-positive criteria were selected. One hundred non-selected samples were provided by Banc de Sang i de Teixits de Catalunya. This panel was used to perform the method-comparison of the new 3a6c-PT1I immunoassay.

8.2.5. Samples for interference and cross-reactivity studies

To perform an IgG interference study, two samples were selected fulfiling *T. gondii* IgM-negative and IgG-positive criteria.

To perform cross-reactivity studies, positive samples for varicella zoster (VZ), systemic lupus erythematosus (SLE), rubella (RUB), rheumatoid factor (RF), parvovirus (Parvo), herpes simplex virus (HSV), human anti-mouse antibodies (HAMA) and cytomegalovirus (CMV) were selected.

All samples were tested in parallel with the BIO-FLASH® Toxo IgG, IgM, and the 3a6c-PT1I. Interference was analyzed using internal validated spreadsheet which follows Clinical and Laboratory Standards Institute (CLSI), Protocol EP7-A2.

8.2.6. Laboratory investigation

All commercial kits used to screen the samples were stored at 2-8°C until use. Testing was performed following the manufacturer's instructions.

8.2.6.1. VIDAS® TOXO Competition

The VIDAS® TOXO Competition is an automated immunoassay to be used on the VIDAS® instrument (VIDAS BioMérieux, France). It uses the ELFA principle, combining a two-step enzyme immunoassay sandwich method with final fluorescence detection. The solid-phase receptacle (SPR) serves as the solid phase for the reaction and is coated with *T. gondii* lysate proteins. Additionally, the SPR acts as a pipetting device. Assay reagents are ready to use and are predispensed in the sealed reagent strips. All the assay steps are performed automatically by the instrument. After the sample is diluted, it is processed on the SPR. The anti-*T. gondii* antibodies present in the sample bind to the

antigens coating the interior of the SPR. The antibodies are detected using a monoclonal anti-P30 antibody labeled with alkaline phosphatase. The fluorescence of the product is measured at 450 nm. The results are analyzed and calculated automatically; a test value (TV) <1.6 indicates a positive result and a TV ≥1.6 a negative result.

8.2.6.2. PLATELIA™ Toxo IgM

PLATELIA™ Toxo IgM (BIO-RAD Laboratories, Marnes La Coquette, France) is a microplate immunoassay using an immuno-capture format for detection of specific IgM against *T. gondii* in human serum or plasma. Briefly, 200 µL of 1/100 diluted samples were distributed in each well, then incubated for 1 h at 37°C. The plate was then washed four times and 200 µL of conjugate was added and incubated for 1 h at 37°C. After a four-time washing step, revelation was carried out with a TMB substrate solution for 30 min at room temperature then stopped with 1N sulfuric acid. Optical densities (OD) were read at 450/620 nm using a plate reader within 30 min after stopping the reaction. Results were expressed in ratio = (OD of tested sample) / (appropriate cut-off). Results were interpreted as positive, negative, or equivocal using the ratio provided with the kit: positive result when ratio was greater than 1, negative lower than 0.8, and equivocal between 0.8 and 1.

8.2.6.3. Bioelisa Toxo IgM

The Bioelisa Toxo IgM (Biokit, Spain) is an immuno-capture assay for the detection of specific IgM against *T. gondii* in human serum or plasma. The test is performed by the incubation of 150 µL of 1/100 diluted samples in the 96-well microplate which is coated with rabbit anti-human IgM antibodies. After 1 h incubation at 37°C, the plate was washed four times and 150 µL of the *T. gondii* antigen labeled with peroxidase was added and incubated for 1 h at 37°C. Then, a second wash step was performed, followed by the addition of the TMB substrate. Finally, the reaction was stopped with 1N sulfuric acid and the optical density read at 450/620 nm using a plate reader. Results were expressed in ratio = relative absorbance units (RAU)= (OD of tested sample) / (appropriate cut-off). Results were interpreted according to manufacturer's instructions: negative if RAU/mL were <9, indeterminate if RAU/mL were ≥9, and positive if RAU/mL ≥10.

8.2.6.4. BIO-FLASH® Toxo IgM and Toxo IgG

The BIO-FLASH® assays are CLIA used on the BIO-FLASH® instrument (Biokit, Spain), a fully automated chemiluminescent immuno-analyzer. The principle of the BIO-FLASH® system has recently been described (105). The BIO-FLASH® assays used in this study were developed using native *T. gondii* antigens (Biokit) coated onto paramagnetic beads. A patient serum sample is pre-diluted with the BIO-FLASH® sample buffer in a small disposable plastic cuvette. Small amounts of the diluted patient serum, the beads, and the assay buffer are all combined into a second cuvette, mixed, and then incubated for 9.5 min at 37 °C. The magnetized beads are sedimented using a strong

magnet in the washing station and washed several times followed by the addition of isoluminol conjugated anti-human IgG or IgM and again incubated for 9.5 min at 37°C. The beads are sedimented and washed repeatedly. The isoluminol conjugate is oxidized when sodium hydroxide solution and peroxide solutions (triggers) are added to the cuvette, and the flash of light produced from this reaction is measured as relative light units (RLU) by the BIO-FLASH® optical system. The RLU are proportional to the amount of isoluminol conjugate that is bound to the human IgG or IgM, which is, in turn, proportional to the amount of antibodies bound to the antigen on the beads.

8.2.6.1. Solving indeterminate result

The PLATELIA™ Toxo IgM, bioelisa Toxo IgM, BIO-FLASH® Toxo IgM, and IgG immunoassay, are all assays that have a gray zone where samples are considered equivocal or indeterminate. In each case, the manufacturer's instructions established what must be performed to solve indeterminate results. In most cases, the result must be confirmed by another test done on a second sample drawn at least three weeks later after the first test. Since this assumption could not be made as the study was performed using retrospective samples, indeterminate results were tested once again in duplicated with the same method. Then, the final result was based on what was reported in two out of the three tests performed. If the sample gave the same indeterminate result the sample was classified as indeterminate.

8.3. *T. gondii* peptide microarray

The epitope mapping of the nine *T. gondii* antigens was done in collaboration with PEPperPRINT GmbH and is briefly explained below.

8.3.1. Protein selection

To select the proteins to be analyzed by the microarray, the Immune Epitope Database (IEDB) was used (https://www.iedb.org/). A list of different *T. gondii* (ID 5811) antigens was obtained. Briefly, the criteria used for the selection were: previous studies involving the antigen, commercialized assays using those antigens or epitopes belonging to those antigens, intellectual property, etc. The sequences of the nine selected proteins to study by the microarray were identified using the UniProt website (https://www.uniprot.org/) (311).

8.3.2. Microarray content

The sequence of nine *T. gondii* proteins (major surface antigen P30, surface antigen P22, dense granule proteins GRA2, GRA3, GRA4, GRA6, granule antigen Protein GRA7, microneme protein MIC3, and rhoptry protein ROP1) were linked and elongated by artificial GSGSGSG linkers to avoid truncated peptides. The sequences were translated into 15 amino acid peptides with a peptide-peptide

overlap of 14 amino acids. The resulting microarray contained 2668 different peptides printed in triplicate (8004 peptide spots) and was framed by polio (KEVPALTAVETGAT, 190 spots) and anti-HA (YPYDVPDYAG, 192 spots) control peptides. The signal intensities of these control peptides indicated the spot uniformity and binding specificities.

8.3.3. Procedure

Initially, a pre-swelling step in standard buffer (PBS, pH 7.4) and blocking in blocking buffer (Rockland MB-070, Rockland Immunochemical Inc., US) was performed. Then, the microarray was incubated with the secondary antibodies to analyze background interactions with the peptides. Goat anti-human IgG (Fc) conjugated DyLight680 and goat anti-human IgM (μ chain) DyLight800 (Rockland Immunochemical Inc., US) was used at dilutions of 1/5000 in the presence of the control antibody monoclonal anti-HA (12CA5)-DyLight800 at a dilution of 1/2000 for 45 min at room temperature. Conjugate dilutions were done in PBS with 0.05% Tween20 and 10% blocking buffer.

Each sample (see 8.2.1) was diluted 1/500 and 1/200 in incubation buffer (PBS, pH 7.4, 10% Rockland blocking buffer MB-070 and 0.05% Tween 20) and incubated with the microarray for 16 h at 2-8°C and shaking at 140 rpm, followed by staining with the secondary antibodies goat anti-human IgG (Fc) conjugated DyLight680 and goat anti-human IgM (μ chain) DyLight800 for 45 min at room temperature, diluted 1/5000 in incubation buffer in the presence of the monoclonal anti-HA (12CA5)-DyLight800 control antibody for 45 min at room temperature, diluted 1/2000 in incubation buffer). Read-out was performed using LI-COR Odyssey Imaging System; scanning offset 0.65 mm, resolution 21 μm, scanning intensities of 7/7 (red = 700 nm/green = 800 nm) (312).

Quantification of spot intensities and peptide annotation were based on 16-bit grayscale tiff files; microarray image analysis was done with PepSlide® Analyzer (SICASYS, Germany). A software algorithm broke down fluorescence intensities of each spot into raw, foreground, and background signal, and calculated the standard deviation (SD) of median foreground intensities. Spots with a deviation of 40% were zeroed to yield corrected averaged foreground intensities. Based on corrected averaged median foreground intensities, intensity maps were generated and binders in the peptide maps highlighted by an intensity color code with red (IgG, 700 nm) (IgM, 800 nm) for high and black for low spot intensities.

The results were plotted by averaged spot intensities of the samples against the linked and elongated total *T. gondii* sequence from the N-terminus of first linked peptide corresponding to major surface antigen P30 to the C-terminus of last linked peptide corresponding to granule antigen protein GRA6, to visualize the overall spot intensities and signal-to-noise ratios. The intensity plots were correlated with peptide and intensity maps as well as with visual inspection of the microarray scan to identify IgG and IgM epitopes of all human serum samples analyzed (data not shown).

8.3.4. Statistical analysis

The statistical analysis of IgG and IgM responses of the microarray panel was performed with the SUMO software (Statistical Utility for Microarray and Omics data (313)) that was developed in the German Cancer Research Center in Heidelberg, Germany, based on two-class t-tests. The statistical analyses were focused on the identification of common IgG and IgM responses, and differential IgG and IgM responses, respectively on averaged spot intensities without data normalization. As a noise filter, a minimum spot intensity of 50 fluorescence units was defined. All interactions below this threshold were set to 50 and did not influence the statistical analysis. To identify common IgG and IgM responses, unpaired two-class t-tests of the IgG and IgM-positive sera against the IgG and IgM-negative sera were performed. An additional unpaired two-class t-test was done with the IgG-positive sera against the IgM-positive sera to screen for differential IgG and IgM responses.

P-value < 1.00E-02 was selected as a threshold to define statistically significant peptides. For each t-test, the results were sorted by decreasing G1-G2 differences (being G1 the IgM-positive sera and G2 the IgG-positive sera) as a measure of the response differences between the groups. High G1-G2 differences corresponded to upregulated antibody responses in group G1, and negative G1-G2 differences values to upregulated antibody responses in the G2 group.

8.4. Solid-Phase Peptide Synthesis

The selected sequences were produced by SPPS. All procedures were carried out at the Proteomics and Protein Chemistry Unit in the Department of Experimental and Health Science of Universitat Pompeu Fabra.

8.4.1. Synthetic versions of the identified antigenic regions

SPPS was done in Prelude (Protein Technologies, Tucson, AZ, US) or Liberty 1 (CEM Corporation, (Mathews, NC, US)) peptide synthesizers running Fmoc protocols at 0.1-mmol or 0.05-mmol scale on 0.1 g Fmoc-Rink-amide ChemMatrix resin (Novabiochem (Läufelfingen, Switzerland)). Double couplings were systematically performed with a 5-fold excess of N^{α}-(9-fluorenylmethyloxycarbonyl) (Fmoc)-amino acid (Senn Chemichals (Dielsdorf, Switzerland)) or O_2Oc in the presence of 2-(1H-benzotriazol-1-yl)-1,1,3,3-tetramethyluronium hexafluorophosphate (HBTU) (Iris Biotech (Marktredwitz, Germany) (5 eq) and N,N-diisopropylethylamine (DIEA) (Merck (Darmstadt, Germany)) (10 eq) with N,N-dimethylformamide (DMF) (SDS (Peypin, France)) as a solvent for 2 × 30 min. Fmoc removal was done with 20% (v/v) piperidine in DMF for 2 × 2.5 min. Coupling and deprotection steps were separated by DMF washes (6 × 30 sec).

8.4.2. Peptide cleavage and work-up

Cleavage and deprotection of the peptide resins was done with trifluoroacetic acid (TFA) (SDS (Peypin, France)) -water-triisopropylsilane (Sigma-Aldrich (Madrid, Spain)) (95:2.5:2.5, v/v/v, 90 min, at room temperature) or with TFA-water-3,6-Dioxa-1,8-octane-dithiol-triisopropylsilane (94:2.5:2.5:1, v/v/v/v, 90 min, at room temperature) for peptides containing cysteine residues. Peptides were isolated by precipitation with chilled diethyl ether (SDS (Peypin, France)), centrifuged for 3 × 10 min at 4°C. Supernatant diethyl ether was discarded by decantation and the pellet solubilized in purified Milli Q water, lyophilized, and stored at -70°C.

8.4.3. Peptide purification

After the synthesis, the lyophilized crude peptides were dissolved in Milli Q water, then RP-HPLC analysis was done in an LC-2010A system (Shimadzu, Kyoto, Japan) using Luna C8 (3 μm, 50 mm × 4.5 mm; Phenomenex, Jupiter, CA, US). Solvents used were; A 0.045% TFA in H_2O (v/v) and B 0.036% TFA in HPLC-grade acetonitrile (ACN) (SDS (Peypin, France)) (v/v). Linear gradients of solvent B into solvent A were used over 15 min at a 1 mL/min flow rate, with UV detection at 220 nm.

RP-HPLC purifications were performed in an SCL-10A semi-preparative system (Shimadzu) using Phenomenex Luna C8 (10 μm, 250 mm × 10 mm; Phenomenex, Jupiter, CA, US). Solvents used were; A 0.1% TFA in H_2O (v/v) and B 0.1% TFA in ACN (v/v). Linear gradients of solvent B into solvent A were used over 30 min, at a 5 mL/min flow rate, with UV detection at 220 nm. Preparative RP-HPLC purifications were performed on Luna C18 (21.2 × 250 mm, 10 μm; Phenomenex, Jupiter, CA, US) columns in a Shimadzu LC8A instrument. Solvents used were; A 0.1% TFA in H_2O (v/v) and B 0.1% TFA in ACN (v/v). Linear gradients of solvent B into solvent A were used over 30 min, at a 7 mL/min flow rate, with UV detection at 220 nm. Peptide elution was obtained within the indicated gradient of B into A, see Chapter 3. The obtained pure fractions were analyzed by analytical RP-HPLC as explained before.

8.4.3.1. Peptide analysis by ESI-MS

After purification, fractions with purity >95% by analytical HPLC were analyzed by HPLC-MS on C18 (4.6 × 150 mm column, 3.5 μm, Phenomenex Jupiter, CA, US) in a Shimadzu LC-MS 2010EV instrument. Solvents used were; A 0.1% TFA (v/v) in H_2O and B 0.08% HCOOH in ACN. Elution was done with the indicated gradient of B into A over 15 min at 1 mL/min flow rate, with UV detection at 220 nm. Purified peptides were characterized by ESI-MS with an LCMS-2010 EV Mass Spectrometer (Shimadzu, Kyoto, Japan) controlled using LabSolutions LC-MS software.

8.4.3.2. Peptide lyophilization and storage

Fractions of satisfactory purity (>95%) and with the expected mass were pooled, lyophilized, and stored at -70°C. To prepare stock solutions at 1 mg/mL, lyophilized peptides were weighed on a high precision analytical microbalance (0.01 mg ± 0.02), dissolved in sterile Milli-Q water, and stored at -70°C.

8.4.4. $(6c)_2K_3$ branched peptide

First, K(Fmoc)KK core matrix and 6c linear peptides with an extra Cys residue in the C-terminus were synthesized and purified following the procedure explained above. Maleimide units were coupled at both α- and ε-amino groups at the N-terminus of the branched K(Fmoc)KK core directly on the resin using two successive coupling steps with 3-maleimidopropionic acid (8 eq.) dissolved in DMF (0.5 mL) and HBTU (8 eq) plus DIEA (16 eq). The resulting solution was incubated with the resin for 1 h at room temperature with three mixing steps in between. The product was washed twice with DMF and DCM (Sigma-Aldrich, Madrid, Spain) before the cleavage and purification steps. Finally, two C-terminally thiol-functionalized 6c branches were coupled via the maleimide linkages of K(Fmoc)KK in phosphate buffer (pH 7.4) (10 mL) after 15 min of reaction stirring.

8.4.5. Biotin peptide conjugation

Biotin was manually coupled to the peptide N-terminus before cleavage using two successive coupling steps (8 eq each), HBTU (8 eq), and DIEA (16 eq) dissolved in DMF (0.5 mL). The resulting solution was incubated with the resin for 1 h at room temperature with 3 mixing steps. The product was washed twice with DMF and DCM before the cleavage and purification.

8.5. Enzyme-linked immunosorbent assay

8.5.1. Multiplex ELISA

The multiplex ELISA was developed in collaboration with InfYnity Biomarkers (Lyon, France).

8.5.1.1. Printing

The *T. gondii* selected peptides and positive controls (PC) were C-terminally printed under controlled temperature and humidity conditions in duplicates in each well of a 96-well plate (Maxisorp Nunc) using a sciFLEXARRAYER printing system (Scienion Dortmund, Germany). Each lyophilized peptide was diluted with carbonate buffer (pH 9.6) to a concentration of 5, 50, and 100 µg/mL. After spotting, plates were incubated overnight, then dried at 37°C ± 1°C for 2 h and washed with PBS-Tween (phosphate-buffered saline with 0.05% Tween 20). Finally, blocking solution (phosphate-buffered saline with BSA) was added and incubated for 2 h at room temperature (314).

8.5.1.2. ELISA procedure

The microplates were incubated with the samples from the screening panel diluted with PBS at 1/50 for 1 h at room temperature and washed three times with PBST in an automatic microplate washer. Next, horseradish peroxidase (HRP)-conjugated goat anti-human IgM antibody (Abliance, France) was diluted with PBS at 1/1500 and 1/3000 and added to the microplate for 1 h at room temperature. The microplates were then washed three times with PBST before adding a TMB solution (SDT GmbH, Baesweiler, Germany). The chromogen solution was incubated for 20 min protected from light. Then, TMB solution was removed and the plates were dried at 37°C for 10 min.

Each plate was imaged using the SensoSpot Microarray Analyzers (Sensovation, Radolfzell, Germany). Additionally, a visual analysis was performed on each plate to detect the presence of possible precipitates, or to validate, if necessary, non-specific intensity detected by the scanner. The software calculated the pixel intensity for each spot. To establish the net intensity for each antigen, the mean value of the paired spots was considered. The net intensity value of each peptide was measured considering the mean value of duplicated spots intensity for each peptide (315).

8.5.1.3. Statistical analysis

Descriptive statistics are presented as mean values for continuous variables. The Mann-Whitney U test was used to compare continuous variables. A cut-off value for each antigen was calculated for determining seropositivity, represented as the 95 percentile of the reactivity in pixel intensity of the serum samples tested. Receiver Operating Characteristic (ROC) was performed using Analyse-it® software (version 4.6) (Analyse-it® software, Ltd., Leeds, UK).

8.5.2. Singleplex ELISA

8.5.2.1. Coating

Polystyrene 96-well plates (Nunc, US) were coated with 150 µL of each peptide appropriately diluted in coating buffer (40 mM carbonate bicarbonate buffer (pH 9.5)) and incubated overnight at room temperature protected from light. The plates were then blocked with 100 µL blocking buffer (BSA 1% - Glycine 0.75% (pH 7.4)) and incubated for 1 h. After aspiration, 200 µL of stabilization buffer (BSA 1% - Sucrose 4% pH 7.4) were distributed and incubated at room temperature for 90 min. Then, the plates were aspirated, and a final dry step was performed overnight at room temperature or in a low humidity chamber for 3 h. Dried plates were used directly or individually packed in aluminum bags thermowell with a silica gel bag of 2 g per plate and stored at 2-8ºC. If needed, the plates were directly used after the stabilization step.

8.5.2.2. ELISA procedure

Samples were diluted as appropriate in PBS-BSA and 150 µL were distributed to each well and incubated for 1 h at 37°C. Then, the microplates were washed three times with wash solution (PBS, 0.1% Tween 20) in an automatic microplate washer. Conjugate (peroxidase-coupled monoclonal antibody anti-human IgM (BD Pharmingen, CA, US)) was diluted as appropriate in PBS-BSA, and 150 µL were transferred to each well of the microplate. The ELISA plates were incubated for 1 h at 37°C. After the incubation, the microplates were washed three times. A quantity of 100 µL of the substrate-TMB were transferred to each microplate well and incubated for 30 min at 20-25°C. Then, 100 µL of stop solution was added to each well. Finally, the microplate absorbance at 450-620 nm was read within a maximum period of 30 min.

8.5.2.3. Statistical analysis

The data were statistically evaluated using the Analyse-it® software (version 4.60). Receiver operating characteristics (ROC) analysis was used to analyze the discriminatory ability of different immunoassays.

8.6. Chemiluminescent immunoassay

The protocols to produce the chemiluminescent reagent (magnetic particles, assay buffer, and tracer), as well as the materials used, are intellectual property of Biokit. Thus, they will be briefly mentioned.

To develop the 3a6c-PT1I CLIA prototype, the RLU measured were transformed into S/CO using the following formula, being Cal1 and Cal2 the commercial BIO-FLASH® Toxo IgM calibrators.

$$S/CO\ sample = \frac{RLU^{sample} - RLU^{Cal1}}{RLU^{Cal2} - RLU^{Cal1}}$$

Once the cut-off of the 3a6c-PT1I was stablished at an appropriate RLU value, it was used as Cal2 RLU value in subsequent calculations. The BIO-FLASH® Toxo IgM Cal 1 RLU was used during the development phase as a negative control.

To perform the DOE study, the variables and the levels selected were introduced in Minitab®19 (Minitab Statistical Software Inc.), and the resulting design combinations were produced. The results were analyzed with Minitab software, establishing 0.05 the p-value to be considered significant. The output variables selected were the bound antigen, the averaged median results of both positive and negative samples, and the span.

8.6.1. Solid-Phase

The paramagnetic particles (Dynal Biotech, Oslo, Norway) were initially resuspended, washed three times using wash buffer, and incubated with the peptide or the antibody (depending on the assay scheme selected) adequately diluted in coating buffer. Then, paramagnetic beads were washed and blocked using a blocking buffer. Blocked particles were resuspended in storage buffer and then sonicated, filtered, and stored until use at 2-8°C. During the sonication process, the absorbance at 500 nm was measured until constant absorbance was reached. Before usage, paramagnetic beads were appropriately homogenized.

To study the solid-phase by DOE, different lots of paramagnetic beads were produced according to the combinations established by Minitab®19. The factors modified were the ratio peptide/magnetic bead, the pH, the salt concentration, and the blocking agent.

8.6.2. Assay buffer

Different lots of assay buffer were produced based on the original formulation of the BIO-FLASH® Toxo IgM assay buffer. To study their formulation by DOE, the factors selected were the pH, the salt concentration, detergents, and blocking agent.

8.6.3. Tracer

Different tracer lots were produced based on the original formulation of the BIO-FLASH® Toxo IgM tracer. To study their formulation by DOE, the factors selected were the pH, the salt concentration, the detergents, the nonionic components, and the blocking agent. Additionally, different tracer concentrations were produced and studied in the final tracer diluent formulation.

8.6.3.1. Immunocapture tracer

A lot of isoluminol-conjugated streptavidin was produced following internal procedures. Briefly, SEC chromatography using Superdex 200 Increase column in 6x FPLC ÄKTA purifier (GE Healthcare, US) was performed monitoring absorbances at 260, 280, and 329 nm. Conjugate complex was produced by mixing and incubating the ABEI-conjugated streptavidin with 3a6c biotinylated peptide in TAN buffer (50mM triethanolamine, 100mM NaCl, pH8.0) for 30 min at room temperature and shaking at 500 rpm.

The complex was purified using Superdex 75 Increase SEC column on 6x FPLC ÄKTA purifier (GE Healthcare, US). The elution volume was collected in fractions of 0.25 mL. An aliquot from each peak fraction was diluted 1/100 in PBS and analyzed for the presence of isoluminol by running the light-check assay in the BIO-FLASH® instrument (data not shown).

8.6.4. Protein quantification

Protein quantification was performed on the microparticles coating supernatants collected before (pre-coating) and after (after-coating) using Pierce Micro BCA Protein Assay Kit (Thermo Scientific, cat #23227) as recommended by the manufacturer. Briefly, the BCA Working Reagent (WR) was prepared by mixing 50 parts of BCA Reagent A with one part of BCA Reagent B (Reagent A:B ratio = 50:1). An amount of 25µL of each BCA standard or sample was pipetted into a microplate well (Nunc, US) and then 200µL of the WR was added to each well. The plate was placed on a plate shaker for 30" and incubated at 37°C for 30 min. After cooled, the absorbance of the plate was measured at 562 nm on a plate reader and a standard curve was created by plotting the average blank-corrected 562 nm reading for each BSA standard vs. its concentration in µg/mL. The standard curve was used to determine the protein concentration of each sample.

8.6.5. BIO-FLASH® assay parameters

The BIO-FLASH® instrument in developer mode was used to modify the pre-defined assay parameters of the BIO-FLASH® Toxo IgM assay definition. The variables modified were the sample dilution factor, and the sample volume incubated with the paramagnetic microparticles.

8.6.6. IgG interference study

The IgG interference study was done according to CLSI EP7-A2. Calculations were based on the measurement of the IgM by the 3a6c-PT1I in a pool containing the IgG, relative to the control pool which did not contain the IgG. Additionally, to assess if IgG concentration affected the measurement of the IgM, two different pools with two different IgG concentrations were tested.

The two samples containing the IgM anti-*T. gondii* were divided into three aliquots, the control (C) diluted 1/4 with the IgG/ IgM-negative sample and the two test (T) spiked each one with the two IgG-positive samples. A total of 30 replicates were performed on each aliquot with the 3a6c-PT1I. For the analysis, the mean value of the 30 replicates (expressed in RLU), the standard deviation (SD), the coefficient of variation (%CV), and the percentage of bias between (C) and (T) was calculated and analyzed using internal validated excel spreadsheet.

8.6.7. Cross-reactivity study

The cross reactivity study was performed analyzing two replicates of different samples containing antibodies against human anti-mouse antibodies (HAMA), varicella zoster (VZ), systemic lupus erythematosus (SLE), rubella (RUB), rheumatoid factor (RF), parvovirus (Parvo), herpes simplex virus (HSV) and cytomegalovirus (CMV) in the BIO-FLASH® Toxo IgM, IgG and the 3a6c-PT1I. The agreement of the results reported between the BIO-FLASH® Toxo IgM and the 3a6c-PT1I was used to determine potential cross-reactivity.

8.6.8. Method comparison study

Method comparison of the 216 preselected serum specimens was performed in parallel with the BIO-FLASH® Toxo IgM and the 3a6c-PT1I prototype. Regression analysis was performed using the Passing-Bablok method (316). The correlation coefficient and slope between the two assays were calculated. ROC curves were generated, and the areas under the curve of both tests were compared and statistically analyzed using Analyse-it® software (version 4.60). Alternative cut-off points were studied by the Youden's index (data not shown).

8.7. Chimeric monoclonal IgM. Cell line generation and characterization

8.7.1. Hybridoma cell line generation

The 3a6c peptide was used to immunize a cohort of five InEps® mice. The immune response of the immunized mice was monitored by an indirect ELISA based on Biokit in-house general procedure (see 8.5.2). As antigens, the 3a, 6c, and 3a6c peptides were used. To compare the reactivity of mice polyclonal response with known samples, two aliquots from the conditional panel (#3 as a positive and #86 as negative) were used.

Sera from the five InEps® were periodically evaluated by Biokit following the procedure explained in section 8.5.2. Once the animals producing 3a6c-specific antibodies were selected, ArkAb initiated the generation of the hybridoma cell lines following ArkAb internal procedures. During the process, hybridoma supernatant samples were sent to Biokit to assess their reactivity and to select those generating specific IgM. The selected ones were used for stabilization, and to generate the master cell bank.

First cloning using limiting dilution was made for all clones selected after fusion. Screening of growing cells was also made by ELISA. The results obtained were assessed to verify the stability and homogeneity of the master banks (seed banks), to select the backup clones, and for following sub-cloning. Once the homogeneity of the master bank was validated, the mycoplasma-contamination status of the cell line was checked by ArkAb. An amount of 50 mL of master cell bank supernatant and the cryopreserved master cell bank were sent to Biokit.

8.7.2. Initial set-up and generation of research master cell bank of A12A and B12A hybridoma cell lines

Upon receipt, both A12A and B12A hybridomas were stored in liquid nitrogen in sterile cryovials inside a liquid N_2 container at -196°C. When thawing, the cryovial was transferred from the liquid N_2 container into a water bath previously warmed at 37°C. Then, 1/10 dilution of the cryovial content

was carried out in a second tube containing pre-warmed media Iscove's Modified Dulbecco's Medium (IMDM) GlutaMAX™ Supplemented (ThermoFisher Scientific™, Spain) + 10% HyClone™ Fetal Clone I (FCI) (ThermoFisher Scientific™, Utah, US) + 1% Penicillin Streptomycin (P/S) (Sigma-Aldrich). The tube containing the mixture was centrifuged at 300 x g for 5 min to remove previous Dimethyl sulfoxide (DMSO) Hybri-Max™ (Sigma-Aldrich)-containing media. After that, the pellet was re-suspended and inoculated in 10 mL of pre-warmed media at 37ºC in a T-Flask-25. To keep the cells in the exponential growth phase, cell passaging was routinely performed. At the time of cell passaging, viability, total and viable cell density, and doubling time were assessed for each cell line. In general, cells were kept between 0.2-1.2x10^6cell/mL, to ensure exponential growth. Cells were incubated at 37ºC incubator with a humidified atmosphere of 5% CO_2.

Before cell passaging, Trypan Blue (TB) (Gibco) staining was used to assess the viable cell density of each cell line using a ½ dilution of the sample of the culture. Trypan Blue penetrates dead cell membranes showing a blue characteristic color, whereas, living cells appear bright under microscope observation. An automated cell counter (Countess II, Invitrogen) was used for viability assessment, the final volume and concentration were established depending on the requirements of the culture.

For cryopreservation, cells were frozen with 90% FCI + 10% DMSO and the cell bank obtained was called Research Master Cell Bank (RMCB). One RMCB vial per cell line was then used to produce the batch culture.

Briefly, the generation of the RMCB required: high cell density (4x10^6 cell/mL) viability higher than 75%, a minimal number of cell passaging, and enough volume to produce the desired number of cryovials (usually 1mL each). For the success of the following cell culture generation, cells must be in the exponential growth phase at the time of harvesting. Thus, to accomplish the stated characteristics, A12A and B12A cell lines were scaled-up after thawing. Conditions at the time of the A12A RMCB was generated, cells were at 1.3x10^6 cell/mL and 89% viability. In the case of B12A, the cell line reached 85% viability before freezing and viable cell densities were 1.3x10^6 cell/mL.

After harvesting, cells were centrifuged at 300 × g for 5 minutes, the culture medium was discarded, and pellet was resuspended by adding freezing medium (FCI + 10% DMSO or 50% of conditioned medium + 50% of a mix of fresh medium and 15% of DMSO). Then, resulting cryovials were frozen at -70°C in an automated controlled-rate freezing apparatus (MR Frosty™, Nalgene or CoolCell, Corning). After 24 h, cells were transferred to liquid N_2 for long-term storage. For both cell lines, fifteen cryovials were frozen in passage four. The generation of RMCB was performed as described in Figure 8-1.

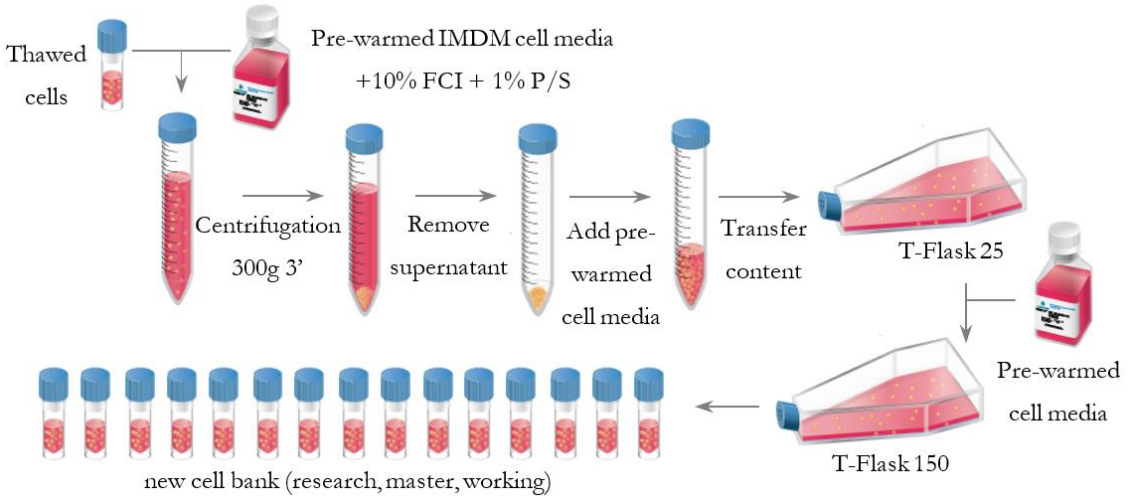

Figure 8-1: General procedure for the generation of research, master, and working cell bank.

8.7.3. Antibody titration

The antibody titer of the two hybridoma cell lines was monitored using CLIA described in section 8.6. The supernatants containing the desired antibody were filtered by a 0.2 μm sterile filter (Corning NY, US). Then serial dilutions were performed to find the one that generated the desired S/CO. As diluent, the BIO-FLASH® assay diluent (Biokit, Spain) and specific IgM calibrators and controls diluent, formulated at Biokit were used. The RLU obtained were used to calculate the Bias % of each checkpoint versus time zero using the following formula:

$$Bias\ \% = \frac{RLU\ Day\ X - RLU\ Day\ 0}{RLU\ Day\ 0} x100$$

CHAPTER 9 – Conclusions

Based on the presented results, this thesis allows us to conclude that:

1. **Epitope mapping by peptide microarray is a powerful technology to identify IgM-specific sequences.** Novel IgM-specific epitopes were identified from nine immunodominant *T. gondii* proteins. The evaluation of the microarray using well characterized serum samples and statistical analysis revealed a complex IgM response pattern, consistent with the difficulties previously encountered in the identification of IgM-specific sequences. Our results demonstrated that most specific sequences upregulated in the IgM-positive vs. the IgG-positive samples belong to dense granule protein GRA3, rhoptry protein ROP1, granule antigen protein GRA7 and major surface antigen P30. In addition, the IgG depletion approach used to evaluate IgM-positive / IgG-negative samples, allowed us to discard epitopes that were reactive to non-depleted samples, reinforcing the specificity criteria that drive our experimental design.

2. **Synthetic replicas of the identified sequences were shown to be functional antigens.** Eighteen synthetic peptides were efficiently synthesized by SPPS and evaluated as antigens via multiplex ELISA. Peptides 3a, 3b, and 6c were the best candidates. The assay parameters stablished in the multiplex approach were assessed in singleplex ELISA format, confirming the IgM-specificity, and validating the suitability of the selected peptides as new diagnostic tools to detect *T. gondii* IgM-positive samples.

3. **High-throughput immunoassay provides a fast and accurate evaluation of multiple antigens in a single step, reducing execution times and allowing manifold data analyses.** Multiplex ELISA demonstrated the feasibility of the synthetic peptides for detecting anti-*T. gondii* IgM in a fast and efficient way, especially considering that samples, in particular those negative for IgG, are a prized asset. Additionally, our reproducibility assessment demonstrated, for the first time, excellent correlation between multiplex and singleplex ELISA based on synthetic peptides to detect IgM anti-*T. gondii*.

4. **Anti-*T. gondii* IgM commercial kits showed poor agreement.** We found that 40% of the samples evaluated gave results showing disagreement between one or more than one of the methods used. This further reinforced the need to improve both sensitivity and specificity to have robust diagnostic methods offering comparable and reliable results.

5. **Chimeric peptides offer superior antigenic properties than single epitope peptides.** Antigenic synergy was first demonstrated by mixing single peptides in solution. Therefore, we produced by SPPS peptide chimeras which combined 3a and 6c sequences into a single peptide molecule. ELISA revealed that the 3a6c chimeric peptide was highly sensitive and specific compared with the 3a and 6c alone, proving it was appropriate for detecting IgM-positive samples instead of *T. gondii* lysate antigen.

6. **Chimeric homotandems bearing two identic 6c sequences do not demonstrate significant antigenic advantages.** None of the homomer peptides evaluated, neither the $6c_2K_3$, a branched construct with two copies of 6c truncated peptide attached to a lysine core, exhibited superior reactivity. This provides conclusive evidence of the importance of combining different epitopes for the specific detection of IgM anti-*T. gondii*. Beyond epitope combination, the layout seems to play a crucial role in terms of reactivity as the reverse heterotandem version of our principal candidate (3a6c), in which we merely changed the sequence order of truncated 6c and 3a peptides (6c3a), showed comparable performance as the other homotandems.

7. **CLIA based on chimeric synthetic peptide display good assay performance.** The prototype initially developed using peptide 3a6c, showed equivalent results to its ELISA homologue. Additionally, sensitivity and specificity were evaluated using well-characterized IgM and IgG-positive and negative samples. Results demonstrate the usefulness of chimeric peptides as antigens and portray our CLIA prototype as an attractive candidate to be further optimized.

8. **Design of experiments is an effective methodology to develop novel immunoassays and/or to optimize product formulations.** Solid-phase, assay diluent and tracer formulation optimization was successfully achieved with significant time and cost savings. Multiple factors per reagent component were evaluated at once by application of DOE strategy. The span variable was used throughout the study and its subsequent increase shows the improvement of the reagent during optimization.

9. **Method comparison study of the peptide-based immunoassay reveled promising features.** A 99.5% sensitivity, 96.7% specificity and 97% agreement were achieved when 316 samples were analyzed in a comparability study versus the BIO-FLASH® Toxo IgM. A *worst-case strategy* was applied to solve the discrepant and indeterminate samples using PLATELIA™. Overall, results using synthetic chimeric peptide match the performance claim

of assays using the native *T. gondii* antigen, improving the results of the BIO-FLASH®, and avoiding the use of animals to produce the antigen. All these features imply big savings in production costs and facilitate obtention of reliable biomaterials.

10. **IgG presence, even at high concentration, does not interfere in the performance of 3a6c-PT1I.** By their very nature, IgGs often cross-react in assays intended for IgM detection. Results from our IgG interference study evidenced strong IgM specificity even in samples containing high IgG concentrations. This reinforces the convenience of exploring the use of "artificial" chimeric peptides as a strategy to overcome the weaknesses of current IgM immunoassays in terms of specificity.

11. **Chimeric humanized IgMs appear as a suitable replacement for plasma-derived samples as standard materials.** In an effort to improve the current source of reference materials, we evaluated the usefulness of mouse monoclonal humanized chimeric antibodies as calibrators and controls in the new 3a6c immunoassay. Results showed these new biomaterials as highly suitable in terms of reactivity and with comparable thermal stability to the current calibrators and controls.

References

1. Nicholson LB. The immune system. Essays Biochem. 2016;60(3):275–301.

2. Sokol CL, Luster AD. The chemokine system in innate immunity. Cold Spring Harb Perspect Biol. 2015;7(5):1–20.

3. Alberts B, Johnson A, Lewis J. Molecular Biology of the Cell. 4th editio. Garland Science, editor. New York; 2002.

4. Riera M, Pérez-Martínez D, Castillo C. Innate immunity in vertebrates: An overview. Immunology. 2016;148(2):125–39.

5. Klose CS, Artis D. Innate lymphoid cells as regulators of immunity, inflammation and tissue homeostasis. Nat Immunol. 2016;17(7):765–74.

6. Netea MG, Schlitzer A, Placek K, Joosten LAB, Schultze JL. Innate and Adaptive Immune Memory: an Evolutionary Continuum in the Host's Response to Pathogens. Cell Host Microbe. 2019;25(1):13–26.

7. Domínguez-Andrés J, Fanucchi S, Joosten L, Mhlanga M, Netea M. Advances in understanding molecular regulation of innate immune memory. Curr Opin Cell Biol. 2020;63:68–75.

8. Besedovsky L, Lange T, Haack M. The sleep-immune crosstalk in health and disease. Physiol Rev. 2019;99(3):1325–80.

9. Netea MG, Quintin J, Van Der Meer JWM. Trained immunity: A memory for innate host defense. Cell Host Microbe. 2011;9(5):355–61.

10. Boehm T, Swann B J. Origin and evolution of adaptive immunity. Annu Rev Anim Biosci. 2014;Feb(2):259–83.

11. Vivier E, Raulet DH, Moretta A, Caligiuri MA, Zitvogel L, Lanier LL, et al. Innate or adaptive immunity? The example of natural killer cells. Science (80-). 2011;331(6013):44–9.

12. Chaplin D. Overview of the immune response. J Allergy Clin Immunol. 2010;125(2):S345.

13. Minervina A, Pogorelyy M, Mamedov I. T-cell receptor and B-cell receptor repertoire profiling in adaptive immunity. Transpl Int. 2019;32(11):1111–23.

14. Burnet FM. A Modification of Jerne's Theory of Antibody Production using the Concept of Clonal Selection. CA Cancer J Clin. 1976;26(2):119–21.

15. Besteiro S. The role of host autophagy machinery in controlling Toxoplasma infection. Virulence. 2019;10(1):438–47.

16. Yarovinsky F. Innate immunity to Toxoplasma gondii infection. Nat Rev Immunol. 2014;14(2):109–21.

17. Hamie M, Sasai M, Yamamoto M. Innate, adaptive, and cell-autonomous immunity against Toxoplasma gondii infection. Exp Mol Med. 2019;51(12).

18. Mellman I. Dendritic cells: master regulators of the immune response. Cancer Immunol Res. 2013;1(3):145–9.

19. Mukherjee S, Huda S, Sinha Babu SP. Toll-like receptor polymorphism in host immune response to infectious diseases: A review. Scand J Immunol. 2019;90(1):1–18.

20. Regenmortel M. What Is a B-Cell Epitope? Methods Mol Biol Ep Mapp Protoc. 2008;524(1):264–81.

21. Dragoş D, Tănăsescu MD. The effect of stress on the defense systems. J Med Life. 2010;3(1):10–8.

22. Simon AK, Hollander GA, Mcmichael A, Mcmichael A. Evolution of the immune system in humans from infancy to old age. Proc Biol Sci. 2015;282(1821):1–12.

23. Racine R, Winslow GM. IgM in microbial infections: Taken for granted? Immunol Lett. 2009;125(2):79–85.

24. Niles MJ, Matsuuchi L, Koshland ME. Polymer IgM assembly and secretion in lymphoid and nonlymphoid cell lines: Evidence that J chain is required for pentamer IgM synthesis. Proc Natl Acad Sci U S A. 1995;92(7):2884–8.

25. Gong S, Ruprecht RM. Immunoglobulin M: An Ancient Antiviral Weapon – Rediscovered. Front Immunol. 2020;11(August):1–9.

26. Halonen S, Weiss LM. TOXOPLASMOSIS. Handb Clin Neurol. 2013;114:125–45.

27. Weiss, Louis M. Dubey JP. Toxoplasmosis: a history of clinical observations. Int J Parasitol. 2009;39(8):895–901.

28. Howe D, Sibley D. Toxoplasma gondii Comprises Three Clonal Lineages: Correlation of Parasite Genotype with Human Disease. J Infect Dis. 2015;172(6):1561–6.

29. Sibley, L. David. Boothroyd J. Virulent strains of Toxoplasma gondii comprise a single clonal lineage. Nature. 1992;359(6390):82–5.

30. Shwab EK, Zhu X, Majumdar D, Hilda F, Gennari S, Dubey J, et al. Geographical patterns of Toxoplasma gondii genetic diversity revealed by multilocus PCR-RFLP genotyping. Parasitology. 2014;141:453–61.

31. Lehmann T, Marcet PL, Graham DH, Dahl ER, Dubey JP. Globalization and the population structure of Toxoplasma gondii. Proc Natl Acad Sci USA. 2006;103(30):11423–8.

32. Shwab E, Zhu X, Majumdar D, Pena H, Gennari S, Dubey J, et al. Genetic Divergence of Toxoplasma gondii Strains Associated with Ocular Toxoplasmosis, Brazil. Parasitology. 2014;141(4):453–61.

33. Dubey J, Frenkel K. Cyst-Induced Toxoplasmosis in Cats. J Protozool. 1972;19(1):155–77.

34. Hutchison, WM., Dunachie, JF. Siim, JC., Work K. Life cycle of toxoplasma gondii. Br Med J. 1969;4:806.

35. Dubey, JP. Lindsay D. Structures of Toxoplasma gondii Tachyzoites, Bradyzoites, and Sporozoites and Biology and Development of Tissue Cysts. Vet Parasitol. 1998;2(11):267–99.

36. Frenkel, JK. Dubey JMN. Toxoplasma gondii in cats: fecal stages identified as coccidian oocysts. Science (80-). 1970;167(3919):893–6.

37. Pittman KJ, Knoll LJ. Long-Term Relationships: the Complicated Interplay between the Host and the Developmental Stages of Toxoplasma gondii during Acute and Chronic Infections. Microbiol Mol Biol Rev. 2015;79(4):387–401.

38. Black MW, Boothroyd JC. Lytic Cycle of Toxoplasma gondii. Microbiol Mol Biol Rev. 2000;64(3):607–23.

39. Hill D, Dubey JP. Toxoplasma gondii: transmission, diagnosis and prevention. Clin Microbiol Infect. 2002;8(10):634–40.

40. Kochanowsky JA, Koshy AA. Toxoplasma gondii. Curr Biol. 2018;28(14):R770–1.

41. Dubey JP. The History of Toxoplasma gondii —The First 100 Years. J Eukaryot Microbiol. 2008;55(6):467–75.

42. Blader IJ, Coleman BI, Chen C-T, Gubbels M-J. Lytic Cycle of Toxoplasma gondii : 15 Years Later . Annu Rev Microbiol. 2015;69(1):463–85.

43. Jung C, Lee CYF, Grigg ME. The SRS superfamily of Toxoplasma surface proteins. Int J Parasitol. 2004;34(3):285–96.

44. Lekutis C, Ferguson DJP, Boothroyd JC. Toxoplasma gondii: Identification of a developmentally regulated family of genes related to SAG2. Exp Parasitol. 2000;96(2):89–96.

45. He XL, Grigg ME, Boothroyd JC, Garcia KC. Structure of the immunodominant surface antigen from the toxoplasma gondii SRS superfamily. Nat Struct Biol. 2002;9(8):606–11.

46. Wang Y, Yin H. Research progress on surface antigen 1 (SAG1) of Toxoplasma gondii. Parasit Vectors. 2014;7(1):180.

47. Mineo JR, Kasper LH. Attachment of Toxoplasma gondii to Host Cells Involves Major Surface Protein, SAG-1 (P-30). Vol. 79, Experimental Parasitology. 1994. p. 11–20.

48. Betancourt ED, Hamid B, Fabian BT, Klotz C, Hartmann S, Seeber F. From entry to early dissemination-Toxoplasma gondii's Initial Encounter with Its Host. Front Cell Infect Microbiol. 2019;9(46):1–9.

49. Boothroyd JC, Dubremetz JF. Kiss and spit: The dual roles of Toxoplasma rhoptries. Nat Rev Microbiol. 2008;6(1):79–88.

50. Besteiro S, Dubremetz JF, Lebrun M. The moving junction of apicomplexan parasites: A

key structure for invasion. Cell Microbiol. 2011;13(6):797–805.

51. Robert-Gangneux F, Dardé ML. Epidemiology of and diagnostic strategies for toxoplasmosis. Clin Microbiol Rev. 2012;25(2):264–96.

52. Tyler JS, Treeck M, Boothroyd JC. Focus on the ringleader: The role of AMA1 in apicomplexan invasion and replication. Trends Parasitol. 2011;27(9):410–20.

53. Rommereim LM, Fox BA, Butler KL, Cantillana V, Taylor GA, Bzik DJ. Rhoptry and Dense Granule Secreted Effectors Regulate CD8+ T Cell Recognition of Toxoplasma gondii Infected Host Cells. Front Immunol. 2019;10(2104).

54. Dubremetz JF. Rhoptries are major players in Toxoplasma gondii invasion and host cell interaction. Cell Microbiol. 2007;9(4):841–8.

55. Mohabati R, Babaie J, Amiri S, Talebzadeh M, Fard-Esfahani P, Darbouy M, et al. Expression and purification of recombinant ROP1 of Toxoplasma gondii in bacteria. Avicenna J Med Biotechnol. 2013;5(4):227–33.

56. Noya O, Patarroyo M, Guzman F, de Noya B. Immunodiagnosis of Parasitic Diseases with Synthetic Peptides. Curr Protein Pept Sci. 2005;4(4):299–308.

57. Montoya JG. Laboratory diagnosis of Toxoplasma gondii infection and toxoplasmosis. J Infect Dis. 2002;185 Suppl:S73–82.

58. Montoya JG, Liesenfeld O. Toxoplasmosis. Lancet. 2004;363:1965–76.

59. Werner Louis Apt Baruch. Parasitología Humana. 1ª ed. 1ª Edicion. Mexico: McGraw-Hill; 2013.

60. Boyer KM, Holfels E, Roizen N, Swisher C, Mack D, Remington J, et al. Risk factors for Toxoplasma gondii infection in mothers of infants with congenital toxoplasmosis: Implications for prenatal management and screening. Am J Obstet Gynecol. 2005;192(2):564–71.

61. Álvarez JB, Serrano MM, Parrado LM, Ortuño SL, Sánchez MDC. Prevalencia e incidencia de la infección por Toxoplasma gondii en mujeres en edad fértil en Albacete (2001-2007). Rev Esp Salud Publica. 2008;82(3):333–42.

62. Muñoz C, Guardià C, Juncosa T, Viñas L, Sierra M, Sala I, et al. Toxoplasmosis and pregnancy. Multicenter study of 16,362 pregnant women in Barcelona. Med Clin (Barc). 2004;123(1):12–6.

63. Dard C, Fricker-Hidalgo H, Brenier-Pinchart MP, Pelloux H. Relevance of and New Developments in Serology for Toxoplasmosis. Trends Parasitol. 2016;32(6):492–506.

64. Paris L. Toxoplasmosis. In: Hunter's Tropical Medicine and Emerging Infectious Diseases. 2019. p. 803–13.

65. Wilking H, Thamm M, Stark K, Aebischer T, Seeber F. Prevalence, incidence estimations,

and risk factors of Toxoplasma gondii infection in Germany: A representative, cross-sectional, serological study. Sci Rep. 2016;6(22551):1–9.

66. Nogareda F, Le Strat Y, Villena I, De Valk H, Goulet V. Incidence and prevalence of Toxoplasma gondii infection in women in France, 1980-2020: Model-based estimation. Epidemiol Infect. 2014;142(8):1661–70.

67. John B, Weninger W, Hunter CA. Advances in imaging the innate and adaptive immune response to Toxoplasma gondii. Futur Microbiol. 2010;5(9):1321–8.

68. Louis M. Weiss, Kami K. Toxoplasma Gondii: The Model Apicomplexan - Perspectives and Methods: Second Edition. Elsevier Ltd; 2013.

69. Blanchard N, Gonzalez F, Schaeffer M, Joncker t N. Immunodominant, protective response to the parasite Toxoplasma gondii requires antigen processing in the endoplasmic reticulum. Nat Immunol. 2008;9(8):937–44.

70. Feliu V, Vasseur V, Grover HS, Chu HH, Brown MJ, Wang J, et al. Location of the CD8 T Cell Epitope within the Antigenic Precursor Determines Immunogenicity and Protection against the Toxoplasma gondii Parasite. PLoS Pathog. 2013;9(6).

71. Frikel E-M, Sahoo N, Hoop J, Gubbels M-J. Parasite stage-specific recognition of endogenous Toxoplasma gondii derived CD8+ T cell epitopes. J Infect Dis. 2008;198(11):1625–33.

72. Grover HS, Chu HH, Kelly FD, Yang SJ, Michael L, Blanchard N, et al. Impact of regulated secretion on anti-parasitic CD8 T cell responses. Cell Rep. 2014;7(5):1716–28.

73. Hunter CA, Remington JS. Immunopathogenesis of toxoplasmic encephalitis. J Infect Dis. 1994;170(5):1057–67.

74. Saadatnia G, Golkar M. A review on human toxoplasmosis. Scand J Infect Dis. 2012;44(11):805–14.

75. Morlat P, Leport C. Prevention of toxoplasmosis in immunocompromised patients. Ann Med Interne (Paris). 2008;14(12):1089–101.

76. Montoya JG, Remington JS. Clinical Practice: Management of *Toxoplasma gondii* Infection during Pregnancy. Clin Infect Dis. 2008;47(4):554–66.

77. Baquero-Artigao F, Martín F, Corripio I, Mellgren A, Guasch C, De La Calle Fernández-Miranda M, et al. Guía de la Sociedad Española de Infectología Pediátrica para el diagnóstico y tratamiento de la toxoplasmosis congénita. An Pediatr. 2013;79(2).

78. Bigna JJ, Tochie JN, Tounouga DN, Bekolo AO, Ymele NS, Simé PS, et al. Global, regional and national estimates of Toxoplasma gondii seroprevalence in pregnant women: A protocol for a systematic review and modelling analysis. BMJ Open. 2019;9(10):1–4.

79. Dunn D, Wallon M, Peyron F, Petersen E, Peckham C, Gilbert R. Mother-to-child

transmission of toxoplasmosis: Risk estimates for clinical counselling. Lancet. 1999;353(9167):1829–33.

80. Park YH, Nam HW. Clinical features and treatment of ocular toxoplasmosis. Korean J Parasitol. 2013;51(4):393–9.

81. Gary, N. Holland M. Ocular Toxoplasmosis: A Global Reassessment. Part I: Epidemiology and Course of Disease. Am J Ophthalmol. 2003;136(6):973–88.

82. Garweg JG. Ocular Toxoplasmosis: An Update. Klin Monbl Augenheilkd. 2016;233(4):534–9.

83. Villard O, Cimon B, L'Ollivier C, Fricker-Hidalgo H, Godineau N, Houze S, et al. Serological diagnosis of Toxoplasma gondii infection. Recommendations from the French National Reference Center for Toxoplasmosis. Diagn Microbiol Infect Dis. 2016;84(1):22–33.

84. Liu Q, Wang ZD, Huang SY, Zhu XQ. Diagnosis of toxoplasmosis and typing of Toxoplasma gondii. Parasites and Vectors. 2015;8(1):1–14.

85. Gan SD, Patel KR. Enzyme immunoassay and enzyme-linked immunosorbent assay. J Invest Dermatol. 2013;133(9):1–3.

86. Kurstak E. Progress in enzyme immunoassays: Production of reagents, experimental design, and interpretation. Bull World Health Organ. 1985;63(4):793–811.

87. Sabin AB, Feldman HA. Dyes as microchemical indicators of a new immunity phenomenon affecting a protozoon parasite (toxoplasma). Science (80-). 1948;108(2815):660–3.

88. Reiter-Owona I, Petersen E, Joynson D, Aspöck H, Dardé ML, Disko R, et al. The past and present role of the Sabin-Feldman dye test in the serodiagnosis of toxoplasmosis. Bull World Health Organ. 1999;77(11):929–35.

89. Wyrosdick HM, Schaefer JJ. Toxoplasma gondii: history and diagnostic test development. Anim Heal Res Rev. 2015;16(02):150–62.

90. Nilgün Tekkesin. Diagnosis of toxoplasmosis in pregnancy. Geburtshilfe Frauenheilkd. 1989;49(7):642–8.

91. Cambiaso CL, Galanti LM, Leautaud P, Masson PL. Latex agglutination assay of human immunoglobulin M antitoxoplasma antibodies which uses enzymatically treated antigen-coated particles. J Clin Microbiol. 1992;30(4):882–8.

92. Thobhani S, Attree S, Boyd R, Kumarswami N, Noble J, Szymanski M, et al. Bioconjugation and characterisation of gold colloid-labelled proteins. J Immunol Methods. 2010;356(1–2):60–9.

93. Terkawi MA, Kameyama K, Rasul NH, Xuan X, Nishikawa Y. Development of an immunochromatographic assay based on dense granule protein 7 for serological detection of toxoplasma gondii infection. Clin Vaccine Immunol. 2013;20(4):596–601.

94. Wang YH, Li XR, Wang GX, Yin H, Cai XP, Fu BQ, et al. Development of an

immunochromatographic strip for the rapid detection of Toxoplasma gondii circulating antigens. Parasitol Int. 2011;60(1):105–7.

95. Boothroyd JC. Toxoplasma gondii: 25 years and 25 major advances for the field. Int J Parasitol. 2009;38(8):935–46.

96. Murat JB, L'Ollivier C, Hidalgo HF, Franck J, Pelloux H, Piarroux R. Evaluation of the new Elecsys Toxo IgG avidity assay for toxoplasmosis and new insights into the interpretation of avidity results. Clin Vaccine Immunol. 2012;19(11):1838–43.

97. Marcolino PT, Silva DAO, Leser PG, Camargo ME, Mineo JR. Molecular markers in acute and chronic phases of human toxoplasmosis: Determination of immunoglobulin G avidity by Western blotting. Clin Diagn Lab Immunol. 2000;7(3):384–9.

98. Khammari I, Saghrouni F, Lakhal S, Bouratbine A, Said M Ben, Boukadida J. A new IgG immunoblot kit for diagnosis of toxoplasmosis in pregnant women. Korean J Parasitol. 2014;52(5):493–9.

99. Murat JB, Hidalgo HF, Brenier-Pinchart MP, Pelloux H. Human toxoplasmosis: which biological diagnostic tests are best suited to which clinical situations? Expert Rev Anti Infect Ther. 2013;11(9):943–56.

100. Saeed AFUH, Wang R, Ling S, Wang S. Antibody engineering for pursuing a healthier future. Front Microbiol. 2017;8(MAR):1–28.

101. Van Dyke K, Woodfork K. Luminescence Biotechnology. Instruments and applications. Press C, editor. London-New York--Whashington D.C; 2002.

102. Holec-Gąsior L, Ferra B, Czechowska J, Serdiuk IE, Krzymiński K. A novel chemiluminescent immunoassay based on original acridinium ester labels as better solution for diagnosis of human toxoplasmosis than conventional ELISA test. Diagn Microbiol Infect Dis. 2018;91(1):13–9.

103. Cinquanta L, Fontana DE, Bizzaro N. Chemiluminescent immunoassay technology: what does it change in autoantibody detection? Autoimmun Highlights. 2017;8(1).

104. Schroeder H, Vogelhut P, Carrico R, Bogdlaski RC. Competitive protein binding assay for biotin monitored by chemiluminescence. Anal Chem. 1976;48(13):1933–7.

105. Mahler M, Bentow C, Serra J, Fritzler MJ. Detection of autoantibodies using chemiluminescence technologies. Immunopharmacol Immunotoxicol. 2016;38(1):14–20.

106. Gasso S, Martinez ML. Magnetic bead coatings : Today and tomorrow. 2000.

107. Sultan F. The Basic Guide for the use of Magnetic Beads in Chemiluminiscent Immunoassays. sepmag. 2000.

108. Byun CK, Kim M, Kim D. Modulating the partitioning of microparticles in a polyethylene

glycol (PEG)-Dextran (DEX) aqueous biphasic system by surface modification. Coatings. 2018;8(3).

109. Diamandis P, Christopoulos K. The Biotin-(Strept)Avidin System: Principles and Applications in Biotechnology. Clin Chem. 1991;37(5):625–36.

110. Dimeski G. Interference testing. Clin Biochem Rev. 2008;29 Suppl 1(August):S43-8.

111. Selby C. Interference in immunoassay. Ann Clin Biochem. 1999;36:704–21.

112. Douet T, Armengol C, Charpentier E, Chauvin P, Cassaing S, Iriart X, et al. Performance of seven commercial automated assays for the detection of low levels of anti-Toxoplasma IgG in French immunocompromised patients. Parasite. 2019;26.

113. Zhang K, Lin G, Han Y, Li J. Serological diagnosis of toxoplasmosis and standardization. Clin Chim Acta. 2016;461:83–9.

114. Landry ML. Immunoglobulin M for Acute Infection : True or False ? Clin Vaccine Immunol. 2016;23(7):540–5.

115. Gras L, Gilbert RE, Wallon M, Peyron F, Cortina-Borja DM. Duration of the IgM response in women acquiring Toxoplasma gondii during pregnancy: implications for clinical practice and cross-sectional incidence studies. Epidemiol Infect. 2004;132(3):541–8.

116. Sensini A. Toxoplasma gondii infection in pregnancy: opportunities and pitfalls of serological diagnosis. Eur Soc Clin Infect Dis. 2006;12(6):504–12.

117. Fricker-Hidalgo H, Saddoux C, Suchel-Jambon AS, Romand S, Foussadier A, Pelloux H, et al. New Vidas assay for Toxoplasma-specific IgG avidity: evaluation on 603 sera. Diagn Microbiol Infect Dis. 2006;56(2):167–72.

118. Gay-Andrieu F, Fricker-Hidalgo H, Sickinger E, Espern A, Brenier-Pinchart MP, Braun HB, et al. Comparative evaluation of the ARCHITECT Toxo IgG, IgM, and IgG Avidity assays for anti-Toxoplasma antibodies detection in pregnant women sera. Diagn Microbiol Infect Dis. 2009;65(3):279–87.

119. Candolfi E, Pastor R, Huber R, Filisetti D, Villard O. IgG avidity assay firms up the diagnosis of acute toxoplasmosis on the first serum sample in immunocompetent pregnant women. Diagn Microbiol Infect Dis. 2007;58(1):83–8.

120. Prince HE, Wilson M. Simplified Assay for Measuring Toxoplasma gondii Immunoglobulin G Avidity. Clin Diagn Lab Immunol. 2001;8(5):904–8.

121. Ashburn D, Joss AWL, Pennington TH, Ho-Yen DO. Do IgA, IgE, and IgG avidity tests have any value in the diagnosis of toxoplasma infection in pregnancy? J Clin Pathol. 1998;51(4):312–5.

122. Weber B, Badiel M, Alvarez-Otero Y, Thulliez P, Montoya JG. Comparative evaluation of AxSYM, VIDAS and VIDIA toxoplasmosis reagent performance in a high

seroprevalence Latin American country. Sci Med (Porto Alegre). 2010;20(1):27.

123. Wilson M, Remington JS, Clavet C, Varney G, Press C, Ware D, et al. Evaluation of Six Commercial Kits for Detection of Human Immunoglobulin M Antibodies to Toxoplasma gondii. Microbiology. 1997;35(12):3112–5.

124. Wilson M, Remington JS, Clavet C, Varney G, Press C, Ware D. Evaluation of six commercial kits for detection of human immunoglobulin M antibodies to Toxoplasma gondii. The FDA Toxoplasmosis Ad Hoc Working Group. J Clin Microbiol. 1997;35(12):3112–5.

125. Kaul R, Chen P, Binder SR. Detection of immunoglobulin M antibodies specific for Toxoplasma gondii with increased selectivity for recently acquired infections. J Clin Microbiol. 2004;42(12):5705–9.

126. Mayo Clinic Laboratories. Testing for IgM-class Antibodies to Determine Acute Infection: Clinical and Diagnostic Considerations. 2019.

127. García-bermejo I, Ory F. Rapid diagnosis in serology. Enferm Infecc Microbiol Clin. 2017;35(4):246–54.

128. Rostami A, Karanis P, Fallahi S. Advances in serological, imaging techniques and molecular diagnosis of Toxoplasma gondii infection. Infection. 2018;46(3):303–15.

129. Tomasi JP, Schlit AF, Stadtsbaeder S. Rapid double-sandwich enzyme-linked immunosorbent assay for detection of human immunoglobulin M anti-Toxoplasma gondii antibodies. J Clin Microbiol. 1986;24(5):849–50.

130. Obwaller A, Hassl A, Picher O, Aspöck H. An enzyme-linked immunosorbent assay with whole trophozoites of Toxoplasma gondii from serum-free tissue culture for detection of specific antibodies. Parasitol Res. 1995;81(5):361–4.

131. Kotresha D, Noordin R. Recombinant proteins in the diagnosis of toxoplasmosis. APMIS. 2010;118(8):529–42.

132. Thiruvengadam G, Init I, Fong MY, Lau YL. Optimization of the expression of surface antigen SAG1/2 of Toxoplasma gondii in the yeast Pichia pastoris. Trop Biomed. 2011;28(3):506–13.

133. Chang PY, Fong MY, Nissapatorn V, Lau YL. Evaluation of Pichia pastoris - Expressed recombinant rhoptry protein 2 of Toxoplasma gondii for its application in diagnosis of toxoplasmosis. Am J Trop Med Hyg. 2011;85(3):485–9.

134. Wang Z, Ge W, Huang SY, Li J, Zhu XQ, Liu Q. Evaluation of recombinant granule antigens GRA1 and GRA7 for serodiagnosis of Toxoplasma gondii infection in dogs. BMC Vet Res. 2014;10(1):1–6.

135. Wang Y, Yin H. Research advances in microneme protein 3 of Toxoplasma gondii. Parasites and Vectors. 2015;8(1):1–12.

136. Tomasz Ferra B, Holec-Gąsior L, Gatkowska J, Dziadek B, Dzitko K, Grąźlewska W, et al. The first study on the usefulness of recombinant tetravalent chimeric proteins containing fragments of SAG2, GRA1, ROP1 and AMA1 antigens in the detection of specific anti-Toxoplasma gondii antibodies in mouse and human sera. PLoS One. 2019;14(6):1–23.

137. Li S, Galvan G, Araujo FG, Suzuki Y, Remington JS, Parmley S. Serodiagnosis of recently acquired Toxoplasma gondii infection using an enzyme-linked immunosorbent assay with a combination of recombinant antigens. Clin Diagn Lab Immunol. 2000;7(5):781–7.

138. Dai J, Jiang M, Wang Y, Qu L, Gong R, Si J. Evaluation of a recombinant multiepitope peptide for serodiagnosis of Toxoplasma gondii infection. Clin Vaccine Immunol. 2012;19(3):338–42.

139. Aubert D, Maine GT, Villena I, Hunt JC, Howard L, Sheu M. Recombinant antigens to detect Toxoplasma gondii- specific Immunoglobulin G and Immunoglobulin M in Human Sera by enzyme immunoassay. J Clin Microbiol. 2016;38:1144–50.

140. Pfrepper KI, Enders G, Gohl M, Krczal D, Hlobil H, Wassenberg D, et al. Seroreactivity to and avidity for recombinant antigens in toxoplasmosis. Clin Diagn Lab Immunol. 2005;12(8):977–82.

141. Woolley CF, Hayes MA. Recent developments in emerging microimmunoassays. Bioanalysis. 2013;5(2):245–64.

142. Maksimov P, Zerweck J, Maksimov A, Hotop A, Groß U, Pleyer U, et al. Peptide microarray analysis of in silico-predicted epitopes for serological diagnosis of Toxoplasma gondii infection in humans. Clin Vaccine Immunol. 2012;19(6):865–74.

143. Nilvebrant J, Rockberg J. An Introduction to Epitope Mapping. Methods Mol Biol. 2018;1785.

144. Greenbaum J, Pernille Andersen, Blythe Martin, Huynh-Hoa Bui. Towards a consensus on datasets and evaluation metrics for developing B-cell epitope prediction tools. J Mol Recognit. 2007;20(5):75–82.

145. Potocnakova L, Bhide M, Pulzova LB. An Introduction to B-Cell Epitope Mapping and in Silico Epitope Prediction. J Immunol Res. 2016;2016.

146. Johnson M. The antigenic structure of Toxoplasma gondii: a review. Pathology. 1985;17:9–19.

147. Döşkaya M, Liang L, Jain A, Can H, Gülçe Iz S, Felgner PL, et al. Discovery of new Toxoplasma gondii antigenic proteins using a high throughput protein microarray approach screening sera of murine model infected orally with oocysts and tissue cysts. Parasites and Vectors. 2018;11(1):1–13.

148. Costa JG, Peretti LE, García VS, Peverengo L, González VDG, Gugliotta LM, et al. P35 and P22 Toxoplasma gondii antigens abbreviate regions to diagnose acquired toxoplasmosis during pregnancy: Toward

single-sample assays. Clin Chem Lab Med. 2017;55(4):595–604.

149. Wang Y, Wang G, Ou J, Yin H, Zhang D. Analyzing and identifying novel B cell epitopes within Toxoplasma gondii GRA4. Parasites and Vectors. 2014;7(1):1–8.

150. Leriche MA, Dubremetz JF. Characterization of the protein contents of rhoptries and dense granules of Toxoplasma gondii tachyzoites by subcellular fractionation and monoclonal antibodies. Mol Biochem Parasitol. 1991;45(2):249–59.

151. He XL, Grigg ME, Boothroyd JC, Garcia KC. Structure of the immunodominant surface antigen from the toxoplasma gondii SRS superfamily. Nat Struct Biol. 2002;9(8):606–11.

152. Tonelli RR, Colli W, Alves MJM. Selection of binding targets in parasites using phage-display and aptamer libraries in vivo and in vitro. Front Immunol. 2012;3(JAN):1–16.

153. Beghetto E, Spadoni A, Buffolano W, Del Pezzo M, Minenkova O, Pavoni E, et al. Molecular dissection of the human B-cell response against Toxoplasma gondii infection by lambda display of cDNA libraries. Int J Parasitol. 2003;33(2):163–73.

154. Beghetto E, Pucci A, Minenkova O, Spadoni A, Bruno L, Buffolano W, et al. Identification of a human immunodominant B-cell epitope within the GRA1 antigen of Toxoplasma gondii by phage display of cDNA libraries. Int J Parasitol. 2001;31(14):1659–68.

155. Robben J, Hertveldt K, Bosmans E, Volckaert G. Selection and identification of dense granule antigen GRA3 by Toxoplasma gondii whole genome phage display. J Biol Chem. 2002;277(20):17544–7.

156. Moreira GMSG, Fuhner V, Hust M. Epitope Mapping by Phage Display. Methods Mol Biol. 2018;1701:321–30.

157. frank R. Spot synthesis: an easy technique for the positionally addressable, parallel chemical synthesis on a membrane support. Tetrahedron. 1992;48:9217–32.

158. Mezzasoma L, Bacarese-Hamilton T, Ardizzoni A, Bistoni F, Crisanti A. Serodiagnosis of infectious diseases with antigen microarrays. J Appl Microbiol. 2004;96(1):10–7.

159. Maksimov P, Zerweck J, Maksimov A, Hotop A, Groß U, Spekker K, et al. Analysis of clonal type-specific antibody reactions in toxoplasma gondii seropositive humans from germany by peptide-microarray. PLoS One. 2012;7(3):1–10.

160. Tighe PJ, Ryder RR, Todd I, Fairclough LC. ELISA in the multiplex era: Potentials and pitfalls. Proteomics - Clin Appl. 2015;9(3–4):406–22.

161. R. B. Merrifield. Solid Phase Peptide Synthesis. I. The Synthesis of a Tetrapeptide. J Am Chem Soc. 1963;85(14):2149–54.

162. Palomo JM. Solid-phase peptide synthesis: An overview focused on the preparation of

biologically relevant peptides. RSC Adv. 2014;4(62):32658–72.

163. Stawikowski M, Fields GB. Introduction to Peptide Synthesis. Curr Protoc Protein Sci. 2002;26:1–17.

164. Mäde V, Els-heindl S, Beck-sickinger AG. Automated solid-phase peptide synthesis to obtain therapeutic peptides. Beilstein J Org Chem. 2014;(Scheme 1):1197–212.

165. Chandrudu S, Simerska P, Toth I. Chemical Methods for Peptide and Protein Production. 2013;4373–88.

166. Gómara MJ, Haro I. Synthetic Peptides for the Immunodiagnosis of Human Diseases. Curr Med Chem. 2007;14(5):531–46.

167. Vlieghe P, Lisowski V, Martinez J, Khrestchatisky M. Synthetic therapeutic peptides: science and market. Drug Discov Today. 2010;Jan(15):1–2.

168. Wiuff C, Jauho ES, Stryhn H, Andresen LO, Thaulov K, Boas U, et al. Evaluation of a novel enzyme-linked immunosorbent assay for detection of antibodies against Salmonella, employing a stable coating of lipopolysaccharide-derived antigens covalently attached to polystyrene microwells. J Vet Diagnostic Investig. 2000;12(2):130–5.

169. List C, Qi W, Maag E, Gottstein B, Müller N, Felger I. Serodiagnosis of Echinococcus spp. infection: Explorative selection of diagnostic antigens by peptide microarray. PLoS Negl Trop Dis. 2010;4(8).

170. Shen G, Behera D, Bhalla M, Nadas A, Laal S. Peptide-based antibody detection for tuberculosis diagnosis. Clin Vaccine Immunol. 2009;16(1):49–54.

171. Kowalczyk W, Monsó M, de la Torre BG, Andreu D. Synthesis of multiple antigenic peptides (MAPs)-strategies and limitations. J Pept Sci. 2010;17(4):247–51.

172. Kong J, Grigg ME, Uyetake L, Parmley S, Boothroyd JC. Serotyping of Toxoplasma gondii infections in Humans Using Synthetic Peptides. J Infect Dis. 2003;187:1484–95.

173. Sousa S, Ajzenberg D, Marle M, Aubert D, Villena I, Da Costa JC, et al. Selection of polymorphic peptides from GRA6 and GRA7 sequences of Toxoplasma gondii strains to be used in serotyping. Clin Vaccine Immunol. 2009;16(8):1158–69.

174. Bastos LM, Macêdo AG, Silva M V., Santiago FM, Ramos ELP, Santos FAA, et al. Toxoplasma gondii-derived synthetic peptides containing B- and T-cell epitopes from GRA2 protein are able to enhance mice survival in a model of experimental toxoplasmosis. Front Cell Infect Microbiol. 2016;6:1–11.

175. Beghetto E, Spadoni A, Bruno L, Buffolano W, Gargano N. Chimeric antigens of Toxoplasma gondii: Toward standardization of toxoplasmosis serodiagnosis using recombinant products. J Clin Microbiol. 2006;44(6):2133–40.

176. Holec-Gąsior L, Ferra B, Drapała D, Lautenbach D, Kur J. A new MIC1-MAG1 recombinant chimeric antigen can be used

instead of the Toxoplasma gondii lysate antigen in serodiagnosis of human toxoplasmosis. Clin Vaccine Immunol. 2012;19(1):57–63.

177. Drapała D, Holec-Gasior L, Kur J. New recombinant chimeric antigens, P35-MAG1, MIC1-ROP1, and MAG1-ROP1, for the serodiagnosis of human toxoplasmosis. Diagn Microbiol Infect Dis. 2015;82(1).

178. Holec-Gąsior L, Ferra B, Drapała D. MIC1-MAG1-SAG1 chimeric protein, a most effective antigen for detection of human toxoplasmosis. Clin Vaccine Immunol. 2012;19(12):1977–9.

179. Dai J, Jiang M, Qu L, Sun L, Wang Y, Gong L, et al. Toxoplasma gondii: Enzyme-linked immunosorbent assay based on a recombinant multi-epitope peptide for distinguishing recent from past infection in human sera. Exp Parasitol. 2013;133(1):95–100.

180. Döşkaya M, Caner A, Can H, Iz SG, Gedik Y, Döşkaya AD, et al. Diagnostic value of a Rec-ELISA Using toxoplasma gondii recombinant SporoSAG, BAG1, and GRA1 proteins in murine models infected orally with tissue cysts and oocysts. PLoS One. 2014;9(9):1–7.

181. Ferra B, Holec-Gąsior L, Kur J. A new Toxoplasma gondii chimeric antigen containing fragments of SAG2, GRA1, and ROP1 proteins—impact of immunodominant sequences size on its diagnostic usefulness. Parasitol Res. 2015;114(9):3291–9.

182. Sousa S, Ajzenberg D, Vilanova M, Costa J, Dardé ML. Use of GRA6-derived synthetic polymorphic peptides in an immunoenzymatic assay to serotype Toxoplasma gondii in human serum samples collected from three continents. Clin Vaccine Immunol. 2008;15(9):1380–6.

183. Wang Y, Wang G, Zhang D, Yin H, Wang M. Screening and identification of novel B cell epitopes of Toxoplasma gondii SAG1. Parasites and Vectors. 2013;6(1):2–6.

184. Jacobson RH. Validation of serological assays for diagnosis of infectious diseases. Rev Sci Tech. 1998;17(2):469–86.

185. Jones ML, Barnard RT. Use of chimeric antibodies as positive controls in an enzyme-linked immunosorbent assay for diagnosis of scrub typhus (infection by Orientia tsutsugamushi). Clin Vaccine Immunol. 2007;14(10):1307–10.

186. Eusebi P. Diagnostic accuracy measures. Cerebrovasc Dis. 2013;36(4):267–72.

187. Leeflang M. Systematic reviews and meta-analyses of diagnostic test accuracy. Clin Microbiol Infect. 2014;20(2):105–13.

188. Milstein C, Alerts E. Continuous cultures of fused cells secreting antibody of predefined. Nature. 1975;256(5517):495–7.

189. Zaroff S, Tan G. Hybridoma technology: the preferred method for monoclonal antibody generation for in vivo applications. Biotechniques. 2019;67(3):90–2.

190. Parray HA, Shukla S, Samal S, Shrivastava T, Ahmed S. Hybridoma technology a versatile method for isolation of monoclonal antibodies,

its applicability across species, limitations, advancement and future perspectives. Int Immunopharmacol. 2020;85.

191. Samoilovich S, Duga C, Macario A. Hybridoma technology: new developments of practical interest. J Immunol Methods,. 1987;101:153–70.

192. Monoclonal Antibody Production. National Research Council (US) Committee on Methods of Producing Monoclonal Antibodies. Washington (DC): National Academies Press (US); 1999.

193. Almeida R, Nakamura CN, de Lima Fontes M, Deffune E, Felisbino SL, Kaneno R, et al. Enhanced immunization techniques to obtain highly specific monoclonal antibodies. MAbs. 2018;10(1):46–54.

194. Yatim KM, Lakkis FG. A brief journey through the immune system. Clin J Am Soc Nephrol. 2015;10(7):1274–81.

195. Otero AJ. 38 Years of Hybridoma Technology as a Source of Analytical Tools for Immunodiagnostics of Infectious Diseases . Some Contributions Developed in Cuba to Improve the Original Procedures and Future P. J Immunol Tech Infect Dis. 2015;(June).

196. Hackett J, Hoff-Velk J, Golden A, Brashear J, Robinson J, Rapp M, et al. Recombinant mouse-human chimeric antibodies as calibrators in immunoassays that measure antibodies to Toxoplasma gondii. J Clin Microbiol. 1998;36(5):1277–84.

197. Morrison SL, Johnson MJ, Herzenberg LA, Oi VT. Chimeric human antibody molecules: Mouse antigen-binding domains with human constant region domains. Proc Natl Acad Sci U S A. 1984;81(21 I):6851–5.

198. Cogné M, Laffleur B, Cuvillier A, Bosselut M. Transgenic non-human mammal for producing chimeric human immunoglobulin E antibodies. PCT/IB2014/062826, 2013. p. 1–40.

199. Smith SA, Crowe JE. Use of Human Hybridoma Technology To Isolate Human Monoclonal Antibodies. Microbiol Spectr. 2015;3(1):1–12.

200. Aubert D, Maine GT, Villena I, Hunt JC, Howard L, Sheu M, et al. Recombinant antigens to detect Toxoplasma gondii-specific immunoglobulin G and immunoglobulin M in human sera by enzyme immunoassay. J Clin Microbiol. 2000;38(3):1144–50.

201. Pietkiewicz H, Hiszczyńska-Sawicka E, Kur J, Petersen E, Nielsen H V., Stankiewicz M, et al. Usefulness of Toxoplasma gondii-Specific Recombinant Antigens in Serodiagnosis of Human Toxoplasmosis. J Clin Microbiol. 2004;42(4):1779–81.

202. Beghetto E, Buffolano W, Spadoni A, Pezzo M Del, Cristina M Di, Minenkova O, et al. Use of an Immunoglobulin G Avidity Assay Based on Recombinant Antigens for Diagnosis of Primary. Microbiology. 2003;41(12):5414–8.

203. Buffolano W, Beghetto E, Del Pezzo M, Spadoni A, Di Cristina M, Petersen E, et al. Use

of recombinant antigens for early postnatal diagnosis of congenital toxoplasmosis. J Clin Microbiol. 2005;43(12):5916–24.

204. Harning D, Spenter J, Metsis A, Vuust J, Petersen E. Recombinant Toxoplasma gondii surface antigen 1 (P30) expressed in Escherichia coli is recognized by human Toxoplasma-specific immunoglobulin M (IgM) and IgG antibodies. Clin Diagn Lab Immunol. 1996;3(3):355–7.

205. Leinikki P, Lehtinen M, Hyöty H, Parkkonen P, Kantanen ML, Hakulinen J. Synthetic Peptides as Diagnostic Tools in Virology. Adv Virus Res. 1993;42:149–86.

206. Gonzalez L, Boyle RW, Zhang M, Castillo J, Whittier S, Della-Latta P, et al. Synthetic-peptide-based enzyme-linked immunosorbent assay for screening human serum or plasma for antibodies to human immunodeficiency virus type 1 and type 2. Clin Diagn Lab Immunol. 1997;4(5):598–603.

207. Nowakowska D, Colon I, Remington JS, Grigg M, Golab E, Wilczynski J, et al. Genotyping of Toxoplasma gondii by Multiplex PCR and Peptide-Based Serological Testing of Samples from Infants in Poland Diagnosed with Congenital Toxoplasmosis. J Clin Immunol. 2006;44(4):1382–9.

208. Muñoz P, Sierra M, Andreu M. Diagnóstico serológico de las infecciones por Toxoplasma gondii. Control Calidad SEIMC. 1989;7.

209. Villard O, Cimon B, Ollivier CL, Fricker-hidalgo H, Godineau N, Houze S, et al. Serological diagnosis of Toxoplasma gondii infection. Recommendations from the French National Reference Center for Toxoplasmosis. Diagn Microbiol Infect Dis. 2016;84:22–33.

210. Drapała D, Holec-Gasior L, Kur J. New recombinant chimeric antigens, P35-MAG1, MIC1-ROP1, and MAG1-ROP1, for the serodiagnosis of human toxoplasmosis. Diagn Microbiol Infect Dis. 2015;82(1):34–9.

211. Holec-Ģsior L, Kur J, Hiszczyńska-Sawicka E. GRA2 and ROP1 recombinant antigens as potential markers for detection of toxoplasma gondii-specific immunoglobulin G in humans with acute toxoplasmosis. Clin Vaccine Immunol. 2009;16(4):510–4.

212. Sibley D, Boothroyd J. Virulent strains of Toxoplasma gondii comprise a single clonal lineage. Nature. 1992;359:82–5.

213. Rezaei F, Sharif M, Sarvi S, Hejazi SH, Aghayan S, Pagheh AS, et al. A systematic review on the role of GRA proteins of Toxoplasma gondii in host immunization. J Microbiol Methods. 2019;165(105696).

214. Bradley PJ, Hsieh CL, Boothroyd JC. Unprocessed Toxoplasma ROP1 is effectively targeted and secreted into the nascent parasitophorous vacuole. Mol Biochem Parasitol. 2002;125(1–2):189–93.

215. Bradley PJ, Boothroyd JC. Identification of the pro-mature processing site of

Toxoplasma ROP1 by mass spectrometry. Mol Biochem Parasitol. 1999;100(1):103–9.

216. Soldati D, Lassen A, Dubremetz JF, Boothroyd JC. Processing of Toxoplasma ROP1 protein in nascent rhoptries. Mol Biochem Parasitol. 1998;96(1–2):37–48.

217. Holec-Gąsior L, Drapała D, Lautenbach D, Kur J. Toxoplasma gondii: Usefulness of ROP1 recombinant antigen in an immunoglobulin G avidity assay for diagnosis of acute toxoplasmosis in humans. Polish J Microbiol. 2010;59(4):307–10.

218. Varro R, Chen R, Sepulveda H, Apgar J. Bead-based multianalyte flow immunoassays: the cytometric bead array system. Methods Mol Biol. 2007;378(3):125–52.

219. Morgan E, Varro R, Sepulveda H, Ember JA, Apgar J, Wilson J, et al. Cytometric bead array: A multiplexed assay platform with applications in various areas of biology. Clin Immunol. 2004;110(3):252–66.

220. Guigue N, Menotti J, Hamane S, Derouin F, Garin YJF. Performance of the BioPlex 2200 flow immunoassay in critical cases of serodiagnosis of toxoplasmosis. Clin Vaccine Immunol. 2014;21(4):496–500.

221. Liesenfeld O, Press C, Montoya JG, Gill R, Isaac-Renton JL, Hedman K, et al. False-positive results in immunoglobulin M (IgM) toxoplasma antibody tests and importance of confirmatory testing: The platelia toxo IgM test. J Clin Microbiol. 1997;35(1):174–8.

222. Prusa AR, Hayde M, Unterasinger L, Pollak A, Herkner KR, Kasper DC. Evaluation of the Roche Elecsys Toxo IgG and IgM electrochemiluminescence immunoassay for the detection of gestational Toxoplasma infection. Diagn Microbiol Infect Dis. 2010;68(4):352–7.

223. Baschirotto PT, Krieger MA, Foti L. Preliminary multiplex microarray igG immunoassay for the diagnosis of toxoplasmosis and rubella. Mem Inst Oswaldo Cruz. 2017;112(6):428–36.

224. Holec-Gasior L. Toxoplasma gondii recombinant antigens as tools for serodiagnosis of human toxoplasmosis: Current status of studies. Clin Vaccine Immunol. 2013;20(9):1343–51.

225. Blanco E, Guerra B, De La Torre BG, Defaus S, Dekker A, Andreu D, et al. Full protection of swine against foot-and-mouth disease by a bivalent B-cell epitope dendrimer peptide. Antiviral Res. 2016;129:74–80.

226. Cañas-Arranz R, Forner M, Defaus S, de León P, Bustos MJ, Torres E, et al. A single dose of dendrimer B2T peptide vaccine partially protects pigs against foot-and-mouth disease virus infection. Vaccines. 2020;8(1):1–11.

227. Liu J, Liu J, Chu L, Wang Y, Duan Y, Feng L, et al. Novel peptide-dendrimer conjugates as drug carriers for targeting nonsmall cell lung cancer. Int J Nanomedicine. 2011;6(1):59–69.

228. Joshi VG, Dighe VD, Thakuria D, Malik YS, Kumar S. Multiple antigenic peptide (MAP): A synthetic peptide dendrimer for diagnostic,

antiviral and vaccine strategies for emerging and re-emerging viral diseases. Indian J Virol. 2013;24(3):312–20.

229. Monsó M, De La Torre BG, Blanco E, Moreno N, Andreu D. Influence of conjugation chemistry and B epitope orientation on the immune response of branched peptide antigens. Bioconjug Chem. 2013;24(4):578–85.

230. Gershoni JM, Roitburd-berman A, Siman-tov DD, Freund NT. Epitope Mapping The First Step in Developing Epitope-Based Vaccines. DRUG Dev. 2007;21(3):145–56.

231. Blanco E, Andreu D, Sobrino F. Peptide Vaccines Against Foot-and-mouth Disease. Foot Mouth Dis Virus Curr Res Emerg Trends. 2017;(Jan):317–32.

232. Adesida, Adetola. Aojula, Raj. Ajoula HCD. Nonepitopic antibody binding sequence: Implications in screening and development of peptide vaccines. Vaccine. 1999;18:315–20.

233. Marussig M, Rénia L, Motard A, Miltgen F, Pétour P, Chauhan V, et al. Linear and multiple antigen peptides containing defined T and B epitopes of the Plasmodium yoelii circumsporozoite protein: Antibody-mediated protection and boosting by sporozoite infection. Int Immunol. 1997;9(12):1817–24.

234. Ossorio PN, Schwartzman JD, Boothroyd JC. A Toxoplasma gondii rhoptry protein associated with host cell penetration has unusual charge asymmetry. Mol Biochem Parasitol. 1992;50(1):1–15.

235. Holec-Gąsior L, Ferra B, Czechowska J, Serdiuk IE, Krzymiński K, Kur J. A novel chemiluminescent immunoassay for detection of Toxoplasma gondii IgG in human sera. Diagn Microbiol Infect Dis. 2016;85(4):422–5.

236. Hajissa K, Zakaria R, Suppian R, Mohamed Z. An evaluation of a recombinant multiepitope based antigen for detection of Toxoplasma gondii specific antibodies. BMC Infect Dis. 2017;17(1):1–8.

237. Lau YL, Thiruvengadam G, Lee WW, Fong MY. Immunogenic characterization of the chimeric surface antigen 1 and 2 (SAG1/2) of Toxoplasma gondii expressed in the yeast Pichia pastoris. Parasitol Res. 2011;109(3):871–8.

238. Pietkiewicz H, Hiszczyńska-Sawicka E, Kur J, Petersen E, Nielsen H V., Paul M, et al. Usefulness of Toxoplasma gondii recombinant antigens (GRA1, GRA7 and SAG1) in an immunoglobulin G avidity test for the serodiagnosis of toxoplasmosis. Parasitol Res. 2007;100(2):333–7.

239. Kim P, Pau CP. Comparing tandem repeats and multiple antigenic peptides as the antigens to detect antibodies by enzyme immunoassay. J Immunol Methods. 2001;257(1–2):51–4.

240. Ram H, Rao JR, Tewari AK, Banerjee PS, Sharma AK. Molecular cloning, sequencing, and biological characterization of GRA4 gene of Toxoplasma gondii. Parasitol Res. 2013;112(7):2487–94.

241. Nigro M, Gutierrez A, Hoffer AM, Clemente M, Kaufer F, Carral L, et al. Evaluation of Toxoplasma gondii recombinant proteins for the diagnosis of recently acquired toxoplasmosis by an immunoglobulin G analysis. Diagn Microbiol Infect Dis. 2003;47(4):609–13.

242. Butler JE. Solid supports in enzyme-linked immunosorbent assay and other solid-phase immunoassays. Methods. 2000;22(1):4–23.

243. Schetters H. Avidin and streptavidin in clinical diagnostics. Biomol Eng. 1999;16(1–4):73–8.

244. Ahmed S, Ning J, Peng D, Chen T, Ahmad I, Ali A, et al. Current advances in immunoassays for the detection of antibiotics residues: a review. Food Agric Immunol. 2020;31(1):268–90.

245. Barreiro F, Maynou X. Arquitectura sanitaria. Diseño del laboratorio de análisis clínicos. Gestión y Evaluación Costes Sanit. 2008;9(2):127–44.

246. Palanca I, Miravalles E. Laboratorio Clínico Central Estándares y recomendaciones de calidad y seguridad. 2013.

247. Weissman SA, Anderson NG. Design of Experiments (DoE) and Process Optimization. A Review of Recent Publications. Org Process Res Dev. 2015;19(11):1605–33.

248. Augustine SAJ, Simmons KJ, Eason TN, Griffin SM, Curioso CL, Wymer LJ, et al. Statistical approaches to developing a multiplex immunoassay for determining human exposure to environmental pathogens. J Immunol Methods. 2015;425:1–9.

249. Montgomery C. Douglas. Design and Analysis of Experiments. Wiley; 1997.

250. Altekar M, Homon CA, Kashem MA, Mason SW, Nelson RM, Patnaude LA, et al. Assay Optimization: A Statistical Design of Experiments Approach. Clin Lab Med. 2007;27(1):139–54.

251. Joelsson D, Moravec P, Troutman M, Pigeon J, DePhillips P. Optimizing ELISAs for precision and robustness using laboratory automation and statistical design of experiments. J Immunol Methods. 2008;337(1):35–41.

252. Reiken SR, Van Wie BJ, Sutisna H, Kurdikar DL, Davis WC. Efficient optimization of ELISAs. J Immunol Methods. 1994;177(1–2):199–206.

253. Chen Z, Wu C, Zhang Z, Wu W, Wang X, Yu Z. Synthesis, functionalization, and nanomedical applications of functional magnetic nanoparticles. Chinese Chem Lett. 2018;29(11):1601–8.

254. Cristea I, Charit B. Conjugation of Magnetic Beads for Immunopurification of Protein Complexes. Physiol Behav. 2016;176(1):100–106.

255. Moyano A, Serrano-Pertierra E, Salvador M, Martínez-García JC, Rivas M, Blanco-López

MC. Magnetic lateral flow immunoassays. Diagnostics. 2020;10(5).

256. Petzold A. The relevance of buffer system ionic strength in immunoassay development. J Immunol Methods. 2019;465(November):27–30.

257. Waritani T, Chang J, McKinney B, Terato K. An ELISA protocol to improve the accuracy and reliability of serological antibody assays. MethodsX. 2017;4:153–65.

258. Zbacnik TJ, Holcomb RE, Katayama DS, Murphy BM, Payne RW, Coccaro RC, et al. Role of Buffers in Protein Formulations. J Pharm Sci. 2017;106(3):713–33.

259. Golovanov AP, Hautbergue GM, Wilson SA, Lian LY. A simple method for improving protein solubility and long-term stability. J Am Chem Soc. 2004;126(29):8933–9.

260. Lim CS, Krishnan G, Sam CK, Ng CC. On optimizing the blocking step of indirect enzyme-linked immunosorbent assay for Epstein-Barr virus serology. Clin Chim Acta. 2013;415:158–61.

261. Sentandreu MÁ, Aubry L, Toldrá F, Ouali A. Blocking agents for ELISA quantification of compounds coming from bovine muscle crude extracts. Eur Food Res Technol. 2007;224(5):623–8.

262. Chapman MD, Keir G, Petzold A, Thompson EJ. Measurement of high affinity antibodies on antigen-immunoblots. J Immunol Methods. 2006;310(1–2):62–6.

263. Hakami AR, Ball JK, Tarr AW. Non-ionic detergents facilitate non-specific binding of M13 bacteriophage to polystyrene surfaces. J Virol Methods. 2015;221(April):1–8.

264. Terato K, Do CT, Cutler D, Waritani T, Shionoya H. Preventing intense false positive and negative reactions attributed to the principle of ELISA to re-investigate antibody studies in autoimmune diseases. J Immunol Methods. 2014;407:15–25.

265. Parvez K, Danish I, Moxley MA. Luminol-Based Chemiluminescent Signals: Clinical and Non- clinical Application and Future Uses. Physiol Behav. 2017;176(12):139–48.

266. Santoro F, Afchain D, Pierce R, Cesbron JY, Ovlaque G, Capron A. Serodiagnosis of toxoplasma infection using a purified parasite protein (P30). Clin Exp Immunol. 1985;62(2):262–9.

267. Cesbron JY, Capron A, Ovlaque G, Santoro F. Use of a monoclonal antibody in a double-sandwich ELISA for detection of IgM antibodies to Toxoplasma gondii major surface protein (P30). J Immunol Methods. 1985;83(1):151–8.

268. Petersen E, Borobio MV, Guy E, Liesenfeld O, Meroni V, Naessens A, et al. European multicenter study of the LIAISON automated diagnostic system for determination of Toxoplasma gondii-specific immunoglobulin G (IgG) and IgM and the IgG avidity index. J Clin Microbiol. 2005;43(4):1570–4.

269. Meylan P, Paris L, Liesenfeld O. Multicenter evaluation of the Elecsys Toxo IgG and IgM tests for the diagnosis of infection with Toxoplasma gondii. Eur J Microbiol Immunol. 2015;5(2):150–8.

270. Schotte L, Rombaut B. A liquid phase affinity capture assay using magnetic beads to study protein-protein interaction: the poliovirus-nanobody example. J Vis Exp. 2012;May 29(63):3937.

271. Ray CA, Patel V, Shih J, Macaraeg C, Wu Y, Thway T, et al. Application of multi-factorial design of experiments to successfully optimize immunoassays for robust measurements of therapeutic proteins. J Pharm Biomed Anal. 2009;49(2):311–8.

272. Hanneman SK. Design, analysis, and interpretation of method-comparison studies. AACN Adv Crit Care. 2008;19(2):223–34.

273. Oosterhuis WP. Analytical performance specifications in clinical chemistry: the holy grail? J Lab Precis Med. 2017;2:78–78.

274. Sandberg S, Fraser CG, Horvath AR, Jansen R, Jones G, Oosterhuis W, et al. Defining analytical performance specifications: Consensus Statement from the 1st Strategic Conference of the European Federation of Clinical Chemistry and Laboratory Medicine. Clin Chem Lab Med. 2015;53(6):833–5.

275. Horvath AR, Bossuyt PMM, Sandberg S, John AS, Monaghan PJ, Verhagen-Kamerbeek WDJ, et al. Setting analytical performance specifications based on outcome studies - Is it possible? Clin Chem Lab Med. 2015;53(6):841–8.

276. Hollis S. Analysis of method comparison studies. Ann Clin Biochem. 1996;33(1):1–4.

277. Magari RT. Statistics for laboratory method comparison studies. BioPharm. 2002;15(1):28–32.

278. Parikh R, Mathai A, Thomas R. Understanding and using sensitivity, specificity and predictive values. Indian J Ophthalmol. 2008;56(1):45–50.

279. Zunic B, Peter S. Interferences in Immunoassays. In: Advances in Immunoassay Technology. 2012. p. 267–322.

280. Tate, Jill Ward G. Interferences in Immunoassay. Clin Biochem Rev. 2004;25(May):403–16.

281. Koskinen MT, Holopainen J, Pyörälä S, Bredbacka P, Pitkälä A, Barkema HW, et al. Analytical specificity and sensitivity of a real-time polymerase chain reaction assay for identification of bovine mastitis pathogens. J Dairy Sci. 2009;92(3):952–9.

282. Miller J. Interference in immunoassays: avoiding erroneous results. Clin Lab Int. 2004;28(April):14–7.

283. Clinical and Laboratory Standards Institute. CLSI. Interference testing in Clinical Chemistry; Approved Guideline - Second Edition. Wayne, PA; 20015.

284. Kricka LJ. Human anti-animal antibody interferences in immunological assays. Clin Chem. 1999;45(7):942–56.

285. Levinson S. Antibody multispecificity in immunoassay interference. Clin Biochem. 1992;25(2):77–87.

286. Da Silva MG, Vinaud MC, De Castro AM. Prevalence of toxoplasmosis in pregnant women and vertical transmission of Toxoplasma gondii in patients from basic units of health from Gurupi, Tocantins, Brazil, from 2012 to 2014. PLoS One. 2015;10(11):1–15.

287. Roberts A, Headman K, Luyasu V. Multicenter evaluation of strategies for serodiagnosis of primary infection with Toxoplasma gondii. Eur J Clin Microbiol Infect Dis. 2001;20(7):467–74.

288. Luyasu V, Rober A, Schaefer L, Macioszek J. Multicenter evaluation of a new commercial assay for detection of immunoglobulin M antibodies to Toxoplasma gondii. Multicenter Study Group. Eur J Clin Microbiol Infect Dis. 1995;14(9):787–93.

289. Liesenfeld O, Press C, Flanders R, Ramirez R, Remington JS. Study of Abbott Toxo IMx system for detection of immunoglobulin G and immunoglobulin M toxoplasma antibodies: Value of confirmatory testing for diagnosis of acute toxoplasmosis. J Clin Microbiol. 1996;34(10):2526–30.

290. Garry DJ, Elimian A, Wiencek V, Baker DA. Commercial laboratory IgM testing for Toxoplasma gondii in pregnancy: A 20-year experience. Infect Dis Obstet Gynecol. 2005;13(3):151–3.

291. Siegel JP, Remington JS. Comparison of methods of quantitating antigen-specific immunoglobulin M antibody with a reverse enzyme-linked immunosorbent assay. J Clin Microbiol. 1983;18(1):63–70.

292. Murat JB, Dard C, Hidalgo HF, Dardé ML, Brenier-Pinchart MP, Pelloux H. Comparison of the Vidas system and two recent fully automated assays for diagnosis and follow-up of toxoplasmosis in pregnant women and newborns. Clin Vaccine Immunol. 2013;20(8):1203–12.

293. Dhakal R, Gajurel K, Pomares C, Talucod J, Press CJ, Montoya JG. Significance of a positive toxoplasma immunoglobulin M test result in the United States. J Clin Microbiol. 2015;53(11):3601–5.

294. Klee GG. Human Anti-Mouse Antibodies. Arch Pathol Lab Med. 2000;124(6):921–3.

295. Golden A, Stevens EJ, Yokobe L, Faulx D, Kalnoky M, Peck R, et al. A Recombinant Positive Control for Serology Diagnostic Tests Supporting Elimination of Onchocerca volvulus. PLoS Negl Trop Dis. 2016;10(1):1–16.

296. Magari RT, Munoz-Antoni I, Baker J, Flagler DJ. Determining Shelf Life by Comparing Degradations at Elevated Temperatures. J Clin Lab Anal. 2004;18(3):159–64.

297. Holzlöhner P, Hanack K. Generation of murine monoclonal antibodies by hybridoma technology. J Vis Exp. 2017;119:1–7.

298. Basu K, Green E, Cheng Y, Craik C. Why recombinant antibodies — benefits and applications. Curr Opin Biotechnol. 2019;Dec(60):153–8.

299. Clinical and Laboratory Standards Institute. EP25-A Evaluation of Stability of In Vitro Diagnostic Reagents. Vol. 29, Clinical and Laboratory Standards Institute. 2009. 1–56 p.

300. Hamilton R. Engineered human antibodies as immunologic quality control reagents. Ann Biol Clin. 1990;48(7):473–7.

301. Chromikova V, Mader A, Steinfellner W, Kunert R. Evaluating the bottlenecks of recombinant IgM production in mammalian cells. Cytotechnology. 2015;67(2):343–56.

302. Wolbank S, Kunert R, Stiegler G, Katinger H. Characterization of Human Class-Switched Polymeric (Immunoglobulin M [IgM] and IgA) Anti-Human Immunodeficiency Virus Type 1 Antibodies 2F5 and 2G12. J Virol. 2003;77(7):4095–103.

303. Van Anken E, Pena F, Hafkemeijer N, Christis C, Romijn EP, Grauschopf U, et al. Efficient IgM assembly and secretion require the plasma cell induced endoplasmic reticulum protein pERp1. PNAS. 2009;106(40):17019–24.

304. Mader A, Chromikova V, Kunert R. Recombinant IgM expression in mammalian cells: A target protein challenging biotechnological production. Adv Biosci Biotechnol. 2013;04(04):38–43.

305. Ito R, Takahashi T, Katano I, Ito M. Current advances in humanized mouse models. Cell Mol Immunol. 2012;9(3):208–14.

306. Tomita M, Tsumoto K. Recent Advances in Antigen-Based Generation of Monoclonal Antibodies. Curr Immunol Rev. 2010;6(1):56–61.

307. Han Q, Li S, Fu B, Liu D, Wu M, Yang X, et al. Stability of important antibodies for kidney disease: Pre-analytic methodological considerations. PeerJ. 2018;2018(7):1–13.

308. Hodgkinson VS, Egger S, Betsou F, Waterboer T, Pawlita M, Michel A, et al. Preanalytical stability of antibodies to pathogenic antigens. Cancer Epidemiol Biomarkers Prev. 2017;26(8):1337–44.

309. Patel A, Gupta V, Hickey J, Nightlinger NS, Rogers RS, Siska C, et al. Coformulation of Broadly Neutralizing Antibodies 3BNC117 and PGT121: Analytical Challenges During Preformulation Characterization and Storage Stability Studies. J Pharm Sci. 2018;107(12):3032–46.

310. Nowak C, K. Cheung J, M. Dellatore S, Katiyar A, Bhat R, Sun J, et al. Forced degradation of recombinant monoclonal antibodies: A practical guide. MAbs. 2017;9(8):1217–30.

311. Bateman A. UniProt: A worldwide hub of protein knowledge. Nucleic Acids Res. 2019;47(D1):D506–15.

312. Maguy A, Tardif JC, Busseuil D, Ribi C, Li J. Autoantibody Signature in Cardiac Arrest. Circulation. 2020;141(22):1764–74.

313. Statistical Utility for Microarray and Omics data [Internet]. Available from: http://angiogenesis.dkfz.de/oncoexpress/software/sumo

314. Zrein M, Granjon E, Gueyffier L, Caillaudeau J, Liehl P, Pottel H, et al. A novel antibody surrogate biomarker to monitor parasite persistence in Trypanosoma cruzi-infected patients. PLoS Negl Trop Dis. 2018;12(2):1–16.

315. Granjon E, Dichtel-Danjoy ML, Saba E, Sabino E, Campos de Oliveira L, Zrein M. Development of a Novel Multiplex Immunoassay Multi-cruzi for the Serological Confirmation of Chagas Disease. PLoS Negl Trop Dis. 2016;10(4):1–15.

316. H Passing B. A new biometrical procedure for testing the equality of measurements from two different analytical methods. Application of linear regression procedures for method comparison studies in clinical chemistry, Part I. J Clin Chem Clin Biochem. 1983;21(11):709–20.

upf.

TESI DOCTORAL UPF / 2021